Evaluation Of Molecular Targets In Clinical Management Of Intra-Ocular Tumors (Retinoblastoma and Uveal Melanoma)

THESIS

Submitted in partial fulfillment

of the requirements for the degree of

DOCTOR OF PHILOSOPHY

By

Nalini Venkatesan
2010PHXF038P

Under the supervision of

Dr. S.Krishnakumar

And

Dr.P.R.Deepa

BIRLA INSTITUTE OF TECHNOLOGY AND SCIENCE
PILANI (RAJASTHAN) INDIA
2014

BIRLA INSTITUTE OF TECHNOLOGY AND SCIENCE, PILANI
RESEARCH AND CONSULTANCY DIVISION

CERTIFICATE

This is to certify that the thesis entitled **"Evaluation Of Molecular Targets In Clinical Management Of Intra-Ocular Tumors (Retinoblastoma And Uveal Melanoma)"** submitted by Ms. Nalini Venkatesan, ID. No. 2010PHXFO38P for award of Ph.D. Degree of the Institute embodies original work done by her under our supervision.

Signature of the Supervisor :

Dr. S Krishnakumar, MD
Professor & Pathologist
Head, Ocular Pathology Department
L & T Department of Ocular Pathology
Vision Research Foundation, Sankara Nethralaya
18, College Road, Nungambakkam,

Name in Block Capital letters : **DR.S.KRISHNAKUMAR**
Designation : Deputy Director
Vision Research Foundation,
Sankara Nethralaya, Chennai 600 006.
Tamil Nadu, India

Signature of the Co- Supervisor :

Dr. P.R. Deepa, Ph.D.,
Associate Professor
Department of Biological Sciences
BITS Pilani (Rajasthan : 333031)
BITS Pilani - Chennai Centre

Name in Block Capital letters : **DR.P.R.DEEPA**
Designation : Associate Professor
Department of Biological Sciences
PS Division BITS Pilani - Chennai Centre
Birla Institute of Technology & Science, Pilani
Pilani Campus

Contents

LIST OF FIGURES

LIST OF TABLES

ACKNOWLEDGEMENT

First, I thank the **Almighty**, for giving me the strength, knowledge and divine blessings through which this study was possible.

This work was possible with the efforts and enthusiasm of my mentor,

Dr. S.Krishnakumar, Deputy Director - Research, Prof of Ocular Pathology Sankara Nethralaya. He gave the best opportunities to learn techniques, write manuscripts and grants and helped me to establish network with the eye research community within and outside Sankara Nethralaya, which was an important stepping-stone in my career.

I owe my heartfelt thanks and gratitude to my co-supervisor **Dr. P.R.Deepa**, Associate Professor, Department of Biological science, BITS, Pilani who helped me to cross this journey very smoothly. She has been a great source of inspiration, enthusiasm and strong motivation.

My sincere thanks to **Padmabushan Dr.S.S.Badrinath**, Chairman Emeritus, and **Dr.Vasanthi Badrinath,** Director of laboratory Services, **Sankara Nethralaya**, Chennai, to pursue this study in their esteemed institution.

My heartfelt thanks to **Dr. H.N. Madhavan**, Director, Department of Microbiology and **Dr. Malathy Madhavan** for their consistent support and encouragement throughout my period in Sankara Nethralaya.

I sincerely thank **Prof. B.N. Jain** Vice-Chancellor and Director, **Prof. G Raghurama,** Director, Pilani Campus, **Prof. S.K.Verma**, Dean, Academic Research Division, **Prof. Ashish Kumar Das,** Former Dean, Research and Consultancy Division, **Prof. Sundar**, Dean, Academic and Resource Planning, **Dr. Hemant Ramanlal Jadhav,** Associate Dean, Academic Research Division **Dr. Dinesh Kumar, Dr. Navin Singh,** Ph.D monitoring of **BITS Pilani**, for providing me with this great opportunity to do my thesis in their esteemed university.

My thanks to **Dr.Vishal Saxena, Dr. Prabhat Nath Jha,** Doctoral Advisory Committee members of BITS, Pilani for their valuable comments.

I thank **Dr. Bhaskaran,** Chairman, **Dr. T. S. Surendran,** Vice-Chairman, of **Medical Research Foundation**, and **Dr. Ronnie George,** Director of Research, **Mr. Rajagopal**

President, and **Dr. Rama Rajaram**, Advisory, of **Vision Research Foundation** for their support.

My sincere thanks to **Dr. S. Meenakshi**, Director of Academics and **Mr. N.Sivakumar**, Academic officer for their support.

I thank **Dr. Jyotirmay Biswas**, Director and **Ms. K.Vanitha,** Senior Executive of Larsen & Toubro Department of Ocular Pathology for their support during my internship period.

My sincere thanks to **Dr. V. Umashankar**, HOD, Department of Bioinformatics, **Mr. N.Vishwanathan**, Department of Biostatistics, **Mr. Madavan Vasudevan**, Bionivid technologies (Microarray analysis) for their technical support.

My sincere thanks to **Dr.Vikas Khetan**, **Dr. G. Sugneeswari**, **Dr. Pukraj Rishi**, of Sri Bhagawan Mahavir Department of Vitreoretinal and Ocular Oncology for their valuable clinical inputs in my study.

I thank all my collegues, technical and non-technical staff of Sankara Nethralaya for their support.

I express my deepest gratitude to the **Patients of Retinoblastoma and Uveal melanoma**, whose samples have been used for this research work.

I express my thanks to **Department of Science and Technology** (DST), **Childhood eye cancer trust** (CHECT) foundation for their funding.

Last, but not least, I cannot end without thanking the most important people in my life, all of my family members for all their sacrifices.

I dedicate this thesis to my parents **Mr. P. Venkatesan** and **Mrs.V. Prema** for being with me and making my journey truly happy and joyful.

V.NALINI

LIST OF ABBREVATIONS

1.	APS	Ammonium Per Sulphate
2.	BSA	Bovine Serum Albumin
3.	cDNA	complementary DNA
4.	CB	Ciliary Body
5.	CI	Choroidal Invasion
6.	CISH	Chromosomal Insitu Hybridisation
7.	CO2	Carbon dioxide
8.	DAPI	4, 6 - Di Amidino -2- Phenyl Indole
9.	DMEM	Dulbecco's modification of eagle's medium
10.	ECL	Electro ChemiLuminescence
11.	EDTA	Ethylene Diamine Tetra Acetic Acid
12.	F	Female
13.	FBS	Fetal Bovine Serum
14.	FITC	Fluorescein Iso Thio Cyanate
15.	FISH	Flourescent Insitu Hybridisation
16.	HRP	Horse Radish Peroxidase
17.	HMG	High Mobility Group
18.	HMGA2	High Mobility Group A2
19.	h	Hs
20.	HSP	Heat Shock Protein
21.	ICMR	Indian Council for Medical Research
22.	IHC	Immunohistochemistry
23.	inv	Invasion
24.	LDH	lactate dehydrogenase
25.	LNA	Locked nucleic acid
26.	MDR	Multi-drug resistance
27.	MRP	Multi-drug resistant Protein
28.	MIO-M1	Mueller glial celline
29.	miRNA	microRNA
30.	mins	Minutes
31.	mRNA	Messenger RNA
32.	MTT	(3-(4,5-dimethylthiazol-2-yl)-2,5-diphenyltetrazolium bromide)
33.	ON	Optic nerve
34.	PBS	Phosphate buffer saline
35.	PBS	Phosphate Buffered Saline
36.	PBST	Phosphate Buffered Saline (0.1% Tween 20)
37.	PCR	Polymerase chain reaction

38.	PLL	Poly L Lysine
39.	PRAME	Preferentially Expressed Antigen of Melanoma
40.	Pre-lam	Pre-laminar Invasion
41.	Post-lam	Post-laminar Invasion
42.	PTEN	Phosphatise and tensin homolog
43.	qRT-PCR	Quantitative Real Time-Polymerase Chain Reaction
44.	RB	Retinoblastoma
45.	RIPA	Radioimmunoprecipitation assay
46.	ROX	Carboxyrhodamine
47.	Rpm	Revolutions Per Minute
48.	RPMI	Roswell Park Memorial Institute medium
49.	RT	Reverse Transcription
50.	Scr	Scramble
51.	SDS	Sodium dodecyl sulphate
52.	SDS-PAGE	Sodium Dodecyl Sulfate-Polyacrylamide Gel Electrophoresis
53.	SELEX	Systematic evolution of ligands by exponential enrichment
54.	siRNA	Small inhibitory RNA
55.	SSC	Saline Sodium Citrate
56.	TAE	Tris Acetic acid EDTA
57.	TBS	Tris buffer saline
58.	TBS-T	Tris buffer containing 0.1% Triton x-100
59.	TF	Transcription factor
60.	TSA	Tumour Suppressor Antigen
61.	TEMED	Tetramethylethylenediamine
62.	UM	Uveal Melanoma
63.	WB	Western blotting

CHAPTER 1: INTRODUCTION

1.1. Cancer

Cancer is a disease of an uncontrolled, undesirable and un-coordinated cell division caused by the cellular DNA damage. DNA damage can be either due to genetic inheritance or sporadic (for e.g. a number of environmental factors namely exposure to tobacco smoke, radiations, etc). Replication of cancer cells results in a clump of cells termed as "tumor". Tumors can be typed either as benign or malignant. Benign type are not life threatening and does not result in cancerous tumors while malignant can metasizes to other body parts due its cancerous nature. To metastasize, primary tumors initially undergo an epithelial-to-mesenchymal transition (EMT), during which they lose the expression of cell adhesion molecules such as E-cadherin and adopt an invasive phenotype, before undergoing a mesenchymal-to-epithelial transition (MET), which enables successful colonization. Plasticity and reversible phenotype switching between these different states generates phenotypic heterogeneity in solid tumors. Cellular senescence is an integrated and widespread component contributing for tumor development, tumor suppression and the response to therapy.

1.1.1. Eye (ocular) cancer

Eye cancer is uncontrolled growth of abnormal cells in or around the eye that develop into tumor. This cancer is categorized as either primary (arising in the tissues of eye), or secondary (spread to eye). Predominant sources of secondary eye cancers are breast cancer and lung cancer.

1.1.1.1. Anatomy of eye

The eye consists of three main parts: the eyeball, the orbit (includes eye socket, muscles, and nerves that surround the eyeball), and the adnexal structures (accessory structures, such as the eyelid and lacrimal gland) **[Figure 1.1]**.

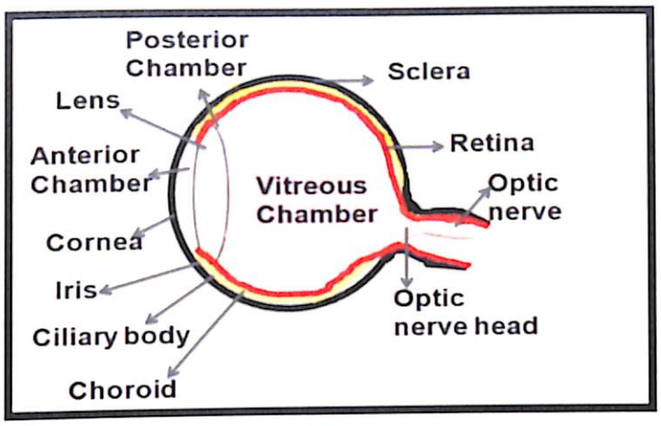

Figure 1.1: Anatomy of Eye.

1.1.1.2. Primary intraocular cancer

Primary eye cancers arise from any of these three parts, when cancer origins in eyeball, it is called primary intraocular cancer. The most common form of primary intraocular cancer in adults is melanoma, followed by lymphoma.

1.1.1.3. Types of primary intraocular cancer

- Melanomas develop in pigment-producing or color-producing cells of uveal tract, such as those in the iris, ciliary body epithelium and choroid of the eye. Most common form of intraocular cancer in adults
- Retinoblastoma arises in retina (light-sensitive tissue of eye) and is the most common form of primary intraocular cancer in children.

Incidence of primary eye cancer is low compared to other cancers, but if untreated it may lead to life-threatening complications and death. Regular eye examination offers the best chance of discovering eye cancer in most curable stage.

1.2. Retinoblastoma (pediatric cancer)

Retinoblastoma (RB), a malignant tumour arising from immature retina, with a relative incidence of 1 in 20,000 live births (Balmer Munier F 2002b et al.), it accounts 3% of all

paediatric tumors worldwide (Dyer et al. 2005) and rates third highest among all intraocular tumors of all ages (Scat et al. 1996). It occurs in infants, children and also in fetus (Maat-Kievit et al. 1993). A few exceptional reports are observed in older children and in young adults (Shields et al. 1991c).

1.2.1. Epidemiology

RB incidence is higher in developing countries, and it is one of the common childhood solid tumor malignancies in some countries of Central and South America (Leal-Leal. et al. 2004). In India, the incidence of high-risk RB tumors (tumors with choroidal and optic nerve invasion) is higher than developed countries (Biswas et al. 2003, Vemuganti G.K. 2000). The reason for this higher incidence remains unclear. The factors namely lower socio economic status, presence of genetic back ground (Pan 2005), presence of human papilloma virus sequences in the retinoblastoma tumor tissue (Orjuela M. et al. 2000) ; (Mohan et al. 2009), and children born through in vitro fertilization implicates the higher risk for this disease (Lidegaard et al. 2005).

RB is confined either to one eye (unilateral) or may occur in both the eyes (bilateral), and can metastasize to primary intracranial neuroblastic tumor, in particular pinealoblastoma ('trilateral' retinoblastoma) (Kivela 1999). The average age of first sign of RB is 7 months for bilateral cases and 24 months for unilateral cases (Balmer A 2000a). It may be non-heritable (60%) or heritable (40%) due to autosomal-dominant transmission with high penetrance (90%) (Balmer Munier F 2002b). The heritable types (both unilateral and bilateral, 60% of all cases) holds high risks resulting in the secondary non-ocular tumors while non- heritable results only in unilateral (15% of cases) (Knudson 1971). Treatment at early stage of the disease shows a better prognosis than at later stages. In very late stages the visual function and rarely the survival too is at risk.

1.2.2. Genetics

Oncogenic mutation ("Two hit hypothesis") in RB1 gene (on chromosome 13q14) between the initial period of third month post-conception and during the age of 4 years

contributes the onset of RB. RB originates either from the cone photoreceptor cells or a multipotent retinoblast (Munier F 2002). In major percentage of RB (heritable), biallelic RB1 inactivation; the first in RB1 mutation (M1) is constitutional, and the second mutation (M2) occurs somatically in one or more of the retinal cells resulting in the formation of RB tumor. In a small percentage of RB (non-heritable), the proband harbors RB1 mutation (M1) in one cell of the multicell embryo resulting in mosaicism, where both RB1 mutational events (M1 and M2) arise in a single somatic retinal cell (Rushlow D. et al. 2009). Among the non-heritable retinoblastoma a small proportion results from *MYCN* gene amplification with normal RB1 gene (Rushlow D. E. et al. 2013). The mutation in RB1 gene makes the RB patients vulnerable to secondary cancers such as lung, bladder, bone, skin and brain cancers (Eng et al. 1993). The inheritance property and high risk of susceptibility to secondary cancers imposes the need of life-long follow up which includes genetic testing and counseling.

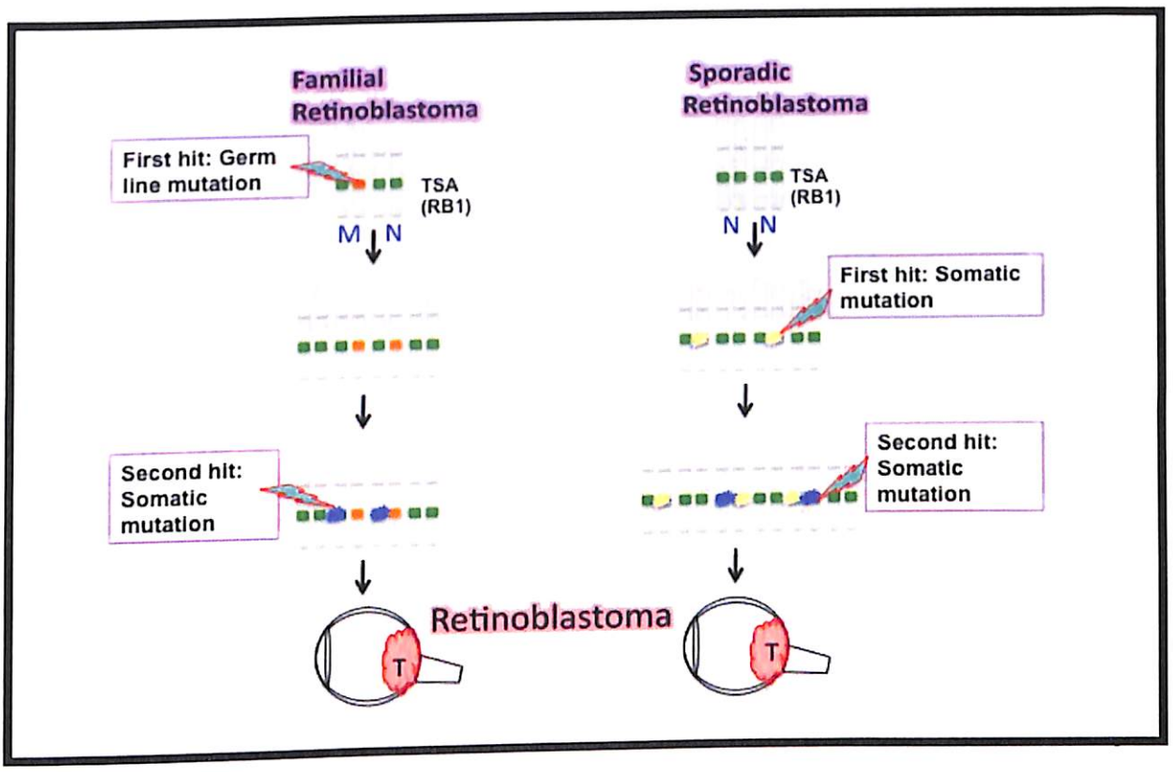

Figure 1.2: Knudson hypothesis. Scheme representation of Knudson "Two hit hypothesis" in familial and sporadic retinoblastoma.TSA: tumor suppressor genes; RB1: RB1 gene; M: mutant phenotype; N: Normal phenotype; T: tumor.

1.2.3. Clinical presentation

The most common clinical presentation of RB is leukocoria (60%) and strabismus (20%). Though it is a late sign, the survival rate is high (88% at 5 years) while the later with the

good chance for globe salvage (Beaverson K and Kirszrot J 2001). The clinical presentation of retinoblastoma depends on

1) Tumor growth pattern

2) Duration and degree of vascularization

3) Presence of calcifications

4) Vitreous seeding, retinal detachment or hemorrhage.

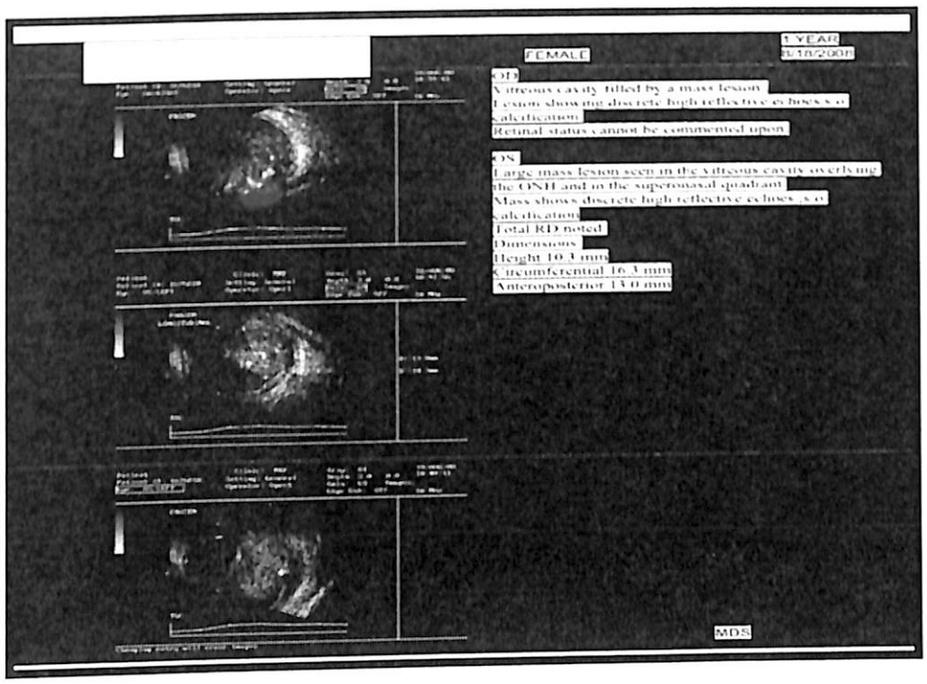

Figure 1.3: Ultrasound report of RB. Reports the presence of whitish tumor mass in both eyes (Right eye: OD; Left eye: OS).

1.2.4. Histopathologic features and risk factors of RB

1.2.4.2. Classifications of RB

Most widely used classification system is the Reese–Ellsworth Classification, developed in 1963 (Reese and Ellsworth 1963). This classification is based on intraocular tumor staging and globe salvage prediction after external beam radiation, and survival has not been taken into account.

Table 1.1: Classification of RB. International intraocular retinoblastoma classification (ABC classification-modified). This classification stages intraocular tumors based on their prognosis after first-line chemotherapy and adjuvant focal therapy. It consists of five groups (A, B, C, D, E) in descending order of favorable prognosis, taking into account the

size of the tumors, their proximity to the macula and the optic nerve, the degree of seeding and importance of retinal detachment and, finally, late complications (Linn Murphree 2005).

Groups	Risk status	Descriptions
Group A	Very low risk	• Tumors 3 mm or smaller, • Eyes with small discrete tumors away from critical structures. • Confined to the retina >3mm from the fovea, >1.5mm from the optic nerve • No vitreous or sub-retinal seeding
Group B	Low risk Tumors	• Eyes with no vitreous or sub-retinal seeding and discrete retinal tumor of any size or location • No vitreous or sub-retinal seeding • Sub-retinal fluid >5mm from the base of the tumor
Group C	Moderate risk	• Seeding local, fine and limited eyes with only focal vitreous or sub-retinal seeding and discrete retinal tumors of any size and location. • Treatable with a radioactive plaque • Tumors discrete and of any size and location up to one quadrant of sub-retinal fluid
Group D	High risk Massive and/or diffuse intraocular disseminated disease	• Eyes with diffuse vitreous or sub-retinal seeding and/or massive, non-discrete endophytic or exophytic disease. • Eyes with more extensive seeding than Group C More than one quadrant of retinal detachment • Fine greasy vitreous seeding or avascular masses • Sub-retinal seeding, plaque-like
Group E	Very high risk	• Irreversible neovascular glaucoma, eyes that have been destroyed anatomically or functionally by the tumor. • Eyes with one or more than the following:

		Massive intraocular hemorrhage, Aseptic orbital cellulitis • Tumor anterior to anterior vitreous face Tumor touching the lens • Diffuse infiltrating retinoblastoma • Phthisis or prephthis

1.2.4.3. Macroscopic Appearance

After enucleation of eyeball, the retinoblastoma tumour tissues are obtained. The gross appearance depends upon the stage of tumor. Generally the tumor appears as a whitish mass with necrotic or calcified tissues. At initial stages, it presents as vitreous seedings and as the disease advances, it totally fills the vitreous cavity and replaces or destroys the entire retina. In the case of acute infarction, the tumor mass have a blood-tinged (hemorrhagic) orange, or soupy, grayish appearance (Eagle 2000).

Figure 1.4: Gross photomicrographs of RB. A: Fresh enucleated eyeball showing Leukocoria (clinical presentation); B: Bread-loaf sections of fresh frozen eyeball; C: Cut-off lobe of a formalin fixed eyeball. Yellow arrowhead indicates the whitish tumor mass, details of the patient is hidden using white colored strip.

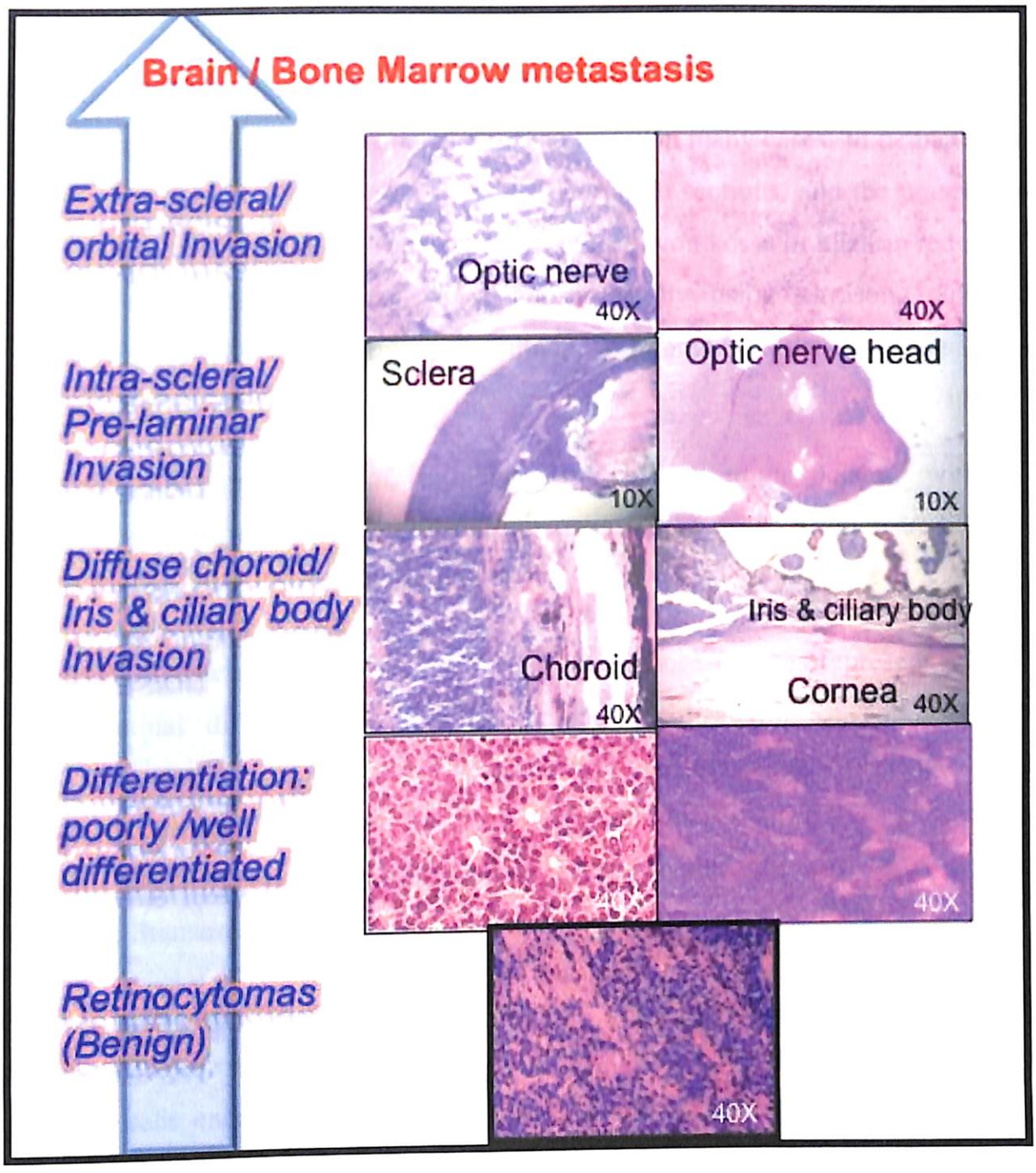

Figure 1.5: Stages of RB. Photomicrographs of different stages of retinoblastoma tumor sections stained with hematoxylin and eosin (H&E) stain.

1.2.4.4. Microscopic Appearance

Microscopically, the cell types are classified as

- Poorly differentiated
- Well differentiated
- Moderately differentiated.

- Among these types, **poorly differentiated** cell type is the predominant one. Round cell with a large basophilic nucleus and scanty cytoplasm, mitotic figures and fragments of apoptotic nuclear debris are usually present. Foci of dystrophic calcification develop in the necrotic parts of the tumor in many cases. In hematoxylin-and-eosin, the calcified foci appear as reddish-purple in sections, and the presence of calcium can be confirmed by the special stains namely von kossa or alizarin red stains. Clinically, the calcification can be demonstrated by using ultrasonography or computed tomography to differentiate the tumour from other simulating lesions (Eagle 2000, Finger et al. 2002a).

  Historically, the prognosis of retinoblastoma has been associated with the differentiation of tumor cells. These differentiations are the signs of which are believed to be the formation of fibrils and rosettes.

- **Flexner-Wintersteiner rosettes**: The formation of these rosettes represent an early stage of retinal differentiation and are composed of a ring of cuboidal cells surrounding a central lumen containing hyaluronidase-resistant acid mucopolysaccharide (AMP), similar to photoreceptor matrix AMP. The presence of abundant Flexner-Wintersteiner rosettes may result in better prognosis (Boxrud 1995, Eagle 2000, Stannard et al. 1979).

- **Homer-Wright rosettes**: These cell types are observed less frequently and are indicative of neuroblastic differentiation. They lack a central lumen, and their constituent cells encompass a central tangle of neural filaments. They are relatively nonspecific because they also occur in neuroblastoma and are a characteristic feature of cerebellar medulloblastoma (Boxrud 1995, Eagle 2000).

- **Fleurettes**: Tso et al; 1969 described another type of arrangement and named as "fleurettes" as they resemble a bouquet of flowers. They appear in the viable portions of tumor cells and believed to represent the greatest degree of differentiation. In retinocytomas (benign variant of retinoblastoma), the tumors are composed entirely of fleurettes (Mashiah and Barishak 1977, Sevel et al. 1974, Ts'o et al. 1969).

- A recent study with extensive analysis of early and late-stages of retinoblastoma has reported that rosette formation is not a hallmark of tumor differentiation, but represents

extensive cell-cell contacts in both tumor stages. So differentiation does not act as a prognostic feature of retinoblastoma (Johnson D. A. et al. 2007).

1.2.4.5. Histopathological risk factors

Many risk factors have been identified for retinoblastoma, which includes age at diagnosis and treatment, previous family history, deletion or inactivation of one allele of RB1 gene, laterality of disease and the local invasion of the tumor (Finger et al. 2002a). Among these risk factors the key predictors of metastasis are invasion of the tumor into the uvea, orbit, and optic nerve, scleral, extrascleral and extra-ocular extension (Finger et al. 2002b, Khelfaoui et al. 1996, Shields et al. 1993, Shields et al. 1994), bilaterality and delay in diagnosis (Finger et al. 2002a). Other reports have stated the risk factors associated with sporadic heritable RB as ethinicity and race (Stiller and Parkin 1996), older parental age (DerKinderen et al. 1990, Moll et al. 1996, Sivakumaran et al. 2000), lower maternal intake of micronutrients during pregnancy (Orjuela M. A. et al. 2005), paternal metal exposure, radiation exposure (Bunin et al. 1990, Hicks et al. 1984).

1.2.4.5.1. Uveal, optic nerve and orbital Extension

Reports by Sheild's et al and Karcioglu et al showed a significant association of choroidal invasion with metastasis and higher stage of disease (stages III or IV of Rees-Ellswaorth classification) (Karcioglu et al. 1997, Shields et al. 1993). There existed a controversy due to lack of adequate histological descriptions whether the choroidal invasion alone contributes to the metastasis. Further, Schilling et al proposed a staging system (stage I- IV) to grade the choroidal involvement and this staging system was clinically significant (Yang H. et al. 1999).

High mortality rate in patients with extension up to the level of optic nerve, sclera, extra-scleral, iris and ciliary body has been reported. An adjuvant therapy of high dose chemotherapy with addition of orbital radiation has been recommended (Honavar and Singh 2005, Rodriguez-Galindo et al. 2007, Sevel et al. 1974). Magnetic Resonance Imaging (MRI) aids evaluating preoperative detection of the optic nerve involvement by the physician (Brisse et al. 2007). The mortality rate is in the range of 13-69%,

when the tumor cells are present in the optic nerve posterior to the lamina cribosa (Chintagumpala et al. 2007, Shields et al. 1994).

One of the worst prognostic factors of the systemic metastasis is orbital retinoblastoma and the mortality rate is in the range of 25-95% (Honavar and Singh 2005). Effective treatment for the orbital RB management has not still proven, but still combination of high dose chemotherapy followed by enucleation (removal of eye) and exentration (removal of surrounding tissue and part of bony socket, the orbit), external beam radiotherapy and extended chemotherapy are advised to improve the survival (Honavar and Singh 2005). These earlier reports indicate the involvement of uvea, optic nerve and orbit as the key predictor risk factors of retinoblastoma.

1.2.4.5.2. Metastatic Retinoblastoma

RB metastasizes to regional lymphnodes, central nervous systems (CNS), spreads to bone and liver (Gunduz et al. 2006, Leal-Leal et al. 2006). The patient with metastatic CNS involvement may rarely survive inspite of the advanced therapies (Chintagumpala et al. 2007, Dunkel et al. 2000, Rodriguez-Galindo et al. 2003). Mc Clean proposed 4 patterns of retinoblastoma metastasis (Mclean 1994).

1) Direct invasive spread of tumor along the optic nerve to the brain
2) Spread to the optic nerve and leptomeninges that disperse to the subarachnoid fluid
3) Hematogenous dissemination, which results in widespread metastasis to the lungs, bones and brain.
4) Presence of anterior tumor leads to massive extra-ocular spread

1.2.5. Treatment modalities

Advancement in the treatment modalities of RB has resulted in a steady increase in the rate of survival from 30% in the 1930s to 80% in the 1960s. RB management varies with intraocular disease and extra ocular spread of the tumor. Patients presenting with unilateral disease and with advanced intraocular disease usually undergo enucleation

(cure rate of greater than 95%). Bilateral RB management requires multimodality therapy (chemotherapy, local therapies) and additional external beam radiation (EBR) therapy are required for tumor regression.

Various treatment modalities in the current RB management are

- Enucleation
- External beam radiation (EBR) therapy
- Brachytherapy
- Chemotherapy
- Laser photocoagulation
- Cryotherapy
- Chemotherapy

Table 1.2: Details of Chemotherapy schedule. List of chemotherapy drug with note on the concentration and the schedule used in RB management (Shields et al. 2013).

Name of drug	Dose	Schedule
Intravenous chemotherapy		
Carboplatin (C)	560mg/M2 in 120 cc/M2 D51/4NS IVSS over 60 min	Day 0 of each cycle (18.6mg/kg for patients <36 months of age)
Etoposide (E)	150mg/M2 in 150 cc/M2 D51/4NS IVSS over 60 min	Days 0 and 1 of each course (5mg/kg for patients <36 months of age)
Vincristine (V)	1.5mg/M2 IVSS over 15 minutes	Day 0 of each cycle (0.05mg/kg for patients <36 months of age). Maximum vincristine dose not to exceed 2mg
Antiemetic drug		
Ondansetron	0.45mg/kg IVSS (maximum dose 24 mg) prior to therapy	Days 0 and 1 of each cycle, with Dexamethasone 0.25mg/kg IVSS prior to therapy days 0 and 1 of each cycle
Phenergen	0.5mg/kg p.o. h.s. on	Day 0 and then every 6h prn with emesis

Name of drug	Dose	Schedule
Diphenhydramine	1mg/kg p.o. h.s.	Day 0 and then every 6h
Therapy continues every 4 weeks for a total of six cycles. Prior to institution of each subsequent cycle, the absolute neutrophil count must be >750cells/μl and platelets must be >75 000 cells/μl		
Intra-arterial chemotherapy		
Melphalan		Slow pulsatile infusion over 30 min
0–2 years old	3mg/30 cc	
2–5 years old	5mg/30 cc	
>5 years old	7.5mg/30 cc	
Carboplatin	30mg/30 cc	Slow pulsatile infusion over 30 min
Topotecan		Slow pulsatile infusion over 30min
0–2 years old	0.5mg/30 cc	
>2 years old	1.0mg/30 cc	
Subtenon's chemotherapy		
Carboplatin	20mg/2 cc	Inject into subtenon's space directly over sclera in area of tumour
Intravitreal chemotherapy		
Melphalan	8–30μg/0.1 cc	Inject intravitreally through pars plana or clear corneal approach, cryotherapy to injection site, jiggle eye to mix chemotherapy. Deliver monthly
Methotrexate	400-800μg/0.1cc	Inject intravitreally through pars plana or clear corneal approach, cryotherapy to injection site. Deliver twice weekly for 1 month, then weekly for 1 month, then monthly for 1 year

Table 1.3: Mode of treatment. Mode of treatment recommended as primary and secondary therapy in RB management. Subtenon's chemotherapy is recommended as primary therapy in conjunction with intravenous chemotherapy for groups D and E. If intravenous chemotherapy is used as primary and secondary therapy, the regimen is changed to different agents in secondary therapy (Shields et al. 2013).

Feature	Intravenous chemotherapy	Intra-arterial chemotherapy	Periocular chemotherapy	Intravitreal chemotherapy
Primary therapy				
Bilateral retinoblastoma	+++	+	+	~
Unilateral retinoblastoma	++	+++	+	~
Secondary therapy for recurrent/persistent tumour				
Retinoblastoma	++	+++	+	~
Sub-retinal seeds	++	+++	+	~
Vitreous seeds	++	++	+	+++

Efficacy of the treatment are indicated as +++: Marked, ++: intermediate, +: minimal, ~: little to none.

Table 1.4: Complications of chemotherapy. Net results and complications (Ocular, brain and systemic) observed during various modes of chemotherapy recommended in RB management (Shields et al. 2013)

Feature	Intravenous chemotherapy	Intra-arterial chemotherapy	Periocular chemotherapy	Intravitreal chemotherapy
Tumour control of				
Retinoblastoma	+++	+++	+	~
Subretinal seeds	+++	+++	++	~
Vitreous seeds	++	++	+	+++
Resolution of retinal detachment	+++	+++	~	~
Prevention of pinealoblastoma	+++	~	~	~
Reduction in long-term second cancers	++	~	~	~

Feature	Intravenous chemotherapy	Intra-arterial chemotherapy	Periocular chemotherapy	Intravitreal chemotherapy
Complications ocular				
Ptosis	~	++	+	~
Eyelid oedema	~	+	++	~
Forehead redness	~	+	~	~
Dysmotility	~	+	+	~
Ophthalmic artery obstruction	~	+	~	~
Retinal artery obstruction	~	+	~	~
Choroidal vascular attenuation	~	++	~	~
Vitreous haemorrhage	~	+	~	~
Retinal vasculitis	~	+	~	~
Optic neuropathy	~	+	~	+
Phthisis	~	++	+	+
	~	+	~	++
Complications brain				
Carotid spasm	~	+	~	~
Stroke	~	+	~	~
Brain haemorrhage	~	~	~	~
Brain vascular perfusion defects	~	+	~	~
Complications systemic				
Renal toxicity	+	~	~	~
Leukaemia	+	+	~	~

Mode of treatment and its outcome are indicated as +++: Marked, ++: intermediate, +: minimal, ~: little to none.

1.2.5.2. Management of extra ocular disease

The survival rate of retinoblastoma with extra ocular disease (includes patients with orbital, pre-auricular disease and patients with tumor found at the optic nerve surgical margin) is minimal. High-dose chemotherapy and EBR in conjunction with bone marrow stem cell transplantation is recommended. A combination of high dose chemotherapy that includes vincristine, doxorubicin, and cyclophosphamide or vincristine, idarubicin, cyclophosphamide, carboplatin, and etoposide has showed a good prognosis in an earlier study (Chantada et al. 2003). The modification in the extra ocular RB management are carried over by Children's Oncology Group (COG) for patients with metastatic disease which includes conventional chemotherapy, stem cell harvest, high-dose chemotherapy with stem cell rescue, and EBR of involved sites.

1.2.5.3. Adjuvant therapy in RB management of unilateral retinoblastoma (with high-risk histopathologic features in patient's enucleated eyes)

In an earlier report by Honavar et al. (2002), incidence of metastasis was 4% in patients (unilateral retinoblastoma underwent primary enucleation and categorized into a high risk group based on pre-determined histopathologic characteristics) who received adjuvant therapy compared with 24% in those who did not. This study indicates the effectiveness of adjuvant therapy in RB (Honavar et al. 2002).

Further, in yet another prospective multi-institutional clinical study in North America, initiated by the Children's Oncology Group (COG), patients with well-defined histopathological features are eligible to receive adjuvant chemotherapy (six cycles of carboplatin, vincristine, and etoposide) (Chintagumpala et al. 2007).

1.3. Ocular melanoma

Ocular melanoma is the most common primary eye cancer. Uveal Melanoma (referred as choroidal melanoma), primary intraocular neoplasms of adults arise from melanocytes of choroidal plexus representing about 5% of all melanomas (Woll et al. 1999). The incidence of UM is 0.02% of outpatients in a referral eye hospital in India

(Biswas et al. 2004). Melanoma has been observed with 3 fold higher incidences in white races compared to dark pigmented races and is rare in Asian populations (1998b, Kuo et al. 1982, Manohar et al. 1991, Margo C. E. and McLean 1984). Melanoma usually occurs in elderly men (Egan et al. 1988), rarly in children/teenagers and less predominantly in women. Mean age of disease onset, in Caucasians, African-Americans, Japanese, Hispanics, Chinese and Asian Indians are 60.1, 51.7, 55.2, 52.4, 43.7, and 45.7 respectively (Biswas et al. 2004, Shields et al. 1991a).

The susceptibility factors associated with the development of UM include: Caucasian race, light eye color, fair skin and the ability to tan (Inskip et al. 2003, Singh et al. 2005, Weis et al. 2006), but evidences are inconsistent to determine occupational UV light or other agents as a risk factor for uveal melanoma (Harris et al. 2001, Singh et al. 2005).

1.3.3. Characteristics, histopathological appearance and risk factors of uveal melanoma

1.3.3.2. Anatomic location

UM arises either in the anterior portion (iris) or the posterior portion of the eye (ciliary body or choroid) uveal tract. Predominantly uveal tract melanomas originate in the choroid (a layer of blood vessels that supplies oxygen and nutrients to eye). Intraocular melanoma of eye (2%) is usually small in size, rarely spreads to the other parts of the body. Iris melanomas are less aggressive and have the best prognosis. Intraocular melanoma of ciliary body (7%) is larger and has a moderate tendency to spread to other parts of the body, and shows poor prognosis (Edge SB 2010, Yap-Veloso et al. 1997). Intraocular melanoma of choroid (90%) is often larger, elevated, dome-shaped sub-retinal mass and has a high tendency to spread to other parts of the body. The degree of pigmentation ranges from dark brown to totally amelanotic (Shields et al. 2014).

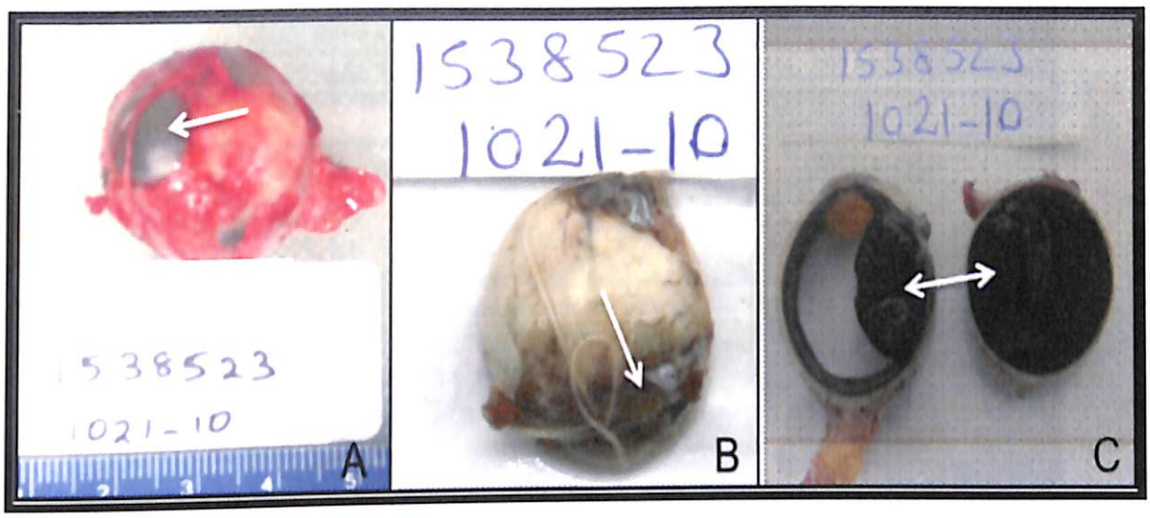

Figure 1.6: Gross photomicrographs of UM. Figure shows the view of a complete eyeball with optic nerve removed from a patient diagnosed with UM (uveal melanoma) at different stages of processing. A: Fresh frozen eyeball (unfixed); B: Formalin Fixed eyeball; C: Bread-loaf sections of formalin fixed eyeball. Number shown is identity of specimen.White arrow head indicates the black-pigmented melanoma tumor.

1.3.3.3. Clinical diagnosis

Ocular melanoma is a malignant tumor that can grow and metastasize (spread) to the other parts of the body especially to liver, which can result in death. Initially, small choroidal melanomas are symptom less. As the tumor enlarges, a few symptoms including light flashes, distortion of the pupil (iris melanoma) floaters, blurred vision (ciliary body melanoma), and vision loss caused by secondary retinal detachment (choroidal melanoma) are observed (Rosai 1996). Clinical diagnosis of uveal melanoma includes the examination of eye through cornea, using opthalmoscopes. Clinical observations that aids to identify melanoma include: Tumor thickness of more than 2 mm, Subretinal fluid, Visual symptoms, Orange pigment on the tumor surface and tumor margin touching the optic disc (Edge SB 2010). The other tests used to diagnose the uveal melanoma include ultrasound or echography, flourescein angiography.

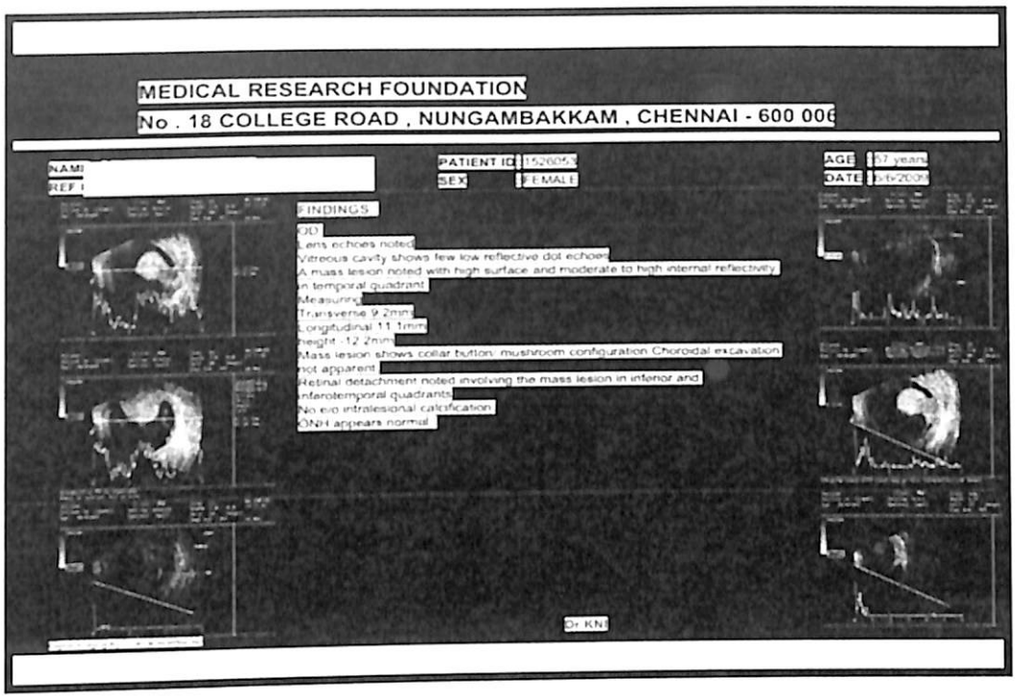

Figure 1.7: Ultrasound report of UM. The report indicates the presence of a mass lesion of collar button/mushroom shaped, measuring about 9.2 mm x 11.1mm x 12.2 mm with retinal detachment in the right eye (OD) of a patient diagnosed with uveal melanoma.

1.3.4. Prognostic factors

Many factors are known to influence the prognosis. The most important of these factors are

1. Cell type.
2. Tumor size.
3. Location of the anterior margin of the tumor.
4. Degree of ciliary body involvement.
5. Extra ocular extension.

The other factors such as microscopic features can affect the prognosis of intraocular melanoma. This includes Mitotic activity, Lymphocytic infiltration and fibro-vascular loops.

1.3.4.2. Cell type

The Cellular Classification of Intraocular (Uveal) melanoma is the classification of UM based on the cell types that predominated in the tumor mass. The primary UM originates from the melanocytes in the uveal tract (Klintworth GK 1999). Four distinct cellular types are recognized in intraocular melanoma McLean's modification of the Callender classification is currently adopted in uveal melanoma's histological classifications and is as follows (Grossniklaus HE 1994) :

- **Spindle-A cells**: spindle-shaped cells with slender nuclei and lacking visible nucleoli).
- **Spindle-B cells**: spindle-shaped cells with larger nuclei and distinct nucleoli).
- **Epitheliod cells**: larger polygonal cells with one or more prominent nucleoli).
- **Intermediate cells**: similar to but smaller than epitheliod cells.

Variable proportions of epitheliod, spindle-A, and spindle-B cells (mixed-cell melanomas) are observed in most of the primary intraocular melanomas. Approximately 3% of cases exhibit pure epithelioid-cell type and are infrequent (Klintworth GK 1999). In the Collaborative Ocular Melanoma Study (COMS), mixed-cell type melanomas predominated (86% of the cases) (1998a).

Spindle cell types carry the best prognosis and the epitheliod cell melanomas carry the least favourable prognosis. But in a report by Dimeras et al, (2012), the epitheliod cell type melanoma has the gene profile matching to the class 1 tumors (low risk tumors) (Albert DM 2011, Singh and Topham 2003b, Weis et al. 2006). This is the pointer for lesser reliability on strictly histological classification of UM for risk assessment. The other prognostic indicator associated with histopathological parameter includes tumor in-filtration by macrophages and/or lymphocytes and mitotic figures (heterogeneous nucleoli size, extracellular matrix patterns).

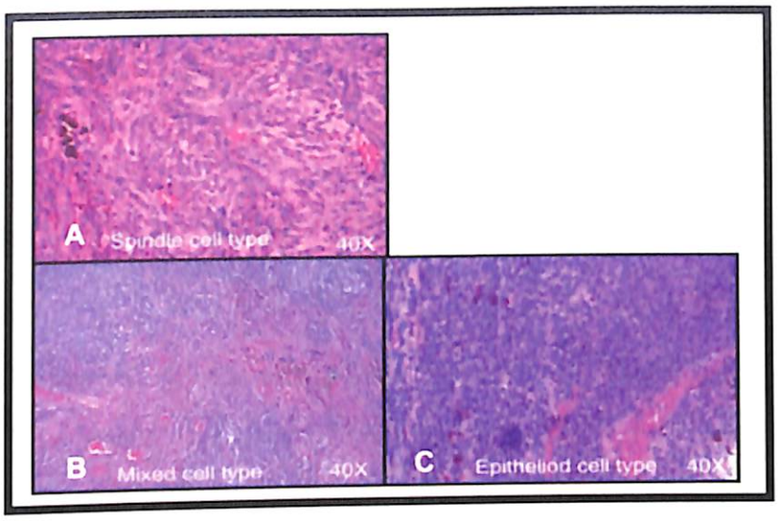

Figure 1.8: Photomicrograph of cell types. Hematoxylin and eosin (H&E) stained sections of eyeball diagnosed with uveal melanoma under 40 X magnifications. A: spindle cell type; B: epitheliod cell type; C: Mixed cell type.

1.3.4.3. Extra-ocular extension

The extraocular extension, recurrence, and metastasis results in extremely poor prognosis, and long-term survival cannot be expected (Gragoudas et al. 1991). The 5-year mortality rate associated with metastasis from ciliary body or choroidal melanoma is approximately 30%, compared with a rate of 2% to 3% for iris melanomas (Shields JA 1992).

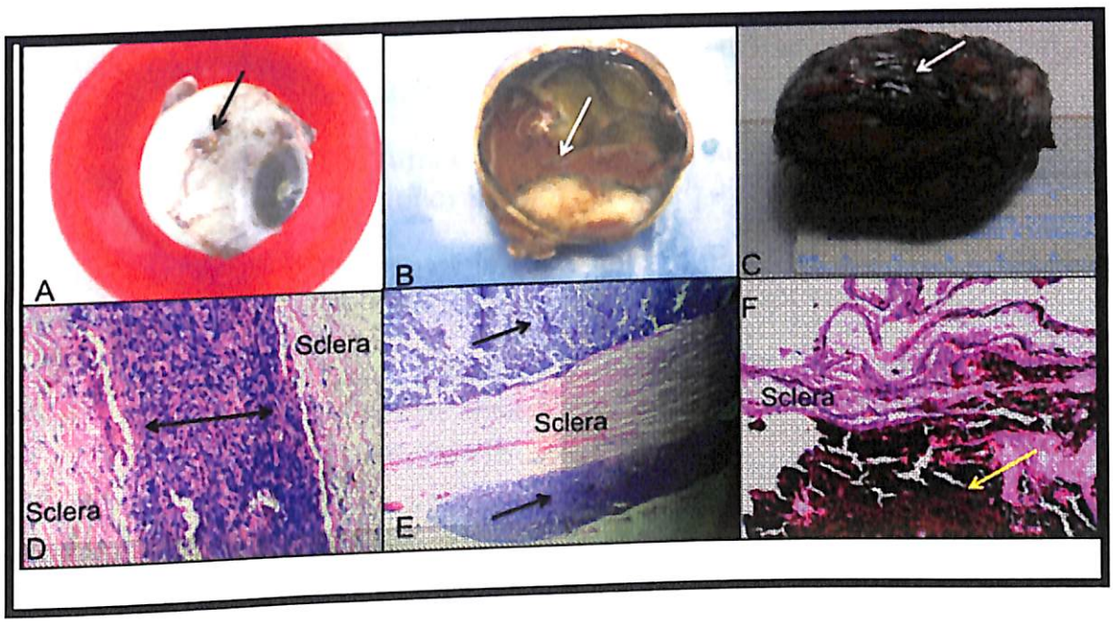

Figure 1.9: Photomicrographs of UM. A-C: Gross photomicrographs of formalin fixed eyeballs. A: Eyeball harboring melanoma tumor mass invasion at emissary veins; B: Eyeball harboring melanoma tumor mass with both at intra-scleral and extra-scleral invasion; C: Exenterated specimen harboring melanoma tumor mass invading the orbital tissues. D-E: Photomicrograph shows hematoxylin and eosin (H&E) stained sections of

eyeball diagnosed with uveal melanoma under 40 X magnifications. D: Intra-scleral invasion; E: Extra-scleral invasion; F: Extra-scleral with orbital invasion. Colored arrowhead indicates the tumor cells.

1.3.5. Classification and stage information for intraocular UM

The clinical information helps to classify the tumors. TNM system used by the American Joint Committee on Cancer is the common system followed by clinicians.

The tumors in TNM classification are based on

T = size of tumor

N = spread to lymph nodes. Choroidal melanoma rarely spreads to the lymph nodes, as there are no lymphatic channels in the eye.

M = metastasis to distant organs

Table 1.5: Stages of uveal melanoma.

S.No	Stages	Definition
1.	Stage 1A	The tumor is 7 mm or less in diameter and is less than 2 mm in height. The tumor has not spread to distant organs.
2.	Stage 1B	The tumor is 7-10 mm in diameter and is 2-3 mm in height. The tumor has not spread to distant organs.
3.	Stage 2	The tumor is 10-15 mm in diameter and is 3-5 mm in height. The tumor has not spread to distant organs.
4.	Stage 3	The tumor is more than 15 mm in diameter or greater than 5 mm in height. The tumor has not spread to distant organs.
5.	Stage 4A	The tumor extends outside the eyeball but it has not spread to distant organs.
6.	Stage 4B	The tumor may be any size, and has spread to distant organs, typically the liver.

1.3.6. Treatment modalities

Ocular tumors, especially the small sized tumors can be completely destroyed. Removal of eyeball (enucleation) is recommended to lessen the probability of metastasize. But management of small choroidal melanomas is still controversial, and it is not clear whether treatment of small tumors prevents metastasis. The rate of growth is a presumed indicator of malignant potential. The likelihood of progression from the time of diagnosis to the time when tumor growth warrants treatment still remains unclear. Some ophthalmologists admit observation to initiate the earlier therapeutic interventions (Augsburger 1993, Robertson et al. 1999, Shields et al. 2002a, Shields et al. 2000).

The treatment options to destroy the tumors depends on site of origin (choroid, ciliary body, or iris), size and location of the lesion, age of the patient, occurrence of extraocular invasion, recurrence, or metastasis. The treatment regimens includes enucleation, pre-enucleation external beam radiation therapy (EBRT), Transcleral local resection, surgical resection of metastasis, plaque therapy or brachytherapy and transpupillary thermotherapy (TTT).

1.3.6.2. Enucleation

The removal of eyeball is the standard treatment for UM especially in the management of large sized tumors. However, this has been largely replaced by radiation therapy (i.e., brachytherapy with radioactive plaques; or external-beam, charged-particle radiation therapy) in order to spare the diseased eye (De Potter et al. 1996, Zimmerman et al. 1980).

1.3.6.3. Plaque therapy

Here, a localized radiation called plaque therapy is used to destroy the tumor cells of small or medium sized melanomas. It consists of a small gold cover or shield with radioactive pellets inserted inside a plastic carrier. The plaque is sutured to the wall of the sclera beneath the base of the tumor. After the completion of the therapy, the

plaque is removed surgically usually after four days. Plaque therapy is generally safe and effective. The advantage of this therapy is the gold cover, which prevents radiation from escaping and affecting the tissues surrounding the eye (the orbit) or brain. Disadvantage of this therapy is that, it can cause damage to sensitive ocular tissues, such as the optic nerve and the macula (Diener-West et al. 2001)

1.3.6.4. Transpupillary thermotherapy

This therapy is used to treat small (less than 3 mm in height), pigmented melanomas that are located in the back of the eye. Here, heat (hyperthermia) is used to destroy the tumor cells. Disadvantage of this therapy is that it results in a high rate of local recurrence and it is ineffective in destroying tumor cells within the sclera, the white wall of the eye. It has resulted in mild to severe visual loss in the treated eye due to the intensity of the laser burns (Char et al. 2002).

1.3.6.5. Metastasis

The prognosis for any patient with recurring or relapsing disease is poor, regardless of cell type or stage. The question and selection of further treatment depends on many factors, including the extent of the lesion, age and health of the patient, prior treatment, and site of recurrence, as well as individual patient considerations. Surgical resection of metastases diagnosed subsequent to initial management of ocular melanoma has been reported. The extent, to which the occasional favorable outcomes are the result of strong selection factors, it still remains unclear. So this approach cannot be considered as standard (Hsueh et al. 2004).

1.3.7. Pointers for improvement in clinical management of RB and UM

Current treatment strategies contributes significantly to vision salvage in patients harboring intraocular disease, and overall survival rates in patients with extra ocular disease. However, therapies such as chemotherapy, brachytherapy, and plaque therapy do result in with significant morbidity. A better understanding of patho-biology of retinoblastoma and uveal melanoma may lead to better outcome in therapies with less

long-term morbidity and may prevent the onset of the secondary cancers. Emphasis is placed on the development of animal models, which may lead to new insights into the development of this disease and opening new avenues for targeted therapies that may lead to high cure rates with minimal toxicities. In this line, a recent study with preclinical models suggested MDMX–p53 interaction as a potential target for chemotherapy in retinoblastoma, which can be efficiently antagonized by nutlin-3 resulting in the death of retinoblastoma cells. Thus local delivery of nutlin-3 is considered as a potential option to treat retinoblastoma (Elison et al. 2006, Laurie et al. 2006).

CHAPTER 2: REVIEW OF LITERATURE

2. Molecular initiation and progression of ocular cancer

Hanahan et al has proposed a review on the acquisition of six hall mark traits which transforms the normal cells to malignant tumor cells such as self-sufficiency in growth signals, insensitivity to antigrowth signals and self-renewal, evasion of apoptosis, limitless replication potential, angiogenesis, invasion and metastasis (Hanahan and Weinberg 2000). Identification of microRNAs (miRNAs) , a new class of small non-protein-coding RNAs that regulate gene expression post-transcriptionally by interacting to various mRNA targets suggests that these molecules could act as molecular switches in the extensive regulatory networks that involves thousands of transcripts (mRNA) (Sotiropoulou et al. 2009).

At present, ongoing studies using higher resolution genomic technologies such as Single Nucleotide Polymorphism (SNP), Next Generation Sequencing (NGS), Epigenetics, miRNA profiling, gene expression studies, have aided to explore the molecular interactions of pathogenic pathways, in turn widening the opportunities for targeted therapies. Integration of the networks from different approaches will facilitate in better understanding of cancer, for example though RB1 loss is the primary genetic alteration involved in the RB tumor initiation, yet other genetic, genomic, epigenetic and gene expression events are involved in the RB tumor progression. In addition, functional evaluation, compilation of multiple data sources in both *in vivo* (animal model) and *in vitro* (cell line model) are of utmost importance.

The discovery of new molecular targets would lead to the concept of individualized medicine, reveal refined information on disease severity, better understanding of molecular patho-physiology assessment of responses to treatments. This, in turn

provides us the prospective validation of the emerging candidate molecules enabling for the better therapeutic strategies and improved prognosis in disease management.

As the focus of this thesis is about the identification of the target molecules in the clinical management of retinoblastoma and uveal melanoma, this chapter will summarize the earlier reports on identification of the genes (mRNA), microRNAs (miRNAs) in these tumors and in other cancers.

2.1. Gene expression studies in Retinoblastoma

A comparative microarray analysis between 10 retinoblastomas and 3 adult retina samples carried out by Chakraborty et al revealed deregulated genes, functionally involved in insulin and Janus Kinase/ Signal Transducer and Activator of Transcription (JAK/STAT) signalling pathways, axon guidance, extracellular matrix-receptor interactions, proteasome, sugar metabolism, ribosomes, cell adhesion molecules and tight junction complexes. Further, on validation of the insulin signalling pathway genes (*PIK3CA, AKT1, FRAP1 and RPS6KB1*) using semiquantitative reverse transcription (RT)-PCR confirmed the significant up-regulation of insulin signalling pathway genes in tumours compared with normal tissues. These results suggested the dysregulation of phosphoinositide-3-kinase/Akt/ mammalian Target of Rapamycin/ribosomal S6 kinase 1 (*PI3K/AKT/mTOR/S6K1*) signalling pathway in retinoblastoma. The study also revealed upregulation of other genes namely CDC25A, a cell cycle progression gene, and ERBB3, involved in cancer development and progression (Chakraborty et al. 2007) Down regulation of LATS2 , a serine-threonine kinase and tumour suppressor, and CHFR , a mitotic checkpoint pathway gene were observed in retinoblastomas.

Though the study was informative in reporting the dys-regulated pathways, there do exist some regional bias of gene expression in the study. The study has highlighted on up-regulated genes, mapping to chromosome 16 and 17 and the down-regulated clusters mapping to chromosome 1. However, the earlier cluster of genes namely

KIF14, MDM4, CDH11 and others are not indicated in the study (Corson and Gallie 2007). Small sample size and normal adult retina as the control could contribute to this bias.

In yet another study by Ganguly et al. (2010), microarray gene expression analysis was compared between six RB tumor tissues and matched normal retina. In this study, an up-regulation of 1116 genes, and down-regulation 837 genes with functional groups including cell cycle regulation, cell death, DNA replication, recombination and repair, cellular growth and proliferation, and cellular assembly and organization were reported. The study reported the DNA damage response pathway genes, breast cancer-associated genes *BRCA1* and *2*, *AHR* and *ATM* signalling genes, and G2 /M DNA damage checkpoint regulation genes, polo-like kinase 1, E2F s, and checkpoint kinase 1 as the most differentially expressed genes. The study implicated the targeting therapy in identified kinases. In addition, reporting of elevated cone cell-specific markers in retinoblastoma's in this study supported the earlier report of a cone progenitor cell of origin for retinoblastoma (Ganguly and Shields 2010, Xu X. L. et al. 2009).

2.3. microRNAs

MicroRNAs (miRNAs) are small, non- protein-coding RNAs, 18-22 nucleotides (nt) in length that regulate gene expression either at post-transcriptional level or at translational inhibition level. It has been estimated that miRNAs regulate ~30% of human genes (Bartel 2004) Interestingly, most of the known miRNAs reside either inside or close to fragile sites and in minimal regions of loss of heterozygosity, minimal regions of amplifications, and common breakpoints associated with cancer (Calin et al. 2004). For example, the *miR-17-92* cluster is located at 13q31, a region commonly amplified in lymphomas (Ota et al. 2004). *miR-143 and miR-145* are located at 5q33, which is frequently deleted in myelodysplastic syndromes (Calin et al. 2004).

Genomic deletion, mutation, epigenetic silencing, and/or miRNA processing alterations are the mechanisms resulting in loss of function of a miRNA. Based on their function they can be termed as oncogenes (oncomirs) or tumor suppressors depending on the tissue and the expression of their targets. For example: *miR-17~92* cluster acts as oncomir promoting the cancer development by negatively regulating the tumor suppressors and genes (*E2F1, Bim, PTEN*) that control cell proliferation and promote apoptosis. miRNAs with a tumor suppressor function frequently have more than one genomic locus. Let-7 family acts as tumor suppressor miRNAs, where its suppression promotes expression of oncogenes (*RAS, c-myc, HMGA2*) that promote cancerous cell growth. Elucidation of mechanism involved in miRNA biogenesis, where they are subjected to intense transcriptional and post-transcriptional regulation has improved the current research on miRNA deregulation and their expression profiles may become candidate genes as surveillance markers and therapeutic targets. In addition, miRNAs might be powerful tool institute new individualized adjuvant treatment strategies in high-risk patients.

2.4. miRNA profiling in Retinoblastoma

Corson et al. (2007) reported the list of deregulated miRNAs for the first time in RB tumors using microarray analysis. In this study, they revealed a substantial down-regulation of *let-7b let-7c, miR-24, miR-125b, miR-191, miR-181a and miR-423* in three RB tumours compared with normal retina. Further, on validation on larger sample size, this group confirmed the down-regulation of let-7b and subsequent up-regulation of its putative target genes *CDC25A* and *BCL7A* (Huang et al. 2007). This study was corroborated with another report by where let-7 family was elevated in retinal tissues, with significant decrease in 39% of primary tumors under study (Huang et al. 2007). There exists a well documentation of *let-7* inverse association with its putative target *HMGA2*. However, this inverse association between lowered let-7 expression and of high mobility group proteins *HMGA1* and *HMGA2* was confirmed by in RB tumor (Reis A. H. et al. 2012a).

Subsequent studies by Zhao et al, Li et al and Martin et al has reported a list of deregulated miRNAs in RB primary tumors (Li B. Q. et al. 2012a, Martin et al. 2013, Zhao J. J. et al. 2009). Conkrite et al has demonstrated that the *miR-17~ 92* cluster, one of the first 'oncomiR' clusters is a potential therapeutic target in retinoblastoma (Conkrite et al. 2011). Further, the role miRNAs in RB tumor progression, proliferation and cell adhesion are well studied using RB cell lines by Dalgard et al, Nittner et al and Jo et al (Dalgard et al. 2009, Jo et al. 2011, Nittner et al. 2012). Madhu et al, has reported total of 33 miRNAs, including 25 upregulated and 8 downregulated miRNAs in both of 14 late stage serum and retinoblastoma tumours. On validation in 20 more RB samples, the authors have revealed five miRNAs, three upregulated (*miR-17, miR-18a and miR-20a*) and two downregulated (*miR-19b and miR-92a-1*) (Beta et al. 2013). All these results provides us the list of exciting candidate miRNAs (tabulated below) **[Table 2.1]** and pave the way for development into predictive biomarkers and for other studies in the identification of therapeutic targets for retinoblastoma management.

Table 2.1: Emerging gene targets in RB. The gene targets are derived from the gene expression analysis using microarray. Modified table from Genomic landscape of retinoblastoma, Clinical and Experimental Ophthalmology 2014; 42: 33–52 (Theriault et al. 2014).

Gene description	Gene symbol	Level of expression	Primary tumors studied (#) and Reference
Phosphatidylinositol-4,5- bisphosphate 3-kinase, catalytic subunit alpha	*PI3KCA*	Up-regulated	Primary tumors n= 10; chakraborty et al, 2007
v-akt murine thymoma viral oncogene homologue 1	*AKT1*	Up-regulated	
FK506-binding protein 12-rapamycin associated protein	*FRAP1*	Up-regulated	
Ribosomal protein S6 kinase, 70 kDa, polypeptide 1	*RPS6KB1*	Up-regulated	
Cell division cycle 25 homologue A	*CDC25A*	Up-regulated	
v-erb-b2 erythroblastic leukemia viral oncogene homologue 3	*ERBB3*	Up-regulated	
LATS, large tumour suppressor, homologue 2	*LATS2*	Down-regulated	
Checkpoint with forkhead and ring finger domains, E3 ubiquitin protein ligase	*CHFR*	Down-regulated	
Breast cancer 1, early onset, Breast cancer 2, early onset	*BRCA1, BRCA2*	Differential gene expression between tumor and normal	Primary tumor tissues n=6; Ganguly et al, 2010
Aryl hydrocarbon receptor	*AHR*		
Ataxia telangiectasia mutated	*ATM*		
Polo-like kinase	*PLK*		
E2F transcription factor	*E2F*		
Checkpoint kinase 1	*CHK1*		

Table 2.2: Differentially expressed miRNAs in RB. Modified table from Genomic landscape of retinoblastoma, Clinical and Experimental Ophthalmology 2014; 42: 33–52 (Theriault et al. 2014).

miRNAs	Expression in tumors	Method	Samples (#)	Reference
let-7b, let-7c, miR-24, miR-125b, miR-191, miR-181a, miR-423	DR	Microarray, qRT-PCR	3	(Huang et al. 2007)
let-7 family	DR	RT-PCR	44	(Mu et al. 2010)
miR-494, let-7e, miR-513-1, miR-513-2, miR-518c, miR-129-1, miR- 129-2, miR-198, miR-492, miR-498, miR-320, miR-503, miR-373	UR	Microarray	9	(Zhao J. J. et al. 2009)
miR-34a	V	qRT-PCR	2(plus 2 cell lines)	(Dalgard et al. 2009)
miR-17~92 and miR-106b~25 (paralog), let-7a, let-7f, miR-2, miR-7, miR-9, miR-16, miR-17a, miR-20a, miR-25, miR-26a, miR-30b, miR- 30d, miR-92a, miR-93a, miR-96, miR-99b, miR-101, miR-103, miR- 106b, miR-124, miR-143, miR-148b, miR-181a, miR-183, miR-216a, miR-217, miR-378, miR-1246	UR	Microarray	32	(Conkrite et al. 2011)
let-7a, let-7b, let-7c, miR-10a, miR-10b, miR-20a, miR-21, miR-28, miR- 29b, miR 30a-3p, miR-30b, miR-30c, miR-30d, miR-99a, miR-99b, miR-100, miR-103, miR-107, miR-124a, miR-125a, miR-125b, miR- 133a, miR-136, miR-141, miR-145, miR-146a, miR-155, miR-181a, miR-181b, miR-182, miR-183, miR-190, miR-191, miR-206, miR-210, miR-222, miR-301, miR-302a, miR-302b, miR-320, miR-330, miR- 335, miR-342, miR-368, miR-373, miR-380-5p, miR-382, miR-423, miR-433, miR-451, miR-452, miR-491	D	Computational	NA	(Li B. Q. et al. 2012a)
miR-129-3p, miR-382, miR-504, miR-22, miR-874, miR-139-3p, miR- 758, miR-655, miR-129-5p, miR-200a, miR-370, miR-485-5p, miR- 193a-5p, miR-330-5p, miR-429, miR-889, miR-499-5p, miR-342-5p, miR-448, miR-200b, miR-196b, miR-518f, miR-34c	DR	Microarray	12	(Martin et al. 2013)

miR-138, miR-155, miR-106b, miR-216a, miR-217, miR-20b, miR-17, miR-106a, miR-25, miR-652, miR-301b, miR-886-5p, miR-93, miR-34a, miR-18a, miR-449a, miR-449b, miR-224	UR	Microarray		
miR-1305, miR-424, miR-532-3p, miR-663b, miR-633, miR-194, miR- 299-3p, miR-142-5p, miR-144, miR-93, miR-545, miR-374a, miR- 374b, miR-665, miR-146b-5p, miR-194, miR-892b, miR-32, miR-501-5p, miR-513c, miR-513b	UR	Microarray	14 serum samples	(Beta et al. 2013)
let-7a, let-7d, let-7c, let-7f, miR-98, miR-let-7b, miR-1254, let-7e, miR- 122, miR-221, miR-1299, miR-198-2, miR-486-3p, miR-375, miR- 1260, miR-1287, miR-720, miR-124, miR-133a, miR-379, miR-129, miR-328, miR-335, miR-1228	DR	Microarray		
miR-199a-3p, miR-99a, miR-125b, miR-214, miR-10b, miR-29b, miR- 100, miR-224, miR-505, miR-29a, miR-363, miR-10a, miR-137, let-7c, miR-193a-3p, miR-374a, miR-130a, miR-29c, miR-335, miR-181a, miR-28-5p, miR-376a	UR	Microarray	SNUOT-Rb1cellline	(Jo et al. 2011)
miR-124, miR-142-3p, miR-34a, miR-135b, miR-96, miR-142-5p, miR- 183, miR-338-3p, miR-193b, let-7i, miR-182, miR-149, miR-let-7g, miR-34c-5p, miR-132, miR-34b	UR	Microarray	Y79 cell line	

DR: Down-regulated; UR: Up-regulated; V: Variable; D: differentially expressed.

Table 2.3: List of validated miRNAs / gene targets. Modified table from Genomic landscape of retinoblastoma, Clinical and Experimental Ophthalmology 2014; 42: 33–52 (Theriault et al. 2014).

miRNAs	Expression in tumors	Target genes	Target gene expression	Samples studied and Reference
let-7b	DR	*CDC25A, BCL7A*	UR	2 RB tumour tissues,(Huang et al. 2007)
let-7 family	DR	*HMGA1, HMGA2*	UR	44 RB tumor tissues (Mu et al. 2010)
miR-34a	V	*CCND1, CCNE2, CDK4, E2F3, EMP1, MDMX, SIRT1, MLLT3, SLC30A3, CNTN2, PLCG1, ACTR1A, CDC25A, EFNB1, KCNH2*	DR to miR-34a induction	2 of each Rb tumor tissues and cell lines (Dalgard et al. 2009)
miR-17~92 and miR-106b~25	UR	*CDKN1A (p21Cip1)*	DR to *miR-17~92* inhibition	32 RB tumor tissues, (Conkrite et al. 2011)
miR-129-3p, 5p, miR382,miR-504, miR-22	DR	*CDK4 and CDK6 (miR- 129); MYC (miR-382); TP53 (miR-504); HDAC4 and MYCP (miR-22)*	NA	12 RB tumor tissues, 2 cell lines and mouse tumor tissues, (Martin et al. 2013)
miR-17, miR-18a,miR-20a	UR	Via consensus regulatory network analysis: *PCNA, CDKN25A*	NA	20 serum samples (Beta et al. 2013)
miR-19b,miR-2a	DR	*CDC25A, KIF15, ERBB, BAX, RAF1, MAP3K5*		

DR: Down-regulated; UR: Up-regulated; V: Variable; D: differentially expressed, NA: Not applicable

2.5. Gene expression in uveal melanoma

UM is divided in to two classes of tumors, class 1 / class 2 based on a validated multigene clinical prognostic assay included in the TNM classification system. Initially, UM was classified into two prognostically significant molecular subtypes as class 1 signature (low risk tumors), class 2 signature (high risk tumors) based on the gene expression profiling of the primary tumors that can exactly identify the patients at high risk of metastasis. Later, a robust, clinically practical, PCR-based 15- gene assay comprising 12 discriminating genes (*HTR2B, GNAQ, ID2, MTUS1, ECM1, ROBO1, SATB1, LTA4H, EIF1B, RAB31, FXR1, LMCD1*) and three endogenous control genes were discovered by onken et al. (2010). This intervention has led to the development of a practical and clinically feasible platform for analyzing the expression profile, which pre-determines high-risk patients through intensified metastatic surveillance, and their earlier intervention for metastasis.

2.6. Gene mutations in UM

The widely mutated genes that are reported in UM are *GNAQ* or *GNA11* and *BAP1*. Onsets of *GNAQ* mutations are reported during early period of UM and they are detected in 22% of metastatic UM. *GNA11* mutations are detected in 57% of metastatic UM. *GNAQ* and *GNA11* encode a heterotrimeric GTP-binding protein α-subunit (Gαq and G α11) that couples G-protein-coupled receptor signaling to the MAPK pathway. Thus, mutations in *GNAQ* or *GNA11* result in constitutive activation of MAPK pathway. Clinical and Experimental Ophthalmology 2014; 42: 33–52 (Theriault et al. 2014).

Another somatic mutation in tumor suppressor gene *BAP1* (BRCA1 associated protein-1), located on chromosome 3p21.1 has been detected in 84% of class 2 uveal melanomas and rarely (1/26) in class 1 tumors. Further, the knockdown of *BAP1* in cultured class 1 cells has resulted in the shift towards class 2 gene expression signature has been reported. This result suggests that *BAP1* loss is linked to metastatic

phenotype. Further, this study has also suggested that *BAP1* germ-line mutation can predispose to uveal melanoma. There is no correlation between GNAQ and BAP1 mutations, however future studies focusing on both genetic mutations could aid us to understand the possible synergistic therapeutic effects in UM management (Harbour et al. 2010).

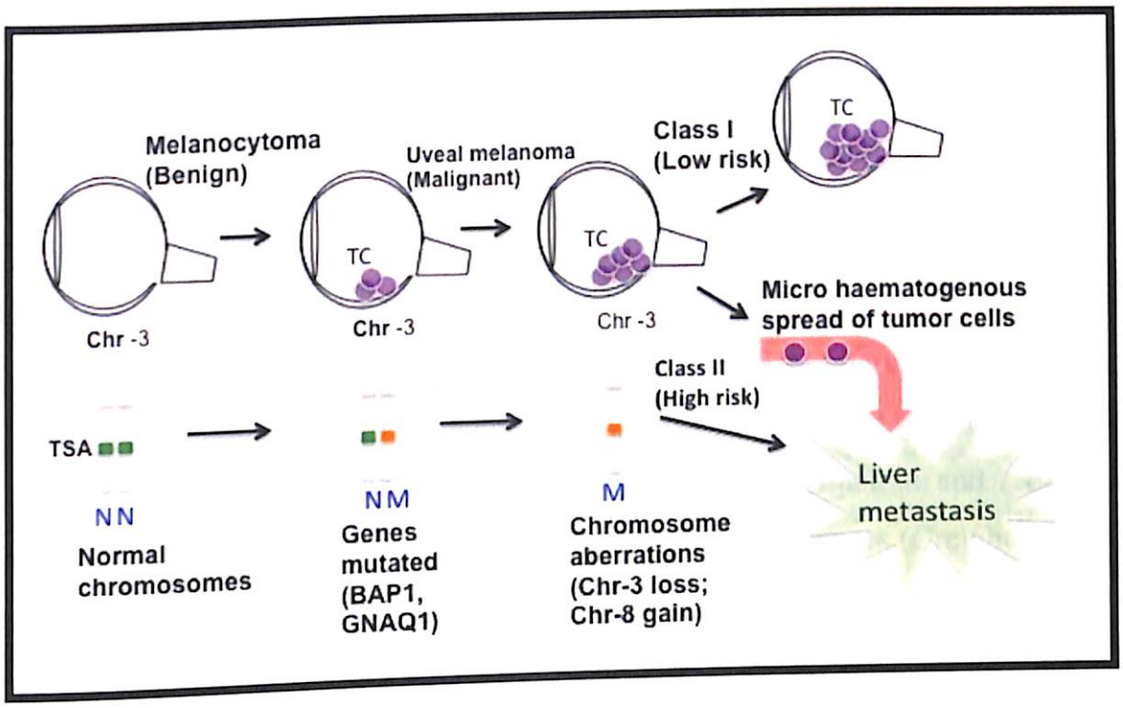

Figure 2.1: Stages of UM. Schematic representation of different stages in uveal melanoma. UM intiates with the gene mutation of tumor suppressor genes (eg: BAP1, GNAQ1) and chromosomal deletion (Chr-3) and/or amplification (Chr-8). These molecular changes results in class I UM (low risk, no metastasis) and class II UM (high risk, liver metastasis). TSA: tumor suppressor genes; M: mutant chromosome; N: Normal chromosome; Chr: chromosome; TC: tumor cells.

2.7. Dys-regulated miRNAs in Uveal melanoma

Lori et al. (2008), generated a genome-wide, microarray based approach in fresh primary UM tumors to screen for differentially expressed miRNAs in predicting metastatic risk. By using unsupervised data analysis (Principal Component Analysis) and Significant Analysis of Microarray (SAM) they reported a list of six miRNAs (*let-7b, miR-143, miR-199a, miR-199a*, miR-214, miR-143*) that were differentially expressed in two groups that corresponded to the gene expression-based subtypes: class 1 (low metastatic risk) and class 2 (high metastatic risk). Among these 6

miRNAs, the major discriminators between the two groups were *let-7b* and *miR-199a* with 100% of accuracy and specificity (Worley et al. 2008).

2.8. miRNAs – mRNA target prediction

Target mRNAs are regulated by miRNAs and so the prediction of targets becomes crucial to understand the role of miRNAs in cancer progression. As there exist an imperfect complementarities and other factors that affect site accessibility, target mRNA prediction becomes challenging (John et al. 2006). The putative target gene can be screened by using sequence-matching algorithms, namely TargetScan (Lewis et al. 2003), miRanda (John et al. 2004), RNA-hybrid (Rehmsmeier et al. 2004), PicTar (Krek et al. 2005), and DIANA-micro T (Maragkakis et al. 2009). Recently established versions such as next generation target prediction and miR databases provides additional features such as sequence conservation and gene ontology (Nam et al. 2008, Roubelakis et al. 2009). However, the experimental and / or functional approaches become mandatory to identify an actual miR targets (Creighton et al. 2008, John et al. 2006). These approaches includes over-expressing or down-regulating specific miRNAs in *in vitro* models (cultured cells) and examining the effects on mRNA and/or protein levels using gene expression studies (microarray, qRT-PCR) or proteomics approaches.

2.9. Summary and leads for molecular research in RB and UM

It is clear from this chapter that the pathogenesis of RB and UM involves general molecular pathways. While some leads are available, there is scope for thorough investigation of several genes and miRNAs that contribute to cancer pathogenesis and control. Thus, in continuation with the discussion in earlier chapter 1.0; section 1.3.7, a better understanding of the patho-biology of retinoblastoma and uveal melanoma is emphasized to explore new prognostic and therapeutic targets in the disease management.

CHAPTER 3: AIM AND OBJECTIVES

The **scope of the study** is to explore the target molecules involved in the patho-biology of intraocular tumors: Retinoblastoma and Uveal melanoma. This report offers the mechanistic insights that widen the application of gene therapy in the clinical management of these tumors.

The **main aim of the study** is to elucidate the regulatory molecular mechanisms and their molecular networks contributing to tumorigenesis and cancer progression in

A. Retinoblastoma, and

B. Uveal melanoma

In order to pursue this aim, the following **objectives** were carried out in this study

A. Retinoblastoma

1. To explore High Mobility Group (HMG) A2 molecule as a potential candidate for gene silencing therapy in RB.

   1.1. To study the expression of an oncogene: High Mobility Group (HMG) A2 in retinoblastoma primary tumors, retinoblastoma cell lines (Y79 and Weri Rb1) and to correlate its expression with the clinico-pathological features of RB.

   1.2. To study the molecular regulatory changes induced by *HMGA2* silencing (using RNAi) in RB cancer cells (Y79 and Weri Rb1), offering mechanistic insights on its anti- cancer potential.

1.3. To study the regulatory involvement of miRNAs at genome-level of molecular dys-regulation in *HMGA2*-silenced RB cells, using integrated miRNA-mRNA network analysis.

1.4. To delineate regulatory molecules through functional obstruction of *HMGA2* protein (using aptamers) contributing to the cell cycle arrest and apoptosis in RB cancer cells (Y79 and Weri Rb1).

2. To study the role of molecular chaperones (heat shock proteins), their association with pro-apoptotic protein survivin in advanced RB. This was studied through inhibition of the physical interaction between these molecules using synthetic peptides (Sherperdin), with therapeutic implication in RB.

3. To elucidate miRNAs regulating major candidate genes in RB: An *in silico* analysis along with experimental validation

4. To gain molecular insights on post-chemotherapy Retinoblastoma by microarray gene expression analysis.

B. Uveal melanoma

1. To identify the chromosomal aberrations - monosomy 3 in uveal melanoma, its association with the clinico-pathological features and metastasis

2. To identify miRNAs associated with the chromosomal aberrations - monosomy 3 in uveal melanoma, its association with the clinico-pathological features, and metastasis free survival. To evaluate genes regulated by candidate miRNAs reported from the above objective that may be the potential target molecules in uveal melanoma.

For better representation, the objectives are presented as a flow chart in the **Figure 3.1.**

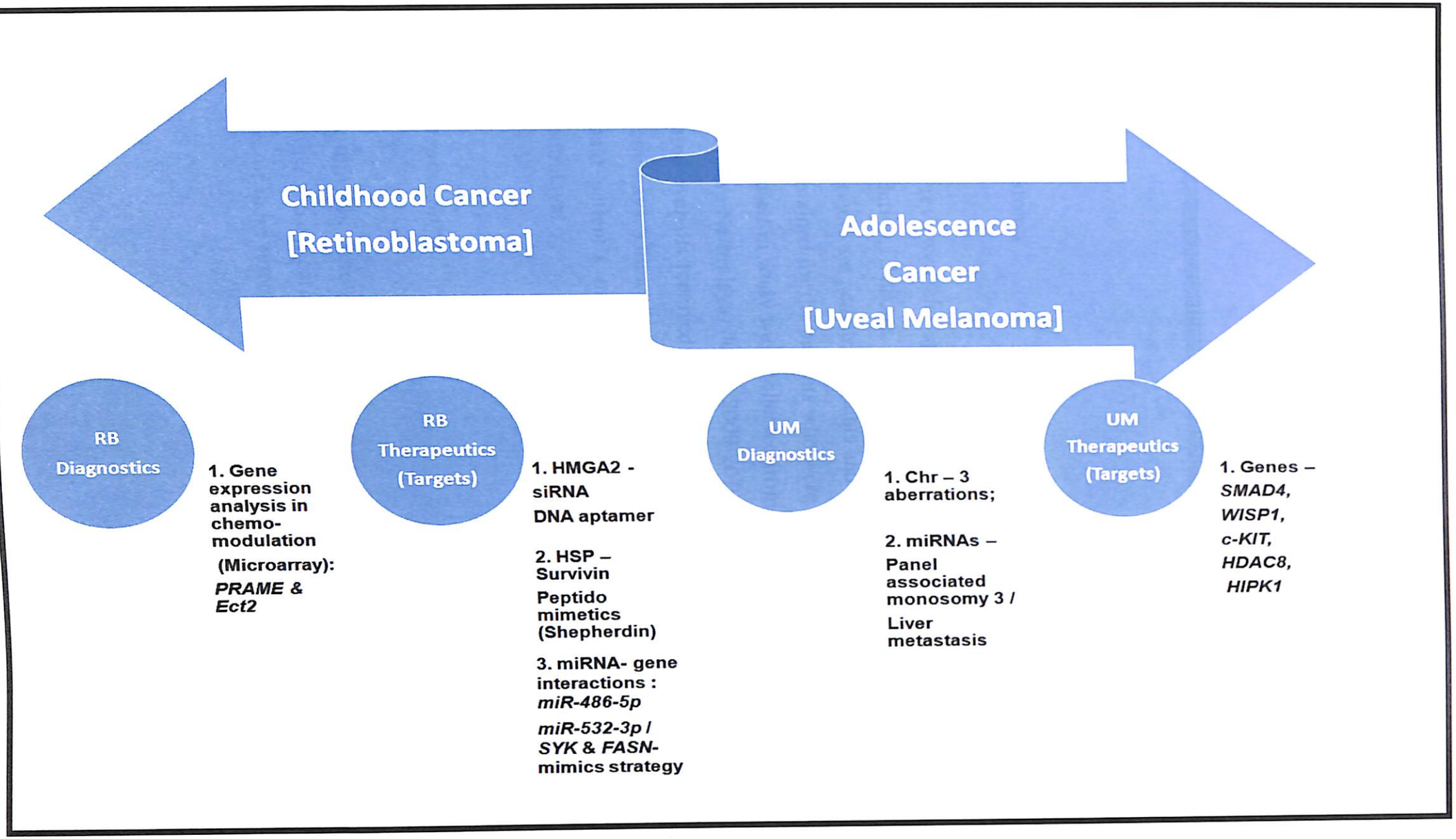

Figure 3.1: Flow chart of objectives

CHAPTER 4: MATERIALS AND METHODS

4. Materials

4.1. Retinoblastoma

The study was reviewed and approved by the institutional ethics committee of Vision Research Foundation, Sankara Nethralaya (Chennai, India). A consent signed by the guardians (as patients are pediatric patients and under the age of 18) for both diagnosis and research were obtained for the patients who were included in the study. Normal or control retinal samples used in study were collected from cadaveric eyeball (received at C.U Shah eye bank, Sankara Nethralaya) during 2009-2013.The tumour samples were collected from the enucleated eyeballs received at Larsen and Toubro Department of Ocular Pathology, Sankara Nethralaya. Clinico-pathological features of the RB tumors were referred from the individual patient's medical record maintained at Medical Research Foundation, Sankara Nethralaya.

4.1.1. Histopathology

All the RB tumours were grouped into A-E groups following International Intraocular Retinoblastoma Classification (IIRC) (Linn Murphree 2005). Haematoxylin and Eosin stained slides of these tumours were observed and classified as reported earlier (Sastre et al. 2009).

4.2. Uveal melanoma

4.2.1. Tumor collection

UM tumor samples (n=86) were collected from the enucleated eyeballs received at Ocular Pathology Laboratory, Medical Research Foundation, Sankara Nethralaya, during the year 2009 – 2013. The snap frozen fresh tumour tissues (n=10) were collected from the enucleated eyeballs received at Ocular Pathology Laboratory, Medical Research Foundation, Sankara Nethralaya, during the year 2011 – 2012. The control choroidal melanocytes (n=5) were collected from the human cadaveric eyeballs received at C.U.Shah Eye bank, Medical Research Foundation, Sankara Nethralaya.

4.2.2. Histopathology

Haematoxylin and Eosin slides were reviewed from 1-2 representative tumor tissue sections and the blocks were selected. All tumor sections were reviewed and examined for invasion of intra and extra-scleral extension, pigmentation and cell types (spindle cell, epitheliod, mixed cell type). The clinical parameters namely the age, sex, type of specimen (eye ball / exentration), follow-up history such as the hepatic secondaries was obtained from individual patient's medical record maintained at Medical Research Foundation, Sankara Nethralaya.

4.2.3. Cell lines

Human RB cell lines (Y79, ATCC, USA; Weri RB 1,Riken cell bank, Japan) cultured in RPMI 1640 medium (Rosewell Park Memorial Institute; Gibco-BRL, Rockville, MD) with 10% heat-inactivated fetal bovine serum (FBS, Gibco- BRL, Rockville, MD), 0.1% ciprofloxacin, 2 mM L-glutamine, 1 mM sodium pyruvate, and 4.5% dextrose (Sigma Aldrich, St. Louis, MD, USA) as supplements were used in the study. The cultures were grown as suspension at 37 °C with 5% CO_2. The human mueller retinal cell line (MIO-M1 derived from human neural cells of retina was a kind gift from G.A. Limb, UCL

Institute of Ophthalmology, London, England) cultured in DMEM (Dulbeccos Minimum Essential Medium) with 10% heat inactivated serum [FBS, Gibco- BRL (Rockville, MD)], 1X antibiotic solution (A-001A, Himedia, India) as supplements were used in the study as non-neoplastic cell line control.

4.3. Methods

4.3.1. Immunohistochemistry

Immunohistochemistry was performed on 4 mm thick formalin fixed, paraffin embedded sections mounted on (3-aminopropyl) triethoxy silane coated slides. After de-paraffinisation and rehydration, endogenous peroxidase activity was quenched by incubation in 3% H_2O_2 (10 minutes) at room temperature. Pre-treatment in a pressure cooker (20 minutes) using citrate buffer (0.1M citric acid and 0.1M trisodium citrate in distilled water, pH 6.0) was performed to unmask epitopes. Next, the sections were incubated in normal rabbit/mouse serum (1: 50 in 1% phosphate buffered saline), and then with the optimally diluted specific antibody. The details of the antibody used in the study are described in the table number 4.1. Bound peroxidase was developed with diaminobenzidine (DAB) /Amino ethyl carbazole (AEC) and hydrogen peroxide and counterstained with haematoxylin.

4.3.1.1. Immunoreactivity scoring

Two observers without knowledge of the clinical data, independently assessed the expression of protein. The distribution of protein expression was semi quantitatively assessed by estimating the percentage of positively stained cells. Randomly 10 tumor fields were scanned for protein expression under 40x magnification. The tumor cells expressing proteins were noted for each field. Then the average of protein expression was calculated from the 10 values for the entire slide and expressed as percentage of positivity. Depending on the percentage of positive cells, 4 categories were established: 0, negative cells; 1+, positive cells in less than one third; 2+, positive cells in 33% to 67%; and 3+, positive cells in more than two thirds of total tumor cell population (Detre et al. 1995).

Table 4.1: Details of antibody. Details of antibodies namely catalogue number, species, dilution, and incubation time used in the Immunohistochemistry.

S.No	Antibody	Catalogue number	Species	Dilution in TBS	Duration of Incubation	Duration of Incubation of Link and Streptavidin-HRPand DAB
1.	HMGA2	SC-30223, Santacruz, Biotechnology, CA	Rabbit polyclonal	1:50	Overnight at 4°c	1.5 h each; DAB (1:50) for 5 mins
2.	HSP-90	4874, cell signalling technology, Danvers.	Rabbit polyclonal	1:100	Overnight at 4°c	1.5 h each; DAB (1:50) for 5 mins
3.	HSP-70	4872, cell signalling technology, Danvers.	Rabbit polyclonal	1:100	Overnight at 4°c	1.5 h each; DAB (1:50) for 5 mins
4.	Survivin	SC-17779, Santacruz, Biotechnology.	Mouse monoclonal	1:50	Overnight at 4°c	1.5 h each; DAB (1:50) for 5 mins
5.	PRAME	ab32185, ABCAM	Rabbit polyclonal	1:50	Overnight at 4°c	1.5 h each; DAB (1:50) for 5 mins
6.	HSP-27	AM171-10M, Biogenex, SanRamon, USA	Rabbit polyclonal	Pre-diluted	Overnight at 4°c	1.5 h each; AEC (1:5 in 0.1M sodium acetate buffer) for 30 mins

4.3.2. Western analysis

4.3.2.1. Protein lysate preparation for HMGA2 protein immunoanalysis

The RB cells (various experimental groups) / RB tumour tissues were treated with 5% perchloric acid. The proteins were precipitated with equal volumes of cold acetone at 20 °C overnight. The precipitate was collected and centrifuged at 20,000 × g for 15 min at 4 °C and washed with acetone at 4 °C. The dried proteins were dissolved directly in sample buffer (2% sodium dodecyl sulfate, 0.0625 M Tris-HCl (pH 6.8), 5 mM EDTA, and 10% glycerol). The protein was resolved by using 18% acrylamide gel. The separated proteins were electrophoretically transferred to the nitrocellulose membrane at 100 V for 1 h.

4.3.2.2. Total protein lysate preparation for proteins immunoanalysis

The total protein cell lysate of the RB cells (various experimental groups)/ RB tumour tissues was extracted using lysis buffer containing 50 mM Tris-HCl (pH 7.6), 5 mM EDTA, 150 mM sodium chloride, 0.1% phenylmethanesulfonyl fluoride (PMSF), and 250 ml of 1 mg/ml protease inhibitor cocktail on ice. A total protein of 50 µg was resolved on by using 12% sodium dodecyl sulfate–PAGE. The separated proteins were electrophoretically transferred to the nitrocellulose membrane at 100 V for 1 h.

The blots were incubated with specific primary antibody for a period of overnight at 4 °C followed by corresponding horseradish peroxidase-conjugated secondary antibody and incubated for 2 h. After intermittent washes with Tween Tris-buffered saline, the membranes were subjected to the chemiluminescence detection method (SuperSignal West Femto Maximum Sensitivity Substrate, Pierce, Rockford, USA). To derive the protein concentration in the individual samples, the intensity of the bands was measured densitometrically (Quantity One, version 4.7 software using GS-800 calibrated Densitometer, Bio-Rad, Gurgaon, India) and normalized with the respective histone/ β-actin expression.

4.3.3. Zymography

The RB cells (various experimental groups) were collected and washed thrice with phosphate buffer. To the washed cell pellet, 200 µl of 10 mg/ml phenylmethanesulfonyl fluoride (P7626; Sigma Aldrich, Florida, USA) and 10 µl of 1 mg/ml protease inhibitor cocktail (Sigma Aldrich) were added, and the samples were sonicated (VirSonicä Virtis, SP Industries Inc., Gardiner, NY) three times for 10 s each, on ice. The samples were then incubated in 4 °C for 15 min and centrifuged under cooling conditions (REMI C-24 Remi High Speed Cooling Centrifuge, Thane, India) at 2,655 × g for 5 min. The supernatant was collected, and the proteins were estimated with the Lowry's method. Ten-percent sodium dodecyl sulfate–PAGE gels incorporated with 1 mg gelatin (Merck Biochemicals, MSD, Pharmaceuticals Private Ltd, Gurgaon, India) was prepared. About 50 µg of each sample with equal volume of Native Loading Buffer (0.1 mg bromophenol blue, 2 ml glycerol, 2.5 ml 0.5 M Tris, pH 7.4) were loaded and run at 100 V for 90 min. The gels were re-natured

in Tris-HCl (pH 6.8) and washed thrice in 5.5 ml milli Q water for 15 min, left overnight in low salt collagenase buffer (LSCB) buffer (50 mM Tris, 0.2 M NaCl, 5 mM $CaCl_2$) for three changes of 30 min each in 2.5% Triton X-100, and then washed with milli Q water, 0.02% Brij 35, and 0.02% sodium azide (pH 7.6) at 37 °C. The gels were then stained with 0.5% Coomassie Blue (Sigma Aldrich, Florida, USA) for 90 min and destained in 10% acetic acid to reveal zones of digestion. The density of the bands were measured using Quantity One, version 4.7 software in GS 800 calibrated Densitometer (Bio Rad) (Hawkes et al. 2010).

4.3.4. Chromogenic in situ Hybridisation

A 4-5mm of Paraffin–embedded tissue sections were taken, baked at 60°C for 4 h for Insitu Hybridisation. The pre-treatment step includes: De-paraffinization using Xylene and Methanol; De-pigmentation using 3.0 % (vol/vol) hydrogen peroxide and 1.0% (wt/vol) disodium hydrogen phosphate, 18 hrs at room temperature (Heavily pigmented tumors) and 0.25% Potassium permanganate and 5% Oxalic acid (moderate pigmented tumors). Followed by de-pigmentation, the heat Pre-treatment using: Tris-EDTA buffer at 98°C for 15 mins, Enzyme digestion using 10 mins with Pepsin at 37°C and the slides were dehydrated using decreasing grades of methanol (100% to 20%). Then co - denaturation of probe and sample was performed at 95°C for 6minutes using a Gradient Insitu PCR thermal cycler. The hybridization was carried out for 18 h at 37°C. The stringent wash was givrn to the slides using saline sodium citrate (0.5 X) at Room temperature and at at 75-80°C for 5min. The slides were counter stained using haematoxylin and mounted using histomount. The slides were air dried for a maximum of 72 h and observed using bright field microscope (dots seen at 50X). The details of the probes used in the study are described in **table 4.3**.

Table 4.2: *Details of antibody. Details of catalogue number, dilution, incubation time of blocking, probing of primary and secondary antibody used in western analysis.*

S.No	Protein (Catalogue number of the antibody)	Blocking of non-specific sites	Primary Antibody (in 0.1% BSA)	HRP-tagged Secondary Antibody (in 0.01% BSA)	Detection System Enhanced Chemiluminescent (ECL)
1.	**HMGA2** (SC-30223, Santa cruz Biotechnology, CA)	5.0 % BSA for 1 h	1:500	1:1000	Supersignal west femto maximum sensitivity substrate: 3 mins
2.	**Histone** (SC-8030, Santa cruz Biotechnology, CA)	5.0 % BSA for 1 h	1:500	1:1000	Supersignal west femto maximum sensitivity substrate: 3 mins
3.	**HSP-90** (4874, cell signalling technology, Danvers, MA)	5.0 % BSA for 1 h	1:500	1:1000	Supersignal west femto maximum sensitivity substrate: 2 mins
4.	**HSP-70** (4872, cell signalling technology, Danvers, MA)	5.0 % BSA for 1 h	1:500	1:1000	Supersignal west femto maximum sensitivity substrate: 2 mins
5.	**Survivin** (SC-17779, Santa cruz Biotechnology, CA)	5.0 % BSA for 1 h	1:250	1:1000	Supersignal west femto maximum sensitivity substrate: 3 mins
6.	**p53** (SC-126, Santa cruz Biotechnology, CA)	5.0 % BSA for 1 h	1:500	1:1000	Supersignal west femto maximum sensitivity substrate: 3 mins
7.	**p21** (SC-6246, Santa cruz Biotechnology, CA)	5.0 % BSA for 1 h	1:500	1:1000	Supersignal west femto maximum sensitivity substrate: 5 mins
8.	**Bim** (SC-126, Santa cruz Biotechnology, CA,)	5.0 % BSA for 1 h	1:500	1:1000	Supersignal west femto maximum sensitivity substrate: 5 mins
9.	**SYK (ab 57465, abcam, UK)**	5.0 % BSA for 1 h	1:1000	1:2000	Supersignal west femto maximum sensitivity substrate: 5 mins
10.	**FASN** (610962, BD biosciences USA)	5.0 % BSA for 1 h	1:250	1:2000	
11.	**ß-actin** (A5316, Sigma Aldrich, USA)	5.0 % BSA for 1 h	1:3000	1:5000	Supersignal west femto maximum sensitivity substrate: 1 min

Table 4.3: Description of probes. Details of probes used in the in situ hybridization.

S.NO.	Probes
1	C-3: Centromeric probe – To detect monosomy in chromosome 3
2	C-18: Centromeric probe – To detect disomy in chromosome 18, acts as the control as no aneuploidy has been reported in chromosome 18

The probes were inherently specific eliminating ALU and LINE elements by *Subtraction Probe Technology* (Invitrogen, USA)

4.3.4.1. Immuno-scoring of hybridised spots

The scoring of cells were counted and assessed by chromosomal index (CI). The chromosomal index is the ratio between the number of hybridization spots and number of nuclei counted. The loss of chromosome is defined as CI< 3 SD from the mean of retina. The signal distribution is assessed by the percentage of nuclei with one hybridization site greater than 30% of nuclei counted. The hybridisation and scoring protocols were followed in the earlier study (Radhakrishnan et al. 2009).

4.3.5. Quantitative Real-Time polymerase chain Reaction

4.3.5.1. Total RNA extraction

4.3.5.1.1. TRIZOL method

To quantify the HMGA2 RNA expression in untreated and siRNA-treated RB (Y79, Weri Rb1) cells, and in tumor tissues, the total RNA was extracted with the guanidine isothiocyanate and chloroform method (TRI Reagent; Sigma Aldrich, Florida, USA). Cells were harvested from cultures and collected in RNase-free vials. To the pellet, 1 ml of TRIzol reagent (TRI Reagent) was added, vortexed vigorously for 2 min, and incubated at room temperature for 5 min. Later, 0.5 ml of chloroform was added to the solution and mixed well for 15 s and centrifuged. The aqueous layer that contains RNA was transferred to new vials. Then 0.5 ml of isopropanol was added and incubated at room temperature for

10 min. After centrifugation, the supernatant was discarded, and 0.5 ml of 75% ethanol was added, mixed well, and centrifuged. Then the supernatant was discarded. The pellet was air dried at room temperature for 2 min and reconstituted in 25 µl of RNase-free water. All centrifugations in the RNA extraction were performed at 15,000 × g for 10 min at 4 °C. All RNA samples were treated with TURBO DNase (Ambion, Genetix Biotech Asia Pvt. Ltd., Chennai, India).

4.3.5.1.2. Total RNA isolation: Fresh tissues

About 10 mg of tumour tissue was homogenised in 300µL of lysis solution using magnetic homogeniser. To the lysate, 600 µL of RNase-free water, 20 µL of reconstituted Proteinase K was added, vortexed, and incubated at 55°C for 15 minutes. The tubes are vortexed occasionally during incubation. The lysate was spinned for 1 minute at 14,000 x g. The supernatant was separated and 450 µL of ethanol was added. The mixture was transferred to the assembled RNA column and the column was washed with 400 µL of wash buffer. The columns are treated with DNAse [25 Kunits/ 100 µLin reaction buffer (140mM Tris pH 7.0, 10mM $MgCl_2$ and 3mM $CaCl_2$)]. The columns were washed with wash buffer, centrifuged at 14,000 rpm / 2 mins. Finally the RNA was eluted using 50 µL using RNAse free elution buffer. Using NanoDrop 1000 Spectrophotometer based on the absorbance at 260/280 assessed the quality and the quantity of the eluted RNA.

4.3.5.1.3. Total RNA isolation from Formalin fixed paraffin embedded tissues

(catalogue number: AM 1975, Ambion/RNA, Life technologies Van Allen Way, Carlsbad, California)

Formalin fixed Paraffin embedded, 5- 8 sections of 20 µm thickness were taken for the miRNA isolation. The sections are treated with xylene while vortexing and heated at 50°C for 3 mins to melt the paraffin. After discarding the xylene, 1ml of 100% ethanol wash was carried out twice and air-dried. Then, 200µL digestion buffer containing Protease was added and incubate at 50°C (15mins) /80°C (15 mins). The mixture was passed through a filter cartridge, 60 µl of DNAse was added to the catridge and incubated for 30 mins in room temperature. Followed by the DNAse treatment, 2 washes of the catridge were carried out using wash buffers. Finally the RNA was eluted in a new 1.5ml PCR vial.

Using NanoDrop 1000 Spectrophotometer assessed the quality and the quantity of the eluted RNA.

4.3.5.2. Complementary DNA (cDNA) synthesis

4.3.5.2.1. cDNA synthesis using Sensiscript II (Qiagen)

For all samples, 1 µg of total RNA was used to synthesize first-strand cDNA with reverse transcriptase (Sensiscript II; catalogue number 205211, Qiagen, Santa Clara,CA) using oligo dT as random primers. The reagents and the reaction volume used for the cDNA synthesis are as follows.

Table 4.4: Reagents for cDNA synthesis I. Details of the reagents including volume per reaction used for cDNA synthesis.

S.No	Reagents	Volume (µl)
1.	10X buffer RT	2.0
2.	dNTP mix (5mM each dNTP)	2.0
3.	Oligo dT primer (10µM)	2.0
4.	RNase inhibitor (10 units/ µl)	1.0
5.	Sensiscript Reverse Transcriptase (RTS)	1.0
6.	RNase free water	Adjusted to 20 µl
7.	Template RNA	500ng
8.	Total volume	20 µl

The reverse transcription was performed at 37 °C for 60 mins using thermalcycler (Eppendroff, Gradient).

4.3.5.2.2. cDNA for miRNA expression studies

4.3.5.2.2.1. Using Taqmann® MicroRNA Reverse Transcription kit (Part number: 4366596, Applied Biosystems, Bangalore, India).

The total RNA is converted into cDNA with specific microRNA primers procured with Taqmann® MicroRNA assays. The reagents used per reaction are described in table 4.6.

Table 4.5: Reagents for cDNA synthesis - II. Details of the reagents including volume per reaction used for cDNA synthesis.

S.No	Component	Master Mix Volume/15 µl reaction
1.	dNTP mix (100mM total)	0.15 µl
2.	Multiscribe ™ RT enzyme (50U/ µl)	1.00 µl
3.	10x RT buffer	1.5 µl
4.	RNase inhibitor (20U/ µl)	0.19 µl
5.	Nuclease free water	4.16 µl
6.	Total	7.00 µl

Each 15µl reaction consists of 7µl mastermix, 3 µl primers and 5 µl RNA sample.

The reverse transcription was carried out in the thermal cycler (Eppendroff, Gradient) as described in table 4.8.

Table 4.6: Protocol for cDNA synthesis. cDNA synthesis carried out in the thermal cycler (Eppendroff, Gradient).

No	Step type	Time (Minutes)	Temperature (°C)
	Hold	30	16
	Hold	30	42
	Hold	5	85
		A	4

5. Total volume
The reverse transcription was
(Eppendroff, Gradient)

New Delhi)

4.3.5.2

Table 4.5: Reagents for cDNA synthesis - II. Details of the reagents including volume per reaction used for cDNA synthesis.

S.No	Component	Master Mix Volume/15 µl reaction
1.	dNTP mix (100mM total)	0.15 µl
2.	Multiscribe ™ RT enzyme (50U/ µl)	1.00 µl
3.	10x RT buffer	1.5 µl
4.	RNase inhibitor (20U/ µl)	0.19 µl
5.	Nuclease free water	4.16 µl
6.	Total	7.00 µl

Each 15µl reaction consists of 7µl mastermix, 3 µl primers and 5 µl RNA sample.

The reverse transcription was carried out in the thermal cycler (Eppendroff, Gradient) as described in table 4.8.

Table 4.6: Protocol for cDNA synthesis. cDNA synthesis carried out in the thermal cycler (Eppendroff, Gradient).

S.No	Step type	Time (Minutes)	Temperature (°C)
1.	Hold	30	16
2.	Hold	30	42
3.	Hold	5	85
4.	Hold	A	4

4.3.5.2.3. Using Exiqon Universal cDNA synthesis kit (Exiqon, New Delhi)

To convert miRNA to cDNA, total RNA was diluted (1:80) and 25ng/µL was reverse transcribed using Exiqon Universal cDNA synthesis kit (Catalog number 203300, Exiqon, New Delhi).

Table 4.7: Details of cDNA synthesis III. Details of the reagents including volume per reaction used for cDNA synthesis.

S.No	Reagents	Volume (µL)
1.	5x Reaction buffer	4.0
2.	Nuclease-free water	6.0
3.	Enzyme mix	2.0
4.	Random RT primer	4.0
5.	Template total RNA (25ng/µl)	4.0

Each sample (20 µL) was incubated for 60 min at 42°C followed by heat inactivation of the reverse transcriptase for 5 min at 95°C, then stored at -20°C.

4.3.5.3. Real Time PCR amplification.

4.3.5.3.1. Taqmann® assays [Applied Biosystems (Bangalore, India)].

The final volume for each PCR was 20 µL including 1µL(100ng) of the investigated sample 1 x Universal PCR Master Mix (Taqman, ABI Applied Biosystem, Bangalore,India) for gene/miRNA expression and 1 µL of taqman probe. The expression of the gene/miRNA in each sample was analysed in triplicates.

Table 4.8: Details of taqmann assays (Gene expression). Details of the taqman assays used in the study of gene expression assays.

S.No	Gene name, catalogue number	Details
1.	HMGA2 (Hs00171569_m1)	NM_003483.4, Exon 1-2, Ampclicon size: 65
2.	Glyceraldehyde-3-phosphate dehydrogenase (GAPDH; Hs99999905_m1)	NM_002046.3, Exon 3,Amplicon size: 122

Table 4.9: Details of taqmann assays (miRNA expression). Details of the taqman assays used in the study of miRNA expression assays.

S.No	Assay ID	Name of miRNA	miRNA Sequence
1.	000459	*hsa-miR-134*	UGUGACUGGUUGACCAGAGGG
2.	000378	*hsa-let-7b*	UGAGGUAGUAGGUUGUGUGGUU
3.	000498	*hsa-miR-199a*	CCCAGUGUUCAGACUACCUGUUC
4.	000517	*hsa-miR-214*	ACAGCAGGCACAGACAGGCAG
5.	001097	*hsa-miR-146b*	UGAGAACUGAAUUCCAUAGGCU
6.	000466	*hsa-miR-143**	UGAGAUGAAGCACUGUAGCUCA
7.	002927	*hsa-miR-1238*	CUUCCUCGUCUGUCUGCCCC
8.	002164	*hsa-miR-149**	AGGGAGGGACGGGGGCUGUGC
9.	001093	*RU6* (endogenous control)	CGCAAGGAUGACACGCAAAUUCGUGAA GCGUUCCAUAUUUUU
10.	001006	*RNU48* (endogenous control)	GAUGACCCCAGGUAACUCUGAGUGUGU CGCUGAUGCCAUCACCGCAGCGCUCUG ACC

4.3.5.3.2. Real Time PCR assay of Universal RT^2 Real Time ™ SyBr Green/ROX PCR master Mix (Qiagen, SABiosciences, USA)

The final volume for each PCR was 20 µL including 1µL (100ng) of the investigated sample 1 x Universal RT^2 Real Time ™ SyBr Green/ROX PCR master Mix (Catalogue NO: 330520, SABiosciences, USA) was used.

The qRT-PCR for the gene/miRNA (menioned in table 4.8 and 4.9) expression using taqmann probes was performed as follows: 2 min at 50 °C, 10 min at 95 °C, and 40 cycles of 15 s at 95 °C, plus 1 min at 60 °C. Commercial software (SDS ver. 1.3; ABI) was used to calculate $^{\Delta\Delta Ct}$. Relative expression values for all these genes/ miRNA were normalized

to the GAPDH / 18s and RNU6B/ RNU48 as endogenous control. The value of each control sample was set at 1.0 fold change and was used to calculate the fold change in target genes and miRNA. The unit of fold change was expressed in log $_2$ transformed ratios.

Table 4.10: Reagents for qRT-PCR assay (Syber-green). Details of the reagents including volume per reaction used for Real-Time assay (qRT-PCR).

S.No	Reagents	Volume (µl)
1.	Mastermix (SyBr Green/ROX)	10.0
2.	Forward primer, 10 µM	0.5
3.	Reverse primer, 10 µM	0.5
4.	RNAse free water	8.0
5.	Template cDNA (100 ng)	1.0
6.	Total volume	20.0

Table 4.11: List of genes with primer sequences (Syber green assay). The gene name and primer sequences used in the gene expression study performed using syber green assay.

Gene name	Sense/ antisense : Sequences
ETS oncogene family (*ELK1*)	FP: 5'GAAGAATCACACCCTTGGAA3' RP: 5'GACAAAGGAATGGCTTCTCA 3'
G-2 and S-Phase expressed1 (*GTSE1*)	FP: 5'ACGTGAACATGGATGACCCTA3' RP: 3'GTTCGGGAACCGGATTATTTA5'
cyclin dependent kinase 6 (*CDK6*)	FP: 5'CTGAATGCTCTTGCTCCTTT3' RP: 5'AAAGTTTTGGTGGTCCTTGA3'
E2Ftranscriptionfactor4, p107/p130binding(*E2F4*)	FP: 5'GGGCAGAAGAAGTACCAGATTCA3' RP: 'GCTCCATGCCTCCTTGTTCA3'

Gene name	Sense/ antisense : Sequences
v – Crk sarcoma virus CT10 oncogenehomolog(avian) (CRK)transcript variant	FP: 5'CCGGGACAAGCCTGAAGAGC3' RP: 5'GGCCCACCCAGTGGCTGTGG3'
CDH1	FP: 5'TCGACACCCGATTCAAAGTGG3' RP: 5'TTCCAGAAACGGAGGCCTGAT3'
SNAIL homolog 1 (Drosophila) (*SNAI1*)	FP: 5'TATGCTGCCTTCCCAGGCTTG3' RP: 5'ATGTGCATCTTGAGGGCACCC3'
MMP 2	FP: 5'AGATCTTCTTCTTCAAGGACCGGTT 3'RP: 5'GGCTGGTCAGTGGCTTGGGGTA3'
MMP 9	FP: 5'GCGGAGATTGGGAACCAGCTGTA3' RP: 5'GACGCGCCTGTGTACACCCACA3'
TGF-β1	FP 5'CAAGGGCTACCATGCCAACT3' RP 5' CAGCAAGGTCCTGGCCCT3'
BAX	FP 5'TCCCCGAGAGGTCTTTT3' RP 5'CGGCCCCAGTTGAAGTTG3'
Bcl2	FP 5'ATGTGTGTGGAGAGCGTCAA3' RP 5'ACAGTTCCACAAAGGCATCC3'
PARP	FP 5'AAGGCGAATGCCAGCGTTAC3' RP 5'GGCACTCTTGGAGACCATGTCA3'
Caspase 3	FP 5'TGCGCTGCTCTGCCTTCT3' RP 5'CCATGGGTAGCAGCTCCTTC3'
SMAD4	FP 5'GTTCAGGTAGGAGAGACGTTTAAGGT3' RP 5'CCTTTACATTCCAACTGCACTCCT3'
c-KIT	FP 5'-CAG GCA ACG TTG ACT ATC AGT-3' RP 5'-ATT CTC AGA CTT GGG ATA ATC-3'
HIPK2	FP 5'GCCGAGAGCGGAGACACA3' RP 5'CTCAGCCTCAGTGGGAATCTG3'
WISP1	FP 5'-AGAGCCGC CTCTGCAACTT-3' RP 5'-GGAGAAGCCAAGCCCATCA-3'
HDAC8	FP 5'- TGGGCAGTCGCTGGT -3' RP 5'- GTGGCTGGGCAGTCATAA-3'
GAPDH	FP 5'AGAAGGCTGGGGCTCATTTG3' RP 5'AGGGGCCATCCACAGTCTTC3'

4.3.6. Whole genome cDNA analysis

The RNA samples (10 µg each) in a 50-µl reaction were treated with 1 µl of TURBO DNase (2 U) in 1× TURBO DNase buffer at 37 °C for 30 min. Followed by the incubation, the RNA sample was extracted with phenol/chloroform to inactivate TURBO DNase. Agilent's (Agilent Technologies Genotypic, Bangalore, India) Low RNA Input Linear Amplification Kit PLUS was used to generate fluorescent complementary RNA (cRNA). T7 RNA polymerase was used in this method, which simultaneously amplifies target material and incorporates cyanine 3-labeled cytidine tri- phosphate (CTP). Qiagen's RNeasy mini spin columns were used for purification of the amplified cRNA samples, and the samples were then hybridized to the Human Whole Genome 44K OliG0 Microarray for 17 h at 65°C, as recommended by the manufacturer (Agilent Technologies). Data analysis was done using Genespring GX version 10 (Agilent Technologies). Agilent Feature Extraction software (G25677AA; Agilent Technologies) was used to analyze the microarray data.

4.3.7. miRNA profiling

Three tumours each of monosomy 3 and disomy 3 was taken for expression studies using Human miRNA V3, 8x15k Agilent arrays. The study was carried out in technical duplicates. The small RNA was extracted from the formalin fixed tissues using miRVANA kit (Ambion, Life technologies,USA) following manufacturer's protocol. The quantity of RNA was measured by Nano Drop spectrophotometer and the quality of small RNA was assessed using Agilent 2100 bio analyzer. The extracted total RNA sample was diluted to 50ng/µl in nuclease free water. About 100ng of total RNA was dephosphorylated along with appropriate diluted spike in control; (Agilent Technologies, microRNA Spike-In Kit, Part Number 5190-1934) using Calf Intestinal Alkaline Phosphatase (CIP) master mix (Agilent Technologies, Part Number: 5190-0456) by incubating at 37°C for 30 minutes. Following the dephosphorylation, miRNA sample was denatured by adding Dimethyl Sulfoxide and heated at 100°C for 10 minutes and transferred to ice-water bath. The miRNA labelling was performed using miRNA Complete Labelling and Hyb Kit (Agilent Technologies, Part Number: 5190-0456). The Ligation master mix (Agilent Technologies, Part Number: 5190-0456) containing Cyanine

3-pCp was added to the denatured miRNA sample and incubated at 16°C for 2 h. The Cyanine 3-pCp labelled miRNA sample was dried completely in the vacuum concentrator (Eppendorf, Concentrator Plus, and catalog Number 5305000) at 45°C to 55°C for 2 h. The dried sample was resuspended in nuclease free water and mixed with Hybridization Mix containing blocking solution (Agilent Technologies, Part Number: 5190-0456) and Hi-RPM Hybridization Buffer (Agilent Technologies, Part Number: 5190-0456) and incubated at 100°C for 5 minutes followed by snap chill on ice for 5 minutes. The samples were hybridized on the Human_miRNA_version 3,8x15k array. The hybridization was carried out at 55°C for 20 h. After hybridization, the slides were washed using Gene expression wash buffer1 (Agilent Technologies, Part Number 5188-5325) at room temperature for 5 minutes and Gene expression wash buffer 2 (Agilent Technologies, Part Number 5188-5326) at 37°C for 5 minutes. The slides were then washed with acetonitrile for 30 seconds. The Microarray slide was scanned using Agilent Scanner (Agilent Technologies, Part Number G2565CA).

4.3.8. Cellular internalization of oligoes / peptides assay

The cellular uptake of the synthetic oligos (AT– rich, Mix sequences, peptides) was analysed using flow cytometry (BD FACS Calibur).

Table 4.12: Protocol of transfection of oligos and peptides. The synthetic oligos, peptido mimetics with the concentration and the time of incubation used for the *in vitro* study in the current dissertation.

S.No	Sequences	Concentrations	Time of Incubation (h)
1	HMGA2-aptamer: AT rich oligo (HS Number 29349920000) G*G*G*A*A*A*A*A*A*T*T*T*T*T*T*A*A*A*A*A*A*C*C*C	0.25, 0.5, 1.0, 1.5 µM	16, 24, 48,72
4	Mix – aptamer: mix sequence (HS Number 29349920000)	0.25, 0.5, 1.0, 1.5 µM	16, 24, 48, 72

	C*C*C*A*C*T*G*C*A*G*T*C*G*G*A*C*T*C*A*C*T*C*G*C		
5	Sherperidin peptide: Biotin-X-YGRKKRRQRRRKHSSGCAFL-CONH2	0.17, 0.25, 0.34, 0.42 µg/ml	4, 8, 16, 24 h of 5% serum supplement
6	Scrambled peptide: Biotin-X-YGRKKRRQRRRSKLACFSHG-CONH2	0.17, 0.25, 0.34, 0.42 µg/ml	4, 8, 16, 24 h of 5% serum supplement

'*'indicates phosphorothioate modification in ssDNA sequences

4.3.9. *In vitro* experiments

4.3.9.1. Transfection

About 1×50,000 cells were plated per well (12 well plates), and allowed to grow for 24–36 hrs (until they were 40% – 60% confluent) and incubated with 0.5 ml of antibiotic-free media containing optimum concentration of specific siRNAs/miRNAs/peptides plus the corresponding concentration of transfection reagent for 24 hrs, 48 hrs, and 72 hrs. 0.5 ml of complete RPMI 1640 medium containing 10% FBS was added after 4 h of transfection. After incubation, the cells were harvested and processed for further analysis. The same protocol was applied using non-target scrambled siRNA/miRNA/peptide as transfected control.

4.3.10. Estimation of Lactate Dehydrogenase (LDH)

The percentage of cellular cytotoxicity in the treated experimental groups was determined by estimating the level of LDH released into the culture medium. The cytopasmic stable enzyme, lactate dehydrogenase (LDH) present in all cells is rapidly released into the cell-culture supernatant when the plasma membrane is damaged. LDH activity is determined in a coupled enzymatic reaction, when the culture supernatant was incubated with the substrate mixture resulting in the reduction of tetrazolium salt INT to formazan. The water soluble formazan dye is measured at the maximum absorption 492nm.

Table 4.13: *Details of oligos and peptides used in transfection.* Gene name, RNA (siRNA, miRNA), peptido-mimetic sequence with its concentration and cell counts optimised for the *in vitro* transfection used in the current study.

Gene	**Catalogue number, company's name**	**siRNA / miRNA / Peptide**	**Concentration of siRNA/miRNA/ Peptide and the transfection reagent Lipofectamine ™ 2000 (Invitrogen) / Lipotransfect (Thermo scientific, Dharmacon) transfection reagent**
HMGA2: siRNA	Hs_HMGA2_6 (SI03029929),Qiagen	FW: 5′-CGG CCA AGA GGC AGA CCU ATT-3′ RW: 5′-UAG GUC UGC CUC UUG GCC GTT-3′	2,00,000 cells / well of 6 well plate, 200nM; 5.0µl of lipofectamine™ 2000 of transfection reagent.
	Hs_HMGA2_7 (SI03067393),Qiagen	FW: 5′-GCG GCG GCA GCC UAA GCA ATT-3′ RW: 5′-UUG CUU AGG CUG CCG CCG CTG-3′	
	HMGA2 siRNA.3 [1146–1164] (1,027,423),Qiagen	FW: 5′-CGC CAA CGU UCG AUU UCU-3′ RW: 5′-GCG GUU GCA AGC UAA AGA-3′	
	Scrambled siRNA(1,022,563), Qiagen	5'-AAT TCT CCG AAC GTG TCA CGT-3'	
DNA aptamer	(HS Number 29349920000)	HMGA2-aptamer: AT rich oligo (HS Number 29349920000) G*G*G*A*A*A*A*A*A*T*T*T*T*T*T*A*A*A*A*A*A*C*C*C	2,00,000 cells/well of 6 well plate at varying concentrations described above and the 6 µg of lipofectamine™ 2000 of transfection reagent
	(HS Number 29349920000)	mix-aptamer (HS Number 29349920000) C*C*C*A*C*T*G*C*A*G*T*C*G*G*A*C*T*C*A*C*T*C*G*C	
PRAME	PRAME cDNA (NM_206955.1), OriGene Technologies	pcDNA3.1 vector:	2,50,000 cells/well of 6 well plate, 2.0 µg plasmid DNA and 6.0µg of lipofectamine™ 2000 of transfection reagent

hsa-miR-106b,	IH-300649-07-0005, Thermo scientific, Dharmacon, Dharmacon, Lafayette, CO, USA	5'UAAAGUGCUGACAGUGCAGAU 3'	2,00,000 cells/well of 6 well plate, 50pM miRNA and 5.0µg of lipotransfect transfection reagent
hsa-miR-93	IH-300512-08-0005, Thermo scientific, Dharmacon	5'CAAAGUGCUGUUCGUGCAGGUAG3'	2,00,000 cells/well of 6 well plate, 50pM miRNA and 5.0µg of lipotransfect transfection reagent
hsa-miR-25	IH-300498-07-0005, Thermo scientific, Dharmacon, Dharmacon, Lafayette, CO, USA	5'CAUUGCACUUGUCUCGGUCUGA 3	2,00,000 cells/well of 6 well plate, 50pM miRNA and 5.0µg of lipotransfect transfection reagent transfection reagent
Scramble miRNA-(antagomir)	Thermo scientific, Dharmacon, Dharmacon, Lafayette, CO, USA	5'GCAACGAUGGUCCAACACCUCGGCC 3'	2,00,000 cells/well of 6 well plate, 50pM miRNA and 5.0µg of lipofectamine™ 2000 of transfection reagent
hsa-miR-486-5p	C-300746-03(Thermo scientific, Dharmacon)	MI0002470: UCCUGUACUGAGCUGCCCCGAG	2,00,000 cells/well of 6 well plate, 50pM miRNA and 5.0µg of lipofectamine™ 2000 of transfection reagent
hsa-miR-532-3p	C-301109-01(Thermo scientific, Dharmacon)	MI0003205: CCUCCCACACCCAAGGCUUGCA	2,00,000 cells/well of 6 well plate, 50pM miRNA and 5.0µg of lipofectamine™ 2000 of transfection reagent
Scrambled miRNA, (mimics	Thermoscientific, Dharmacon	MIMAT0000039: UCACAACCUCCUAGAAAGAGUAGA	2,00,000 cells/well of 6 well plate, 50pM miRNA and 5.0µg of lipofectamine™ 2000 of transfection reagent
Sherperidin peptide	USV synthesis	Biotin-X-YGRKKRRQRRRKHSSGCAFL-CONH2	0.17, 0.25, 0.34, 0.42 µg/ml
Scrambled peptide	USV synthesis	Biotin-X-YGRKKRRQRRRSKLACFSHG-CONH2	0.17, 0.25, 0.34, 0.42 µg/ml

LDH enzyme activity in the culture supernatant increases as the number of dead cells (or cells with damaged plasma membranes) increases.The increase in supernatant LDH activity directly correlates to the amount of formazan formed over time.

The cells were transfected with the DNA aptamers with the above-mentioned conditions. The experiments were carried out using RPMI 1640 as assay medium containing 1% BSA, sodium bicarbonate. After 16 hrs, 24 hrs, 48 hrs of incubation the culture supertanants was collected and proceeded for the estimation of LDH using cytotoxicity assay kit (product number: 04744926001, Roche).

Table 4.14: Protocol of Lactate Dehydrogenase assay. Protocol followed for the estimation of Lactate Dehydrogenase (LDH) in the cytotoxicity assay.

S.No	Reagents	Volume (µl)
1	Background	200 µl of assay medium
2	Low control	100 µl assay medium and 100 µl of culture supernatant
3	High Control	100 µl assay medium and 100 µl 1% Triton X 100
	Incubate at 37° C, 15 mins	
4	Experimental groups	100 µl of the culture supernatants
	Incubate at 25° C- 28° C, 30 mins	
5	Stopping solution	50 µl
	Read the absorbance at 490nm/492nm	

The percentage of cytotoxicity = Experimental Value – Low control / High control- Low control. The experiments were carried out in triplicates and the mean ± SD was calculated.

4.3.11. Cell proliferation assay

Transfected Y79 and WERI Rb1 cells (5,000 cells per well) were plated in 96 well plates on day 0. On day 1, cells were incubated with specific concentration of oligos and corresponding concentration of Lipofectamine transfection reagent as described in table 4.13 above (Invitrogen) for 24 h. This was repeated on days 2 and 3. On the days from 1 to 3, serum-free RPMI medium containing 10µl of 5 mg/ml 3-(4,5- Dimethylthiazolyl) 2,5diphenyltetrazolium bromide (MTT) was added to the wells, and the cells were incubated at 37 °C for 4 h. Then 100 µl of MTT solubilization solution dimethyl sulfoxide

(DMSO, Sigma Aldrich, St Louis, MO) was added, and the cells were incubated at 37°C for 10 min. Colorimetric measurements were made using a spectrophotometer (Beckman Coulter India Private Ltd, New Delhi, India) at 562 nm, and the background was subtracted at 650 nm. The assay was performed in triplicates with and without scrambled siRNA/miRNA as controls.

4.3.12. CyQUANT cell proliferation assay

This assay is based on the DNA binding dye (cell permeable) in combination with a background suppression reagent. Estimation of cell number is based on the DNA content of the cell. Dead cell and cells with compromised cell membranes are masked by the "masking dye". Thus, the CyQUANT® Direct assay measures both proliferation as well as cytotoxicity.

Detection reagent (2X) was prepared as per manufactures instruction (by adding the supplied direct nucleic acid stain and direct background suppressor I). About 50ml of 2X detection reagent was then added directly to the cell plates (stored in -80°c after treatment for overnight), incubated at 37°C for 30 mins in the dark. Fluorescence was measured at 508 nm excitation and 527 nm emissions on a SpectraMax M5 series (Molecular devices). A linear graph was derived for the cell densities ranging from 1750 – 25,000 cells/96 well. The cell number propotionate to RFU were measured using SoftMax Pro software.

4.3.13. Apoptosis assay

The RB cells from the experimental groups were harvested and washed with ice cold 1X PBS twice. The cells were incubated with annexin V FLOUS stain and propidium iodide for 1 h at 4 °c. The cells were washed with ice-cold 1X PBS twice and analysed using flow cytometer by gating 10,000 cells / experiment (FACS Calibur, Becton-Dickinson, Franklin Lakes, and New Jersy).

4.3.14. Cell cycle analysis

RB cells (various experimental groups) were harvested. Cells were fixed for 30 min with 70% cold ethanol, washed twice with ice cold 1X PBS twice, and then incubated at 37 °c for 2 h in 1X PBS buffer containing 100 µg/ml RNase A, propidium iodide 5 µg/ml and cells were analysed using flow cytometer by gating 10,000 cells/ experiment (FACS Calibur, Becton-Dickinson, Franklin Lakes, NJ).

4.3.15. Scratch assay

After transfection, when the RB cells were fully confluent, single uniform scratch was made along the centre of each well to create a cell-free area. The wells were then washed with PBS to remove detached cells. Media was added to the culture immediately before taking the images. Number of cells in the scratch area infiltrated by migrating cells at regular intervals, was calculated using ImageJ (Image J, NIH, USA).

4.3.16. Statistical analysis

Microarray data was analyzed using Gene spring software (GX version 12.5, Agilent technologies, Santacruz, California, USA). Unpaired Student's t-test for p-value calculation and Benjamini Hocheberg based FDR correction was applied. Genes/miRNAs that are lesser than or greater than 1.0 fold differentially expressed with a $p<0.05$ is considered as true differentials. Independent sample't' test and Mann-Whitney 'U' test were used to compare the variables among primary tumor tissues. One-way ANOVA (Post Hoc, Dunnett t-test), Two-way ANOVA and ANOVA with repeated measures were used to compare the controls and test variables for cell proliferation and scratch assay experiments using SPSS software (version 12.0). Polynomial regression analysis was used to derive the IC_{50}/IC_{70} values. Normal p value ≤ 0.05 was as significant results. Values expressed for cell proliferation, apoptosis, cell cycle analysis and scratch assay are mean ± SD of at least three experiments.

CHAPTER 5: HMGA2 AS A MOLECULAR TARGET IN RB MANAGEMENT

CHAPTER 5.1: EXPRESSION OF HMGA2 IN RB: CORRELATION WITH CLINICO-PATHOLOGICAL FEATURES

5.1. Introduction

[#] Newer molecules and pathways have to be identified for designing novel targeted therapies in managing RB to avoid enucleation and to prevent metastasis (Boutrid et al. 2008). EpCAM, Stathmin, and Connexin 46 are recent examples of newer therapeutic and drug delivery targets in RB (Burr et al. 2011, Krishnakumar et al. 2004a, Mitra et al. 2010, Mitra et al. 2011a, Mitra et al. 2011b).

The high mobility group A (HMGA) proteins are small non-histone chromosomal proteins that are characterized by 3 highly conserved DNA-binding motifs called "AT-hooks" and an acidic tail. They preferentially bind to the minor groove of AT-rich B form DNA by recognizing a particular DNA structure rather than a specific nucleotide sequence (Reeves and Nissen 1990). Members of the HMGA protein family are often referred to as "architectural transcription factors" (Wolffe 1994) because of their ability to regulate expression of a large number of target genes through alteration of chromatin structure (Bustin and Reeves 1996). The HMGA family consists of HMGA1a, HMGA1b, HMGA1c, and HMGA2 (Boo et al. 2005, Reeves 2001). HMGA1 (HMGA-1/Y) and

1. [#] *The results presented in this chapter is published: Venkatesan N, Kandalam M, Pasricha G, Sumantran V, Manfioletti G, Ono SJ, Reddy MA, Krishnakumar S. Expression of high mobility group A2 protein in retinoblastoma and its association with clinicopathologic features. J Pediatr Hematol Oncol. 2009 Mar; 31(3): 209-14.*

HMGA2 (HMG1-C) have similar functions and are found relatively abundantly in the early embryo, where cells are proliferating rapidly (Hebert et al. 2007, Sgarra et al. 2004).

HMGA proteins are multifunctional and are involved in many fundamental cellular processes, including gene regulation, cell cycle, differentiation, and viral integration (Reeves 2001). Not surprisingly, therefore, HMGA mutations contribute to many common diseases, including benign and malignant tumors (Sgarra et al. 2004), obesity (Anand and Chada 2000), diabetes (Foti et al. 2005) and atherosclerosis (Schlueter et al. 2005). HMGA proteins are relatively abundant in the early embryo where cells are proliferating rapidly, whereas they are undetectable in terminally differentiated cells (Sgarra et al. 2004).

HMGA2 protein expression is increased in several tumors such as oral squamous cell carcinoma (Rogalla et al. 1996), breast cancer (Wikman et al. 2002), pancreatic cancer (Abe et al. 2003), non-small cell lung cancer (Rogalla et al. 1998) and leukemia (Rommel et al. 1997). Re-activation of the HMGA2 gene was observed in the cells of many human malignancies such as breast and non-small lung cancers (Meyer et al. 2007), pancreatic carcinoma (Abe et al. 2003), breast cancer (Rogalla et al. 1997), squamous cell carcinomas (Miyazawa et al. 2004), and myeloproliferative disorders (Andrieux et al. 2004). HMGA2 is being studied for its oncogenic properties (Hristov et al. 2009, Peng et al. 2008), stem cell self-renewal (Nishino et al. 2008, Tzatsos and Bardeesy 2008), DNA damage response (Park et al. 2007), and tumor cell growth and differentiation (Li A. Y. et al. 2009a, Shell et al. 2007, Wu et al. 2011).However, the precise role of HMGA2 in malignant transformation and the gene's regulation of tumorigenesis are still not clear. Previous studies on HMGA2 gene silencing inhibited Ras-induced transformation of thyroid cells resulting in growth inhibition and increased apoptosis of liposarcoma cells (Berlingieri et al. 1995, Pentimalli et al. 2003). Using a nude mice model of retinoblastoma, Ono et al. suggested a potential role for HMGA2 derepression in the tumorigenesis of retinoblastoma (Chau et al. 2003).

4.	4/M	OD: PD, NI	0	0
5.	2/F	OD: UD, NI	40	3
6.	7mon/M	OD: WD, NI	50	3
7.	1.8/F	OD: WD, NI	10	3
8.	2/M	OD: WD, NI	20	1
9.	3/M	OD: WD, NI	40	3
10.	7mon/M	OD: PD, NI	30	1
11.	3/F	OS: WD, NI	20	1
12.	5/M	OS: PD, NI	10	2
13.	8/M	OS: PD, NI	40	1
14.	5mon/M	OD: WD, NI	50	1
15.	4/F	OD: PD, NI	60	1
16.	/M	OS: WD, NI	70	2
17.	5/M	OS: MD, NI	30	1
18.	5/M	OS: MD, NI	20	1
19.	4/F	OD: PD, NI	20	1
20.	3/F	OD: PD, NI	30	1
21.	4/F	OD: PD, NI	40	1
22.	1.4/M	OD: WD, NI	30	1
23.	1/F	OD: WD, NI	40	1
24.	2/M	OD: WD, NI	20	3
25.	6mon/M	OS: WD, NI	40	1
26.	11mon/F	OD: UD, NI	0	0
27.	7mon/M	OS: PD, NI	40	2
28.	1/F	OS: MD, NI	30	2
29.	2mon/F	OS: WD, NI	0	1
30.	3/F	OD: PD, NI	10	2
31.	1.8/F	OD: WD, NI	20	3
32.	10mon/F	OS: WD, NI	0	1

33.	1/F	OD: WD, NI	0	1
34.	7mon/F	OD: PD, NI	0	0
35.	3mon/M	OD: WD, NI	0	1

F: Female; M: Male; MD: moderately differentiated; PD: poorly differntiated; WD: well differentiated; NI: No Invasion; OD: right eye; OS: left eye.

Table 5.1.2: HMGA2 expression in RB (Invasion).The clinico-pathologic features and HMGA2 expression of the tumors with invasion of choroids/optic nerve/orbit.

S/No	Age(Yrs) /Sex	Clinico-pathologic Features	HMGA2 protein expression (%)	HMGA2 protein expression : Intensity
1.	2/M	OU: OD: WD, focal Ch inv	80	3
2.	7/M	OD: PD, rectus orbital inv	100	3
3.	2/M	OS: PD, diff Ch, pre lam ON inv	80	1
4.	3/M	OD: PD, focal Ch, post lam ON inv	70	1
5.	2/F	OU: OS: PD, diff Ch inv	60	1
6.	4/M	OS: PD, focal Ch, post lam ON inv	80	3
7.	2/F	OD: PD, pre lam ON inv	50	1
8.	2/M	OU:OS: MD, focal Ch inv	70	2
9.	7/M	OS: MD, post lam ON inv	80	1
10.	2/M	OS: PD, post lam ON inv	70	1
11.	5mon/M	OS: PD, pre lam ON inv	20	2
12.	3/M	OD: PD, focal Ch, post lam, orbital inv	60	2
13.	1/F	OS: PD, focal Ch, pre lam ON inv	70	2
14.	3mon/F	OU: OD: WD, focal Ch, pre lam ON	40	1
15.	3/M	OD: PD, focal Ch inv	40	2
16.	4/F	OS: PD, pre lam ON inv	80	3
17.	2/M	OD: WD, diff Ch, post lam and SE inv	60	1
18.	13mon/F	OD: PD, focal Ch, post lam ON inv	10	2
19.	4/F	OD: MD, focal Ch, pre lam ON inv	40	2
20.	1mon/M	OU: OD: MD, diff Ch inv	80	1
21.	4/M	OD: PD, focal Ch, pre lam ON inv	70	3

22.	1/F	OD: PD, diff Ch inv	10	1
23.	3/M	OS: PD, diff Ch, pre lam ON inv	10	2
24.	4/M	OU: OS: PD, diff Ch inv	20	2
25.	3/M	OS: PD, post lam ON inv	10	1
26.	4/F	OD: WD, pre lam ON inv	70	1
27.	2/M	OD: PD, diff Ch, post lam ON inv	20	1
28.	3/F	OD: PD, post lam ON inv	70	2
29.	3/M	OU: OS: PD, diff Ch, post lam ON inv	80	3

F: Female; M: Male; MD: moderately differentiated; PD: poorly differntiated; WD: well differentiated; OD: right eye; OS: left eye; Inv: invasion; pre-lam: pre-laminar; post-lam: post-laminar

5.1.2.2. Association of HMGA2 expression with differentiation and laterality

Among the 64 RBs, there were 37 poorly differentiated tumors and 27 moderately/well-differentiated tumors. There were 10 bilateral tumors and 54 unilateral tumors in the study.

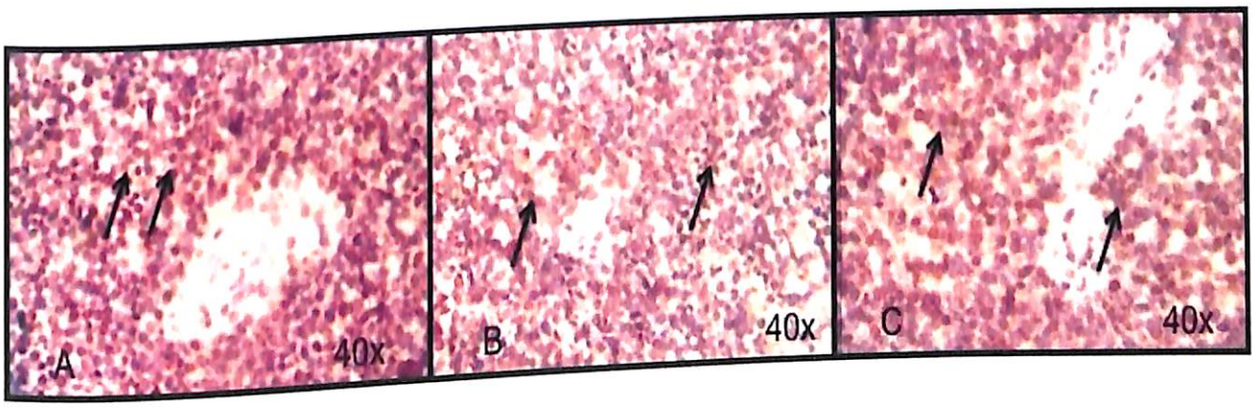

Figure 5.1.1: HMGA2 protein expression. Photomicrographs of HMGA2 protein expression in RB primary tumour tissues. A: HMGA2 protein expression in RB tumour with no invasion (strong positive); HMGA2 protein expression in RB tumour with invasion B: Moderate nuclear positive; C: Strong nuclear positive. The arrow indicates the HMGA2 positive RB cells determined by using diaminobenzaldehyde substrate in immunohistochemistry.

5.1.2.3. HMGA2 Protein Expression in the overall cohort

Among 64 tumors, HMGA2 protein was strongly positive (++) in 16 tumors, moderately positive (+) in 17 tumors and faint/absent (±) in 31 tumors **[Figure 5a: A–C]**

5.1.2.4. *HMGA2 protein expression in tumors without invasion*

Among 35 tumors without invasion, HMGA2 protein was strongly positive (++) in 6 tumors, moderately positive (+) in 6 tumors, and faint/absent (±) in 23 tumors.HMGA2 protein expression in tumors with invasion

Among 29 tumors with invasion, HMGA2 protein was strongly positive (++) in 10 tumors, moderately positive (+) in 11 tumors, and faint/absent (±) in 8 tumors.

5.1.2.5. *Correlation of HMGA2 Protein Expression with Invasion /Differentiation/Laterality of the Tumors*

We observed significantly higher expression of HMGA2 protein in tumors with invasion compared with tumors without invasion ($P < 0.01$). There was no correlation between the HMGA2 protein expression and differentiation/laterality of the tumors.

5.1.2.6. *Western Blotting Analysis of HMGA2 Protein*

We observed a protein in the blot that corresponded to 12 kda molecular weight. Among 12 tumors studied by Western blotting, 7 tumors were strongly positive, 2 tumors were moderately positive, and 1 was faintly positive **[Figure 5.b].**

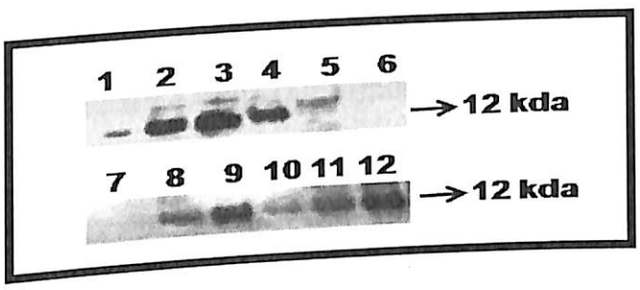

Figure 5.1.2: Western analysis of HMGA2. Western analysis of HMGA2 proteins in primary RB tumour tissues: Lanes 2 t o 4, 8, 9, 11, and 12 show strong expression of HMGA2 protein in the fresh tumors. Lanes 1 and 5 show moderate expression and lane 10 shows faint expression. Lane 7 shows negative expression for HMGA2 protein in non-neoplastic retina (donor eye).

There was no correlation of HMGA2 protein expression with invasion or differentiation of the tumors. Among 6 tumors with invasion, HMGA2 is strongly positive in 4 tumors,

moderately positive in 1 tumor, and negative in 1 tumor. Among 6 tumors without invasion, HMGA2 is strongly positive in 3 tumors, moderately positive in 1, faint in 1, and negative in 1 tumor. As the sample size was very low in each group, the power of the statistics is not significant. Hence, we could not attempt to statistically correlate HMGA2 expression with invasion. We have attempted to correlate the immunoblotting results with the IHC staining grades by agreement correlation statistics and achieved k value of 0.745 with P value < 0.001.

5.1.2.7. HMGA2 mRNA expression in RB tumors

Among 20 RB tumors, HMGA2 mRNA expression was positive in all the tumor samples analysed under study (100%).

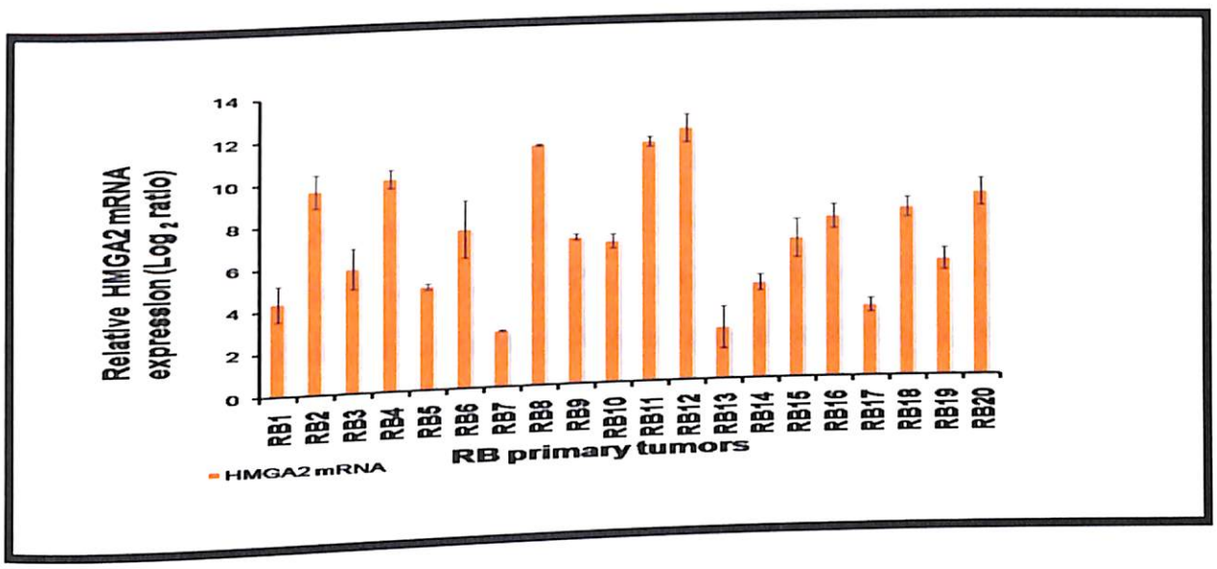

Figure 5.1.3: HMGA2 mRNA expression. The bar graph represents the relative HMGA2 mRNA expression in RB primary tumors (n=20), determined by qRT-PCR, compared with donor retina.

5.1.2.8. HMGA2 expression in RB cell lines (Y79 and Weri Rb1)

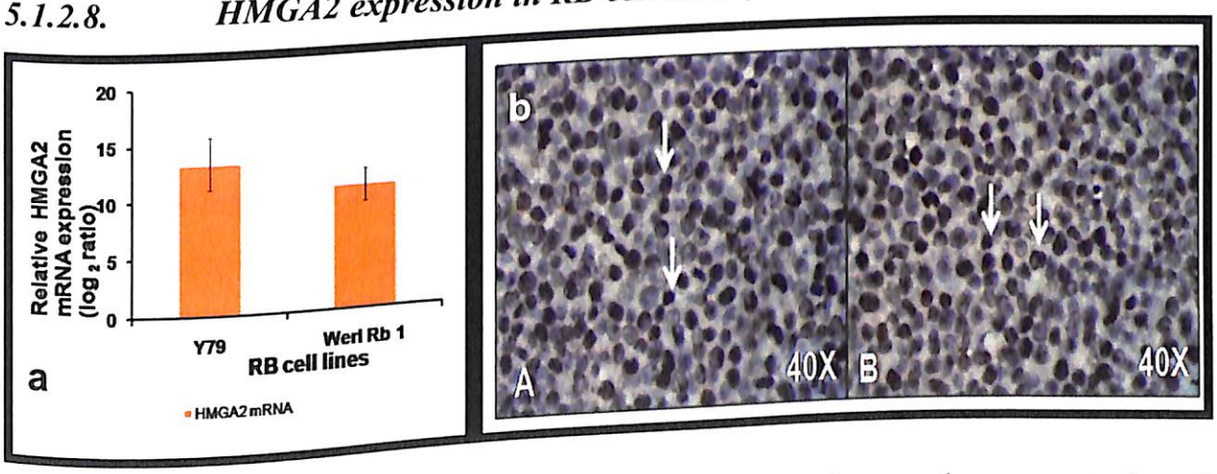

Figure 5.1.4: HMGA2 expression in RB cell lines. **a:** The bar graph represents the relative HMGA2 mRNA expression determined by qRT-PCR in RB cell lines (Y79 and Weri Rb

1) compared with donor retina. **b:** HMGA2 protein expressions in RB cell lines (A: Y79 and B: Weri Rb 1 cell blocks) determined by immunohistochemistry. White arrowhead indicates the nuclear positivity of HMGA2 protein expression.

5.1.3. Discussion

In our study, we have demonstrated the HMGA2 protein expression in RB sections by IHC [**Figure 5.1.1; Table 5.1.1; Table 5.1.2.**] and confirmed the results on fresh tumor samples by Western blot. Among 64 tumors, HMGA2 protein was strongly positive (++) in 16 (25%) tumors, moderately positive (+) in 17 (26%) tumors, and faint/absent in 31 (48%) tumors. Among 35 tumors without invasion, HMGA2 protein was strongly positive (++) in 6 tumors, moderately positive (+) in 6 tumors, and faint/absent (±) in 2 3 tumors. Among 29 tumors with invasion, HMGA2 protein was strongly positive (++) in 10 tumors, moderately positive (+) in 11 tumors, and faint/absent (±) in 8 tumors. We observed significantly higher expression of HMGA2 protein in tumors with invasion compared with tumors without invasion ($P < 0.01$). We did not find any correlation with differentiation or laterality of the tumors. We have confirmed the expression of HMGA2 protein by Western blotting in the fresh tumor samples. We observed a protein band at 12kd in the blotting **[Figure 5.1.2]**. Among 12 tumors processed by Western blot, 7 tumors were strongly positive and 2 tumors were faintly positive. To the best of our knowledge this is the first report showing the clinico-pathologic correlation of HMGA2 protein expression in a large cohort.

HMGA2 protein is abundantly expressed in embryonic tissue, including the retina, but its expression is repressed in virtually all adult tissues, also including the retina (Rogalla et al. 1996) (Chieffi et al. 2002, Hirning-Folz et al. 1998, Zhou et al. 1995, Zhou et al. 1996). In the present study, the strong expression of HMGA2 in the unaffected retina of RB tumor could not be explained clearly at this moment. However, it could be hypothesized that HMGA2 de-repression might be an early oncogenic event required for initiating the neoplastic transformation. Earlier, Chau et al.2003, have shown the reactivation of HMGA2 gene expression in the RB cell lines Y79, Weri-Rb1, and TOTL-1, in tumors derived from some of these cells propagated in nude mice, and in a high frequency of RBs excised from human patients. Their discovery of de-repression of HMGA2 gene expression in RB suggests that this protein might contribute to neoplastic transformation

of retina cells. However, HMGA2 protein was negative in the non-neoplastic donor retina. In addition, Chau et al. 2003, have demonstrated specific blockade of HMGA2 (in which HMGA1 remained unchanged) gene expression, with an antisense adenoviral-mediated approach, resulted in a decrease in cell number/ proliferation of RB cells. In our study, interestingly, the tumors with invasion showed significantly higher expression compared with the tumors without invasion. Several mechanisms have been proposed to account for the transforming ability of the HMGA proteins. Because of their main function of regulating gene transcription, most of these mechanisms are based on the ability of the HMGA proteins to down-regulate or up-regulate the expression of genes that have a crucial role in the control of cell proliferation and invasion. It has been recently reported that HMGA2 induces pituitary adenomas in HMGA2- transgenic mice by binding to pRB and enhancing E2F1 activity, which facilitates the entry of cells to S-phase (Fedele et al. 2006). It has also been reported that HMGA proteins increases the activity of AP-1 complex (Vallone et al. 1997) that include 3 Jun proteins and 4 Fos proteins giving rise to a large variety of homodimers and heterodimers. This AP-1 complex is responsible for the activation of various target genes involved in the control of cell proliferation tumorigenesis and metastasis (Angel and Karin 1991, Karin et al. 1997).

5.1.4. Conclusion

Thus, understanding the role that HMGA2 protein plays in patho-biology and molecular mechanisms of RB occurrence is biologically and clinically significant and HMGA2 protein may become a therapeutic target. Further studies are carried out in forth-coming chapters to prove the contribution of HMGA2 protein in the tumor invasion property of RB.

CHAPTER 5.2: MOLECULAR DE-REGULATIONS IN POST-HMGA2 SILENCED RB CELLS

5.2. Introduction

[#]In continuation with the reports of previous chapter (5.1) and other earlier reports i.e, the strong correlation between HMGA2 protein expression and tumor invasiveness has prompted further research on this molecule and related pathways (Chau et al. 2003, Venkatesan et al. 2009). However, the *HMGA2* gene is not detectable in adult human tissues where it is probably completely silenced (Gattas et al. 1999, Rogalla et al. 1996). The ectopic expression of HMGA2 protein in RB (Chau et al. 2003), and the clinico-pathological correlations of HMGA2 protein in primary RB tissues (Venkatesan et al. 2009) suggest its role in the genesis and maintenance of the transformed phenotypes (Wunderlich and Bottger 1997).

In this chapter, we have established the suppression of cell proliferation in cultured RB cells of differing tumor aggressiveness (Y79 and Weri Rb1) using the HMGA2 gene-silencing technique. The DNA binding sites in the *HMGA2* gene are being identified (Cui and Leng 2007, Watanabe M. et al. 2012) with possible implications for developing DNA-based therapeutics (aptamers). However, molecular understanding of *HMGA2*-mediated cell signaling is limited. Here, we present the key findings on the molecular effects of *HMGA2* gene silencing in cell signaling, apoptotic, and cell adhesion regulation in RB. The deregulated genes in the post-silenced RB cells were compared with primary tumors for constitutive expression levels.

---

2. [#] ***This chapter has been published : Nalini Venkatesan, Subramanian Krishnakumar, Perinkulam Ravi Deepa, Murali Deepa, Vikas Khetan, M. Ashwin Reddy, Molecular deregulation induced by silencing of the high mobility group protein A2 gene in retinoblastoma cells, Molecular Vision 2012; 18:2420-2437.***

5.2.3. Materials and Methods

The study was reviewed and approved by the local ethics committee of our institute, and conformed to the generally accepted principles of research, in accordance with the Helsinki Declaration.

5.2.3.1. Cell Culture

We employed in this study human RB cell lines (Y79, Weri Rb1, Riken cell bank, Japan). Cells were cultured in Rosewell Park Memorial Institute (RPMI; Gibco-BRL) 1640 medium as described in the section 4.1.3.

5.2.3.2. Tumour Samples

The present study includes tumour samples collected from 10 enucleated eyeballs of RB patients (2010 – 2011). The RB sections were reviewed and graded microscopically by an ocular pathologist. The tumour samples were recorded for their clinico-pathological features based on their predominant pattern of differentiation and tumour invasion of the choroid, optic nerve, or orbit (with or without metastasis) following the International Intraocular RB Classification (IIRC) **[Table 5.2.2]**

5.2.3.3. siRNA sequences of HMGA2 transcripts

The transfection protocol was carried out using three different siRNA sequences of three regions targeting the HMGA2 gene. Human *HMGA2* siRNA.1 (Hs_*HMGA2*_6 catalogue number SI03029929: Forward strand: CGGCCAAGAGGCAGACCUATT and the reverse strand: UAGGUCUGCCUCUUGGCCGTT) *HMGA2* siRNA.2 (Hs_*HMGA2*_7 catalogue number SI03067393: Forward strand: GCGGCGGCAGCCUAAGCAATT and the reverse strand: UUGCUUAGGCUGCCGCCGCTG and scrambled siRNA (catalogue number 1022563) *HMGA2* siRNA.3 (1146–1164) (catalogue number 1027423, Forward strand: 5'-CGCCAACGUUCGAUUUCUA3' Reverse strand: 3'GCGGUUGCAAGCUAAAGAU-5') were used in this study.

5.2.3.4. Transfection of HMGA2 siRNA in RB cells

The transfection is carried as described in the section 4.2.9.

5.2.3.5. *Experimental validation in post-HMGA2 silenced RB cells*

Protocol for cDNA microarray, qRT-PCR, western analysis of HMGA2, p53, p21 proteins, cell proliferation assay, cell cycle analysis, expression of caspase 3 using FACS in post-*HMGA2* silenced RB cells, scramble treated and un-treated RB cells are followed as described under the methods section **[chapter 4.2]** of this dissertation.

5.2.3.6. *Statistical analysis*

For microarray analysis, independent't' test was performed using SPSS version 12.0 software (Chicago, IL). $P < 0.05$ was considered significant.

5.2.4. Results

5.2.4.1. *Optimization of short interfering RNA–mediated downregulation of HMGA2 in retinoblastoma (Y79) cell lines*

Initially, the *HMGA2* gene silencing protocol was optimized in cultured RB cells. Using qRT–PCR analyses, we found that over a period of 48 h, transfection with the siRNA.1 (Hs_*HMGA2*_6) sequence led to a -4.65 $\log_2$ ratio decrease, while the other sequences, siRNA.2 (Hs_*HMGA2*_7) and siRNA.3 sequence, led to a $\log_2$ ratio of -2.0 and 1.76 decrease, respectively, when compared with and without scrambled siRNA as controls in RB cells **[Y79; Figure 5.2.1]**. The qRT-PCR results were consistent with the decreased HMGA2 protein levels determined by western analysis **[Y79; Figure 5.2.1]**.

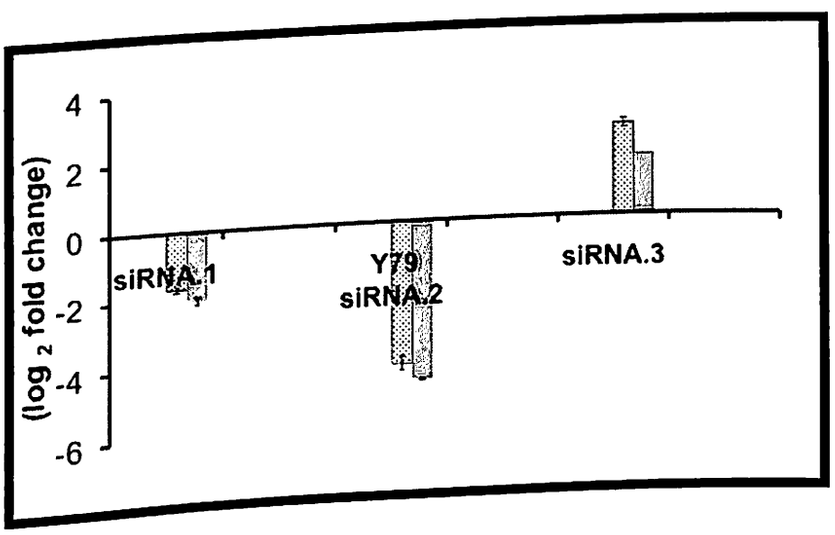

Figure 5.2.1: HMGA2 siRNA effect in RB cells. A: The mRNA levels of High mobility group A2 (HMGA2) in RB cells (Y79) treated with HMGA2 short interfering (si) RNAs

namely siRNA.1 (Hs_HMGA2_6) sequence led to a decrease of 4.65 log_2 ratio, siRNA.2 (Hs_HMGA2_7) led to a decrease of 2.0, siRNA.3 sequence led to an increase of 1.76 log $_2$ ratio when compared with HMGA2 mRNA levels in control (solid bar) and to decrease of 1.68 Log $_2$ ratio, 4.175 Log $_2$ ratio, increase of 2.65 Log_2 ratio respectively to cells treated with scrambled (SCR) siRNA (dotted bars) at the end of 48 h. The error bars represents the standard deviation of triplicate values. Effect of small interfering RNA on the expression of High mobility group A2 (HMGA2) in RB Y79 cells in vitro.

5.2.4.2. Comparison of HMGA2 gene mRNA and protein expression in pre- and post-silenced Y79 and Weri Rb1 cells

The effect of *HMGA2* gene silencing in the pre- and post-silenced Y79 and Weri Rb1 cells using the siRNA.1 (Hs_*HMGA2*_6) sequence showed decreased expression (log_2 ratio of −4.65 and −3.17, respectively). The protein expression of *HMGA2* was confirmed with western blot analysis **[Figure 5.2.3]**.

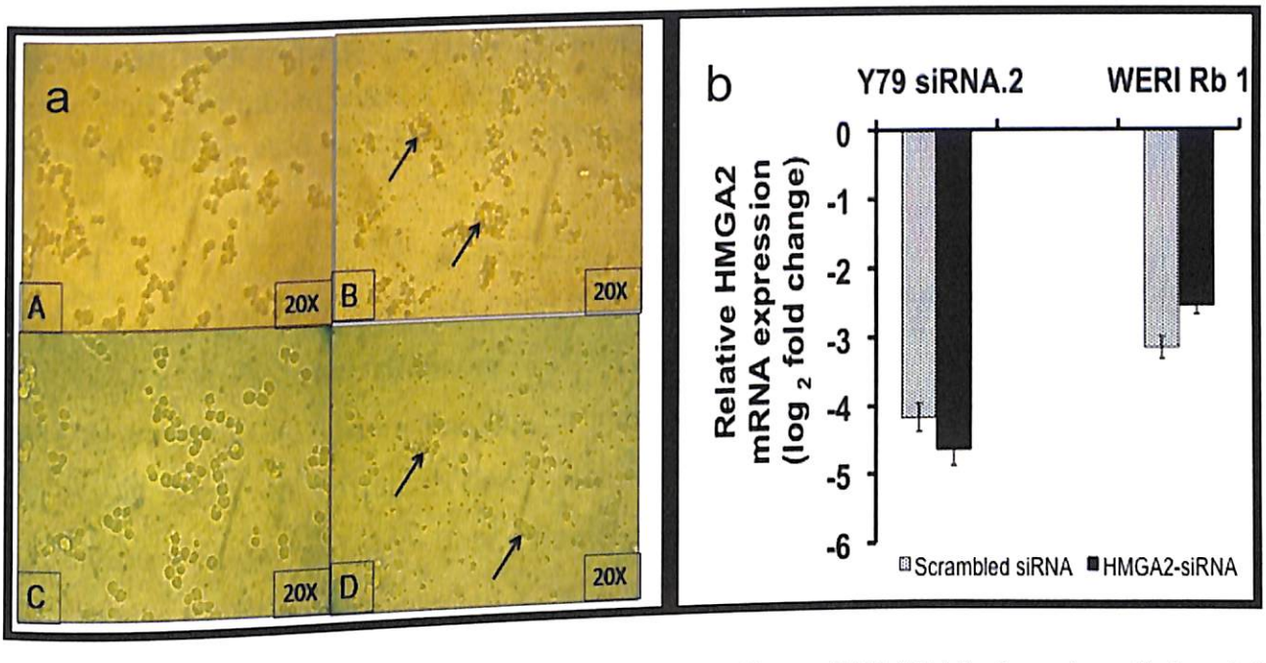

Figure 5.2.2: HMGA2 siRNA effect in RB cells. Effect of HMGA2 short interfering (si) RNA [siRNA.1 (Hs_HMGA2_6) sequence] treatment in RB cells. a: Photomicrographs of RB cells after 48 h of HMGA2 siRNA treatment A: untreated Y79 cells, B: HMGA2 siRNA treated Y79 ; A: untreated Weri Rb1 cells, b: HMGA2 siRNA treated Weri Rb1 cells. The arrow head indicates the morphological changes of RB cells treated with HMGA2 siRNA; b:The mRNA levels of high mobility group A2 (HMGA2) in Y79 cells treated with HMGA2 short interfering (si) RNA [siRNA.1 (Hs_HMGA2_6) sequence] led to a decrease of HMGA2 by log_2 ratio of 4.65 and in Weri Rb1 led to a decrease in HMGA2 log_2 ratio of 2.56 when compared with HMGA2 mRNA levels in RB control cells (solid bar) and to a decrease of 4.175 log_2 ratio, 3.17 log $_2$ ratio respectively in RB (Y79, Weri Rb1) cells treated with scrambled siRNA (dotted bars at the end of 48 h). The error bars represents the standard deviation of triplicate values.

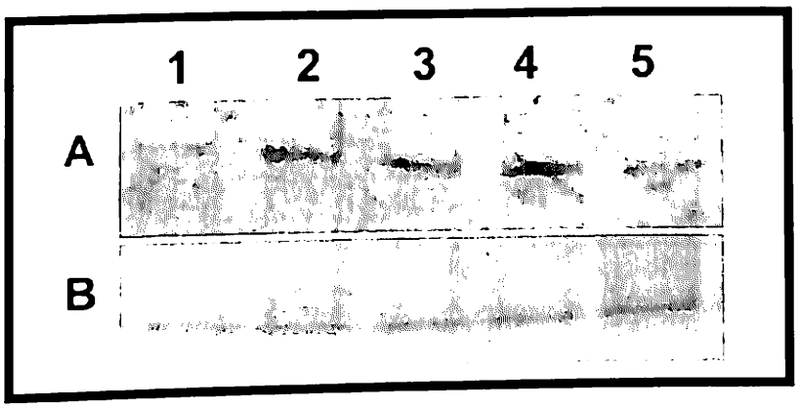

Figure 5.2.3: Western analysis of HMGA2 protein. Effect of siRNA on high mobility group A2 (HMGA2) protein expression in RB (Y79,Weri Rb1) cells. A: Western blot analysis demonstrates markedly reduced HMGA2 expression in Y79 cells treated with HMGA2-siRNA (lane 1), strong expression of HMGA2 in non-transfected Y79 cells (lane 2), strong expression in Y79 cells treated with scrambled siRNA (lane 3), strong expression of HMGA2 in non transfected Weri Rb1 cells (lane 4), and markedly reduced HMGA2 expression in Weri Rb1 cells treated with HMGA2-siRNA (lane 5). B: Western blot analysis demonstrates expression of Histone (normalization control) in Y79 cells treated with HMGA2-siRNA (lane 1), in non-transfected Y79 cells (lane 2), Y79 cells treated with scrambled siRNA (lane 3), non-transfected Weri Rb1 cells (lane 4), and in Weri Rb1 cells treated with HMGA2-siRNA (lane 5).

5.2.4.3. Arrest of cell cycle progression in retinoblastoma cells (Y79, Weri Rb1) with HMGA2 gene silencing

The effect of *HMGA2* gene silencing on modulating RB cell growth was studied using a cell cycle assay after transfection with *HMGA2* siRNA **[Table 5.2.4]**. Cell cycle distribution was assessed with flow cytometry. Compared to the untreated cells, the G_0/G_1 and S phases in the post-transfected Y79 cells, and the G_0/G_1, S, and G_2/M phases in post-transfected Weri Rb1 cells showed marked cell cycle arrest (increase in polyploidy) when *HMGA2* is silenced, which in turn further contributed in the cellular apoptosis **[Figure 5.2.4]**.

Table 5.2.1: Cell cycle analysis. Cell cycle analysis in treated and controls, Y79 and Weri Rb1 cells.

Cell cycle/group	G_0/G_1 (%)	G_2/M (%)	S (%)
Y79 (Control)	56.15 ± 0.33	13.00± 0.97	25.73± 0.48
Y79 (Scrambled siRNA)	50.82± 0.71	26.23± 0.22	14.70± 0.61
Y79 (*HMGA2* siRNA Treated)	39.53± 0.57	19.57± 0.5	12.64± 0.37
Weri Rb1 (Control)	52.05± 0.41	13.58± 0.57	19.20± 0.18
Weri Rb1 (Scrambled siRNA)	54.42± 0.67	9.86± 0.51	34.28± 0.0
Weri Rb1 (*HMGA2* siRNA Treated)	42.19± 0.91	9.84± 0.25	15.65± 0.69

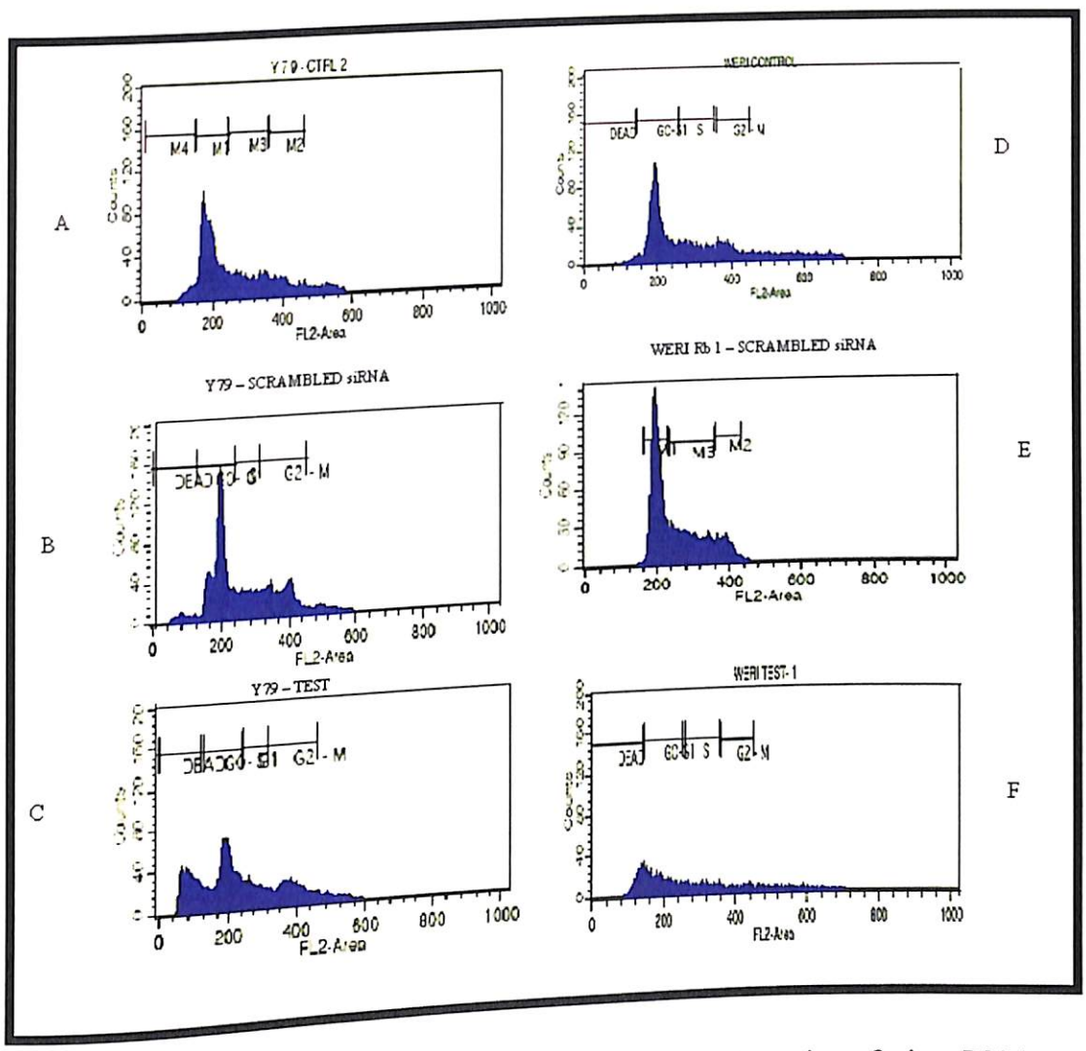

Figure 5.2.4: Cell cycle analysis of RB cells. HMGA2 short interfering RNA treatment results in the marked arrest of the cell cycle phase A: Untreated Y79 cells, B: Scrambled siRNA treated Y79 cells, C: HMGA2 siRNA treated Y79 cells showing marked G_0/G_1 and S phases cell cycle arrest compared to the control cells, D: untreated Weri Rb1 cells, E:

Scrambled siRNA treated Weri Rb1cells, and F: HMGA2 siRNA treated Weri Rb1 cells showing marked G_2/M phases cell cycle arrest compared to the control cells.

5.2.4.4. Suppression of retinoblastoma cell proliferation by HMGA2 gene silencing

The effect of *HMGA2* gene silencing on modulating cell proliferation was studied using an MTT assay. The MTT assay in the RB (Y79, Weri Rb1) cells treated with the anti-*HMGA2* siRNA, scrambled siRNA (a control for non-specific effects of siRNA treatment on cell growth), and the untreated Y79 cells at the end of 24 h, 48 h, and 72 h resulted in a significant decrease in cell proliferation to 81.7%, 67.5%, and 45.5% in Y79 cells and 75.4%, 69.4%, and 49.9% in Weri Rb1 cells, respectively **[Figure 5.2.5]**. There was no significant difference in the cell proliferation rate between the scrambled siRNA and untreated Y79 cells.

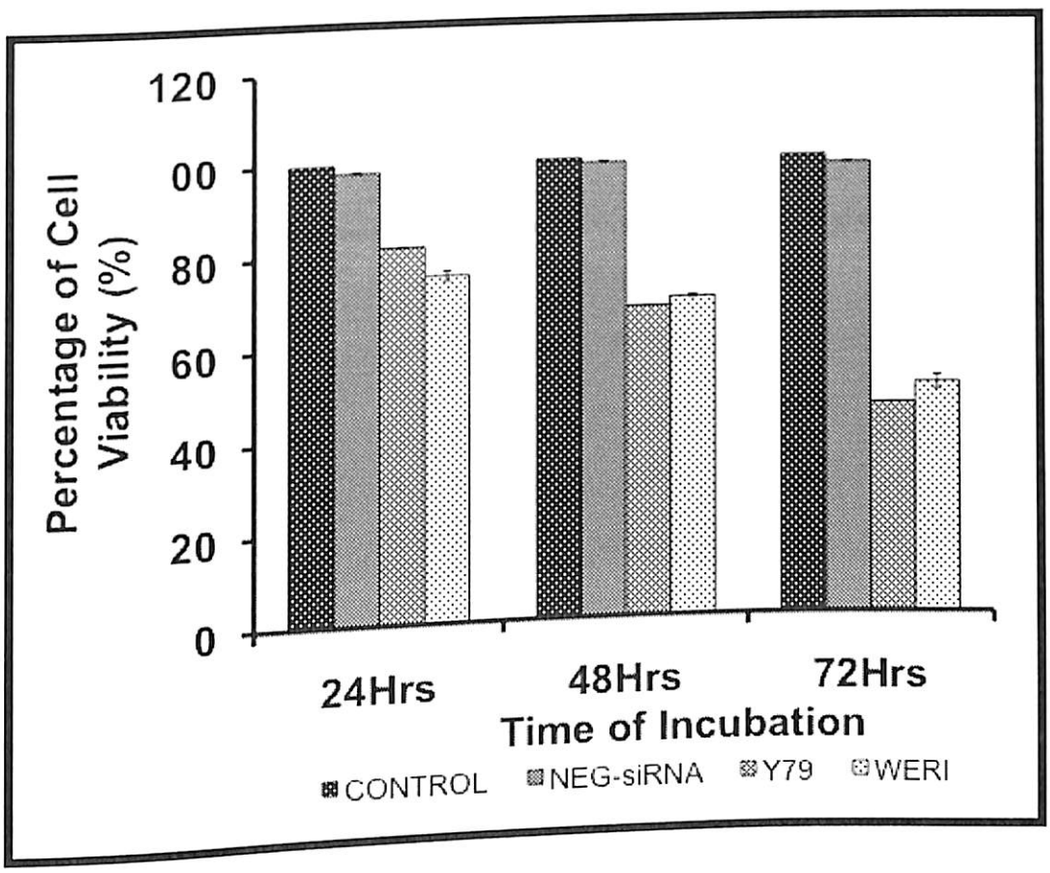

Figure 5.2.5: Cell viability assay in RB cells. HMGA2 short interfering RNA treatment decreases the proliferation of RB (Y79, Weri Rb1) cells. The Y79 cells were treated with High mobility group A2 (HMGA2) short interfering (si)RNA and the cell proliferation was assessed at 24, 48, and 72h using 3-(4,5-dimethylthiazol-2- yl)-2,5-diphenyltetrazolium bromide (MTT) assay. The cell viability decreased to 81.7%, 67.5%, and 45.5% in Y79 cell line, and to 75.4%, 69.4%, and 49.9% in Weri Rb1 respectively

when compared to Y79 cells that were not treated with siRNA. The error bars represents the standard deviation of triplicate values.

5.2.4.5. CDNA microarray analysis

The genome-wide expression of anti-*HMGA2* siRNA treated and untreated Y79 cells were analyzed to probe the genes regulated by the HMGA2 gene. As a result of the anti-HMGA2 siRNA treatment in Y79 cells, a total of vital 227 gene transcripts involved in various cellular functions were modulated, which includes 150 up-regulated (66.07%) and 77 down-regulated (33.9%). Significantly, dysregulated pathways were identified using several databases such as Biologic Pathway Exchange (BioPAX) pathways from Biocarta, Human Protein Reference Database (HPRD), Reactome, KEGG, and NCI-cGAP, by querying the differentially expressed gene list against all the genes annotated with pathway information in the microarray. A total of 100 upregulated and downregulated genes of interest are shown [**Figure 5.2.6**]. The data discussed in this publication have been deposited in NCBI's Gene Expression Omnibus (GEO) and are accessible through GEO Series accession number GSE31687.

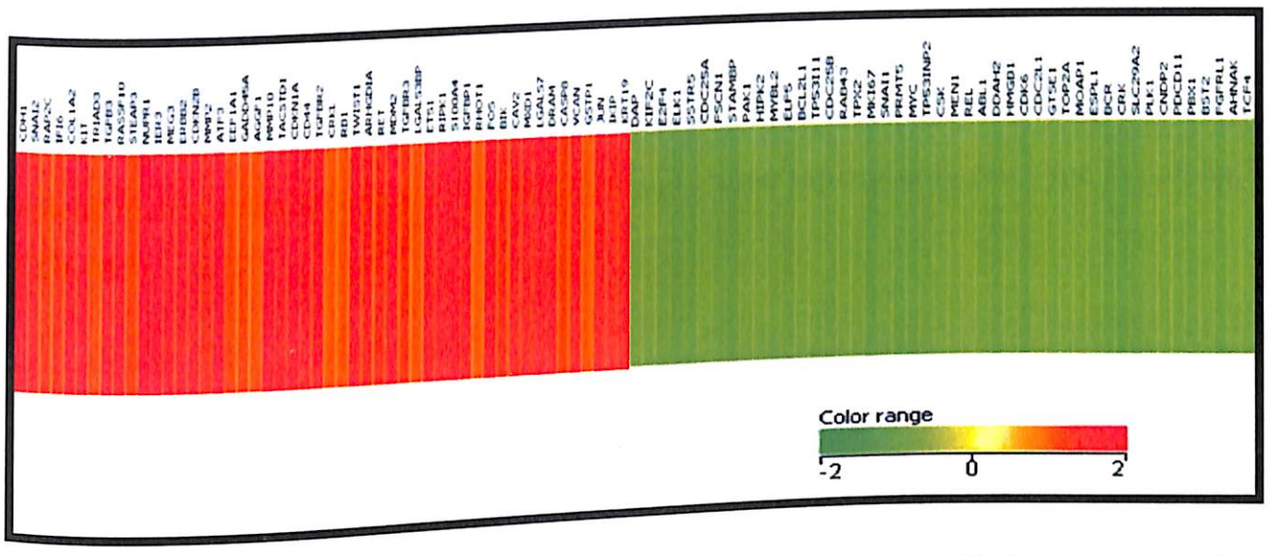

Figure 5.2.6: Gene expression profile in RB. HMGA2 short interfering RNA treatment resulted in changes in gene expression profile in Y79 cells. The heat map represents the expression profile of 100 genes differentially modified in response to knockdown of High mobility group A2 (HMGA2) in Y79 cells compared to untreated cells. The horizontal lines represent the relative fold change in the expression of individual genes modified by the HMGA2-short interfering siRNA. Red and green indicates increased and decreased gene expression, respectively, relative to non-silenced control Y79 cells.

5.2.4.6. *Up-regulation of genes modulated by the treatment of anti-HMGA2 short interfering RNA in Y79 cells*

In the Y79 cells, silencing of the HMGA2 gene resulted in up-regulating gene transcripts involved in the cellular functions, namely, the **apoptosis genes**—lactalbumin, alpha- (*LALBA*), phorbol-12-myristate-13-acetate-induced protein 1 (*PMAIP1*), insulin-like growth factor binding protein 1 (*IGFBP1*), IKK interacting protein (*IKIP*), tumor necrosis factor receptor superfamily, member 10b (*TNFRSF10B*), Homo sapiens receptor (*TNFRSF*)-interacting serine-threonine kinase 1 (*RIPK1*), Homo sapiens damage-regulated autophagy modulator (*DRAM*), ataxin 3 (*ATXN3*), mitogen-activated protein kinase 13 (*MAPK13*), Homo sapiens activating transcription factor 3 (*ATF3*), Homo sapiens nuclear protein 1 (*NUPR1*), Homo sapiens cyclin-dependent kinase inhibitor 1A (*p21, Cip1; CDKN1A*), lectin, galactoside-binding, soluble, 7 (*galectin 7; LGALS7*); **cell cycle and differentiation genes**—Homo sapiens 5-hydroxytryptamine (serotonin) receptor 5A (*HTR5A*), tachykinin 3 (neuromedin K, neurokinin beta; *TAC3*), Homo sapiens activating transcription factor 3 (ATF3); **anti-proliferation**—Homo sapiens maternally expressed 3 (*MEG3*); and **cell adhesion**—Homo sapiens cadherin 11, type 2, OB-cadherin (osteoblast; *CDH11*), Homo sapiens cadherin 1, type 1, E-cadherin (epithelial; *CDH1*), Homo sapiens integrin, alpha 1 (*ITGA1*), Homo sapiens integrin, alpha 2 (*ITGA2*), Homo sapiens laminin, alpha 3 (*LAMA3*), Homo sapiens laminin, beta 3 (*LAMB3*), Homo sapiens laminin, gamma 2 (*LAMC2*), Homo sapiens matrix metallopeptidase 2 (*MMP2*), Homo sapiens matrix metallopeptidase 9 (*MMP9*), and Homo sapiens collagen, type IV, alpha 3 (*COL4A3*).

5.2.4.7. *Down-regulation of genes modulated by the treatment of anti-HMGA2 short interfering RNA in Y79 cells*

In the Y79 cells, silencing of the *HMGA2* gene resulted in downregulating gene transcripts such as the **oncogenes**— Homo sapiens v-abl Abelson murine leukemia viral oncogene homolog 1 (*ABL1*), Homo sapiens v-raf murine sarcoma 3611 viral oncogene homolog (*ARAF*), Homo sapiens v-crk sarcoma virus CT10 oncogene homolog (avian; *CRK*), Homo sapiens ELK1, member of ETS oncogene family (*ELK1*), Homo sapiens v-yes-1 Yamaguchi sarcoma viral related oncogene homolog (*LYN*), Homo sapiens v-myb myeloblastosis viral oncogene homolog (avian)-like 2 (*MYBL2*), Homo sapiens v-myc myelocytomatosis viral oncogene homolog (avian; *MYC*); **cell cycle, proliferation, and**

differentiation genes—Homo sapiens transcription factor 4 (*TCF4*), Homo sapiens cyclin-dependent kinase 6 (*CDK6*), Homo sapiens cell division cycle 25 homolog A(*CDC25A*), Homo sapiens E2F transcription factor 4, p107/p130-binding (*E2F4*), Homo sapiens cyclin-dependent, Homo sapiens antigen identified by monoclonal antibody Ki-67 (*MKI67*), Homo sapiens polo-like kinase 1 (Drosophila; *PLK1*)—Homo sapiens CNDP dipeptidase 2 (metallopeptidase M20 family; CNDP2), pre-B-cell leukemia transcription factor 1 (Homeobox protein PBX1), Homo sapiens snail homolog 1 (Drosophila; *SNAI1*); apoptosis genes—Homo sapiens cDNA FLJ13706 fis, clone, Homo sapiens T-box 3 (ulnar mammary syndrome; *TBX3*), transcript variant 2, Homo sapiens topoisomerase (DNA) II alpha; and angiogenesis genes—Homo sapiens fascin homolog 1, actin-bundling protein (Strongylocentrotus purpuratus; *FSCN1*), Antiapoptosis gene: Homo sapiens G-2 and S-phase expressed 1 (*GTSE1*).

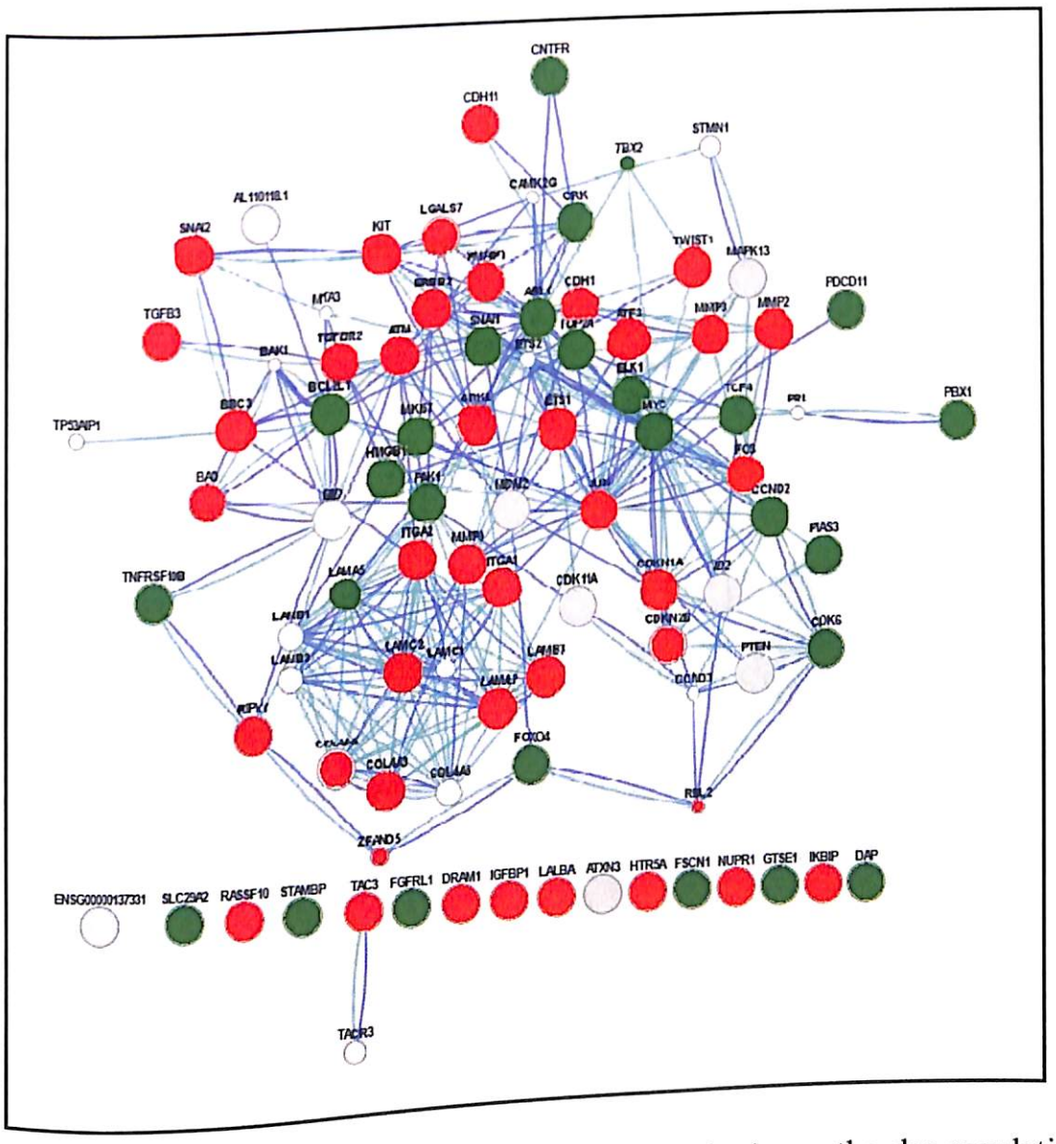

Figure 5.2.7: Interlinking of Genes. The network shows the dys-regulation of the gene cascade identified for their known biological functions drawn using gene mania tool. The dys-regulation of the interlinking such as *SNAI1, CDH1, ELK1, MYC, CDK6, CRK,*

MMP1, *MMP2*, *BCL2L1*, *BBC3*, *BAD* and *TGFB3* indicates suppression of cell proliferation. Dys-regulation of the non-linked genes namely *DRAM1*, *NUPRI* and *GTSEI* in the *HMGA2* siRNA treated RB cells indicates their role in cell proliferation and apoptosis. Green colour indicates down-regulated genes while red colour indicates up-regulated genes in the post- *HMGA2* siRNA Y79 cells.

5.2.4.8. Deregulated pathways modulated by the treatment of the anti-HMGA2 gene short interfering RNA in Y79 cells

In the current study, we found deregulation of genes associated with the mitogen-activated protein (MAP) kinase, Ras, Janus kinase/signal transducers and activators of transcription (Jak/STAT), and p53 signaling pathways. The downregulated genes involved in the **MAP kinase pathway** are *CRK*, *ELK1*, *MYC*, *CDC25B*, and *GRB2*. The downregulated genes involved in the Ras pathway are *Rac1*, *RALGDS*, and *ELK1*. The downregulated genes involved in the **Jak/STAT pathway** are *SPREAD2*, *PIAS3*, *CCND2*, and *CNTFR*. The increased levels of *ATM*, *PUMA /BB3*, *PTEN*, and *DRAM*, the downstream molecules of p53-mediated apoptosis, reveal the modulation of cell apoptosis. The role of **p53-mediated apoptosis** was confirmed by the over-expression of p53 and p21 proteins as well as the caspase 3 protein in HMGA2-silenced Y79 and Weri Rb1 cells [**Figure 5.2.8: A, B**].

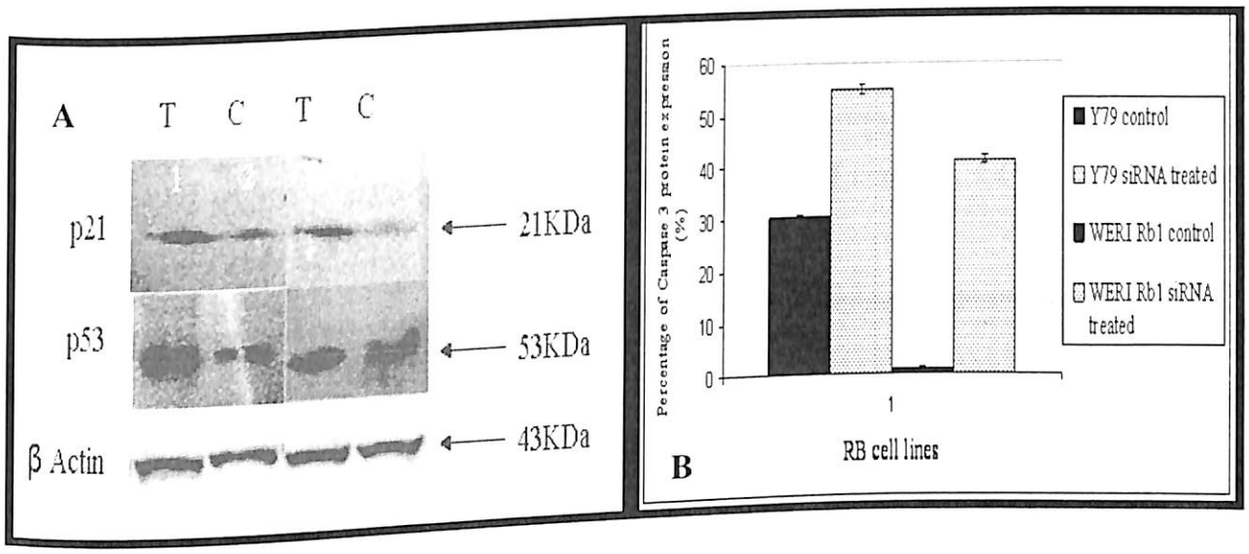

Figure 5.2.8: Effect of HMGA2 siRNA in RBcells. Effect of small interfering RNA on the expression of p21, p53 and caspase 3 in RB (Y79, Weri Rb1) cells. A*:* Western blot analysis demonstrates marked increase of p21,p53 expression in Y79 cells treated with HMGA2-siRNA (lane 1), and p21, p53 expression of HMGA2 in non-transfected Y79 cells (lane 2), marked increase of p21, p53 expression in Weri Rb 1 cells treated with HMGA2 siRNA (lane 3), p21, p53 expression in non transfected Weri Rb1 cells (lane 4). 'T' indicates HMGA2-siRNA treated and 'C' indicates untreated control. B: The graphical

representation of increased caspase 3 expression in HMGA2 siRNA transfected RB cells compared to the non transfected RB cells by flow cytometric analyses. The error bars represent the standard deviation of triplicate values.

5.2.4.9. qRT–PCR confirmation of microarray analysis in HMGA2 silenced retinoblastoma cells (Y79 and Weri Rb1)

The gene expression level of nine genes (*ELK1, CDK6, E2F4, GTSE1, DRAM, CDH1, SNAI1, MMP 2, and MMP 9*) in the microarray analysis was consistent with the qRT–PCR findings in the transfected Y79 cells. However, a few genes in the post-transfected Weri Rb1 cells differed in levels of expression with respect to microarray findings of transfected Y79 cells. These genes include *ELK1, CDK6, E2F4* and especially *SNAI1* gene which were significantly down-regulated in Y79 cells but was not down-regulated to the same extent in the *HMGA2*-silenced Weri Rb1 cells [that is, the expression level was not below the −1.0 cut off value; **Figure 5.2.9**].

5.2.4.10. Constitutive gene expression of deregulated genes in retinoblastoma primary tumors with qRT–PCR

The expression of the selected panel of genes (*ELK1, CDK6, E2F4, GTSE1, DRAM, CDH1, and SNAI1*) was compared for their relative expression in non-transfected primary RB tumors. We observed an inverse correlation of gene expression between the untransfected tumors and the *HMGA2*-silenced RB cells **[Figure 5.2.9; 5.2.10]**. For the ten RB tumor samples analyzed, the average levels of gene expression were as follows: *ELK1* (9.21), *GTSE1* (6.23), *CDK6* (10.76), *E2F4* (10.51), *DRAM* (−4.79), *CDH1* (−0.430), and *SNAI1* (3.60) **[Table 5.2.2]**

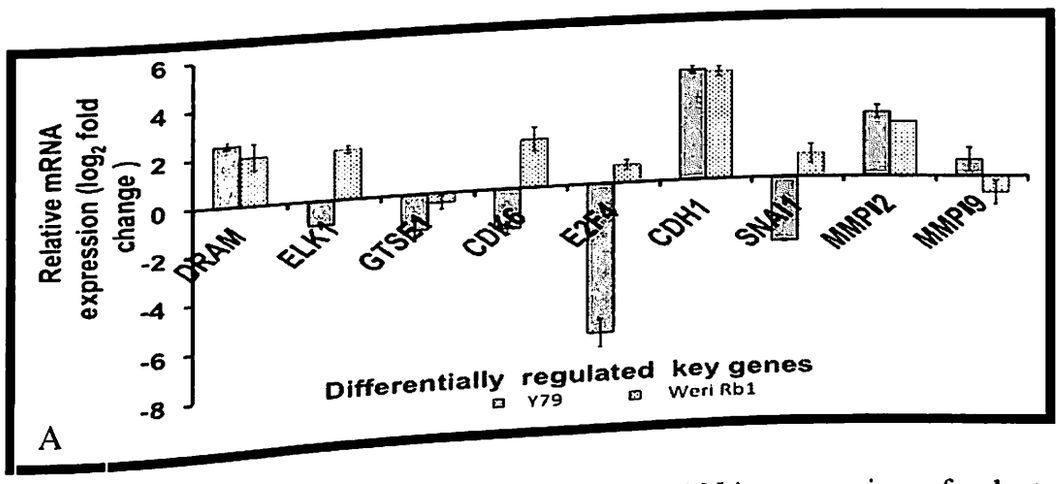

Figure 5.2.9: Microarray results validation. A: The mRNA expression of selected genes from microarray data was confirmed using real time quantitative reverse transcriptase PCR (qRT– PCR). The black bars represent the mRNA levels quantified by qRT–PCR in the

HMGA2-short interfering siRNA treated Y79 cells and the spotted bars represent the fold expression of genes in the HMGA2-short interfering siRNA treated Weri Rb1 cells. The error bars represent the standard deviation of triplicate values. Abbreviations: *DRAM represents damage-regulated autophagy modulator, ELK1: member of ETS oncogene family, GTSE1: G-2 and S-phase expressed 1, CDK6: cyclin-dependent kinase 6, E2F4:E2F transcription factor 4, p107/p130-binding, CDH1: cadherin 1, type 1, E-cadherin (epithelial) (1), SNAI1: snail homolog 1 (Drosophila), MMP2: matrix metallopeptidase 2, MMP 9: matrix metallopeptidase 9.*

B: Schematic representation of the difference in the gene expressions between the two RB cell lines (Y79 and Weri Rb1) in post-*HMGA2* siRNA transfection.

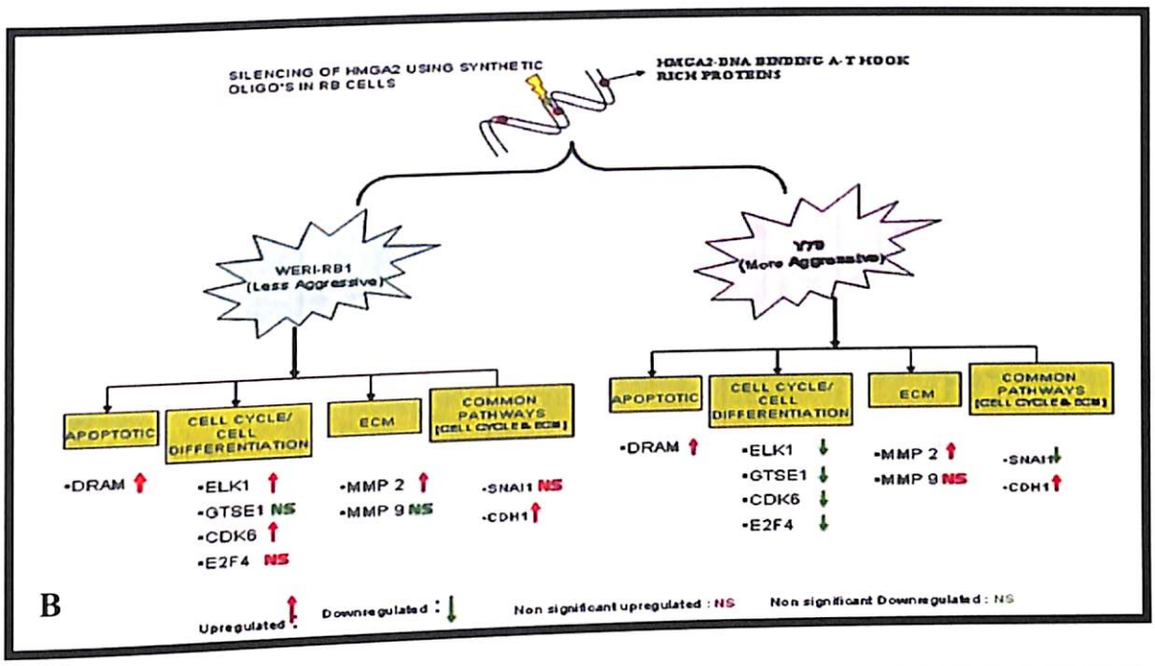

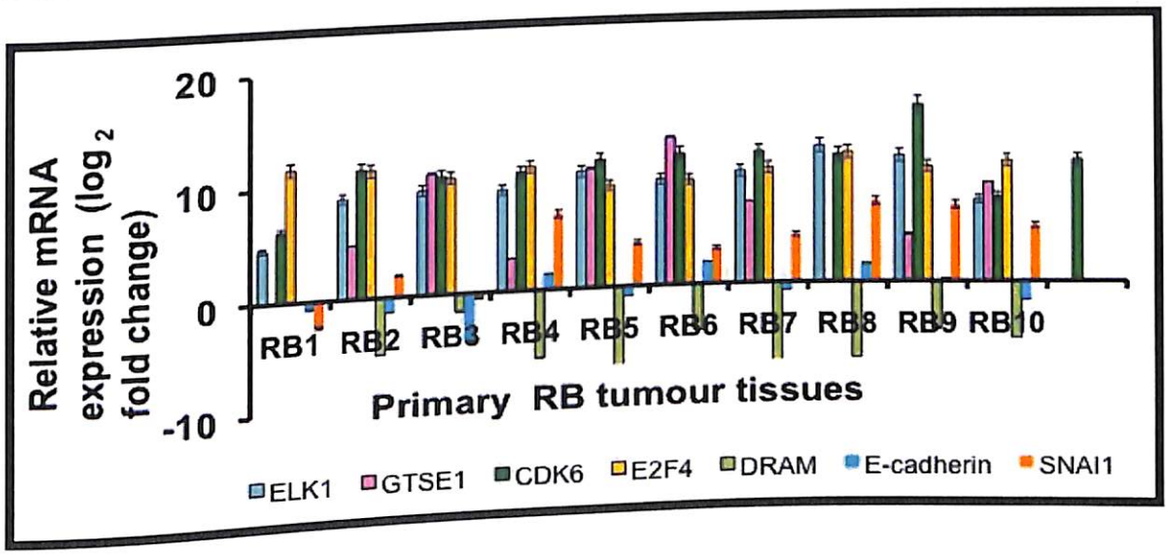

Figure 5.2.10: Gene expression in RB. The constitutive mRNA expression of selected genes from microarray data in RB primary tumour tissues (n=10) using real time quantitative reverse transcriptase PCR (qRT– PCR). The error bars represent the standard deviation of triplicate values.

Table 5.2.2: *Gene expressions in RB. Clinico-pathological features of the primary RB tumours following the International Intraocular Retinoblastoma Classification (IIRC) with gene expression (by qRT-PCR)*

S.NO	Age (Yrs)/ Sex	Clinico-Pathological features	Log $_2$ ratio fold change						
			ELK1	GTSE1	CDK6	E2F4	DRAM	CDH1	SNAI1
1	4/M	OS:PD, CI >3mm thickness, pre-lam,inv of anterior & middle portion of sclera by the tumor cells	++	-	++	++	-	NS	+
2	3/F	OS: WD with formation of fleurettes, pre-lam inv ON	++	++	++	++	+	NS	++
3	2/M	OS: WD, CI >3mm, tumor cells invading the anterior, middle and posterior border of sclera	++	++	++	++	+	+	NS
4	4/M	OD: PD, full thickness diffuse CI >3mm, tumor cells touching the anterior border of scelra, pre-lam of ON	++	++	++	++	+	NS	++
5	8/ F	OD: UD, CI >3mm, tumor touching anterior fibres and outer margins of sclera, inv of pre-lam, post lam portion of ON.	++	++	++	++	+	NS	++
6	6mon/F	OS: MD, CI>3mm, pre-lam inv and post-lam inv ON.	++	++	++	++	+	+	++
7	3/ M	OS: PD, focal CI <3mm.	++	++	++	++	+	NS	++
8	5/M	OD: UD pre-lam invn of ON	++	-	++	++	+	NS	++
9	2/F	OD: PD, CI-10mmx7mm. Tumor cells are invading the anterior & middle portion of sclera.	++	++	++	++	+	NS	++
10	1/F	OS: WD, focal CI <3m.	++	++	++	++	+	NS	++

F: female; M: male; MD, moderately differentiated; PD, poorly differentiated; WD, well differentiated; OD, right eye; OS, left eye; CI: Choroidal invasion; inv: Invasion; pre-lam: pre-laminar; post-lam: post-laminar; ON, optic nerve. ++: Up-Regulated genes; +: Down – Regulated; -: Negative; **NS**: Not significant fold change.

5.2.4.11. *Zymographic determination of matrix metalloproteinase activity in the transfected Y79 and Weri Rb1 with zymography*

Though there was increased expression of MMPs in post-transfected RB cells especially *MMP2* at the mRNA level, activity staining with zymography did not reveal a substantial difference between the pre- and post-transfected cells [Y79 showed a 5.6% increase and Weri Rb1 showed a 4.6% decrease compared to the control; **Figure 5.2.11**]

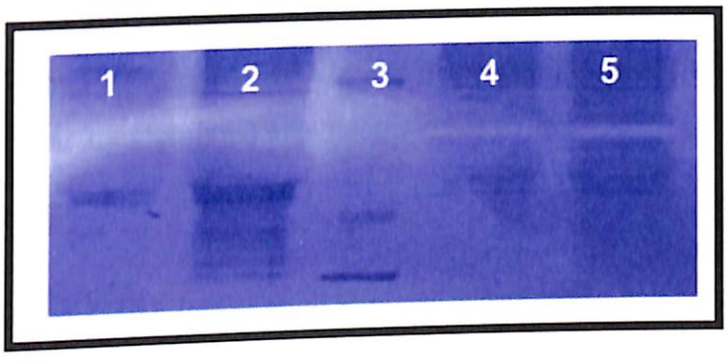

Figure 5.2.11: Zymography in RB cell lines. Effect of small interfering RNA on the expression of high mobility group A2 (HMGA2) in RB (Y79, Weri Rb1) cells *in vitro.* Zymography analysis demonstrates strong activation of MMPs in Y79 cells (lane 4), mild increase of MMPs activation in Y79 cells treated with HMGA2-siRNA (lane 5), strong activation of MMPs in Weri Rb1 cells (lane 2), mild decrease of MMPs activation in Weri Rb1 cells treated with HMGA2-siRNA (lane 1), protein molecular weight ladder (lane 3).

5.2.5. Discussion

Chau et al. 2003, reported that the HMGA2 protein contributed to the neoplastic transformation of retinal cells, and the authors mapped two transcription initiation sites and positive regulatory elements within the Weri Rb1 cells (Chau et al. 2003). The findings of Chau et al.2003, suggested that *HMGA2* could become a therapeutic target, either by blocking HMGA2 protein expression in RB cells or by inhibiting expression of the *HMGA2* gene by targeting its promoters (Chau et al. 2003). In the present study, we investigated the molecular pathways deregulated by HMGA2 in RB cells, by transient silencing of the *HMGA2* gene in *in vitro* models of RB (Y79 and Weri Rb1).

The cell cycle assay **[Figure 5.2.4]** showed a marked transition in the G_1/S phase with an increase in dead cell percentage. Further, this result is substantiated with the significant up-regulation of p21/CDKN1A (log transformed ratio = 2.93), which is a direct target of

miR-106b as it plays a key role in miR-106b induced cell cycle growth (Ivanovska et al. 2008).

HMGA2, as DNA binding proteins often referred to as architectural transcriptional factors, specifically interact with several transcription factors (NF-κB, ATF-2/c-Jun, Elf-1, Oct-2, Oct-6, SRF, NF-Y, PU-1, RAR) and participate in forming stereospecific multiprotein enhanceosome complexes (Reeves and Nissen 1990). Silencing the *HMGA2* gene in the RB cell lines (Y79, Weri Rb1) revealed deregulation of many functional genes. Their possible molecular mechanisms are discussed as follows.

The down-regulation of *GTSE1* (G2 and S phase-expressed-1), a microtubule localized protein (Monte et al. 2003), in the *HMGA2* siRNA treated RB cells (Y79 and Weri Rb1) and its up-regulation in primary RB tissues were validated. The *GTSE-1* protein negatively regulates p53 transactivation and p53-dependent apoptosis. The inhibition of *HMGA2* gene expression in RB cells inhibited cell proliferation, which corroborates with earlier studies in the nude mice model of RB (Chau et al. 2003). This study reveals the up-regulation of the apoptotic genes, namely, *DRAM*, (damage-regulated autophagy modulator), a critical effector of p53- induced autophagy (Crighton et al. 2006) in post-*HMGA2* silenced RB cells (Y79 and Weri Rb1). The constitutive expression of *DRAM* was down-regulated in primary RB tumors. The up-regulation of other p53-regulated genes involved in initiating apoptosis such as *ATM*, *PUMA/BB3*, *NOXA*, *FOXO4*, and *PTEN* (from the whole genome cDNA microarray analysis of *HMGA2* siRNA treated Y79 cells) is indicative of p53-dependent apoptosis (Yu et al. 2001). This was further validated by the observed protein over-expression of p53, p21, and caspase 3 in post-transfected Y79 and Weri Rb1 cells **[Figure 5.2.8]**. The induction of PUMA (p53 up-regulated modulator of apoptosis) by the downstream molecules of TNF-α mediated apoptosis may mediate p53-independent apoptosis. The genes involved in this pathway are ATF and CREB families, which are increased in the post-*HMGA2* silenced RB cells (Jeffers et al. 2003). Taken together, p53-dependent and independent pathways seem to be involved in inducing apoptosis of *HMGA2*-silenced RB cells.

The study also shows the down-regulation of various transcription factors and cyclin-dependent kinases involved in cell cycle regulation, namely, *E2F4* and *CDK6* in *HMGA2* post-silenced Y79 cells. Cyclin-dependent kinases (CDKs) are important regulators of cell cycle progression. *CDK6*, which first appears in the mid-G_1 phase, is important for G_1 phase progression and G_1/S transition. Coupled with *CDK4*, they negatively regulate the activity of the RB tumor suppressor protein (The PubMatrix database). Exit from the G_1 phase of cell cycle division is regulated by phosphorylation of pRb by cyclin D/*CDK4* and cyclin D/*CDK6* complexes. This results in the suppression of the cell cycle. The constitutive expression of *E2F4* and *CDK6* genes was increased in our study cohort of RB tumor tissues analyzed here [**Figure 5.3.10**]. Another *E2F* family transcription factor, *E2F3*, was earlier reported to be overexpressed in RB (Orlic et al. 2006). Increased expression of *CDK6* in other primary tumors such as in squamous cell carcinoma (Ch'ng et al. 2006, Piboonniyom et al. 2002), basal cell carcinoma (Eshkoor et al. 2009), medulloblastoma, and B-cell lymphoproliferative disorder (Chen D. et al. 2009) have been reported in which increased *CDK6* expression has been correlated with induced cell proliferation and malignant transformation coupled with cyclins. Thus, the significant down-regulation of *CDK6* coupled with the cyclins, *CCND2* and *E2F4*, in post-*HMGA2* silenced Y79 cells substantiates the suppression of cell proliferation. There are a few differences in the gene expression of *E2F4*, *CDK6*, and *ELK1* between the two RB cell lines (Y79, Weri Rb1) [**5.2.9 A&B**]. This is possibly because of the differential activation and dominance of specific apoptotic and cell cycle pathways that may relate to tumor aggressiveness. Weri Rb1 represents a non-metastatic model of RB while Y79 represents more aggressive and metastatic characteristic of RB (Chevez-Barrios et al. 2000).

The other gene modulations in the current study include the significant down-regulation of SNAI1 (Snail, a transcriptional repressor of E-cadherin) along with simultaneous up-regulation of E-cadherin in the post-*HMGA2* silenced RB cells. *HMGA2* silencing induced transcriptional derepression of E-cadherin with decreased Snail has been reported in a pancreatic cancer cell line (Watanabe S. et al. 2009). The constitutive expression of *SNAI1* and *CDH1* in RB tumor tissues revealed the inverse correlation between them [**Figure 5.2.10**]. This has also been confirmed in hepatocellular carcinoma (Jiao et al. 2002), oral squamous cell carcinoma (Yokoyama et al. 2001), melanoma (Poser et al. 2001), and breast carcinoma (Blanco et al. 2002). Increased Snail expression resulted in tumor

progression and metastasis in MDA-MB-231 cells (Olmeda et al. 2007), mouse skin carcinoma cell lines (Olmeda et al. 2008), and tongue squamous cell carcinoma (Wang C. et al. 2012). This deregulation of Snail and E-cadherin may contribute to the up regulation of the extracellular matrixes such as laminins α3, β3, γ2 (laminin 5: LN 5), and type IV collagen, and down regulation of laminin α5 and integrin α5. The enhanced expression of laminins, especially laminin 5 and type IV collagen observed here in the HMGA2 silenced Y79 cells, may indicate decreased cell detachment (Haraguchi et al. 2008). The present finding of *SNAI's* regulation in the expression of laminins, integrins, and other extracellular matrix proteins supports the role of *SNAI's* cell adhesion mechanisms involved in cancer progression. Thus, Snail-mediated modulation of ECM proteins serves as one of the mechanisms by which cancer progression is controlled by *HMGA2* silencing (Barrallo-Gimeno and Nieto 2005, Haraguchi 2009).

Matrix metalloproteinases (MMPs) have a role in tumor progression that is determined by a balance of its activators and inhibitors (Adithi et al. 2007, Bein and Simons 2000, Rodriguez-Manzaneque et al. 2001, Taraboletti et al. 2000, Yang Z. et al. 2001). In the present study, the increase in the expression of some MMPs in the treated cancer cells may not be sustained, as their positive and negative regulators do not show any significant increase or decrease in their expression. Up-regulation of *MMPs* (*MMP2, MMP3, MMP7, and MMP9*) with no significant change in the expression of their inhibitors (TIMPs) was observed in post-HMGA2 silenced RB cells. The microarray analysis did not reveal significant changes in the levels of thrombospondin-2 (activator of MMP2) and thrombospondin-1 (activator of MMP9) (Poser et al. 2001, Yokoyama et al. 2001). Thus, the increased level of MMPs is only a transient expression while there is no corresponding increase of their activators. This is further confirmed by our zymography assay of MMP activity that revealed only a mild change in MMP activity in the *HMGA2*-silenced RB cells compared with control cells. In the post-*HMGA2* silenced Y79 cells, a 5.6% increase in MMP activity while a 4.6% decrease in MMP activity in Weri Rb1 cells was observed relative to control cells [**Figure 5.2.11**].

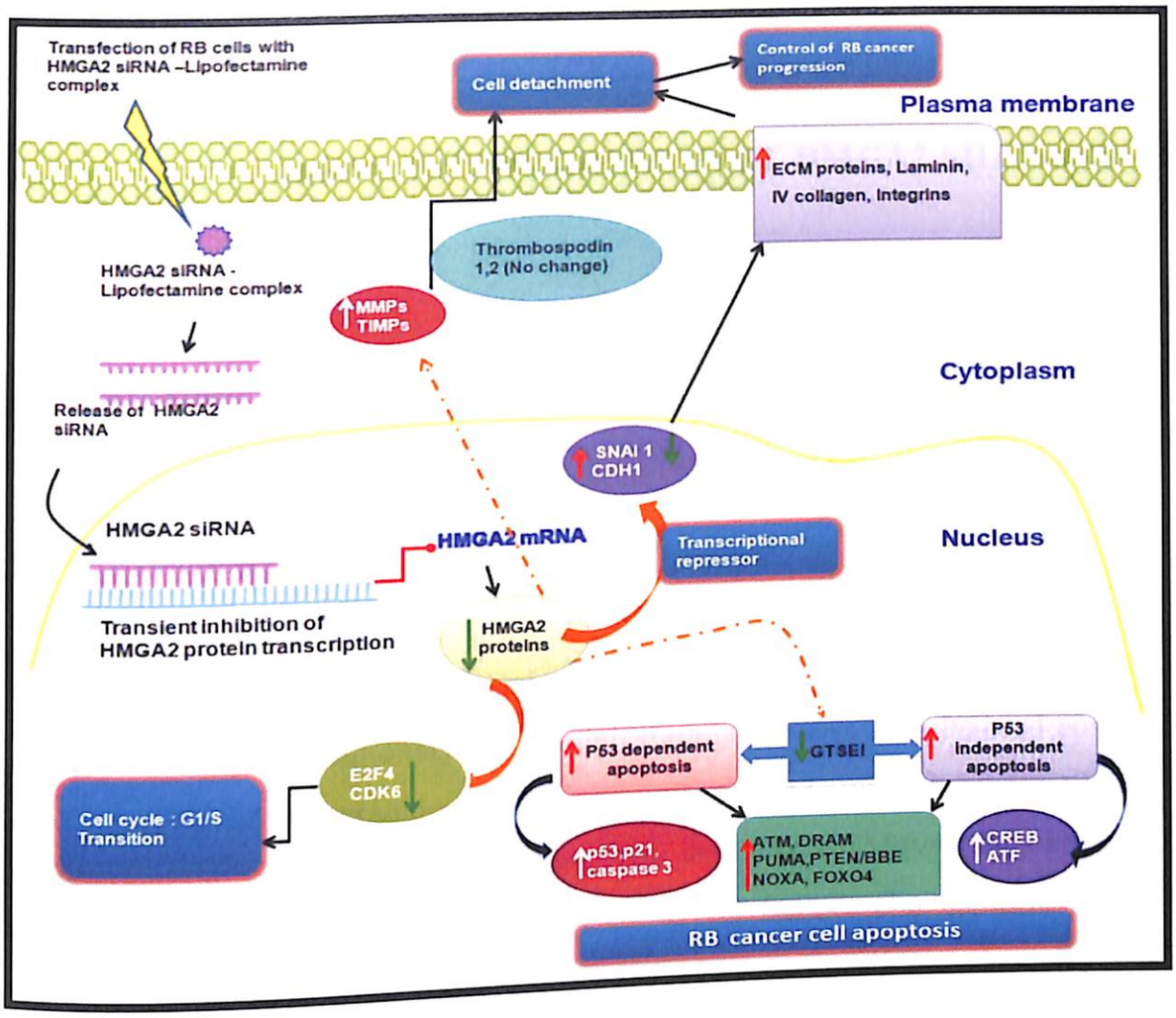

Figure 5.2.12: Dys-regulation of genes. Schematic representation of dys-regulation of genes at various cellular process.The effect of *HMGA2* gene silencing has resulted in the activation of CDH1, its transcriptional repression *SNAI1*, suppression of *GTSEI* , resulting in the activation of p53 dependent and independent apoptotic pathways and suppression of *E2F4*, *CDK6* contributing to the alteration in the cell cycle phase.

5.2.6. Conclusion

In conclusion, *HMGA2* silencing in RB cancer cells resulted in the deregulation of genes responsible for apoptotic, cell cycle, and cell adhesion mechanisms. These may be some of the mechanisms by which cancer cell progression are suppressed in *HMGA2*-silenced RB cells. These findings are further substantiated by the inverse correlations between the deregulated gene expression in the *HMGA2*-silenced RB cells and in the primary RB tumor tissues. The *HMGA2* gene silencing approach is thus suggested to be a promising strategy in RB therapy.

CHAPTER 5.3: INTEGRATED APPROACH TO ELUDICATE THE GENE-miRNA NETWORKING POST-HMGA2 SILENCED RB CELLS

5.3. Introduction

[#]Computational tools are widely used to complement biological investigations, especially in global gene expression analysis and high throughput assays. Advanced computational analyses such as integrated analyses of mRNA and miRNA expression, provide information on several regulatory networks in cancers (Moser and Fritzler 2010), including retinoblastoma (RB), a peadiatric ocular tumor. The identification of these molecular networks could implicate potential genes and miRNAs that may behave as biomarkers. It will also help better understand RB biology and clinical management.

The current RB management is enucleation (removal of eye), chemotherapy and/or focal therapy. Targeted therapy is gaining importance in the management of RB (Hanahan and Weinberg 2011, Sachdeva and O'Brien 2012, Zhang J. et al. 2012a); Gene expression profiling of RB tumors has helped to characterize cell signalling and the molecular pathways involved in its pathogenesis (Enerly et al. 2011, Ganguly and Shields 2010, Nalini et al. 2013). Earlier reports on relative miRNA profiling between normal and RB tumor tissues, and global gene dys-regulation studies (*HMGA2, Tiam 1, EpCAM*) have indicated several aberrant miRNAs and their regulatory genes (Conkrite et al. 2011,

3. [#] ***The results presented in this chapter have been published: Nalini Venkatesan P. R. Deepa, Madavan Vasudevan, Vikas Khetan, Ashwin M. Reddy, Subramanian Krishnakumar, Integrated analysis of dysregulated miRNA-gene expression in HMGA2-silenced retinoblastoma cells, Bioinform Biol Insights. 2014 Sep 4; 8: 177-91.***

Kandalam et al. 2012, Martin et al. 2013, Mitra et al. 2010, Mitra et al. 2011b, Subramanian et al. 2013, Venkatesan et al. 2012, Xu X. et al. 2011b).

We had earlier reported in the previous chapter 5.2, that silencing of *HMGA2* reduced cell proliferation in cultured RB cells (Venkatesan et al. 2012). HMGA2, a non-histone chromosomal protein, is highly expressed during embryogenesis and in various malignant tumors including RB (Fusco and Fedele 2007, Venkatesan et al. 2009). This protein contains structural DNA binding AT-rich domains, and at the C-terminus these domains undergo conformational change due to their interaction with the B form of DNA. This conformational change plays a crucial role in the transcriptional regulation of other proteins which are also involved in the epithelial mesenchymal transition (EMT) pathways (Wu et al. 2011). Over-expression of HMGA2 protein is seen in several malignancies and may be due to the suppression of miRNAs, namely miR-15, miR-16, miR-196 (De Martino et al. 2009, Kaddar et al. 2009) and let-7 (Lee and Dutta 2007). In a study on pituitary tumors, E2F1 activation through displacement of HDAC1 by HMGA2 resulted in pRB inactivation (Fedele et al. 2006).

Reports from, *in vivo* and *in vitro* studies have demonstrated a reduction in cell proliferation in various cancers including RB by blocking the HMGA2 protein synthesis using antisense methodology (Chau et al. 2003, Fedele et al. 2006). Our previous study (Please refer chapter 5.2) (Venkatesan et al. 2012), implicated changes of several abnormal gene networks including mitogen-activated protein kinase (MAP) kinase, JAK/STAT, Ras pathway, Ras induced ERK1/2 and tumor protein 53 (P53) dependent pathways in HMGA2 silenced RB cells.

In the present chapter, using computational and experimental tools, the role of dys-regulated miRNAs in HMGA2-silenced retinoblastoma cells was investigated. Their association with the gene targets has been analysed using integrated array analysis. The specific role of miR-106b-25 cluster in RB has also been examined.

5.3.3. Methods

5.3.3.1. Primary RB tumor samples

Fresh frozen tumor samples were collected from 20 enucleated eyeballs of RB patients reported at Larsen & Toubro Department of Ocular Pathology, Medical Research Foundation, Sankara Nethralaya as part of RB management (2010 – 2011) and utilised for research purpose. The Institutional Ethics Committee of Vision Research Foundation, Sankara Nethralaya (Chennai, India) has reviewed and approved the study (Institutional ethics clearance number: 2009-146p). The fresh adult retina were collected from 3 cadaveric eyeballs (received at C.U Shah eye bank, Medical Research Foundation Sankara Nethralaya, http://www.sankaranethralaya.org/eye-bank.html) during the year 2010 were included in the study. The collected tumour samples and the normal retina were snap frozen in liquid nitrogen and stored at -80°C until further use.

The haematoxylin and eosin stained RB sections were reviewed microscopically and graded by an ocular pathologist. The clinico-pathological features tabulated in table 3 are based on the tumour invasion of the choroid, optic nerve or orbit. These RB tumors were recorded as per the earlier report (Sastre et al. 2009).

5.3.3.2. Cell culture

Human RB cell lines (Y79, Weri Rb1, Riken cell bank, Japan) were used as *in vitro* model udy the significance of the *HMGA2*, *hsa-miR-106b-25* clusters in RB. The cultures are d as described in the section 4.1.3.

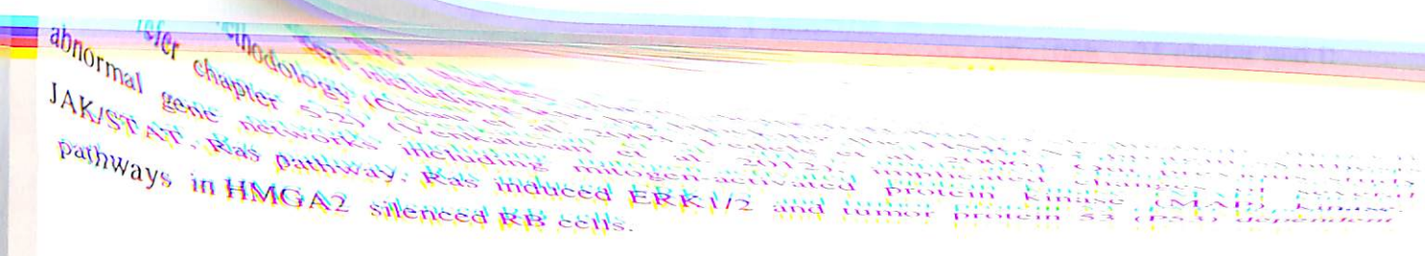

In the present chapter, using computational and experimental tools, the role of dys-regulated miRNAs in HMGA2-silenced retinoblastoma cells was investigated. Their association with the gene targets has been analysed using integrated array analysis. The specific role of miR-106b-25 cluster in RB has also been examined.

5.3.3. Methods

5.3.3.1. Primary RB tumor samples

Fresh frozen tumor samples were collected from 20 enucleated eyeballs of RB patients reported at Larsen & Toubro Department of Ocular Pathology, Medical Research Foundation, Sankara Nethralaya as part of RB management (2010 – 2011) and utilised for research purpose. The Institutional Ethics Committee of Vision Research Foundation, Sankara Nethralaya (Chennai, India) has reviewed and approved the study (Institutional ethics clearance number: 2009-146p). The fresh adult retina were collected from 3 cadaveric eyeballs (received at C.U Shah eye bank, Medical Research Foundation Sankara Nethralaya, http://www.sankaranethralaya.org/eye-bank.html) during the year 2010 were included in the study. The collected tumour samples and the normal retina were snap frozen in liquid nitrogen and stored at -80°C until further use.

The haematoxylin and eosin stained RB sections were reviewed microscopically and graded by an ocular pathologist. The clinico-pathological features tabulated in table 3 are based on the tumour invasion of the choroid, optic nerve or orbit. These RB tumors were recorded as per the earlier report (Sastre et al. 2009).

5.3.3.2. Cell culture

Human RB cell lines (Y79, Weri Rb1, Riken cell bank, Japan) were used as *in vitro* model to study the significance of the *HMGA2*, *hsa-miR-106b-25* clusters in RB. The cultures are maintained as described in the section 4.1.3.

5.3.3.3. Transient transfection in RB cells (Y79, Weri Rb1)

The transfection method of silencing *HMGA2* using Human *HMGA2* siRNA (Hs_*HMGA2*_6) was performed as described in section 4.2.9.

5.3.3.4. miRNA profiling of post-HMGA2 silenced Rb cells (Y79)

The miRNA profiling in the post-*HMGA2* silenced cells (Y79) was performed using Human_miRNA_version 3.8 x 15k array (Agilent Technologies, Part Number G2565CA) as described in the section 4.2.7.

5.3.3.5. *Integrated miRNA- mRNA analysis in HMGA2 silenced RB cells (Y79)*

The methods followed in the integrated miRNA-mRNA analysis in HMGA2 silenced RB cells is described schematically below [**Figure 5.3**].

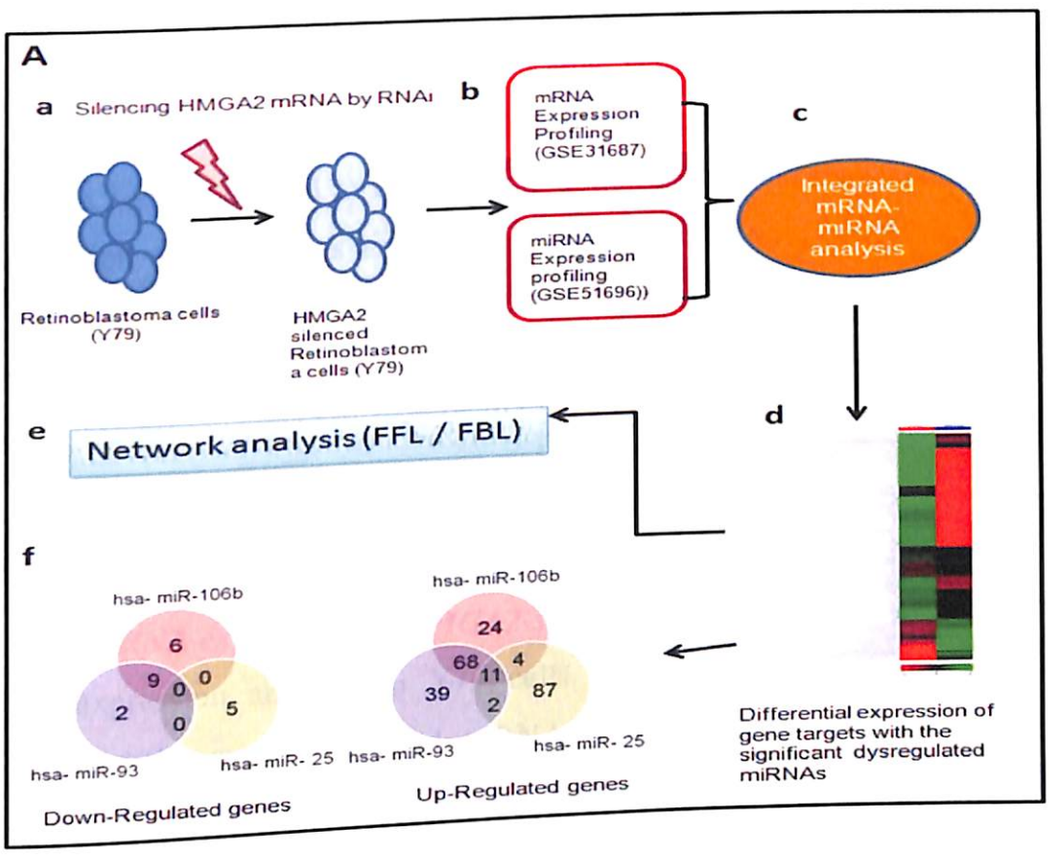

Figure 5.3.1: Steps followed in the study. Schematic representation for the overall steps in the determination of de-regulated miRNAs in *HMGA2* silenced Y79 cells: a: Silencing of HMGA2 in the RB cells (Y79) using synthetic oligos using RNAi method, b: mRNA transcripts and miRNA expression levels were profiled using microarray, c: Integration of significantly dysregulated mRNA transcripts with its regulatory miRNA was annotated, d: Hierarchical cluster of the GO functions of the up/down regulated genes by the 3 miRNAs of miR-106b ~ 25 cluster; e: The number of up-regulated and the down-regulated genes targeted by the miR-106b ~ 25 cluster and f: Network analysis (Feed Forward Loop (FFL) / Feed Backward Loop(FBL) was annotated.

5.3.3.6. *Experimental validation in antagomirs (anti-hsa-miR-106b-25) treated RB cells*

qRT-PCR, cell proliferation assay (MTT assay), apoptosis assay (Annexin V FLUOS stain), scratch assay (wound assay) and western analysis (p21, Bim) antagomirs treated RB cells were analysed by following the protocol described in chapter 4.2.5.

5.3.3.7. Statistical analysis

Microarray data was analyzed using Gene spring software (GX version 12.5, Agilent Technologies, Santacruz, California, USA). Unpaired Student's *t*-test for *p*-value calculation and Benjamini Hocheberg based FDR correction was applied. Genes/miRNAs that are lesser than or greater than 1.0 fold differentially expressed with a $p<0.05$ were considered as true differentials. ANOVA (*Post Hoc, Dunnett t-test*) was used to compare the controls and test variables for cell proliferation using SPSS software (version 12.0). Paired student's *t*-test was used to compare the untransfected and transfected experiment groups for scratch assay. Values expressed for cell proliferation, apoptosis and scratch assay are mean ± SD of at least three experiments. There were considered statistically significant for $p \leq 0.05$.

5.3.4. Results

5.3.4.1. miRNA expression in HMGA2-silenced RB (Y79) cells

The miRNA expression analysis in Y79 cells revealed 188 differentially expressed miRNAs. These differentially regulated miRNAs (supplementary file 1) include 86 up-regulated and 102 downregulated miRNAs. The family cluster classification of up-regulated miRNAs using TAM tool (Lu et al. 2010) revealed three main clusters: hsa-miR-let7e clusters (miR-99b, miR125a), hsa-miR-506 cluster (miR-513a, miR-513b, miR-513c), and hsa-miR-1283 cluster. Functionally, the filtered 82 up-regulated miRNAs were found to be involved in the activation of the caspase cascade (miR-150, miR-155), angiogenesis (miR-150) and activation of apoptosis, cell cycle regulation (miR-494, miR-150, and miR-155), cell proliferation (miR-150), and tumor suppression (miR-125a, miR-150, and miR-155). From this, it appears that miR-150 and miR-155 expressions are common to the key regulatory cellular functions in RB.

The down-regulated 102 miRNAs were categorized into 15 families using TAM tool. **Table 5.3.1** lists the various miRNA clustering in the specific families along with their function. The suppression of hsa-miR-17 cluster, its paralogs, hsa-miR-106a cluster, hsa-miR-106b cluster, hsa-miR-23b family, hsa-miR-130 family following the silencing of HMGA2 oncogene indicates a positive regulation of these miRNAs by *HMGA2*. The pathway analysis of these dysregulated miRNA's using TAM tool revealed the down

regulation of AKT pathway ($p<0.001$). The miRNA involved in this pathway was determined as miR-20a, miR-18a, miR-7, miR-17, miR-19a, miR-331, miR-19b, miR-26a, miR-92a, miR-21 and miR-221. The functional annotations of these deregulated miRNAs are found to be involved in angiogenesis, apoptosis, cell cycle regulation, cell differentiation, cell proliferation, tumor suppression and oncomirs. These data have been submitted to the NCBI: GEO data base (GSE51696).

Table 5.3.1: List of de-regulated miRNAs. Shows the list of miRNAs de-regulated in the post-HMGA2 RB cells (Y79) revealed in the microarray analysis and their functional annotations.

S.No	Functional annotation of dysregulated miRNA	Dysregulated miRNAs	
		Up-regulated miRNA	Down-regulated miRNA
1.	Angiogenesis	*miR-150*	*miR-15a, miR-let7b, miR-18a, miR-let7f, miR-21, miR-126, miR-16, miR-19a, miR-19b, miR-378, miR-27b, miR-130a, miR-20a, miR-92a, miR-17, miR-221*
2.	Apoptosis	*miR-494,miR-150,miR-155*	*miR-15a, miR-15b, miR-21, miR-148a, miR-221, miR-7g, miR-19a, miR-19b, miR-182, miR-27a, miR-34b, miR-34c, miR-29b, miR-29a, miR-20a, miR-17, miR-16, miR-92a, miR-96, miR-18a, miR-7, miR-26a, miR-195*
3.	Cell cycle	*miR-494,miR-150,miR-155*	*miR-15a, miR-24, miR-15b, miR-21, miR-19a, miR-140, miR-107, miR-221, miR-let-7b, miR-7a, miR-124, miR-7g, miR-331, miR-19b, miR-182, miR-27a, miR-27b, miR-34b, miR-185, miR-29b, miR-20a, miR-17, miR-16, miR-34c, miR-92a, miR-424, miR-96, miR-18a, miR-9, miR-195.*
4.	Cell differentiation	-	*miR-15a, miR-424, miR-16*
5.	Cell proliferation	*miR-150*	*miR-15a, miR-24, miR-15b, miR-124, miR-21, miR-let7d, miR-16, miR-9, miR-27b, miR-130a, miR-34b, miR-34c, miR-140, miR-29b, miR-221*
6.	Tumour suppressors	*miR-125a*	*miR-15a , miR-let7b, miR-7a, miR-7f, miR-7g, miR-7d, miR-16, miR-7i, miR-7e, miR-26b, miR-26a, miR-101, miR-34b, -c, miR-195, miR-124, miR-125a, miR-126, miR-29a*
7.	Oncomirs	*miR-150,miR-155*	*miR-24, miR-20a, miR-20b, miR-21, miR-17, miR-106b, miR-19a, miR-19b, miR-107, miR-27a, miR-18a, miR-92a, miR-93, miR-18b, miR-221*
8.	Akt pathway	-	*miR-20a, miR-18a, miR-17, miR-19a, miR-331, miR-26a, miR-21 and miR-221*

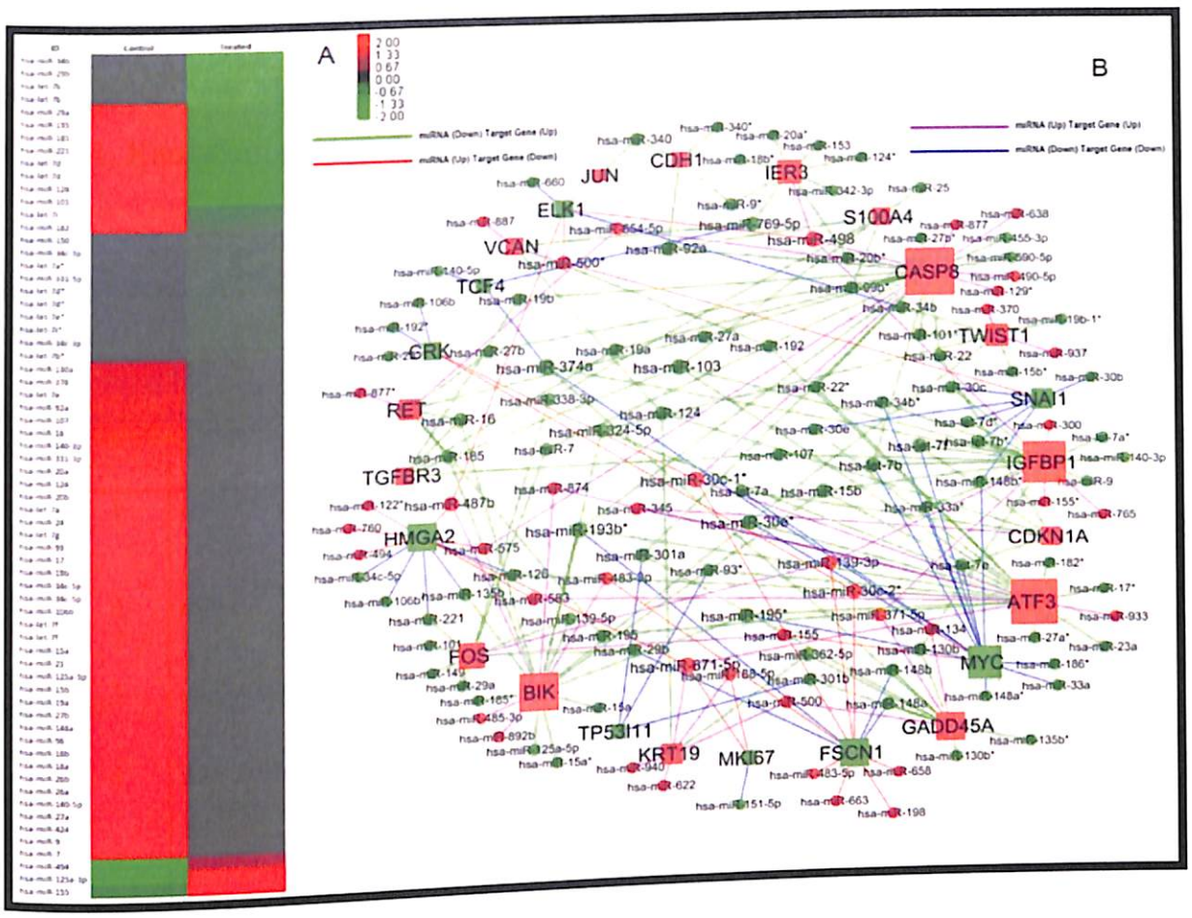

Figure 5.3.2: Molecular changes in the study

A: The miRNA expression profile in *HMGA2* siRNA treated Y79 cells: Hierrarchial cluster represents the expression profile of 100 differentially altered miRNAs in post *HMGA2* silenced Y79 cells compared with untreated RB cells. Red line indicates up-regulation, while green line indicates down-regulation in fold change relative to untransfected Y79 cells.

B: miRNA and Target Gene Regulatory Network Modeling: The key miRNAs that targets differentially expressed genes are presented here (Cytoscape v 2.8). Circles and squares indicate miRNA and genes respectively, red colour indicates up-regulation and green colour indicates down-regultion, Red colour indicates up-regulation while green colour indicates down-regulation in fold change relative to untreated Y79 cells. The colour lines represent: green line describes the positive regulation between miRNA (down) and target gene (up); red line describes the positive regulation between miRNA (up) and target gene (down); pink line describes the positive regulation between miRNA (up) and target gene (up) and blue line describes positive regulation between miRNA (down) and target gene (down).

The sequence alignment of the HMGA2 mRNA with the conserved miRNAs described above was carried out using the online tool: microRNA.org-Targets and expression

(www.microRNA.org) to confirm its regulatory networks. The output of this analysis has been tabulated in [**Table 5.3.2**]. Among this list, we could identify the suppression of two oncomir families - hsa-miR-17-92 cluster and hsa-miR-106b cluster with good miR-SVR scores, which are also found in other cancers, including RB (Cai et al. 2011, Conkrite et al. 2011, Kandalam et al. 2012).

Table 5.3.2: Alignments of conserved miRNAs with HMGA2 mRNA. The alignments of the conserved miRNAs identified in HMGA2 silenced RB (Y79) cells with the HMGA2 mRNA.

S.No	miRNAs	Location	Alignment	mirSVR score
1.	*miR-150*	2615	3' gugaccauguucccaACCCUCu 5' 5' uauaguuuauuuuugUGGGAGa 3'	-0.6787
2.	*miR-17*	1197	3' gauGGACGUGACAUU--CGUGAAAc5' 5' aucUCUUCAUUCAAACUGCACUUUu 3'	-0.5950
3.	*miR-106a*	1197	3'gauGGACGUGACAUU--CGUGAAAa5' 5'aucUCUUCAUUCAAACUGCACUUUu3'	-1.2030
4.	*miR-106b*	1199	3'uaGACGUGA--CAGUCGUGAAAu 5' 5'cuCUUCAUUCAAACUGCACUUUu 3'	-0.5950
5.	*miR-93*	1197	3'gauGGACGU--GCUUGUCGUGAAAc 5' 5'aucUCUUCAUUCAAACUGCACUUUu 3'	-0.5950
6.	*miR-23b*	1979	3'ccauuagggaccgUUACACUa 5' 5'uguauuuuacacaAAUGUGAu 3'	-1.0962
7.	*miR-20a*	1197	3'gauGGACGUGAUAUU--CGUGAAAu 5' 5'aucUCUUCAUUCAAACUGCACUUUu 3'	-0.5950
8.	*miR-129-5p*	982	3'cguUCGGGUCUGGCGUUUUUc 5' 5'aucAAUUUAAAAAGCAAAAAa 3'	-1.2030
9.	*miR-26a*	546	3'ucggaUAGGAC--CU---AAUGAACUu5' 5'guauaAUCUUGUAGACACUUACUUGAu3'	-0.5528

5.3.4.2. Integrating differentially expressed miRNAs and their gene targets in HMGA2 silenced RB cells

To understand the interactions between the dysregulated miRNAs and the genes involved in cancer progression, a computational approach was adopted. The dysregulated genes in HMGA2 silenced Y79 cells obtained from cDNA microarray analysis (discussed in previous chapter 5.2) may be referred to at the NCBI: GEO database (GSE31687).

The present analysis revealed a total of 337 genes that are under the regulatory control of dysregulated miRNAs in HMGA2-silenced RB cells. Biological networks were generated by connecting the nodes (genes) and edges (type of regulation) based on Microcosm

some highly interconnected genes and their regulatory

been tabulated in [Table 5.3.2]. Among this list, we could identify

oncomir families - hsa-miR-17-92 cluster and hsa-miR-[illegible]

scores, which are also found in other cancers [illegible]

al. 2011; Sathipati et al. 2012).

Table 5.3.2: *Alignments of*

the

et al. 2012), the functional role of the miR-106b~25 cluster in RB is not understood. The present study, therefore, attempts to characterize the miR-106b~25 cluster in primary RB tissues, and in *HMGA2*-silenced RB cells.

5.3.4.3. Analysis of transcription factors, mRNA – miRNA Feed Forward Loops (FFL) and Feed Backward Loops (FBL) in HMGA2 silenced RB cells

In order to evaluate the interactions between transcription factors, genes (mRNA) and miRNAs, we carried out the feed forward and feed backward loop analysis based on data obtained from Circuits Database (Friard et al. 2010). Enriched loop connections were visualized using Cytoscape V 2.8 with nodes coloured by their fold change [**Figure 5.3.2**]. Transcription factors that were shown to regulate the differentially expressed miRNA and mRNA were identified based on its role in promoting tumorigenesis. Among these loops, we observed that the key transcription factor, *SOX5*, is regulated by the miRNAs - *hsa-miR-29a*, and *hsa-miR-9* family (*hsa-miR-9*, hsa-miR-9-3*). This has been analyzed with the corresponding dysregulated genes, as given below.

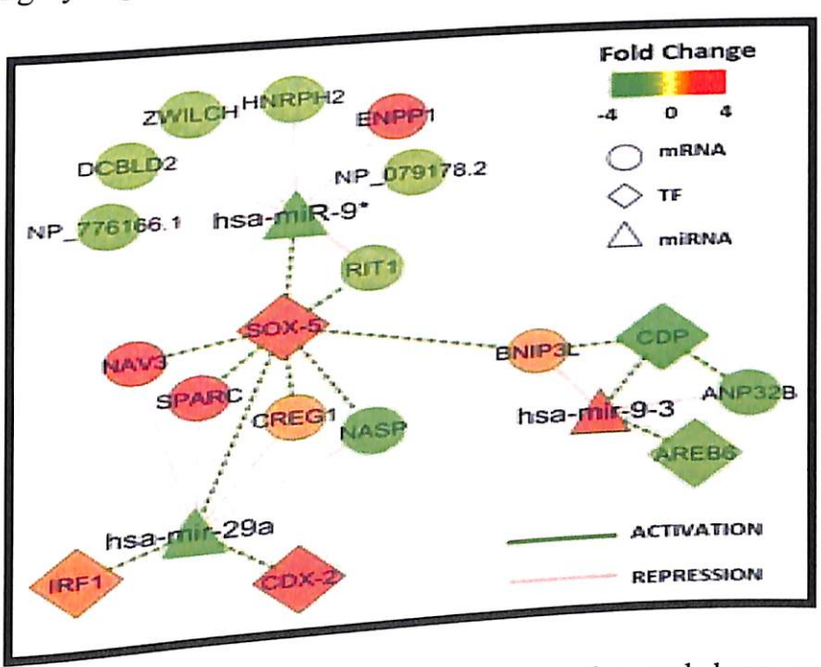

Figure 5.3.3: miRNA-TF regulatory networks. Feed forward loop network analysis representing miRNA-TF regulatory network. The network pinpoints the regulations

Database. The BAN shows some highly interconnected genes and their regulatory miRNAs. These networks are vital for tumorigenesis and cancer control [**Figure 5.3.2.B**].

Interestingly, we observed elevated numbers of cell cycle genes with a positive correlation to miR-17 ~ 92 clusters and its paralog miR-106b~25 cluster. While the biological role of the miR-17~92 cluster has been reported in RB tumorigenesis (Conkrite et al. 2011, Kandalam et al. 2012, Nittner et al. 2012), the functional role of the miR-106b~25 cluster in RB is not understood. The present study, therefore, attempts to characterize the miR-106b~25 cluster in primary RB tissues, and in *HMGA2*-silenced RB cells.

5.3.4.3. Analysis of transcription factors, mRNA – miRNA Feed Forward Loops (FFL) and Feed Backward Loops (FBL) in HMGA2 silenced RB cells

In order to evaluate the interactions between transcription factors, genes (mRNA) and miRNAs, we carried out the feed forward and feed backward loop analysis based on data obtained from Circuits Database (Friard et al. 2010). Enriched loop connections were visualized using Cytoscape V 2.8 with nodes coloured by their fold change [**Figure 5.3.2**]. Transcription factors that were shown to regulate the differentially expressed miRNA and mRNA were identified based on its role in promoting tumorigenesis. Among these loops, we observed that the key transcription factor, *SOX5*, is regulated by the miRNAs - *hsa-miR-29a*, and *hsa-miR-9* family (*hsa-miR-9*, hsa-miR-9-3*). This has been analyzed with the corresponding dysregulated genes, as given below.

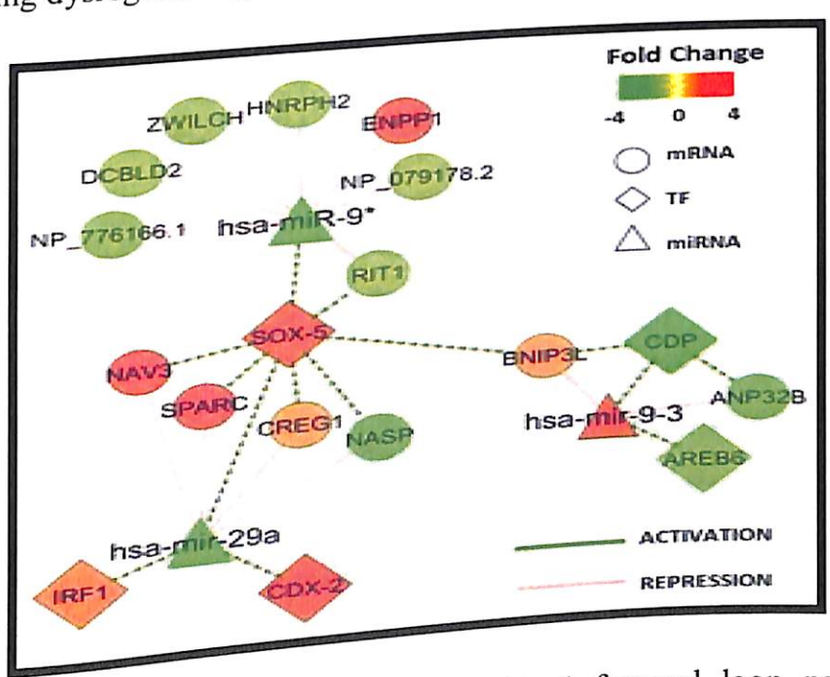

Figure 5.3.3: miRNA-TF regulatory networks. Feed forward loop network analysis representing miRNA-TF regulatory network. The network pinpoints the regulations

between the transcriptions factors (TFs), miRNA and their regulatory gene targets. The circle denotes genes, rhombus denotes transcription factors and triangle denotes miRNA. The pink line describes the repression of genes and the green line describes the activation of genes.

5.3.4.3.1. Network regulation between SOX 5, hsa-miR-29a and TFs / Genes

The predicted regulatory networks between *SOX5*, *miR-29a* and the other key regulatory transcription factors/genes derived from the integrated array in *HMGA2*-silenced RB cells shows the up-regulation of *IRF1* (gene involved in nuclear apoptosis (Kim P. K. et al. 2004)), *CDX2* (tumor suppressor gene (Zhang J. F. et al. 2013)), *SPARC* (apoptosis mediator and chemo-sensitizer (Tang M. J. and Tai 2007)), *NAV3* (navigator gene (Carlsson et al. 2012)), *CREG1* (involved in cellular senescence (Moolmuang and Tainsky 2011)) and down-regulation of *NASP* (involved in cell growth arrest (Ma W. et al. 2012).

5.3.4.3.2. Network regulation between SOX5, hsa-miR-9* and RIT1 gene

In this network, the down-regulation of *RIT1*, an oncogene (Li J. T. et al. 2003) mediated through *SOX5* and *hsa-miR-9** may be a part of the molecular dysregulation contributing to the arrest of cell proliferation in the *HMGA2*-silenced RB cells.

5.3.4.3.3. Network regulation between SOX5, hsa-miR-9-3 and TFs (AREB6/ZEB1, CDP, and ANP32B)

The present analysis reveals the link between *SOX5*, *hsa-miR-9-3*, and the down-regulated genes - *AREB6/ZEB1*, *CDP* (transcription factors (Liu Y. et al. 2012)), *ANP32B* (negative regulator of caspase 3 (Shen S. M. et al. 2010)). These gene down-regulations were observed with the concomitant induction of the pro-apoptotic gene *BNIP3L*. These results explain in part the contributors to cell growth arrest in *HMGA2* silenced RB cells.

The current FFL analysis has predicted the various networks existing between the SOX5, miRNAs (*hsa-miR-29a*, *hsa-miR-9** and *hsa-miR-9-3*) and the key regulatory genes and their gene targets in *HMGA2* silenced RB cells can be experimentally validated. [**Figure 5.3.3**]. These predicted outcomes of integrating differentially expressed miRNAs

5.3.4.4. *Experimental validation to understand the role of miR-106b ~ 25 clusters in RB*

The BAN results clearly implicated the dys-regulation of miR-106b~25 cluster in HMGA2 silenced RB cells. In order to understand the role of miR-106b~25 in RB tumorigenesis, the following experiments were performed: (a) Assessment of miR-106b~25 cluster expressions in primary RB tissues (discussed in section 5.3.3.4.1), and (b) Implication of miR-106b~25 in RB cancer cell proliferation using specific antagomirs (discussed in sections 5.3.3.4.2- 5.3.3.4.5).

5.3.4.4.1. The miR-106b~25 cluster, its direct target MCM7 are over expressed in RB primary tumors

Initially, to understand the role of *miR-106b~25* cluster in RB, the expression of this miRNA cluster was determined in RB primary tumors (n=20), using qRT-PCR. The median fold change of *miR-106b*, *miR-93*, *miR-25* and *MCM7* were 6.56, 7.67 and 11.25 and 7.9 respectively. Relative to donor retina control, *miR-106b ~ 25* cluster was over expressed in most of the RB tumor samples: *miR-106b*: 17/21 (85%), *miR-93*: 19/21 (95%), *miR-25*: 21/21 (100%), and *MCM7*: 21/21 (100%) of positivity **[Figure 5.3.4]**. Among the cluster, *miR-106b* and *miR-93* showed a significant difference ($p \leq 0.05$) between the invasive and no invasive RB tumors while no significant difference was observed based on tumor differentiation and status of chemotherapy. This reveals the presence of the oncogene *MCM7* and its resident intronic miRNAs (*miR-106b-25* clusters) in RB tumors.

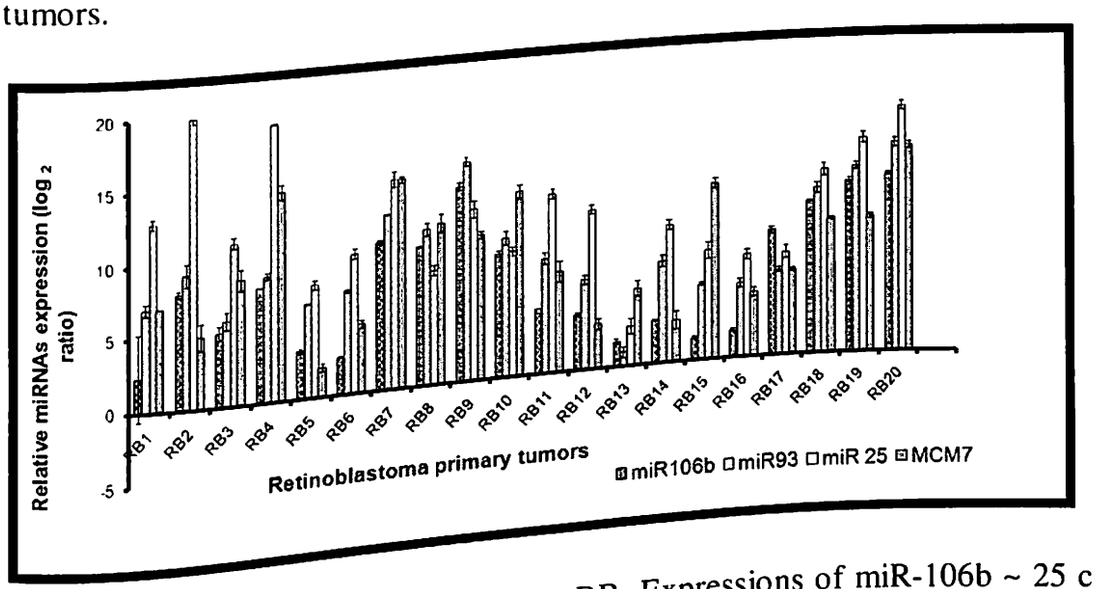

Figure 5.3.4: miRNA /mRNA expressions in RB. Expressions of miR-106b ~ 25 cluster and MCM7 in primary retinoblastoma tumours (n=20). The bar graph represents the

relative miRNA expressions of miR-106b ~ 25 clusters, mRNA expression of MCM7 determined by qRT-PCR. The median fold change of miR-106b is 6.56; miR-93 is 7.67, miR- 25 is 11.25 and MCM7 is 7.9 in RB tumor sample, compared with donor retina.

5.3.4.4.2. Silencing of miR-106b~25 cluster using antagomirs down regulates *HMGA2* and *MCM7* oncogene

The link between miR-106b ~ 25 clusters and its gene target (HMGA2) was further established using the short antisense oligos (antagomirs) against the individual miRNAs of this family. A transient transfection with these antagomirs was induced in the RB cell lines resulting in the down-regulation of miR-106b ~ 25 cluster (fold change in the order miR-106b, miR-93 and miR-25): -6.68, -6.60, -10.26 versus untreated cells and a fold change: -4.96, -4.48, -8.06 versus scrambled miRNA-treated control) in Y79 cells [**Figure 5.3.5.A**]. In Weri Rb1 cells, we observed the suppression of miR-106b ~ 25 family in the order miR-106b, miR-93 and miR-25: -8.27, -6.17, 7.06 compared with untreated cells and fold change of -5.88, -7.77, and -6.17 (in the order miR-106b, miR-93 and miR-25) compared with scrambled miRNA-treated control [**Figure 5.3.5.B**]. The expression of miR-106b~25 family in the RB cells treated with the mixture of all the 3 antagomirs showed a down regulation of miRNAs, by a fold change in the order miR-106b, miR-93 and miR-25: -1.79,-7.34,-6.51 in Y79 cells and -8.15, -4.50, -6.07 in Weri Rb1 cells, respectively [**Figure 5.3.5. A and B**].

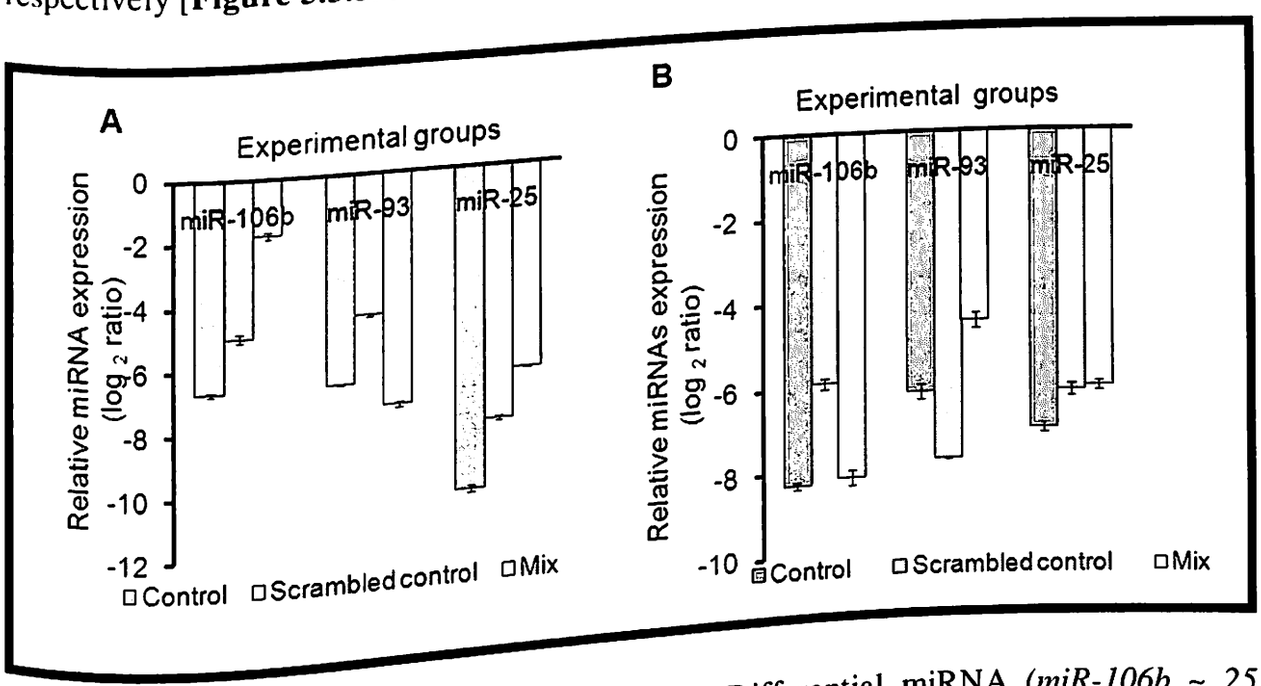

Figure 5.3.5: miRNA expressions in RB cells. Differential miRNA *(miR-106b ~ 25 clusters)* levels in antagomirs - mix treated RB cells. Relative to non-transfected and scrambled siRNA treated RB cells; the fold change in expressions of *miR-106b ~ 25 clusters* is presented. The figures A and B represent Y79 and Weri Rb 1 respectively. The values are expressed as mean fold change (log_2 fold change) ± SD of triplicates.

Table 5.3.3: *miRNA/ mRNA expressions in RB. Clinico-pathological Features of primary RB tumours following the International Intraocular Retinoblastoma classification (IIRC) with HMGA2, MCM7* gene expression and *miR-106b ~ 25 cluster* (by qRT-PCR).

S.No	Age (Yrs)/sex	Chemotherapy	RB Groups (IIRC)	Clinico-pathological parameters	Expression of miRNAs /mRNA in primary RB tum				
					miR-106b	miR-93	miR-25	MCM7	HMGA2
1.	3/F	Pre-operative, 2 cycles of adjuvant chemotherpy	G- E	OU: PD; viable TC, thickened sclera, NI	2.40	7.08	12.95	7.08	4.36
2.	3/M	NC	D	OD: UD; a focal retinoma component, NI	8.01	9.32	20.01	4.92	9.66
3.	2 /M	NC	G-E	OS: MD; NI	5.12	5.93	11.25	8.69	5.9
4.	5/M	NC	D	OD: PD, NI	8.04	8.78	19.22	14.5	10.09
5.	3/F	NC	D	OS: WD; formation of fleurettes, prelam inv of ON	3.31	6.59	7.87	2.04	4.91
6.	1/M	Focal therapy	A	OU:OS; WD; Focal CI <3mm	2.62	7.19	9.74	4.77	7.56
7.	1/F	Pre-operative, 2 cycles	G-D	OU:OD: WD, prelam ON inv, No CI	10.34	12.2	14.64	14.5	2.64
8.	3/M	NC	D	OS: MD; with focal retinoma component, prelam inv of ON, No CI	9.81	10.9	8.05	11.2	11.45
9.	2/M	NC	D	OS: MD; retinoma, Focal CI<3mm	13.70	15.4	12.03	10.1	7.01
10.	4/M	NC	G-E	OD: PD; CI measuring >3mm.	8.71	9.80	8.83	12.9	6.78
11.	3 mon/F	post-operative chemotherapy,6 cycles	E	OD: PD; iris neovascularization, CI >3mm, pre & post lam inv of ON	4.61	8.10	12.61	7.11	11.45
12.	3/M	NC	B	OD: UD; CI<3 mm, pre & post lam inv	3.97	6.37	11.25	3.14	12.05

				of ON					
13.	3/F	Post-operative chemotherapy, 6 cycles	E	OD: PD;f ocal CI <3mm, pre & post lam ON,1.5mm in height & 1mm thickness	1.79	0.99	2.791	5.44	2.46
14.	2/F	Post-operative chemotherapy, 6 cycles	G-E	OS: CI>3mm, TC invading the anterior, middle & posterior border of sclera with spill over into the orbital tissue	3.09	7.24	9.74	2.95	4.58
15.	4/M	Post-operative, 2 cycles (Expired)	E	OS: PD; massive CI>3mm,	1.60	5.41	7.74	12.44	6.69
16.	2/M	Post- operative, 6 cycles	E	OU:OS; diffuse CI >3mm thickness (>60%),pre & post lam inv of anterior & middle portion of sclera	1.94	5.29	7.27	4.61	7.71
17.	8/M	Pre-operative, 7cycles	E	OD: UD; diffuse full thickness CI >3mm, inv of pre & post lam of ON.	8.90	6.09	7.31	6.05	3.39
18.	3/M	Post- operative, 2 cycles	B	OD: MD CI measuring >3mm, pre & early post inv of ON.	10.84	11.7	13.05	9.57	8.11
19.	4/F	NC	E	OD: PD, massive CI >3mm, Pre, post lam, and meningeal sheath of ON inv, hemorrhage in ON.	12.22	13.2	15.21	9.64	5.6
20.	3/M	Pre-operative, 7 cycles of adjuvant chemothrapy	E	OD: PD. Pre & post lam inv of ON, meningeal sheath of ON inv, hemorrhage in ON,	12.60	14.8	17.38	14.5	8.81

M: Male, F: Female, NC: No chemotherapy, OU: Both eyes, OD: Right eye, OS: Left eye, WD: Well differentiated, MD: Moderately differentiated, PD: Poorly differentiated, CI: Choroid invasion, pre-lam: pre-laminar, Post-lam: post-laminar, ON: optic nerve, Inv: Invasion

After antagomirs transfection (miR-106b, miR-93, miR-25 and mixture) in RB cells, the *HMGA2* gene was down-regulated by -2.20, -1.89, -1.74, -2.24 fold change in Y79, and by a fold-change of -1.03, -0.71, -1.6, -0.33 in Weri Rb1 cells respectively [**Figure 5.3.6.A**]. The suppression of *HMGA2* transcripts confirms the regulation of these oncogenes by *miR-106b ~ 25 clusters*. The down-regulation of *MCM7* to a fold change -3.51,-1.04, -9.48 and -0.06 in $\log_2$ fold change was observed in anti–miRs (*miR-106b, miR-93, miR-25* and mixture) treated Y79 cells and -1.72, -2.55, -1.25, -3.03 $\log_2$ fold change in anti–miRs (*miR-106b, miR-93, miR-25* and mixture) treated Weri Rb1 [**Figure 5.3.6.B**]. Further we probed the role of this miRNA family in mediating RB cell proliferation.

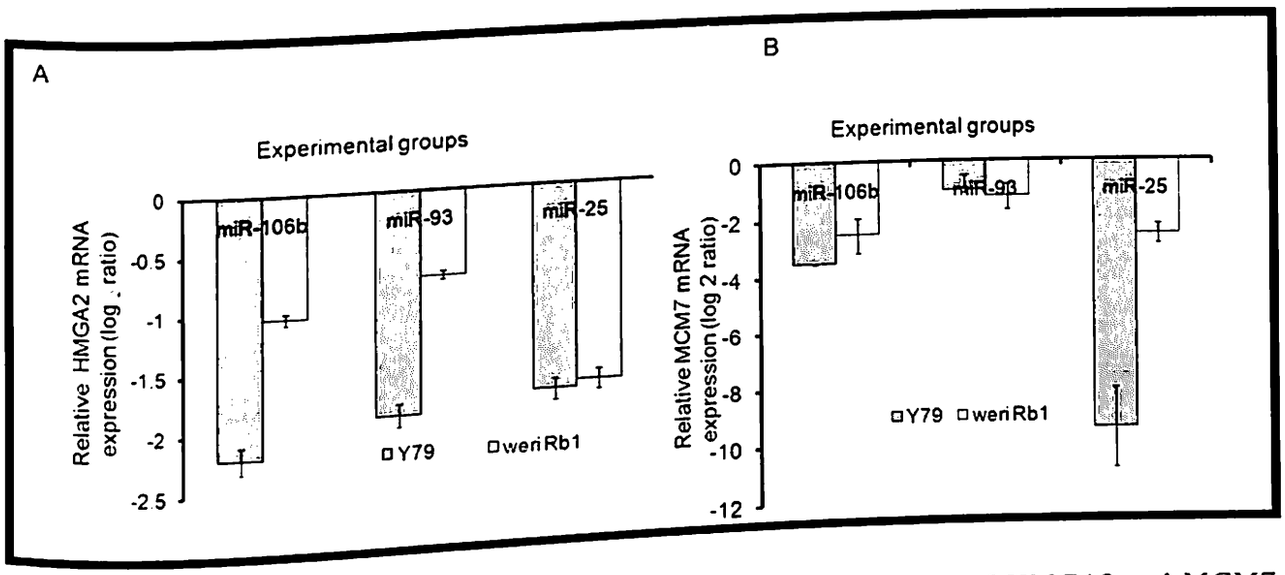

Figure 5.3.6: mRNA expressions in RB cells. Differential expressions of *HMGA2* and *MCM7* in antagomirs treated RB cells. Relative to scrambled siRNA treated RB cells, the fold change in expressions of *HMGA2* and *MCM7* is presented. The figure A and B represent *HMGA2* and *MCM7* respectively. The black bar represents Y79 while grey bar represents Weri Rb1 respectively. The values are expressed as mean fold change ($\log_2$ fold change) ± SD of triplicates.

5.3.4.4.3. Role of the miR-106b ~ 25 cluster in RB cell proliferation and cell apoptosis

The MTT assay and Annexin V fluorescence binding assay results reflected the effects of the anti- miR-106b ~ 25 cluster in RB cells. **Figure 5.3.7.A and B** shows decreased cell proliferation compared to the untransfected RB cells at the end of 24 hrs, 48 hrs, and 72 hrs. At the end of 48 hrs, the percentage of viable cells in the antagomirs treated RB cells in comparison with untreated cells in the order of *miR-106b, miR-93, miR-25* and mix were (i)

Y79 cells: 67.52%, 64.87%, 64.72%, 67.68%; (ii) Weri Rb1: 66.37%, 68.44%, 64.46%, 66.09% respectively. Moreover, the Annexin V flourescence staining and FACS analysis showed an increased level of apoptosis significantly in the RB cells transfected with the anti-miRs compared to the untransfected RB cells [**Figure 5.3.7. C, D and E**]. The average percentage of early apoptotic cells induced at the end of 48 hrs in the anti–miRs treated RB cells (in the order of untreated control, *miR-106b, miR-93, miR-25* and the mix) are (i) Y79 cells: 1.2%, 33.54%, 28.00%, 38.91%, 31.02%; (ii) Weri Rb1: 0.22, 39.86%, 39.82%, 38.417%, 22.09%, respectively. These results suggest that these miRNAs promote the cell proliferation and suppress the apoptosis in RB cells (Y79 control: 1.2%, Weri Rb1 control: 0.22%).

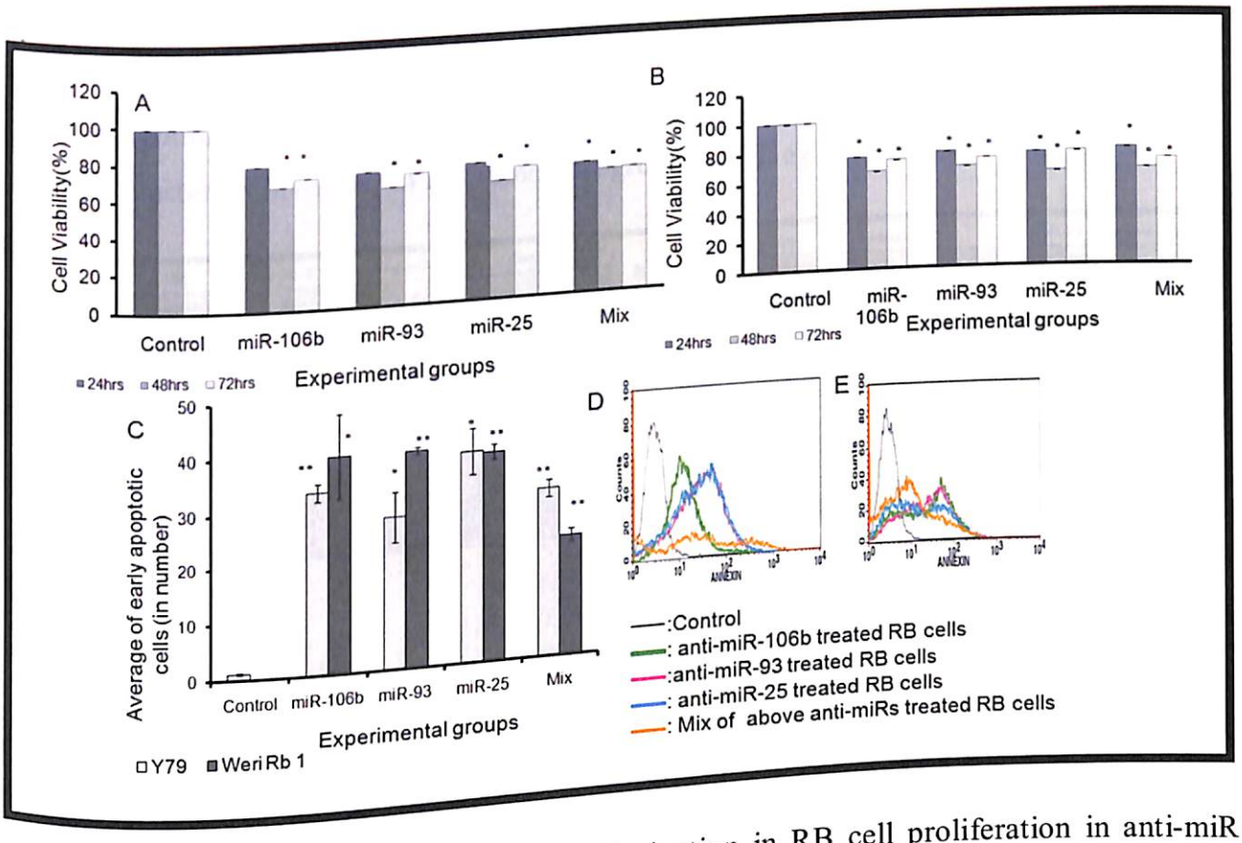

Figure 5.3.7: Cell viability assays in RB. Reduction in RB cell proliferation in anti-miRs (*miR-106b~25*, mix) treated cells. The anti-miRs treated Y79 (A) and Weri Rb 1 (B) cells were compared for cell viability with the untreated and scrambled treated RB cells as controls. Percentage of cell proliferation was obtained after treating the RB cells with antagomirs at 24 hrs, 48hrs and 72 hrs of time interval. C: The graph represents the average number of apoptotic cells in anti-miRs treated RB cells (*miR-106b ~ 25 cluster*, mix) performed in triplicate, Mean ± SD of triplicates were expressed. The grey bar represents Y79 cells, and the black bar represents Weri Rb1 cells. Figure D and E show a representative graph of annexin V Flour staining using flow cytometry in RB cells (Y79 and Weri Rb-1). Asterisks

represent the significant difference between the controls and the antagomirs transfected RB cells (*p≤0.05, ** p≤0.01).

5.3.4.4.4. Role of the miR-106b~25 cluster in RB cell growth and cell migration

To further understand the role of the *miR-106b~25* cluster in cell growth and cell invasion, scratch assay was carried out in the antagomirs-transfected and untransfected RB cells. The average area of scratch invaded by the Y79 cells in the order (untreated, antagomirs treated: *miR-106b, miR-93, miR-25*) at the end of 24 hrs: 17.91 %, 10.6%, 9.4%, 9.79% and 48 hrs 25.25 %, 4.5%, 4.18%, 4.81% respectively. The average area of scratch invaded by the Weri Rb1 cells in the order (untreated, antagomirs treated: *miR-106b, miR-93, miR-25*) at the end of 24 hrs: 34.71 %, 19.96%, 15.33%, 14.31% and 48 hrs 36.16 %, 19.28%, 11.15%, 9.06% respectively. These experiments showed a marked reduction in migrating cell populations in the antagomirs transfected RB cells [**Figure 5.3.7. A and B**], suggesting that the *miR-106b~25* cluster is involved in RB tumor progression (Liang et al. 2007).

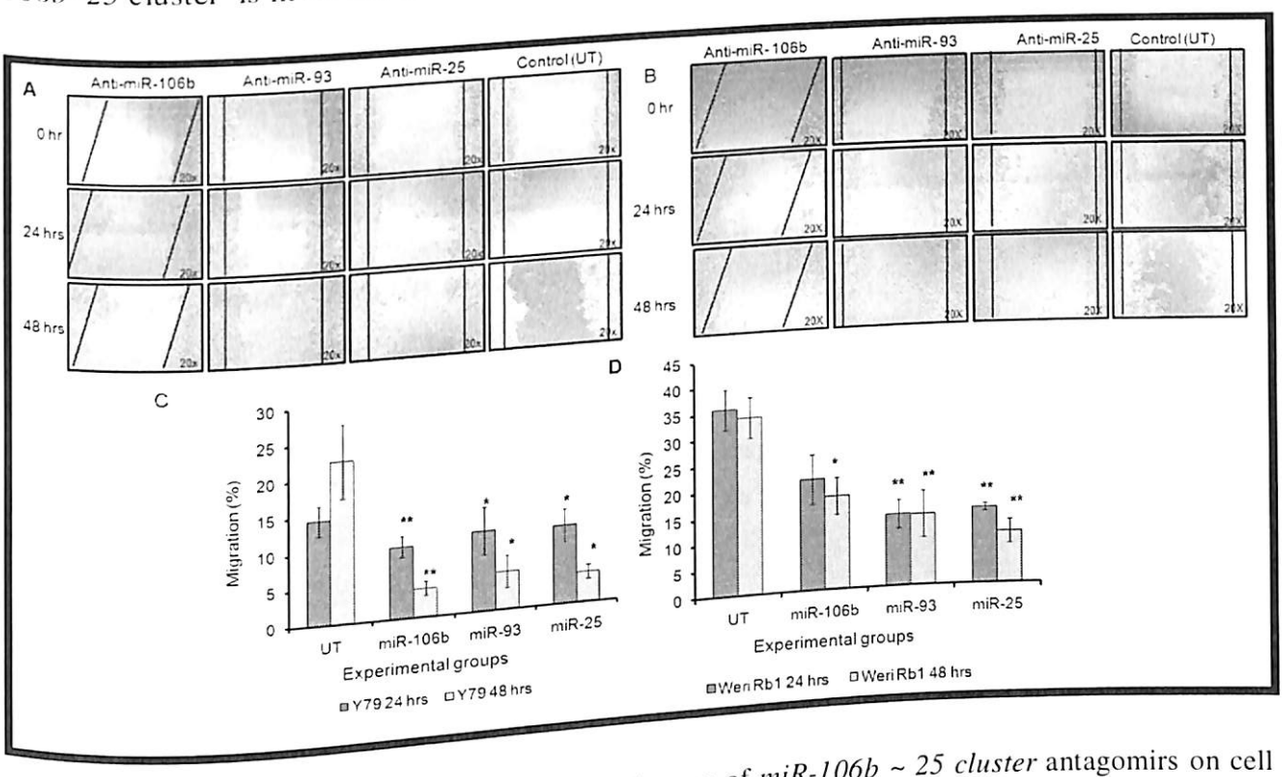

Figure 5.3.8: Cell Migration assay in RB. Influence of *miR-106b ~ 25 cluster* antagomirs on cell migratory behavior in RB cells. Photomicrographs show the migratory behavior between the untreated and antagomirs treated Y79 (A) and Weri Rb 1 (B); Figure C represents the percentage of area migrated by Y79 cells at 24 h (black bar) and 48 h (grey bar). Figure D represents the percentage of area migrated by Weri Rb 1 cell at 24 h (black bar) and 48 h (grey bar). Asterisks represent the

significant difference between the controls and the antagomirs treated RB cells (* $p \leq 0.05$, ** $p \leq 0.05$).

5.3.4.4.5. *miR-106b~25* clusters mediates cell cycle by down-regulating the expression of p21 and BIM in RB

The expression of apoptotic proteins - p21 and BIM (direct targets of miR-106b and miR-25 (Ivanovska et al. 2008)) was measured in the anti-miR-transfected RB cells by immunoblot analysis [**Figure 5.3.9. A and B**]. This experiment revealed the increase in p21 and BIM protein levels in the antagomirs transfected RB cells compared to the untransfected RB cells. This indicated the apoptotic mechanisms were, in part, regulated through the *miR-106b ~25*, and its relationship with the oncogene HMGA2.

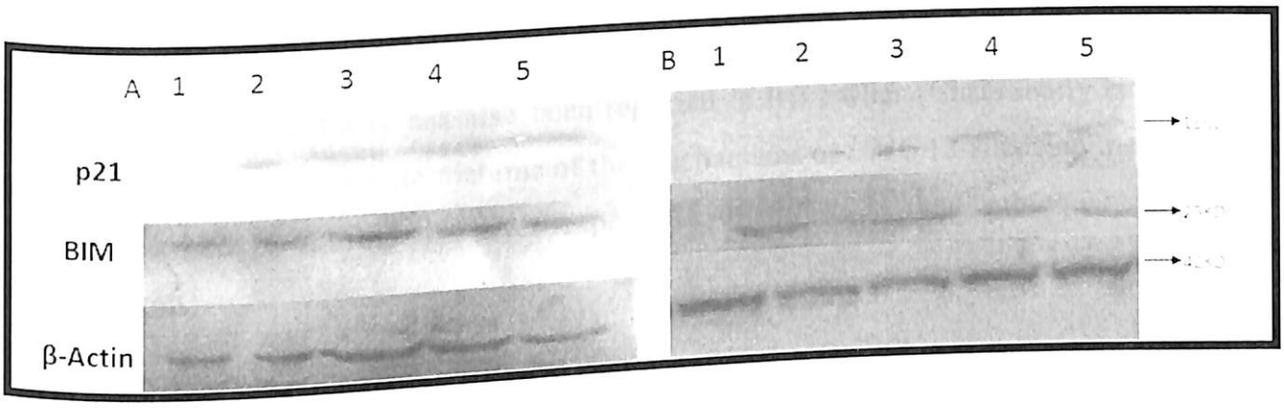

Figure 5.3.9: Western analysis in RB cells.

Western blot of p21 and BIM proteins in antagomirs treated cells: Expression of p21 and BIM proteins in Y79 (A) and Weri Rb 1(B) cells are presented here. The intensity of protein (p21 and BIM) bands was normalized with beta-actin expression in RB cells (control and antagomirs treated cells). [Lanes 1-5: control RB cells, antagomirs to *miR-106b, 93, 25*, mix respectively].

5.3.5. Discussion

5.3.5.1. HMGA2 induced miRNA-gene regulatory pathways in RB

We explored the global miRNA expressions in HMGA2-silenced RB cells. Through an integrated miRNA- mRNA expression analysis, we were able to correlate the dys-regulated miRNAs and corresponding mRNAs (genes) that are involved in various cellular processes

[**Figure 5.3.1**]. The study mainly focuses on the dysregulated miRNAs which have been reported to play a vital role in cancer development [**Figure 5.3.10**] and their roles in HMGA2-silenced RB cancer cells (He L. et al. 2007, He L. et al. 2005, O'Donnell et al. 2005).

The *HMGA2* siRNA treatment induced up-regulation of *miR-125a, miR-150, miR-155*, and *miR-494* which may contribute to cell growth arrest in RB tumor cells through alterations in expression of cancer regulatory genes. *miR-125a*, known as a tumor suppressor, regulates *ERBB* oncogene (*ERBB2 and ERBB3*) via ERK1/2 and AKT phosphorylation. The suppression of this oncogene, through the over-expression of *miR-125a* was reported to alter the cancer cell phenotype of SKBR3 cells (ERBB2-dependent human breast cancer cell line) (Scott et al. 2007). *miR-125a* has also been suggested as a prognostic and therapeutic marker in gastric cancers (Nishida et al. 2011). High expression of ERBB3, along with the dys-regulation of AKT pathway has also been reported in RB earlier (Chakraborty et al. 2007). These studies strongly indicate that one of the mechanisms of *HMGA2*-silencing mediated RB cell death could be through the over expression of *miR-125a* (and subsequent oncogene modifications).

miR-150 is reported as a tumor suppressor in lymphoma (Watanabe A. et al. 2011) and corticotropinomas (Amaral et al. 2009). Watanabe et al. (Watanabe A. et al. 2011) showed that *miR-150* directly down-regulated the expression of gene targets DKC1 and AKT2 while increasing that of the tumor suppressors, Bim and p53 in lymphoma. This is in line with the present finding of over-expressed miR-150, along with increased level of Bim protein [**Figure 5.3.9. A and B**], and our earlier finding of elevated p53 proteins (Venkatesan et al. 2012) in HMGA2-silenced RB cells. These findings strongly point to the tumor suppressor mechanisms of *miR-150* induced by the silencing of *HMGA2* gene in RB (Amaral et al. 2009). (Watanabe A. et al. 2011). The up-regulated *miR-155* in the current study has been previously reported to reverse EGF-induced epithelial-mesenchymal transition (EMT) resulting in inhibition of proliferation, metastasis, invasion, and contributing to increase cisplatin sensitivity in cervical cancer cells (Lei et al. 2012). *miR-494* is reported to induce cellular senescence by suppressing *IGF2BP1* in lung cancer cells (Ohdaira et al. 2012). Thus, the up-

regulation of *miR-155* (fold change=7.421) and *miR-494* (fold change=2.421) observed here can be linked to cell growth arrest in post-*HMGA2* silenced RB cells.

The *HMGA2* siRNA treatment has induced down-regulation of major oncomirs such as such as *miR-21, miR-9, miR-221* and the 2 major families *miR-17~92* cluster and its paralogs *miR-106a~363* and *miR-106b ~ 25 clusters.*

miR-21 is known to be an oncomir with its regulatory target genes involved in tumor invasiveness and micro vascular proliferations in cancers such as glioblastoma, breast cancer, pre-cell lymphoma (Chan J. A. et al. 2005, Medina et al. 2010, Qi et al. 2009, Yan et al. 2008).The gene targets *RECK* (a matrix metalloproteinase regulator, fold change: 0.93) (Reis S. T. et al. 2012b), *PTEN* (fold change: 0.64), *PDCD4*, and *TM1* are modulated by this *miR-21* in breast cancer (Qi et al. 2009). Thus the observed down-regulation of *miR-21* (fold change: -1.821) links the anti-proliferative effect of *HMGA2*-silencing with the suppression of the oncomir *miR-21*. Another oncomir, miR-9, was down–regulated (fold change:-2.878) along with increased expression of E-cadherin gene in *HMGA2* silenced RB cells (Ma L. et al. 2010). E-cadherin (*CDH1*), a gene target of *miR-9*, is involved in tumor angiogenesis through the activation of ß-catenin that promotes cancer metastasis (Ma L. et al. 2010).

miR-21 from an earlier report (Chen Y. et al. 2008), and miR-9 from our current integrated data analysis [**Figure 5.3.3**] are known to regulate *SOX5*, a member of (SRY-related HMG-box) family of transcription factors. The over-expression of *SOX5* results in regulation of embryonic development and cell fate (Lefebvre 2010), malignant B cell proliferation (Edwards et al. 2014) and reduction of glioma cell proliferation with induction of acute cell senescence (Tchougounova et al. 2009). The up-regulation of *SOX 5* (fold change: 1.93), together with down-regulation of miR-9 family and miR-21 contributes to *HMGA2* - silencing, mediated RB cell growth arrest.

In addition, *miR-221*, which is a suppressor of cell cycle inhibitor proteins p27/Kip1 and p57, and a promoter of RAS-RAF-MEK signalling pathway (Ma L. et al. 2010, Shah and Calin 2011) was found to be down-regulated (fold change: -6.838). This miRNA down-regulation may result in the inhibition of cell migration as reported earlier in MDA MB-231, breast cancer cell line (Lambertini et al. 2012, Zhang J. et al. 2010) and thus may contribute to the reduction of RB tumor cell proliferation, invasiveness and motility in post-*HMGA2* gene silencing.

We also observed the suppression of two major oncomir clusters namely *miR-17~92* and *miR-106b~25* due to the silencing of *HMGA2* in RB. The miRNA family, *miR-17~92* clusters and one of its paralogs *miR-106a~363* cluster reside on c13ORF25 genes of chromosome 13 and chromosome X, respectively. The over expression of these clusters have been reported earlier in various cancers such as leukemias (Mi et al. 2010), breast cancer (Negrini and Calin 2008) and AIDS associated non-Hodgkin's lymphoma (Thapa et al. 2011). *miR-17~92* expression was reported in RB (Kandalam et al. 2012).

In *HMGA2* silenced cells, we observed the suppression of the other paralog *miR-106b~25* and its host gene *MCM7*. *HMGA2* is known to be a positive regulator of *MCM7*, where one of the reported mediators is the *E2F* family. The involvement of *E2F* in tumor promotion has been implicated in RB primary tumors (Orlic et al. 2006, Venkatesan et al. 2012). Further, the *HMGA2* silencing also induced suppression of E2F family (Venkatesan et al. 2012). Thus the silencing of gene induces down-regulation of *MCM7* (via E2F family) which in turn prevents the biosynthesis of miR-*106b ~25* [please refer **Figure 5.3.10**]. In addition, the sequence complementarity between 3'UTR of HMGA2 and miR-106b~25 may also be a direct target for regulation. The miR-*106b ~25* has been investigated in detail and is discussed in the next section.

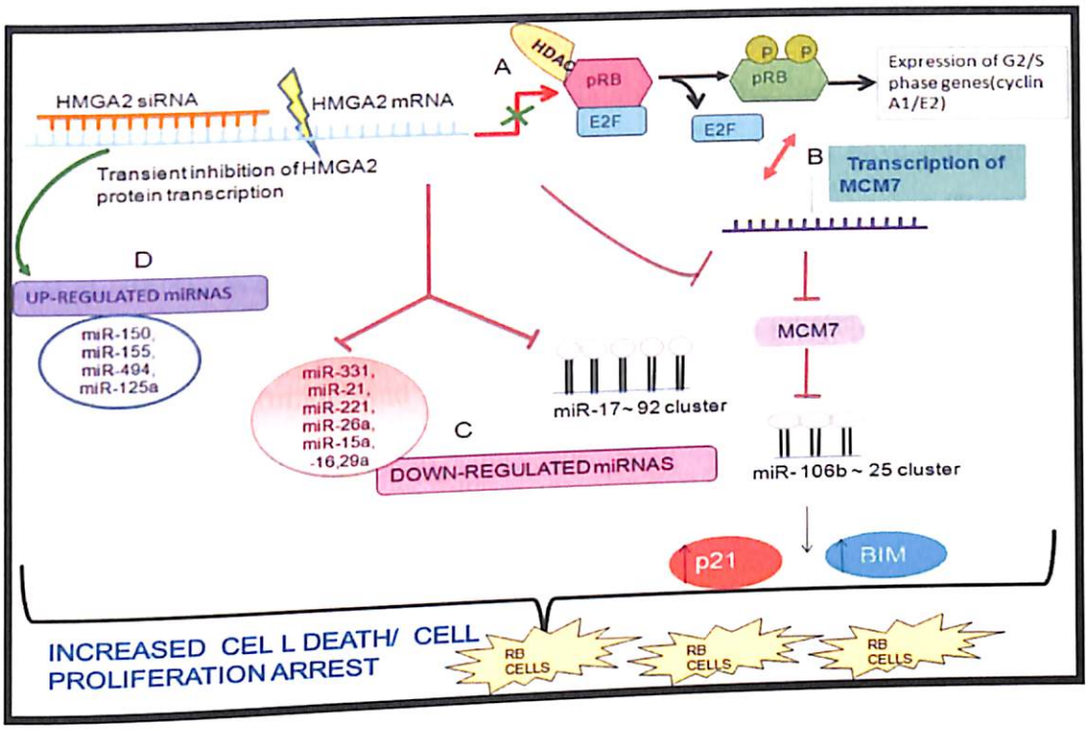

Figure 5.3.10: Dysregulated genes and miRNAs. Schematic representation of the key dysregulated genes and the miRNAs in the post-*HMGA2* silenced RB cells contributing to apoptosis and cell proliferation arrest.

A: Down-regulation of the HMGA2 protein resulting in the activation of Rb protein resulting in the up-regulation of cyclin A1/E2 (expressed in the G2/S phase of cell cycle).

B: Suppression of the *miR-106b-25* cluster through down-regulation of its host gene, *MCM7* via the reduced E2F family proteins. This, in turn results in the up-regulation of the p21 and BIM, which are the direct targets of *miR-106b-25* cluster contributing to the RB cell death.

C: Down-regulation of the key oncomirs and cell cycle regulatory miRNAs namely*; miR-331, miR-21, miR-221, miR-26a, miR-15a, miR-16, miR-29a.*

D: Up-regulation of tumour suppressor miRNAs and cell cycle regulatory miRNAs namely *miR-150, miR-155, miR-494, miR-125a.*

5.3.5.2. Implication of miR-106b~25 in RB pathogenesis, validation of its host gene MCM7 and target genes p21, BIM

The *miR-106b~25* family includes three miRNAs namely *miR-106b, miR-93* and *miR-25*. This family is highly conserved in vertebrates and resides in the 13th intron of *MCM7* gene on chromosome 7 (Smith et al. 2012);(Zhao Z. N. et al. 2012). The MCM7 is well known for its

regulation of the replication fork assembly on chromosomal DNA during G_1/S phase transition (Blow and Hodgson 2002). The suppression of this cluster using inhibitors had resulted in increased apoptosis and G_0/G_1 cell cycle arrest in oesophageal adenocarcinoma and laryngeal cancer (Cai et al. 2011, Kan et al. 2009). Earlier studies have correlated its over expression with poor prognosis in prostrate, endometrial and gastric cancers (Ren et al. 2006) (Petrocca et al. 2008). We have observed over-expression of *MCM7* in a cohort of 20 primary RB cases [**Table 5.3.3, Figure 5.3.4**]. Although miR-106b~25 cluster, (especially *miR-106b*) has been reported in RB tumor and serum samples (Beta et al. 2013), their gene regulation mechanisms are not known.

In the present study, the over-expression of *miR-106b ~ 25* cluster was identified in primary RB tumors (n=20) relative to donor retina. Secondly, we have used a model of RB cells where the *miR-106b ~ 25* cluster was inhibited by specific antagomirs to study its functional and regulatory mechanisms.

In a study on unrestricted somatic stem cells, the various gene targets of *miR-106b* such as (i) *cyclinD1 (CCND1)*, (ii) *E2F1* (iii) *CDKN1A* (p21), (iv) *PTEN*, (v) *RB1*, (vi) *RBL1* (p107), and (vii) *RBL2* have been reported indicating enhanced G_1/S transitions with increased levels of E2F transcription factors using bioinformatics and experimental validation protocols (Trompeter et al. 2011). In addition, this cluster of miRNAs have been known to repress the p21 and BIM which are downstream mediators of the TGF-ß signalling pathway (Petrocca et al. 2008).

Our results showed the activation of p21 and BIM [**Figures 5.3.9.A and B**], along with decreased cell proliferation and invasion, and with concomitant increase in apoptosis in the antagomirs treated RB cells. The observed up-regulation of oncogene, *MCM7* in primary RB tumor tissues was complimented by the down-regulation of *MCM7* gene [**Figure 5.3.5**] in *miR-106b ~ 25* specific antagomirs treated RB cells. These result strongly points to the role of *miR-106b ~ 25* cluster in promoting RB cell proliferation (Ivanovska et al. 2008).

To summarize, the integrated analysis between the deregulated miRNAs and genes due to the suppression of HMGA2 mRNA in the RB cells revealed the down-regulation of two main clusters of miRNAs namely *miR-106b~25* and *miR-17~92*. These miRNA clusters are known to regulate various key genes such as *MCM7*, *CDKN1A* (p21), *BIM* and *EpCAM*. These oncomir clusters can be further investigated for their role in RB tumor progression and also during chemotherapeutic interventions.

5.3.6. Conclusions

Improvement in RB management may be achieved by understanding the regulatory gene – miRNA networks involved in RB tumorigenesis and tumor suppression along with their ...latory miRNAs. We have reported the various miRNAs deregulated in the *HMGA2*-...B cells, have been reported. The integrated mRNA-miRNA network analysis ... associations between important genes and miRNAs following ... silencing induced

Figure 5.3.10: Dysregulated ... apoptotic ...

suggested that (a) *miR-106b~25* cluster itself may be a potential biomarker or target in RB management, and (b) down-regulation of the *miR-106b~25* cluster is one of the key mechanisms of cell death induced by *HMGA2* silencing in RB.

To summarize, the integrated analysis between the deregulated miRNAs and genes due to the suppression of HMGA2 mRNA in the RB cells revealed the down-regulation of two main clusters of miRNAs namely *miR-106b~25* and *miR-17~92*. These miRNA clusters are known to regulate various key genes such as *MCM7*, *CDKN1A* (p21), *BIM* and *EpCAM*. These oncomir clusters can be further investigated for their role in RB tumor progression and also during chemotherapeutic interventions.

5.3.6. Conclusions

Improvement in RB management may be achieved by understanding the regulatory gene – miRNA networks involved in RB tumorigenesis and tumor suppression along with their regulatory miRNAs. We have reported the various miRNAs deregulated in the *HMGA2*-silenced RB cells, have been reported. The integrated mRNA-miRNA network analysis revealed the regulatory associations between important genes and miRNAs following *HMGA2* silencing that result in RB tumor control. Particularly, *HMGA2* silencing induced down-regulation of the *miR-106b~25* cluster. The tumor promoting role of *miR-106b~25* in RB was clearly documented using specific antagomirs. Taking the results together, it is suggested that (a) *miR-106b~25* cluster itself may be a potential biomarker or target in RB management, and (b) down-regulation of the *miR-106b~25* cluster is one of the key mechanisms of cell death induced by *HMGA2* silencing in RB.

CHAPTER 5.4: FUNCTIONAL OBSTRUCTION OF HMGA2 PROTEIN BINDING WITH DNA: AN APTAMER STRATEGY IN RB CANCER CELLS

5.4. Introduction

At present, about 70% of retinoblastoma reported in developing countries is at an advanced stage (Dimaras et al. 2012). Though chemotherapy and/or chemo regressed enucleation is the current RB management, advancements like gene therapy are being researched as better interventions (Philiponnet et al. 2014). It becomes mandatory at this stage for the researchers to identify the key regulatory molecules and pathways for designing novel targeted therapies in managing RB and to prevent metastasis (Boutrid et al. 2008). In this lineage, High mobility group (HMG) of proteins has the significant potential.

High mobility group A (HMGA) proteins, referred to as ''architectural transcription factors'' (Wolffe 1994) are small non-histone chromosomal proteins that are characterized by 3 highly conserved DNA-binding motifs called ''AT-hooks'' and an acidic tail. These proteins preferentially interact with the minor groove of AT-rich B form DNA by recognizing a particular DNA structure rather than a specific nucleotide sequence (Reeves and Nissen 1990). The HMGA family consists of HMGA1a, HMGA1b, HMGA1c, and HMGA2 (Boo et al. 2005, Reeves 2001). HMGA1 (HMGA-1/Y) and HMGA2 (HMG1-C) have similar functions and are found abundantly in the rapidly proliferating early embryo cells and get repressed in the adult or mature cells

HMGA2 proteins are known to involve in many cellular regulation which includes, gene regulation, cell cycle progression, differentiation, and viral integration (Reeves 2001). Thus, alterations at transcription and translation levels of HMGA2 contribute to many common diseases, including (Sgarra et al. 2004), obesity (Anand and Chada 2000), diabetes (Foti et al. 2005) and atherosclerosis (Schlueter et al. 2005) and in several benign and malignant tumors such as breast cancer (Sgarra et al. 2004, Wikman et al. 2002), pancreatic cancer (Abe et al. 2003), retinoblastoma (Venkatesan et al. 2009) and leukemia (Rommel et al. 1997). In addition to its oncogenic properties (Hristov et al. 2009, Peng et al. 2008), other properties such as stem cell self-renewal (Nishino et al. 2008, Tzatsos and Bardeesy 2008) DNA damage response (Park et al. 2007), and tumor cell growth and differentiation (Li A. Y. et al. 2009a, Shell et al. 2007, Wu et al. 2011) have been reported.

Owing to the prominent role of HMGA2 in the molecular regulation of RB, it has been attempted to suppress either the biogenesis (transcription) using siRNAs or function. In this order,(Venkatesan et al. 2012), earlier have reported the genome wide changes by HMGA2 silencing in RB cancer cells using RNAi tool, with an analysis of its anti- cancer potential (Please refer the chapter 5.2). Further, in continuation with this study, Venkatesan et al, 2014 have reported the miRNAs dys-regulated (especially the two oncomir clusters: miR-17-92 cluster and miR-106b-25 cluster) due to HMGA2 silencing in RB cells. Similar results have been reported in a nude mice model of retinoblastoma and liposarcoma cells (Berlingieri et al. 1995, Chau et al. 2003, Pentimalli et al. 2003). All these studies indicate HMGA2 plays a potential role in the tumorigenesis of retinoblastoma (Chau et al. 2003) and that it could be a potential target molecule in RB management.

Here, we introduce another class of nucleic acid based molecular tool 'aptamers' to inhibit the HMGA2 protein function. Aptamers being small nucleic acid molecules are derived from *in vitro* selection experiments namely Systematic Evolution of Ligands by Exponential Enrichment (SELEX). Aptamer has a wide range of biomedical applications namely detection of biomarkers in cancer diagnostic tools, imaging pathological tissues and treating cancers (Zhou and Rossi 2010), (Ni et al. 2011, Zhou and Rossi 2008, 2009). Due to their high

specificity, affinity, non-immunogenic, greater ease of *in vitro* modification and tissue penetration, aptamers are recognised as potential therapeutic agents than monoclonal antibodies and small molecules (Jayasena 1999, Nakamura et al. 2012). Aptamers are synthesized and manipulated with high versatility in structure and function similar to target proteins. After 2 decades of aptamer invention, the first FDA approved aptamer drug (Macugen) for treatment of age related macular degeneration has reached the level of clinical trials and this proves its therapeutic application. At present, attempts are also made to synthesize aptamers-targeted nano platforms capable to ferry cargo and load onto them for both imaging and therapeutic functions creating so called nano-theragnostics agents. In the future, aptamers are likely to play an important role in diagnosis and treatment of several pathologies including cancer (Lassalle et al. 2012).

Here in this study, we have used DNA aptamer modified with phosphothiorate to inhibit the HMGA2 protein function. In order that these antagonists work in animal models of disease, and in humans, it is necessary to modify the aptamers. Modifications in the aptamers such as sugar modifications of nucleoside triphosphates are carried out to render them resistant to nucleases that exist in serum. Generally, modification in 2'OH groups of ribose to 2'F or 2'NH2 groups has yielded aptamers which are stable in the body fluids such as blood. As the aptamers are relatively in low molecular weight (8000-12000 daltons) it rapidly clears from the blood (Brody and Gold 2000). Because of these advantages, aptamers are designed to deliver the cancer inhibitory molecules namely siRNA or chemotherapeutic drugs namely *EpCAM* aptamer-Dox conjugate to deliver the doxorubicin drug into the retinoblastoma cancer cells (Subramanian et al. 2012).

previous report, the effect of DNA-HMGA2 aptamers as chemo sensitizer in pancreatic
er cell line model has been reported (Watanabe M. et al. 2012). In the present study, we
explored the efficacy of DNA aptamers against HMGA2 protein in RB cells, offering
tic insights in the dys-regulation of *TGF-ß* mediated *SMAD4* dependent apoptosis

specificity, affinity, non-immunogenic, greater ease of *in vitro* modification and tissue penetration, aptamers are recognised as potential therapeutic agents than monoclonal antibodies and small molecules (Jayasena 1999, Nakamura et al. 2012). Aptamers are synthesized and manipulated with high versatility in structure and function similar to target proteins. After 2 decades of aptamer invention, the first FDA approved aptamer drug (Macugen) for treatment of age related macular degeneration has reached the level of clinical trials and this proves its therapeutic application. At present, attempts are also made to synthesize aptamers-targeted nano platforms capable to ferry cargo and load onto them for both imaging and therapeutic functions creating so called nano-theragnostics agents. In the future, aptamers are likely to play an important role in diagnosis and treatment of several pathologies including cancer (Lassalle et al. 2012).

Here in this study, we have used DNA aptamer modified with phosphothiorate to inhibit the HMGA2 protein function. In order that these antagonists work in animal models of disease, and in humans, it is necessary to modify the aptamers. Modifications in the aptamers such as sugar modifications of nucleoside triphosphates are carried out to render them resistant to nucleases that exist in serum. Generally, modification in 2'OH groups of ribose to 2'F or 2'NH2 groups has yielded aptamers which are stable in the body fluids such as blood. As the aptamers are relatively in low molecular weight (8000-12000 daltons) it rapidly clears from the blood (Brody and Gold 2000). Because of these advantages, aptamers are designed to deliver the cancer inhibitory molecules namely siRNA or chemotherapeutic drugs namely *EpCAM* aptamer-Dox conjugate to deliver the doxorubicin drug into the retinoblastoma cancer cells (Subramanian et al. 2012).

In a previous report, the effect of DNA-HMGA2 aptamers as chemo sensitizer in pancreatic cancer cell line model has been reported (Watanabe M. et al. 2012). In the present study, we have explored the efficacy of DNA aptamers against HMGA2 protein in RB cells, offering mechanistic insights in the dys-regulation of *TGF-β* mediated *SMAD4* dependent apoptosis and cell cycle arrest.

expression levels of *TGFβ, SMAD4, SNAI1, CDH1, HDAC8, Bcl2, BAX, BIM, PARP and CASP 3* were detected by following qRT-PCR protocol (please refer section 4.3.5.3.2) using the specific primers tabulated in section 4.11.

5.4.3.5. *Internalization assay*

The intake of the HMGA2 – aptamers within RB cells (Y79 and Weri Rb 1) and in MIO-M1 cells were measured qualitatively using Axio observer microscope and quantitatively by the cellular uptake assay using FACS. After the transient transfection, the cells were harvested and processed for the internalisation as described in the section 4.2.8. The internalised FITC conjugated oligos were observed using AXIO observer (Zeiss microscope). The photomicrographs were further documented. In continuation with the internalisation assay, the quantitative estimation of the aptamers penetrated within the RB cells and MIO-M1 cells are estimated using flow cytometry as described in the section 4.2.8.

5.4.3.6. *Cell proliferation and viability assays*

The percentage of cell proliferation relative to untreated control cells were analysed using CYQUANT proliferation assay in aptamer treated RB cells and MIO-M1 cells were carried out as described in the section 4.11.4 at 1.0 μM aptamer concentration for a period of 48 hrs of incubation.

The percentage of cell viability relative to untreated control cells were analysed using MTT assay in aptamer treated RB cells and MIO-M1 cells were carried out as described in the section 4.11.3 at 0.25μM to 1.0μM concentration for the period of 24hrs, 48 hrs and 72 hrs of incubation respectively.

5.4.3.7. *Apoptosis Assay*

The percentage of apoptotic cells in aptamer treated RB cells and in untreated control RB cells were carried out as described in the section 4.11.5 at 0.5 μM concentration for a period of 48 hrs of incubation (optimized from previous section 5.4.2.6).

5.4.3.8. Cell cycle analysis

The percentage of various stages of cell cycle in aptamer treated RB cells and in untreated control RB cells were carried out as described in the section 4.11.6 at 0.5 µM concentration at the end of 48 hrs of incubation.

5.4.3.9. Statistical analysis

One-way ANOVA was used to derive the significance for the variable groups in cell viability and cell proliferation assays. Independent sample t-test and Mann-whitney 'U' was carried out to compare the variable groups in apoptosis and cell cycle analysis assay.

5.4.4. Results

5.4.4.1. Internalisation assay of DNA aptamers

After transfection with 0.5 µM of aptamers (HMGA2 and mix-aptamers), RB cells and MIO-M1 cells were observed microscopically to evaluate the penetration of the aptamers in the nucleus of cells. Presence of FITC-conjugated aptamers in the nucleus **[Figure 5.4. A, B, C]** indicates the internalisation of aptamers inside the cells. Further, the quantitative cellular uptake of the HMGA2-aptamer by the Y79 cells at 0.5 µM showed 92.4%, 93.1%, 85.43%, 86.41%, and 91.83% uptake during the period of 12, 24, 48, 72, and 96hrs of incubation respectively. Similarly, the cellular uptake of mix-aptamer sequences in Y79 cells at 0.5 µM showed 69.59%, 93.73%, 91.2%, 88.04%, and 92.16 respectively during the period of 12, 24, 48, 72, and 96hrs of incubation **[Figure 5.4.D]**. In Weri Rb 1 cells, an internalisation of HMGA2-aptamer of 87.15%, 95.5%, 97.88%, 98.72% and 98.81% was observed while mix-aptamer showed 87.17%, 98.25%, 97.55%, 99.40%, and 99.74% during the period of 12, 24, 48, 72, and 96hrs of incubation **[Figure 5.4.D]**. These qualitative and quantitative aptamer internalisation results showed the efficiency of transfection of HMGA2 aptamers carried out in RB cancer cells, and in MIO-M1 normal retinal cells.

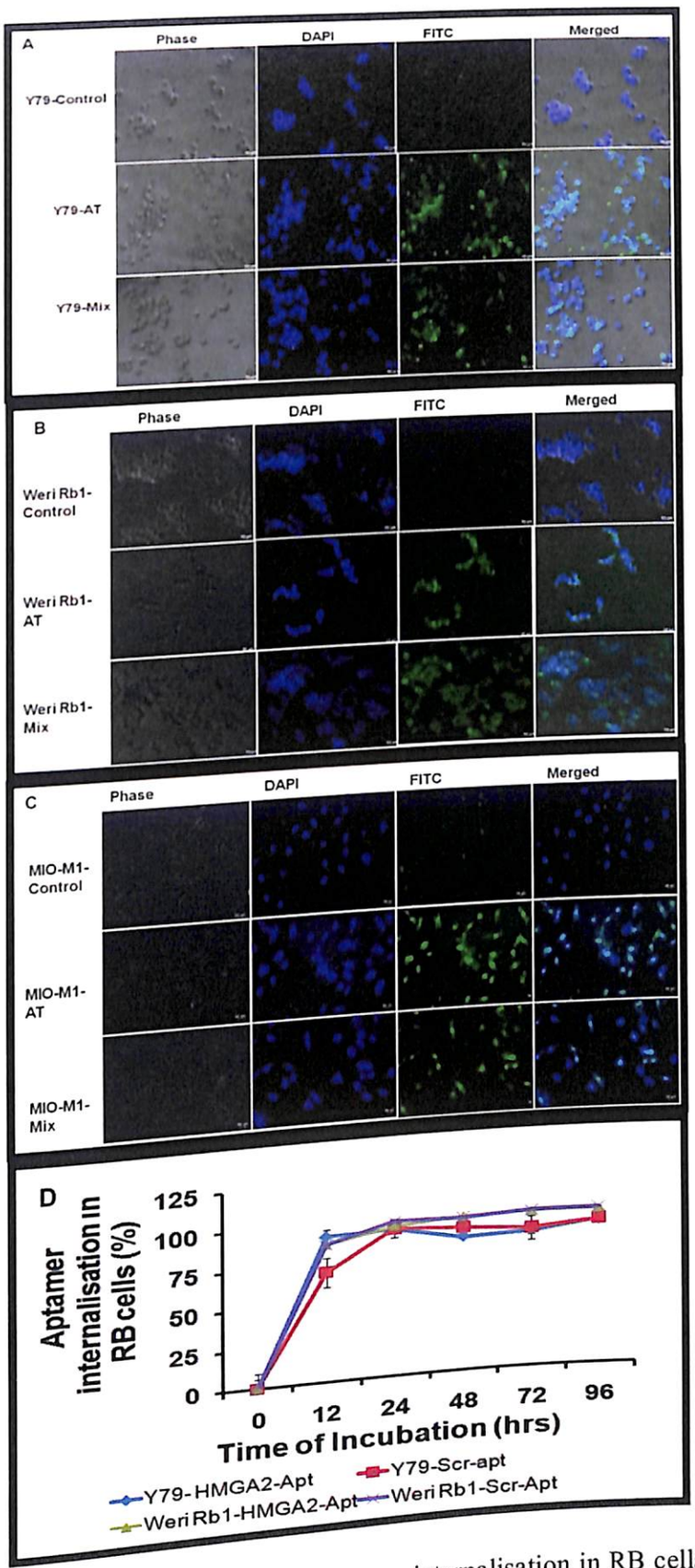

Figure 5.4.1: Internalisation of aptamers. Aptamers internalisation in RB cells and MIO-M1 cells. A-C: Photomicrographs of HMGA2-aptamer and mix-aptamer treated RB cells and non-neoplastic MIO-M1 cells in 0.5μM at the end of 48 h of incubation. A: Y79 cells; B: Weri Rb1 cells; C: MIO-M1

cells. Microscopic observartion in the order of phase-contrast, DAPI stained, FITC stained and merged images are indicated in rows. Microcropic observations of un-tranfected control, HMGA2-aptamer (AT) and scramble transfected control (mix) are indicated in columns. D: Quantitative estimation of aptamers internalised within RB cells are represented graphically in RB cells. Error bars represent the SD of the triplicates.

5.4.4.2. Effect of aptamers on cell toxicity, cell proliferation and cell viability

The spectrophometric analyses of lactate dehydrogenase (LDH) in RB cells after treatment with HMGA2-aptamers for 24 h revealed at the maximum of 107.99% of LDH activity relative to untransfected control in Y79 cells, while Weri Rb1 revealed 72.41 % relative to the untransfected control cells. In non-neoplastic cells, MIO-M1, a maximum of 62.06% of LDH activity at 1.5 µM at end of 24 h of HMGA2-aptamer was observed. In the presence of mix-aptamer sequences, lactate dehydrogenase activity of about 30% were observed in RB cells while about 50% observed in MIO-M1 cells at the maximum concentration of 1.5 µM treatment for 24 hrs of time. These results indicate 1.0 µM of HMGA2-aptamer as the cytotoxicity concentration in RB cells.

At the end of 48 h of 1.0 µM HMGA2-aptamer transfection, cell proliferation analyzed by CYQUANT assay, revealed a decrease to 15.3% in Y79 cells, 13.49% in Weri Rb 1 cells while an increase of 159.7% in non-neoplastic cells (MIO-M1) in comparison with un-transfected cell control. Treatment of mix- aptamer in RB cells for 48 h, revealed a decrease in proliferation to 59.4% in Y79 and 47.5% in Weri Rb1 cells while an increase to 125% compared to un-transfected control was observed in MIO-M1 cells.

In 1.0 µM HMGA2-aptamer transfected RB cells, MTT assay revealed, a decrease in cell viability in the order of 54.65% in Y79 cells, 59.25% in Weri Rb1 cells while an increase of 90.25 % in MIO-M1 cells were observed with relative to the un-transfected cell control at the end of 48 h of incubation. At the same concentration and at the same time of incubation, with mix sequence transfection in RB cells, a cell viability of 81.87% in Y79 cells, 105.68% in Weri Rb1 while 90.75% cell viability was observed in MIO-M1 cells.

Taken together, these results indicate that HMGA2 aptamer regulates cell viability and proliferation. As mild to moderate regulation of cell viability was observed with mix sequence transfection, attention need to be paid in using them in further *in vivo* studies. At 0.5 µM concentration, the HMGA2-aptamer transfection revealed 67.03% of cell viability in Y79 and 83% in Weri Rb1 cells while 89.14% in non-neoplastic MIO-M1 cells. This concentration was selected to analyze the synergistic activity of the HMGA2 aptamers in chemo modulation (etoposide) of RB cells. Thus, this concentration of 0.5 µM of aptamers was selected for the cell cycle analysis and apoptosis assay.

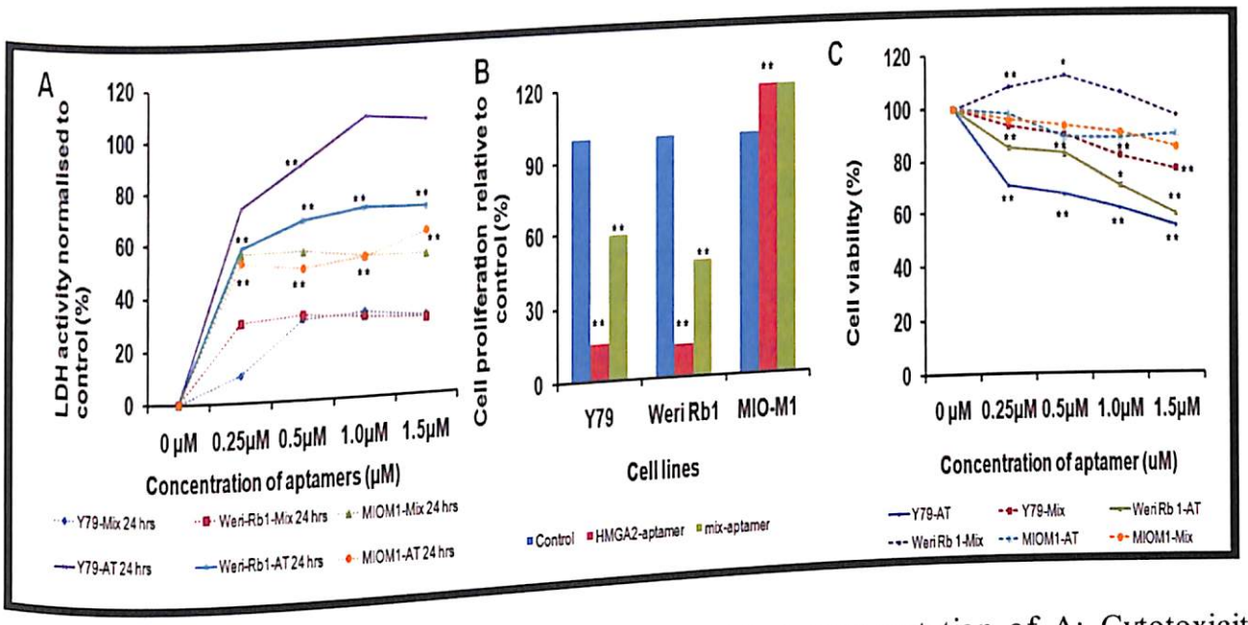

Figure 5.4.2: Toxicity / Proliferation assays. Graphical representation of A: Cytotoxicity assay-Lactate Dehydrogenase (LDH) activity; B: Cell proliferation assay (CyQUANT assay); C: Cell viability assay (MTT assay). A: Percentage of LDH activity measured at 0.25µM, 0.5 µM, 1.0 µM, 1.5 µM at the end of 24 h of HMGA2-aptamer (AT) and mix-aptamer treated RB cells and MIO-M1 cells. Straight line indicates LDH activity in HMGA2-aptamer treated RB cells. Dotted line indicates LDH activity in HMGA2 – aptamer treated non-neoplastic, MIO-M1 cells, and mix-aptamer treated RB cells and MIO-M1 cells. Error bars represent the SD of the triplicates. B: Percentage of proliferation relative to untransfected cells as control in 0.5µM HMGA2-aptamer and mix-aptamer treated RB cells and MIO-M1 cells at the end of 48 h of incubation. C: Percentage of cell viability measured at 0.25µM, 0.5 µM, 1.0 µM, 1.5 µM at the end of 48 h of HMGA2-aptamer (AT) and mix-aptamer treated RB cells and MIO-M1 cells. Straight line indicates cell viability in HMGA2-aptamer treated RB cells. Dotted line indicates cell viability in HMGA2 – aptamer treated non-neoplastic, MIO-M1 cells, and

mix-aptamer treated RB cells and MIO-M1 cells. Error bars represent the SD of the triplicates, (*p<0.05, ** p<0.01).

5.4.4.3. Effect of aptamers on cellular apoptosis

At 0.5 µM of HMGA2 aptamer treatment for 48 h of incubation, the cellular apoptosis using Annexin V FLUOS stain, revealed a mild percentage of cell death, of about 9.25% in Weri Rb1 cells compared to 1.67 % in untreated and 4.49 % in mix aptamer treated Weri Rb1 cells as control. At the same concentration, no remarkable change in cell death was observed in HMGA2 aptamer treated Y79 cells compared to untreated and mix aptamer treated Y79 cells.

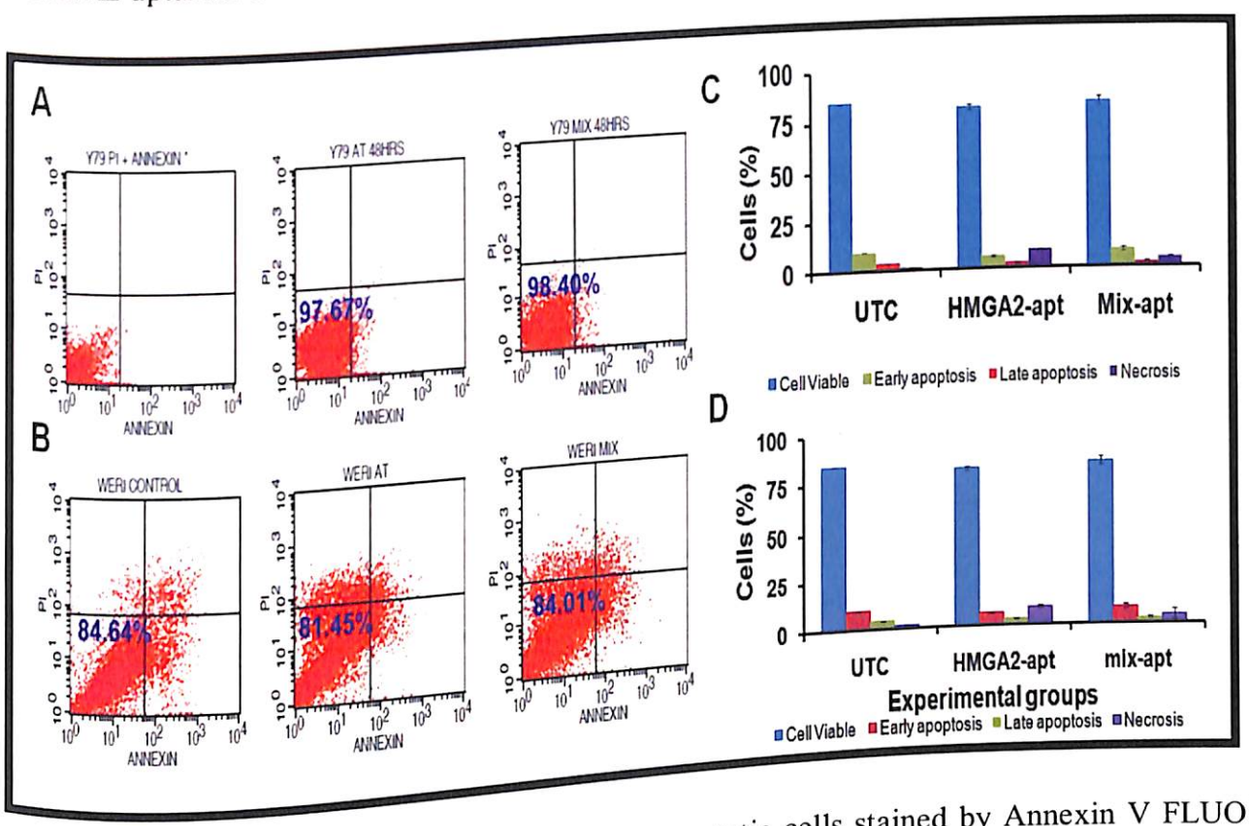

Figure 5.4.3: Apoptotic assay. Scatter plot of apoptotic cells stained by Annexin V FLUOS stain in 0.5 µM of aptamers at the end of 48 h of incubation. A: (i) Measurement of apoptotic Y79 cells in HMGA2-aptamer (AT) and mix-aptamer treatment; (ii) Measurement of apoptotic Weri Rb1 cells in HMGA2-aptamer (AT) and mix-aptamer treatment. B: The bar graph of RB cells at various stages of apoptosis in HMGA2-aptamer (AT) and mix-aptamer treatment. Error bars represent the SD of the triplicates (*p<0.05, ** p<0.01).

5.4.4.4. *Regulation of cell cycle by aptamers*

At 0.5μM of HMGA2 aptamer treatment, the regulation of cell cycle was analysed using PI stain. In this experiment, the HMGA2-aptamer treated RB cells showed a compromised cell proliferation [G2/M and S phase: Y79 (31.75%) and Weri Rb1 (27.94%)] while the mix-aptamer treated RB cells synchronized at S-phase [Y79: 58.29% and Weri Rb1: 31.76%].

Table 5.4.2: Cell cycle analysis. Percentage of cells distributed in different phase of cell cycle in untreated RB cells, HMGA2-aptamer treated RB cells and mix-aptamer treated RB cells. AVG: Average of triplicate experiments; SD: Standard deviation of triplicate experiments.

Experimental groups	Y79				Weri Rb1			
	G0-G1 (%)	G2-M (%)	S (%)	Dead (%)	G0-G1 (%)	G2-M (%)	S (%)	Dead (%)
CONTROL	58.57	18.55	20.03	0	61.4	20.1	16.23	0
	57.78	18.75	20.31	0	61.39	19.75	16.45	0
	58.32	19.35	19.31	0	60.74	20.66	16.51	0
AVG	58.22	18.88	19.88	0.00	61.18	20.17	16.40	0.00
SD	0.33	0.34	0.42	0.00	0.31	0.37	0.12	0.00
HMGA2-aptamer	63.6	6.24	28.44	0.94	73.3	9.26	17.89	0.02
	69.67	5.27	23.73	0.69	73.28	3.01	23.81	0.02
	66.45	11.86	19.72	0.44	72.08	3.06	24.88	0.01
AVG	66.57	7.79	23.96	0.69	72.89	5.11	22.19	0.02
SD	2.48	2.91	3.56	0.20	0.57	2.93	3.07	0.00
mix-aptamer (Scramble)	17.22	16.7	55.49	0	42.09	20.88	31.21	0
	13.04	16.28	59.25	0	41.26	21.32	31.63	0
	12.19	16.12	60.12	0	40.84	20.76	32.44	0
AVG	14.15	16.37	58.29	0.00	41.40	20.99	31.76	0.00
SD	2.20	0.24	2.01	0.00	0.52	0.24	0.51	0.00

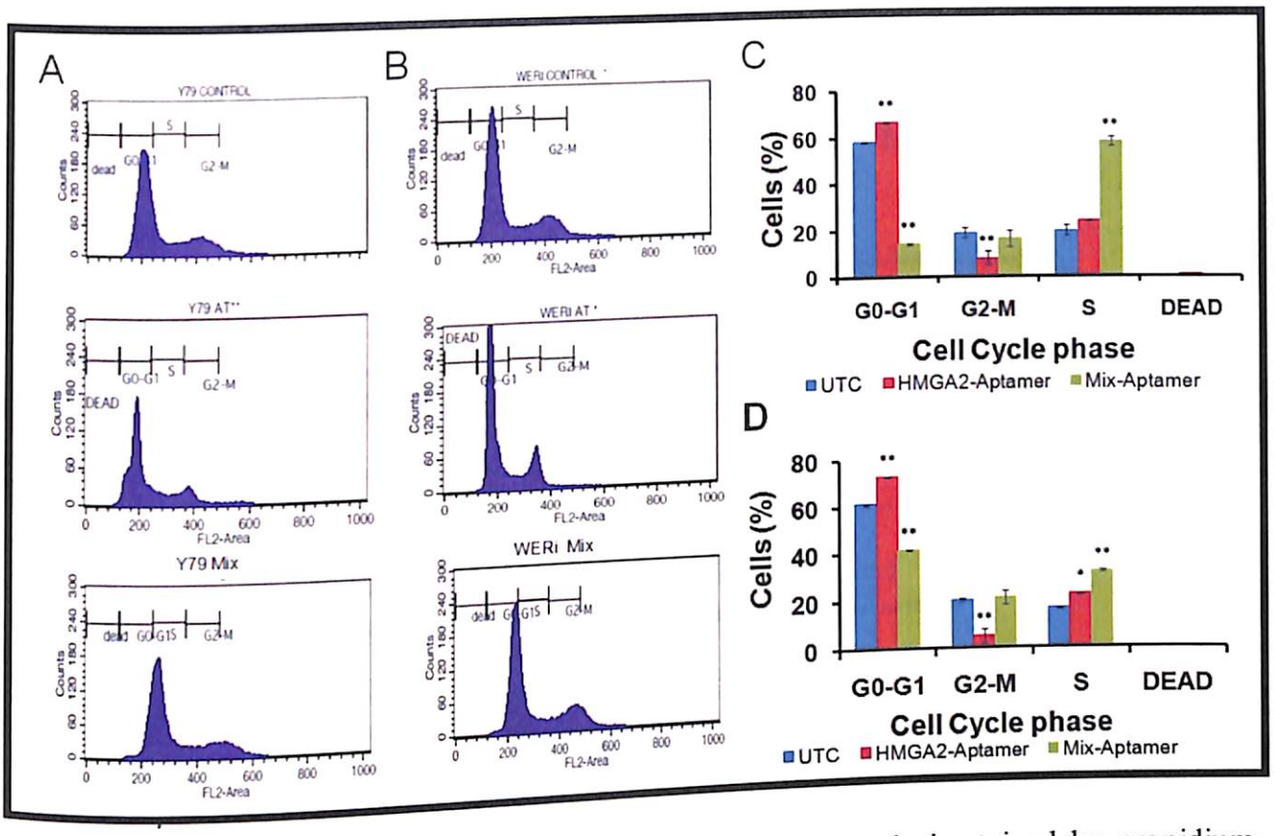

Figure 5.4.4: Cell cycle analysis. Scatter plot of cell cycle analysis stained by propidium iodide stain in 0.5µM of aptamers at the end of 48 h of incubation. (i) Measurement of various cell cycle stage in HMGA2-aptamer (AT) and mix-aptamer treated Y79 cells; (ii) Measurement of various cell cycle stage in HMGA2-aptamer (AT) and mix-aptamer treated Weri Rb 1 cells. B: The bar graph of RB cells at various stages of cell cycle in HMGA2-aptamer (AT) and mix-aptamer treatment. Error bars represent the SD of the triplicates, (*p<0.05, ** p<0.01)

5.4.4.5. Synergistic effect of HMGA2-aptamer treatment in etoposide drug modulation of RB cells

We observed that the constant dosage of 0.5µM of HMGA2-aptamer in combination with increase concentrations of the standard chemotherapeutic drug, etoposide resulted in substantial decrease in RB cancer cell viability. The IC_{70} dose of etoposide, at the end of 48 h of treatment in the Y79 and Weri Rb1 cells were determined as 4.35µg/ml and 4.12 µg/ml respectively. Interestingly, we could observe 70% of cell viability at 2-3µg/ml of etoposide in the presence of HMGA2-aptamer in RB cells while no significant change was observed in mix-aptamer treated RB cells compared to the un-transfected control cells **[Figure 5.4.4.A and B]**. In addition, we observed a significant change in the cell viability percentage of

etoposide treated RB cells (p-value in the order of Y79=0.02; Weri Rb1=0.05) compared to the mix-aptamer treated RB cells. This result indicates that the molecular changes due to the treatment of HMGA2-aptamer in RB cells contribute to the chemotherapeutic drug (etoposide) modulation.

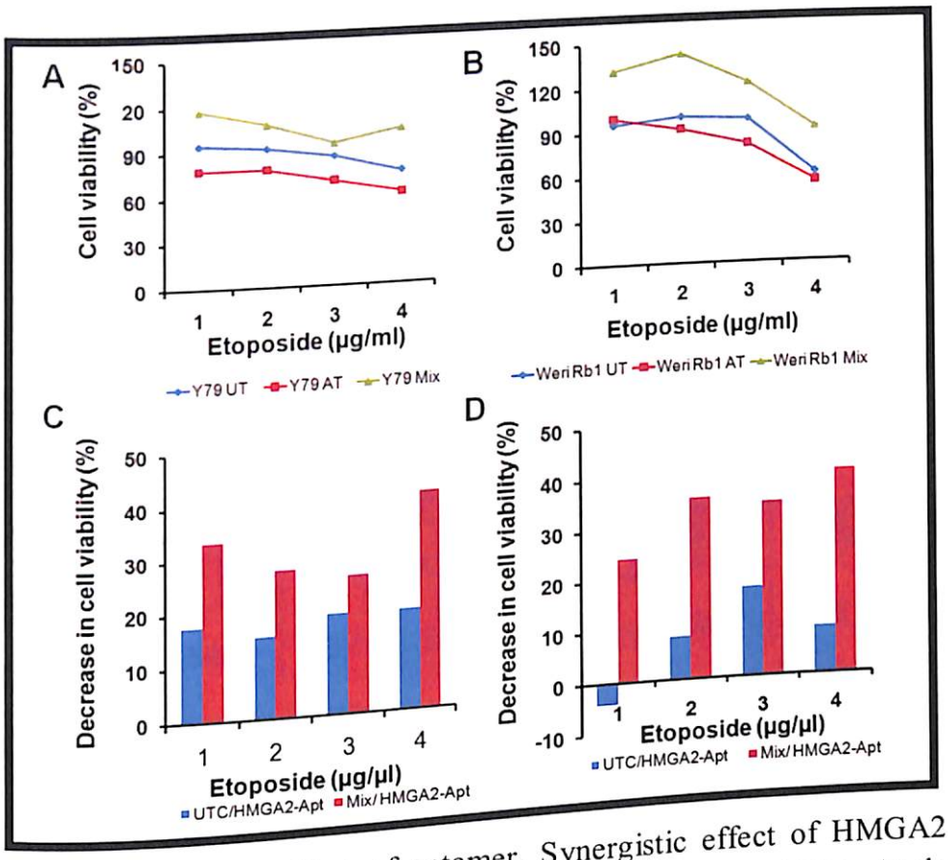

Figure 5.4.5: Synergistic effect of aptamer. Synergistic effect of HMGA2 aptamer in the modulation of etoposide treatment in RB cells; A: Y79; B: Weri Rb1. At the end of 48 h of 0.5 µM HMGA2-aptamer and mix-aptamer treatment, cell viability was measured after 1.0 to 4.0 µg of etoposide treatment. The decrease in cell viability relative untransfected control (UTC) and transfected control (mix-aptamer) in RB cells was computed and represented as bar graphs-C: Y79; D: Weri Rb1. Blue colour bar represents comparison of the transfected cells with respect to untransfected cells, while red colour bar represents the comparison of tranfected cells with respect to transfected control cells (mix- aptamer). Error bars represent the SD of the triplicates.

5.4.4.6. *Molecular dys-regulation in aptamer treated RB cells*

The expression of select panel of genes (*TGFß, SNAI1, CDH1, SMAD4, HDAC8, Bcl2, BAX, PARP, and CASP 3*) was compared for their relative expressions in untransfected RB cells. We observed an inverse correlation of gene expressions between the HMGA2-aptamer

transfected and mix-aptamer transfected RB cells while no inverse correlations was observed in MIO-M1 cells. For the HMGA2–aptamer treated cells , the average levels of gene expression in Y79 cells as follows *TGFß* (5.29), *SNAI1*(-5.865), *CDH1*(4.505), *SMAD4* (4.17), *HDAC 8*(-1.97), *Bcl2* (-4.3), *BAX* (2.32), *PARP* (7.62), and *CASP 3* (3.5). For the HMGA2–aptamer treated cells, the average levels of gene expression in Weri Rb1 cells as follows *TGFß* (5.15), *SNAI1*(-4.01), *CDH1*(6.47), *SMAD4* (3.15), *HDAC8* (-6.34), *Bcl2* (5.11), *BAX* (1.59), *PARP* (3.35), and *CASP 3* (4.60).

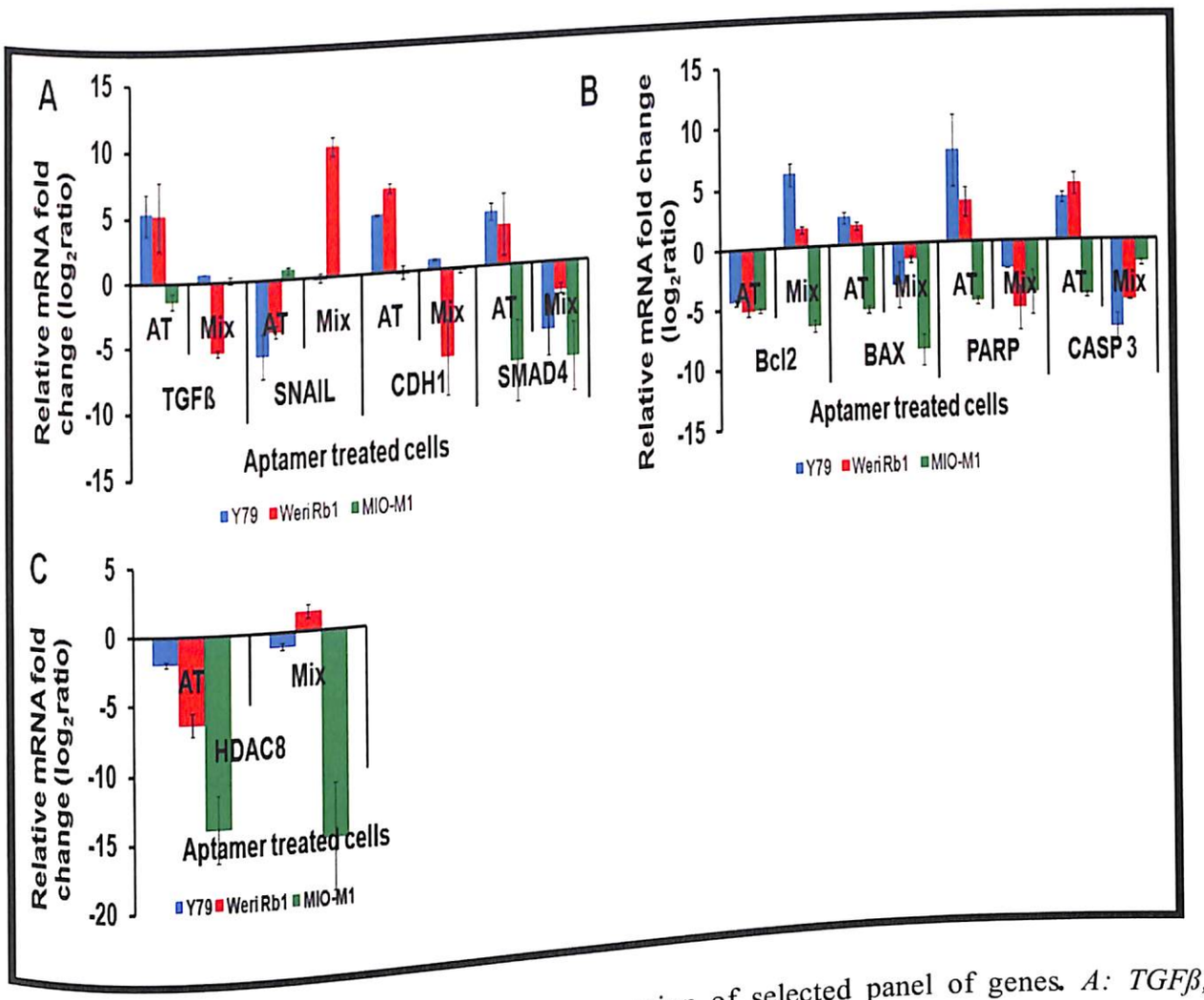

Figure 5.4.6: Gene expressions in RB. Expression of selected panel of genes. *A: TGFß, SNAI1, CDH1, SMAD4, B: Bcl2, BAX, PARP, and CASP 3 and C: HDAC8 measured by qRT-PCR*. The transcript expression was compared for their relative expressions in untransfected RB cells with HMGA2-aptamer transfected, mix-aptamer transfected RB cells and non-neoplastic MIO-M1 cells. Error bars represent the SD of the triplicates.

Table 5.4.3: Gene expressions in RB. Gene levels in the HMGA2-aptamer treated mix-aptamer treated RB cells and MIO-M1cells.

S.No	Genes	Aptamer	Y79	Weri Rb1	MIO-M1
			Average fold change (log_2 ratio)	Average fold change (log_2 ratio)	Average fold change (log_2 ratio)
1.	*TGFβ*	AT	5.300 (1.5)	5.160 (2.5)	-1.325(0.6)
		Mix	0.698 (0.0)	-5.435(0.2)	0.135(0.2)
2.	*SNAIL*	AT	-5.865 (1.6)	-4.015(0.4)	0.718(0.2)
		Mix	-0.016 (0.3)	9.935(0.7)	0.100(0.0)
3.	*CDH1*	AT	4.505 (0.0)	6.471(0.3)	-0.040(0.5)
		Mix	0.818(0.0)	-6.838(2.8)	-0.122(0.2)
4.	*SMAD4*	AT	4.173 (0.6)	3.152 (2.3)	-7.480 (3.1)
		Mix	-5.193 (2.1)	-2.115 (0.4)	-7.415 (2.6)
5.	*HDAC8*	AT	-1.977 (0.2)	-6.341 (0.8)	-13.940 (2.4)
		Mix	-1.030 (0.2)	1.465 (0.5)	-15.005 (3.9)
6.	*Bcl2*	AT	-4.302 (0.2)	-5.110 (0.4)	-5.057 (0.2)
		Mix	6.075 (0.9)	1.485 (0.2)	-6.655 (0.5)
7.	*BAX*	AT	2.321 (0.4)	1.590 (0.3)	-5.399 (0.3)
		Mix	-3.455 (1.9)	-1.350 (0.2)	-9.045 (1.3)
8.	*PARP*	AT	7.620 (0.9)	3.354 (1.2)	-4.962 (0.3)
		Mix	-2.265 (0.0)	-5.629 (1.8)	-4.335 (1.8)
9.	*CASP 3*	AT	3.571 (0.3)	4.682 (0.9)	-4.577 (0.2)
		Mix	-7.435 (1.2)	-5.075 (0.0)	-1.922 (0.2)

5.4.5. Discussion

HMGA2 proteins are known to contribute to neoplastic transformation of retinal cells. Further, the transcription initiation sites and positive regulatory elements have been mapped within the Weri Rb1 cells (Chau et al. 2003). In yet another report, the mechanistic insights inducing apoptosis, G1/ S phase cell cycle arrest and inhibition of cell adhesion mechanism, thereby indicating RB cancer cell suppression due to HMGA2-silencing substantiates HMGA2 as a therapeutic target. This could be further achieved, either by functional obstruction of HMGA2 protein in RB cells, or by suppressing HMGA2 protein expression by targeting its promoters (Chau et al. 2003). In the current study, we investigated the molecular changes involved in RB cells suppression, by functional blocking of synthesized HMGA2 protein in *in vitro* models (Y79 and Weri Rb1) using a DNA Aptamer. In order to determine the specific action of the aptamers, the study included mix-aptamer as the scramble control and also the HMGA2 negative cell line, non-neoplastic MIO-M1cells (as HMGA2 proteins are absent in adult differentiated cells).

Transfection of HMGA2 aptamers in RB cells have resulted in the modulation of cell proliferation while no significant change of cell proliferation was observed in the mix-aptamer treatment in RB cells and in non-neoplastic MIO-M1 cells **[Figure 5.4.2A-C]**. This decrease in RB cell proliferation (in the order of Y79: 59.4% and Weri Rb1: 47.5% with 1.0 µM HMGA2-aptamer treatment) indicates the inhibition of HMGA2 proteins interacting with B-form of DNA. This presents the transcription of E2F family proteins, thus dys-regulating pRB/E2F1 pathway (Fedele et al. 2006). Suppression of RB cell proliferation is further substantiated by the level of lactate dehydrogenase released by HMGA2-aptamer (1.0 µM) treated RB cells for a period of 24 h, which in turn indicates the initiation of cytotoxicity. Further, the decrease in the RB cell proliferation measured by using CYQUANT assay (in the order of Y79: 15.3%, Weri Rb1: 13.49%, MIO-M1 cells: 159.7%) corroborates with the current results of RB cell growth suppression due to the HMGA2-aptamer treatment. In addition, HMGA2-aptamer treated RB cells have resulted in the compromised cell proliferation, while the mix-aptamer treated RB cells synchronised at S-phase of cell cycle

[Figure 5.4.4.A and B, Table 5.4.2]. A few of the molecular changes contributing to these results occuring with in the HMGA2-aptamer treated RB cells are further discussed below.

5.4.5.1. ***Suppression of SNAI1 and activation of CDH1 gene expression levels***

Addition of HMGA2-aptamer in RB cells resulted in the suppression of *SNAI1* gene expression with corresponding increase of *CDH1* (E-cadherin) mRNA levels **[Figure 5.4.6.A]**. This result corroborates with our earlier report, where we observed the similar molecular changes contributing to suppression of RB cell adhesion mechanisms (with decreased *MMP2* activity) due to silencing of *HMGA2* transcripts using RNAi (The published work is also part of the present thesis, chapter 5.2 , (Venkatesan et al. 2012)). Further, the inverse correlation of *SNAI1* and *CDH1* in primary tumors namely retinoblastoma (Venkatesan et al. 2012), breast cancer (Fearon 2003), hepatocellular carcinoma (Jiao et al. 2002) has indicated their contribution in tumor progression and metastasis. So, the change in levels of these two genes could contribute to the arrest of RB cell progression. No significant changes were observed in mix-aptamer treated RB cells and in non-neoplastic MIO-M1 cells.

5.4.5.2. ***Dissecting the tumor suppressor role of TGFß in HMGA2 silenced RB***

TGFß is reported to have dual property of being a tumor suppressor or a tumor promoter (Yamazaki et al. 2011). Hence the molecular complement accompanying the expression of TGFß assumes importance. In this present study, it is evident that HMGA2 silencing activated the *TGFß-SMAD4* pathway resulting in apoptotic cell death in RB cells.

Functional obstruction of DNA-binding HMGA2 proteins using HMGA2-aptamer resulted in the inverse correlation of TGFß gene expression compared to the mix-aptamer transfected RB cells **[Figure 5.4.6.A]**. Earlier reports indicates tumor suppressor role of *TGFß* (Derynck et al. 2001), *SMAD 2* and 4 (Bakri et al. 2014, Kelly and Rizzino 1999). Further, TGFß could induce cell cycle arrest through many interlinked mechanisms such as suppression of c-Myc, cyclin dependent kinases (CDK2/CDK4), E2F transcription factors and dephosphorylation of pRb (Growth inhibition by *TGF-β* linked to suppression of retinoblastoma protein

phosphorylation). In the current study, activation of *TGF-ß* levels in the HMGA2- aptamer treated RB cells has resulted in the G_0/G_1 cell cycle transition. We had previously reported *CDK6* and *E2F4* gene down-regulations in *HMGA2* transcript silenced Y79 cells. This along with the current result of activated *TGFß* mRNA together with compromised cell proliferation (from cell cycle analysis results in HMGA2- aptamer treated model) substantiates its role in the RB cell cycle synchronisation **[Figure 5.4.4.A, B].**

Further, in the HMGA2-aptamer treated RB cells, we observed activation of SMAD4 and an inverse correlation with mix-aptamer treated RB cells **[Figure 5.4.6.A]**. Tumour suppressor role of *SMAD4* gene has been well reported earlier (Hahn et al. 1996). Though, *SMAD4* plays a central component in *TGFß-SMAD* pathway, it still remains unclear if loss of SMAD4 would suppress the tumor suppressive property of *TGFß* (de Winter et al. 1997, Jazag et al. 2005). Further, in few other studies, the activation of SMAD4 in the presence of *TGFß* has resulted in the cell cycle arrest and cell migration (de Winter et al. 1997, Levy and Hill 2005). Taken together with these reports, the activation of SMAD4 together with *TGFß* genes in the current study indicates its contribution towards the RB cell cycle arrest in HMGA2 aptamer treated RB cells while no significant changes were observed with mix-aptamer RB cells. This concomitant evaluation of *TGFß* and *SMAD4* is significant in the light of another report in estrogen receptor α positive breast cancer cells.

In a previous report on colorectal cancer, loss of SMAD4 had contributed to chemo-resistance in malignant tumor (Zhang B. et al. 2014). Since we observed activation of SMAD4 in the HMGA2-aptamer treated RB cells, we were interested to analyse the synergistic effect of these aptamers in the modulation of the chemotherapeutic drugs namely etoposide. In another study, the HMGA2-aptamers phosphorothioarate DNA aptamers had increased the gemcitabine sensitivity in human pancreatic cancer cell lines. However, the molecular mechanism contributing to the chemo-sensitisation of pancreatic cancer cells was not known. Interestingly, in the current study, we observed a significant decrease in cell viability (p-value for Y79=0.02; Weri Rb1=0.05) in the presence of etoposide and HMGA2-aptamer treated RB cells compared to that etoposide and mix-aptamer treated RB cells. Further, we observed the

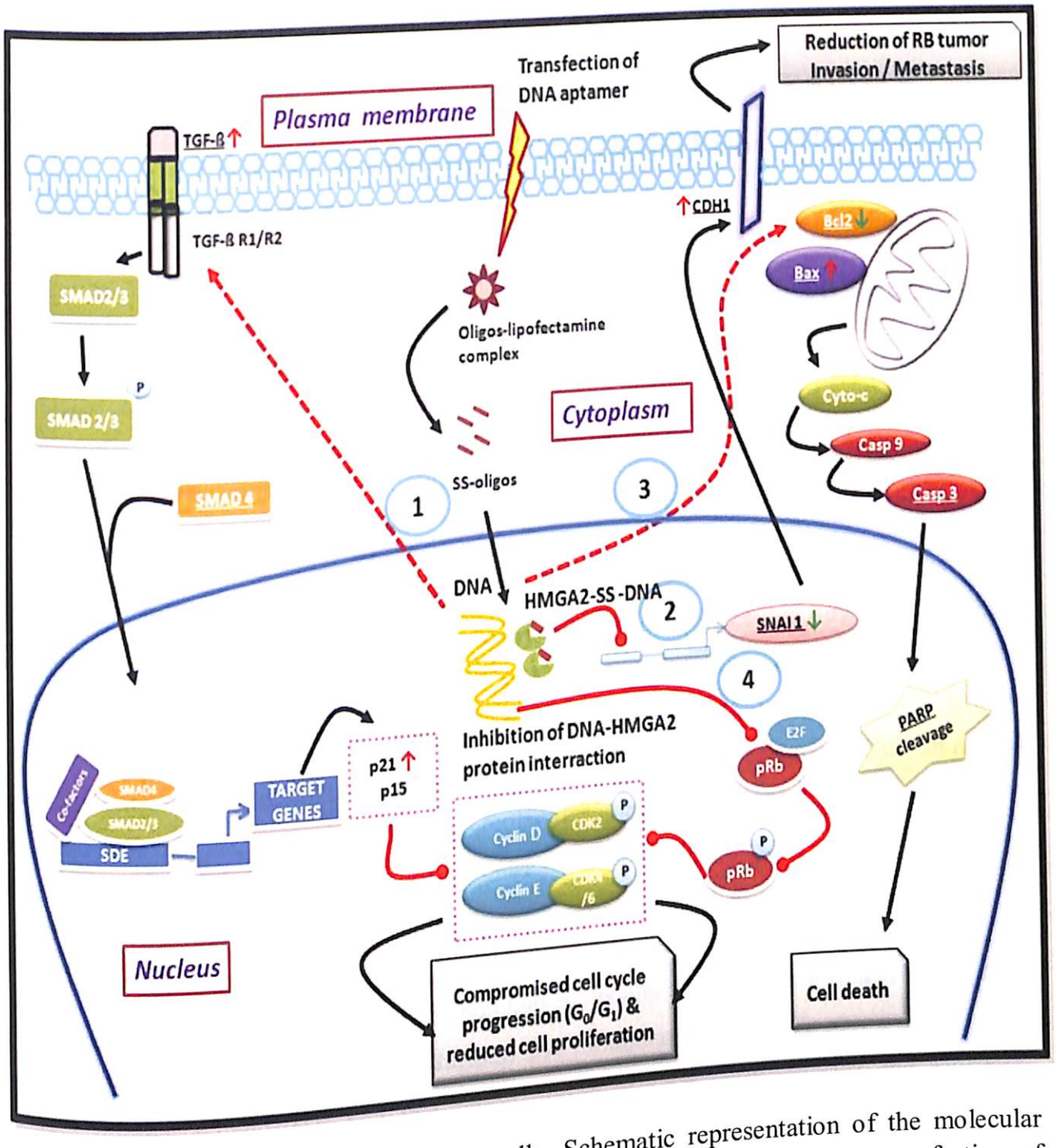

Figure 5.4.5: Molecular changes in RB cells. Schematic representation of the molecular changes in RB cells in the presence of HMGA2 aptamers. 1. Transient transfection of HMGA2 aptamers in RB cells resulted in the activation of TGFß and SMAD4 contributing to compromised cell cycle progression (G_0/G_1); 2. Activation of CDH1 and its transcriptional repressor SNAI1; 3. Suppression of Bcl2 which in turn activates Bax, Casp3 and PARP contributing to the induction of cell death.

CHAPTER 6: FUNCTIONAL OBSTRUCTION OF HEAT SHOCK PROTEINS: INHIBITING ITS INTERACTION WITH SURVIVIN

6. Introduction

Genetic instability of cells results in uncontrolled cell proliferation, resulting in cancer. Novel therapeutic agents are being identified based on specific molecular targets to signaling pathways with great efficacy and reduced systemic toxicity. Although moderate to severe stress resides within the tumor, cancer cells inherit the ability to adapt to the noxious environment even during chemotherapy, which needs to be addressed during selection process of molecular targets. One of the basic molecular machinery involved in these adaptive signaling pathways is the molecular chaperones – heat shock proteins.

Heat shock proteins (HSPs) are highly abundant molecular chaperones in tissues under stress conditions to enhance cell survival (Whitesell and Lindquist 2005). HSPs play a major role in protein folding, homeostasis and maturation during proteotoxicity (Mosser and Morimoto 2004). In addition, these foldosomes are involved in numerous cellular signaling pathways such as cell cycle regulation, proliferation, apoptosis and cytoskeleton (Soti et al. 2002). Based on their molecular sizes, HSPs has been categorized as HSP100, HSP90, HSP70, HSP60, HSP40 and other small heat shock proteins (Jolly and Morimoto 2000). HSPs especially HSP90, HSP70 and HSP27 are predominantly over-expressed in several cancer types such as glioblastoma, prostate carcinoma, retinoblastoma (Graner et al. 2007, Jiang et al. 2008, Sherman and Multhoff 2007, Tang D. et al. 2005) where a significant association

was reported with tumor progression (Ciocca et al. 2003, Gyrd-Hansen et al. 2004, Nylandsted et al. 2000). In particular, HSP90 has emerged with prime importance in the survival of cancerous cells. This unique cancer chaperone molecule is highly conserved and constitutively expressed in cancers to maintain genetic instability and tumor cell survival (Neckers 2007, Whitesell and Lindquist 2005). HSP 90 accounts for 1-2 % of total normal cellular protein and its level is elevated to approximately 4-6% under stress (Stravopodis et al. 2007). The functional activity of HSP90 is attained through the interaction of this protein with numerous client proteins mainly like HER2, AKT, CDK4, HIF, MMP2 and Survivin (Pearl and Prodromou 2000, Workman et al. 2007).

Among these client proteins, Survivin is an inhibitor of apoptosis (IAP) gene family member and is over-expressed in many cancers and its expression was earlier reported in retinoblastoma (Sudhakar et al. 2013). Survivin exhibits an essential role in apoptosis inhibition, tumor progression and cell cycle regulation (Altieri 2003, Andersen and thor 2002). Suppression of Survivin induces mitochondrial apoptosis, inhibits cell proliferation and increases the susceptibility of tumor cells to chemotherapy (Blum et al. 2006, Liu X. et al. 2010, Trabulo et al. 2011, Tu et al. 2003, Wang Z. et al. 2005). HSP90 controls proteostasis of survivin, a tumour antigen by refolding the unfolded/denatured protein to a native state. With respect to other co-chaperone molecules, namely HSP70, HSP40, p23 and an adapter, HOP (HSP organizer protein) (Cintron and Toft 2006, Johnson B. D. et al. 1998, Pratt and Toft 2003) a sequential binding and hydrolysis of ATP takes place resulting in multi-chaperone complex (Pratt and Toft 2003, Young et al. 2001).

Rather than targeting a single molecule, targeting multiple biologically significant molecules in cancer pathways has provided a wide tool for various cancer therapies. Thus, disruption of HSP90/Survivin physical interaction by targeting the ATP-binding pocket of HSP90 inhibits the down-stream signaling cascade of Survivin, leading to the ubiquitin mediated degradation and deactivation of Survivin signaling pathways resulting in the arrest of tumor growth and development (Fortugno et al. 2003, Meli et al. 2006). Thus HSP90/ Survivin may serve as a potential target for RB cancer therapies. RB arises from the primitive retinal layers of eye

usually due to the *de-novo* mutation of RB1 gene. Incidence of the extra-ocular and metastatic RB is almost two-third of cases in the developing countries. Betterment in the disease management is achieved with the combination of therapies namely chemotherapy, radiotherapy and the enucleation (Bakhshi S 2007).

Earlier, a structure–based mimicry, shepherdin (K79-L83), which intervenes the survivin-HSP90 interaction has been tested to be potent and selective anti-cancer agent (rationale design). Previous reports by Plesica et al., 2005 and Morris et al., 1998 signify the interaction of peptido-mimetic, shepherdin with HSP90 both structurally (AutoDock program package) and experimentally (using cell-permeable variants in HeLa cells). In addition, these studies revealed that shepherdin is a potential anti-cancer agent compared to geldanamycin (GA) (structural analysis) and 17-AAG (*in vitro* tumor models) (Sausville et al. 2003).

In the current study, initially, we report the over-expression of HSP90, HSP70, survivin and their association in advanced retinoblastoma (RB) primary tumors. Secondly, we have studied the dose dependent efficacy of a peptido-mimetic, shepherdin using *in vitro* RB tumor model (Y79 and Weri Rb1) and non-neoplastic cell line Muller glial cells (MIO-M1). Attempts to identify the molecular targets aiding in implementation of peptides to sensitize the tumors may contribute to the good results in combination therapies.

6.1. Materials and Methods

6.1.3. Primary RB tissues

The institutional ethics committee of Vision Research Foundation, Sankara Nethralaya (Chennai, India) has reviewed and approved the study. RB primary tumor samples were collected from 29 enucleated eyeballs of RB patients as part of RB management (2010 – 2012). The study includes 17 male and 12 female patients with median age of 2.0 years.

Among them, 15 tumor samples were collected from right eye and 14 from left eye. Grading of tumors was performed from the microscopic observations of haematoxylin and eosin stained RB sections by the ocular pathologist. Histopathological information namely tumor invasion of the choroid, optic nerve, or orbit **[Table 6.1]** was obtained from surgical pathology reports. Among the tumors analyzed, there were 17 invasive tumors and 12 non-invasive tumors with high risk histopathological features. From these samples, a representative of 10 tumor samples was analyzed for the respective mRNA expression (using qRT-PCR) and protein expression (Using flow cytometry analysis and western analysis).

Based on the clinical presentation of the patients, the tumors were classified as per International Intraocular Retinoblastoma Classification (IIRC). There were 6 tumors under group B, in which 2 were invasive, 4 non-invasive. Of the 10 tumors under group D, 6 were invasive, 4 non-invasive. Of the 15 tumors under group E, 9 were invasive, 6 non-invasive (Sastre et al. 2009). Normal adult retina collected from 3 cadaveric eyeballs (received at C.U. Shah eye bank, Sankara Nethralaya, http://www.sankaranethralaya.org/eye-bank.html) during the year 2011were included in the study.

6.1.4. Cell culture

Human RB cancerous cell lines (Y79, Weri Rb1, Riken cell bank, Japan) and human non-neoplastic cell line, Muller glial cell line (MIO-M1) used in the study was maintained as described in section 4.1.3.

6.1.5. Nutrient- deprivation RB cell model

Cells were treated with peptidomimetics in serum- free condition for an initial period of 4 h and supplemented with 5% growth medium, incubated further at 37 °C in a 5% CO_2 for 20 hrs. HSP90 and survivin levels were analyzed at the end of 4hrs of serum deprivation and after 20 hrs of 5% serum supplementation

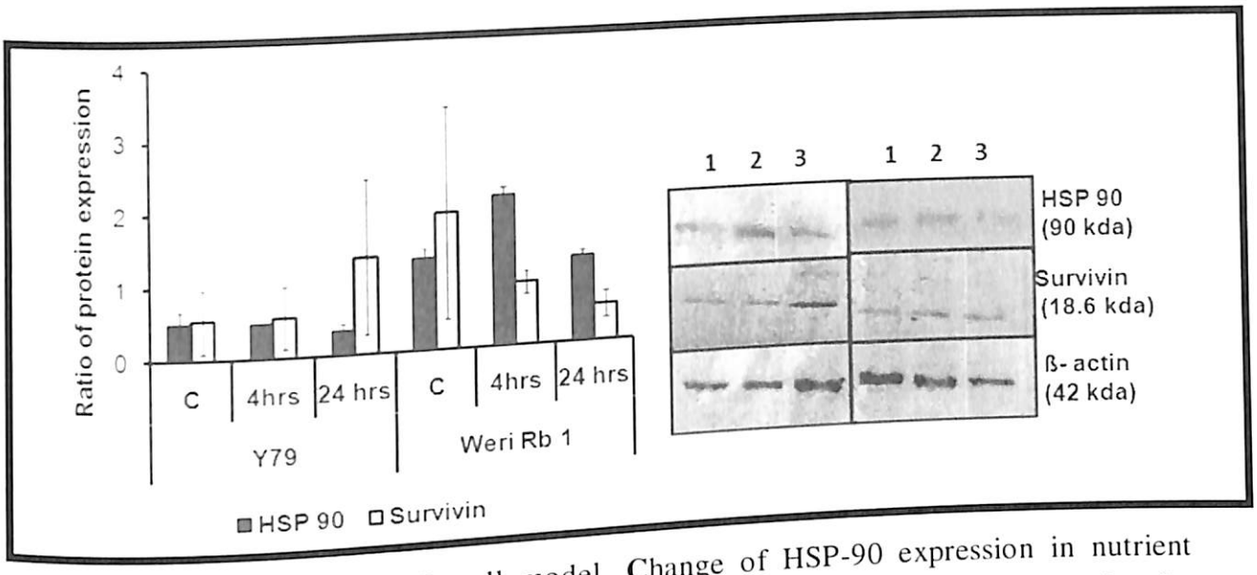

Figure 6.1: Nutrient deprived RB cell model. Change of HSP-90 expression in nutrient deprived (4 hrs starvation of serum) RB cells, followed by the 5% serum supplementation for 20 hrs).

6.1.6. Antibodies and Peptides

Monoclonal antibodies to HSP90 (catalogue No: 4874, Cell signaling Technology, Danvers, MA), HSP70 (catalogue No:4872, Cell signaling Technology, Danvers, MA), Survivin (SC-17779, santa cruz, CA,USA), Bax (catalogue No: Ab7977, 0.2mg/ml; Abcam), Bcl-X S/L (4H33, catalogue No SC 70418, Santacruz biotechnologies, CA, USA), Bim(H-191, catalogue No: Sc 11425,, Santacruz biotechnologies, CA, USA), caspase 9 (F7, catalogue No: Sc 17784 Santacruz biotechnologies, CA, USA), β-actin (Sigma Aldrich, St. Louis, MD, USA), Horse raddish peroxidase (HRP) conjugated secondary antibodies conjugate (santacruz),anti-mouse-FITC conjugated (catalogue No: , Santacruz biotechnologies, CA, USA) and anti-rabbit-cy3 conjugated (catalogue No: A(10520), 2mg/ml, Invitrogen CA, USA) and fluorescence isothiocyanate (FITC) conjugated streptavidin (Invitrogen) were used in the study. N-terminal end of Shepherdin and its scrambled peptides, tagged with a biotinylated cell permeable HIV-TAT protein. The amino acid sequences of shepherdin peptide used in the study is as follows: biotin-X-YGRKKRRQRRRKHSSGCAFL-$CONH_2$ ($shepherdin^{Tat}$) for shepherdin, biotin-X-YGRKKRRQRRRSKLACFSHG-$CONH_2$ for scrambled peptide, X = EAHX, hexanoic acid spacer. These peptides were procured from Custom peptide sythesis, Mumbai.

6.1.7. Immunohistochemistry

HSP 90, HSP 70, Survivin protein expressions in RB primary tumour samples were analysed by immunohistochemistry. The protocol of immunohistochemistry was followed as described in section 4.2.1.

6.1.8. RNA isolation and qRT-PCR

Primers used for qRT-PCR were,

1. HSP70: sense-5'ACCAAGCAGACGCAGATCTTC3'
   antisense-5'CGCCCTCGTACACCTGGAT3'
2. HSP90: sense-5'CCTTCTATTTGTCCCACG3'
   antisense-5'ATCCTCCGAGTCTACCAC3'
3. Survivin: sense-5'GACCACCGCATCTCTACATTC3'
   antisense-5'TGCTTTTTATGTTCCTCTATGGG3'.

Experiments were performed in triplicates in the same reaction. Comparative quantification was determined by using $2^{-\Delta\Delta Ct}$ and relative expression values were normalized to GAPDH as endogenous control.

6.1.9. Western analysis and Flow cytometry

Western analysis of HSP 90, HSP 70, and Survivin are performed as described in the section 4.2.2. The treated and un-treated cells for Survivin, Bcl2-XL, Bax, Bim, caspase 9 expressions are analysed by FACS following the protocol described in section 4.2.

6.1.10. Internalization assay

Cells are treated with various concentrations of peptides ranging from 0.17, 0.25, 0.34, 0.42 µg/ml in serum free media for 4hrs. Following this treatment, 5% serum supplementation was provided to the cells and the cellular uptake of peptides at 0, 4, 8, 16 hrs of serum supplementation was measured using flow cytometer. At the end of incubation, the treated cells were harvested, washed twice with chilled 1x phosphate buffered saline (PBS), incubated with FITC conjugated streptavidin (1:500) at 4°c for 2 hrs. Following this incubation, the cells were washed thrice with chilled 1X PBS and the cells harboring peptides were quantified using flow cytometer (FACS caliber, BD Biosciences, San Jose, CA), installed with CellQuest software program (BD Biosciences). Further the presence of peptides within the cultured cells at 0.42 µg/ml of concentration at end of 24 hrs was examined by using Axio observer microscope (Zeiss, Berlin, Germany).

6.1.11. Cell proliferation, viability and Apoptosis assays

For cell viability and proliferation assays, $5X10^3$ cells /well in 96 well plates and incubated at 37°C overnight. The cells were then treated with varying concentrations of peptido-mimetic ranging from 0.17, 0.25, 0.34, 0.42 µg/ml and incubated for specific time periods (0, 4, 8, 16 hrs of serum supplementation). The MTT assay, CyQUANT assay and cytotoxicity assay (estimation of lactate dehydrogenase activity) in treated and untreated cells were carried out as stated in section 4.2.11.

6.1.12. Zymography

Activity of matrix metallo proteinase was assayed using zymography. Conditioned media from cells cultured in the absence of serum for 4 h were collected and concentrated 10-fold using speed vac concentrator (Thermo Scientific). Concentrated conditioned media were

mixed with 2X Laemmli loading buffer (without reducing agent) and subjected to gelatin (Merck chemicals) zymography as previously descrambleibed (Hawkes, Li et al. 2010). Briefly, samples were electrophoresed on 10% SDS-polyacrylamide gel containing 0.1% gelatin. Gels were then washed in 2.5% Triton X-100 at room temperature to remove SDS, followed by incubation at 37°C for 20 h in 50 mM Tris-HCl (pH 8.0), 5 mM CaCl2. MMP activity was visualized as clear bands with Coomassie Brilliant Blue R-250 staining. The density of the bands were measured using Quantity One, version 4.7 software in GS 800 calibrated Densitometer (Bio-Rad) (Hawkes et al. 2010).

6.1.13. Statistical analysis

Independent sample t-test and pearson-correlation analysis was used to compare the variables among RB tumor tissues. A repeated measure ANOVA and one-way ANOVA was used to derive the significance for the variable groups *in vitro* assay. The normal measure of p-value≤0.05 was considered as significant values.

6.2. Results

6.2.3. Immunostaining of HSPs and survivin in primary RB tumors

HSP90, HSP70 and survivin expression did not show any immuno-reactivity in non-neoplastic, cadaveric human adult retina **[Figure 6.2]** while higher to moderate expressions of these proteins were observed in RB tumors. Among 29 RB tumors, HSP90 expression as cytoplasmic positivity was in the order: higher expression in 4 tumors (23.50%), moderate expression in 2 tumors (11.76%) and less expression in 11 tumors (64.70%). Higher cytoplasmic expression of HSP 70 in 5 tumors (29.4%), moderate expression in 3 tumors (17.64%) and less expression in 9 tumors (52.94%) was observed. Similarly, nucleus and cytoplasmic expression of Survivin was in the order of higher expression in 1 tumor (5.8%), moderate expression in 5 tumors (29.4%) and less expression in 9 tumors (64.70%). **Table 6.1**

shows the distribution of immuno-positivity of HSP90, HSP70 and Survivin in RB tumors. No significant difference with respect to invasion and no invasion were observed. Further, we observed a significant association between HSP 90 / HSP 70 (r=0.59, p value=0.001) while no significant association was observed between HSP 90/70 with Survivin. These results were concurrent with the relative mRNA and the protein expressions in the representative 10 tumor samples studied.

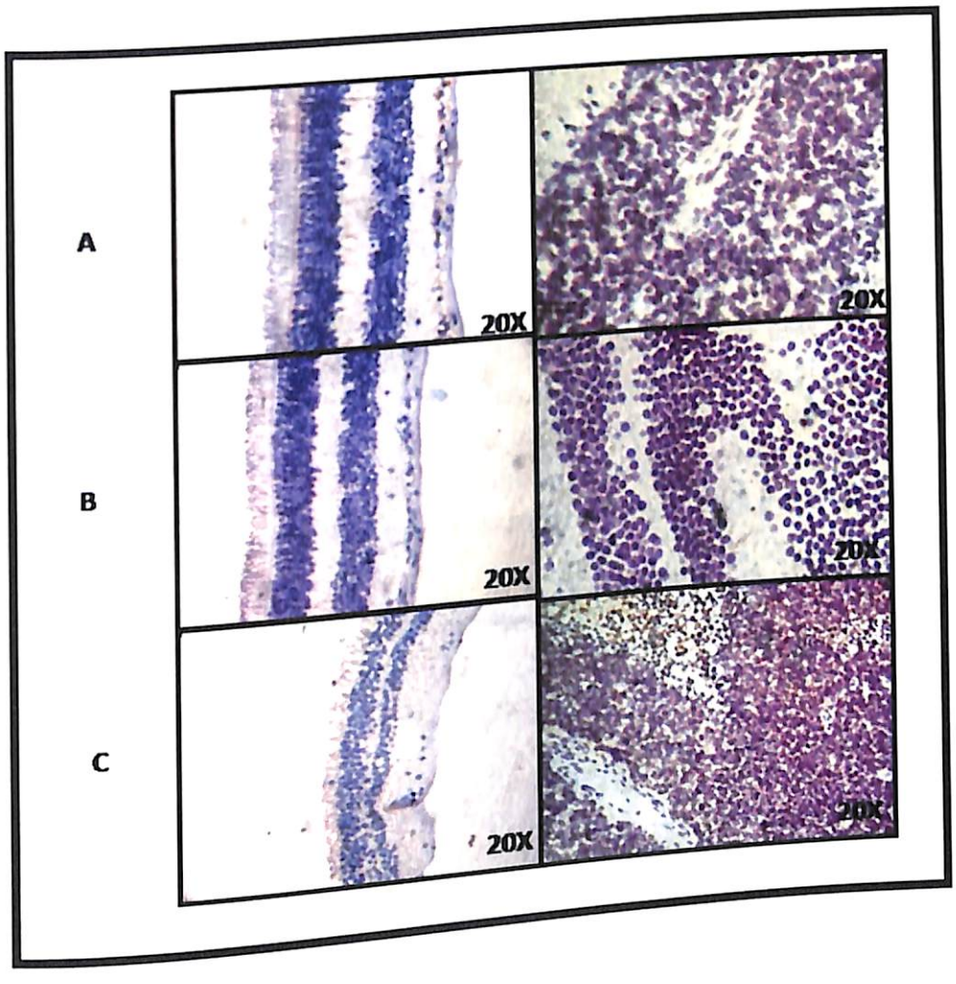

Figure 6.2: Protein expressions in RB. HSP90, HSP70 and Survivin protein expression in RB primary tumors, non-neoplastic cadaveric human retina (IHC): Photomicrographs of HSP90 (A), HSP70 (B) and survivin (C) expressions in RB primary tumors, non-neoplastic cadaveric human retina.

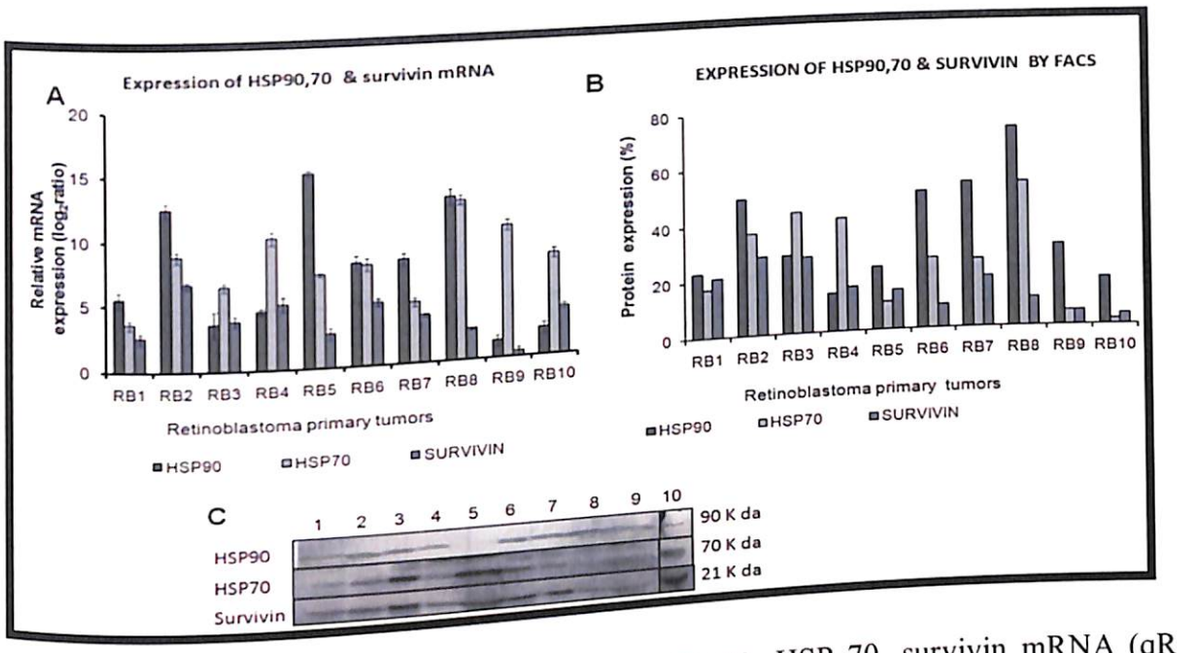

Figure 6.3: HSPs / Survivin expressions in RB. HSP 90, HSP 70, survivin mRNA (qRT-PCR) and protein expressions (western analysis). A: Bar graph representing the relative mRNA expressions in RB primary tumor samples (n=10) and in RB cell lines relative to non-neoplastic cadaveric human retina (n=3); B: Bar graph representing the protein expressions in RB primary tumor samples and in RB cell lines (n=10); C: Western analysis of HSP90, HSP70 and survivin in primary RB tumor samples. Error bars represent the SD of the triplicates.

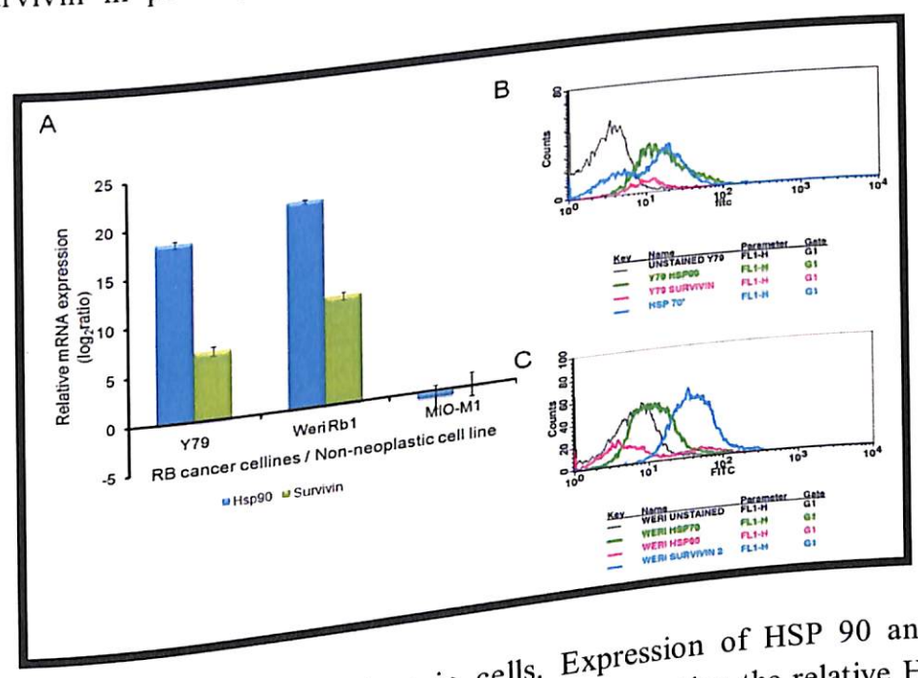

Figure 6.4: HSP90 / Survivin expressions in cells. Expression of HSP 90 and Survivin proteins in RB cells and MIO-M1 cells A: Bar graph representing the relative HSP 90 and Survivin mRNA expressions in RB cell lines (Y79 and Weri Rb 1) and in non-neoplastic cell line (MIO-M1); B-C: Protein expression of HSP90, HSP70 and survivin in RB cell lines (B: Y79 and C:Weri Rb 1). Error bars represent the SD of the triplicates.

Table 6.1: *HSP 90 / HSP 70 / Survivin protein expressions in RB. Clinico-Pathological features of primary RB tumours: Protein expression of HSP90, HSP70 and survivin (IHC).*

S.No	RB primary tumors	RB Group (IIRC)	Age (Yrs) /Sex	Clinico-pathological descriptions	HSP 90		HSP 70		Survivin	
					Positive (%)	Score	Positive (%)	Score	Positive (%)	Score
1	RB1	G-E	6MON/F	OD; MD; CI; >3mm; pre-lam,post-lam of ON	60	3	90	2	40	1
2	RB2	B	2/M	OS; UD; CI; <3mm; pre-lam of ON	50	1	60	1	30	1
3	RB3	G-E	3/M	OD; UD; CI<3mm	30	1	40	1	40	2
4	RB4	B	3/M	OS; UD,NI	50	2	80	2	60	1
5	RB5	B	2/M	OS; NO CI,pre-lam of ON	60	2	40	1	20	1
6	RB6	D	7MON/M	OD; WD; CI; >3mm; pre-lam	10	1	30	1	60	2
7	RB7	D-E	3/M	OS; MD; NI	60	2	80	2	40	1
8	RB8	D	1/F	OS; WD; CI; <3mm	30	1	70	2	40	1
9	RB9	D-E	2/F	OD; CI; 10mmX7mm; scleral inv	40	1	80	2	40	1
10	RB10	G-E	4/M	OS; PD; CI; >3mm; pre-lam of ON	70	1	60	1	20	1
11	RB11	E	2/M	OD;WD; focal RPE inv, pre-lam and post-lam of ON	60	2	85	2	50	1
12	RB12	E	3/M	OD;PD; CI; >3mm; pre-lam of ON	70	2	90	2	60	2
13	RB13	B-E	6MON/F	OS; WD; focal RPE inv; pre-lam	60	2	60	2	40	2
14	RB14	D	1/M	OS; PD; CI; multiple foci of RPE	60	1	40	1	50	1

15	*RB15*	*E*	*4/F*	*OS; PD; focal RPE inv; pre-lam inv OF ON; <3mm; scleral inv*	40	1	40	1	20	1
16	RB16	E	4/F	OD; UD; CI; >3mm; pre-lam ON	10	1	40	1	20	1
17	RB17	D	3/F	OS; WD; CI<3mm; post-lam of ON	30	1	40	1	30	1
18	RB18	D	2/F	OD; PD; pre-lam of ON	30	1	50	2	30	1
19	RB19	E	2/M	OD; CI; >3mm; pre-lam and post-lam of ON	70	2	60	2	40	1
20	RB20	D	1/F	OS; WD; focal RPE inv; <3mm; pre-lam of ON	60	2	40	1	40	2
21	RB21	E	2/F	OD; PD; CI; >3mm;pre-lam and post lam	60	1	50	2	40	2
22	RB22	E	7MON/M	OD; WD; no CI; focal RPE, pre and post laminar invasion	40	1	50	1	30	1
23	RB23	B	2/M	OD; UD; CI; 1.5mm & 2mm	80	2	70	2	60	1
24	RB24	E	2/M	OS; PD; CI; >3mm;; pre-lam, post-lam ON	30	1	20	1	20	1
25	RB25	D	2/F	OD; PD; pre-lam inv of ON	60	1	30	1	50	3
26	RB26	B	2/M	0S;RB;UD	30	1	40	1	60	2
27	RB27	D	2/M	OS;UD;CI<3mm, focal RPE	20	1	40	1	80	3
28	RB28	E	2/M	OD;WD;CI;<3mm; inv of CB	60	1	30	1	20	1
29	RB29	D	3MON/F	OD;WD; focal CI, pre-lam	60	2	40	1	60	2

M: Male; F: Female; OD: Right eye; OS: Left eye; PD: Poorly differentiated; UD: undifferentiated; WD: Well differentiated; CI: Choroidal invasion; inv: invasion, CB: Ciliary body; Pre-lam: Pre-laminar, post-lam: Post-laminar, RPE: Retinal Pigment Epithelium and SE: Surgical end

6.2.4. Internalization and cellular uptake of peptido-mimetic shepherdin molecules

Flow cytometry and microscopic analysis revealed that a shepherdin and scramble-peptide molecule penetrated into RB cells (Y79 and Weri Rb 1) and non-neoplastic cells (MIO-M1) in a concentration dependent manner (figure 2). A maximum uptake of (M2 population: 98%) shepherdin peptide and scramble-peptide, at 0.42ug/ml dosage at the end of 16 h of 5% serum supplementation was observed. The presence of TAT-peptides conjugated to the shepherdin provides the effective membrane penetration (Brooks et al. 2005). Internalization of peptido-mimetic molecules inside these cells was also confirmed by the fluorescent photomicrographs. The photomicrographs show the presence of peptido-mimetic in cytoplasm and in nucleus (as specks) while the scramble-peptide localizes in the cytoplasm of the cells [**Figure 6.5**]. As maximum internalization of the shepherdin and scramble-peptide in RB cells and MIO-M1 cells were at 0.42 µg/ml concentration, the functional evaluation of shepherdin were carried out at this concentration.

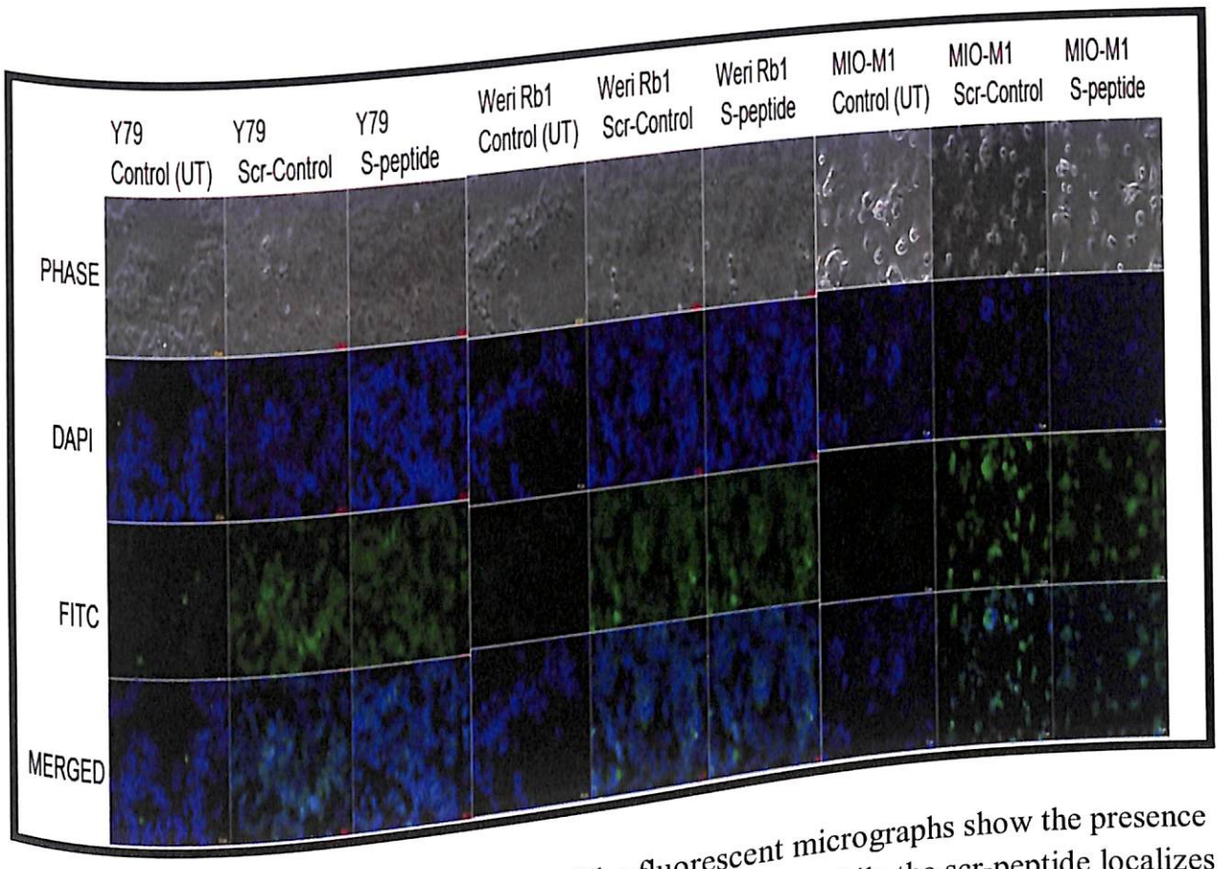

Figure 6.4: Peptide internalisation assay .The fluorescent micrographs show the presence of peptido-mimetic in cytoplasm and in nucleus (as specks) while the scr-peptide localizes in the cytoplasm of the cells.

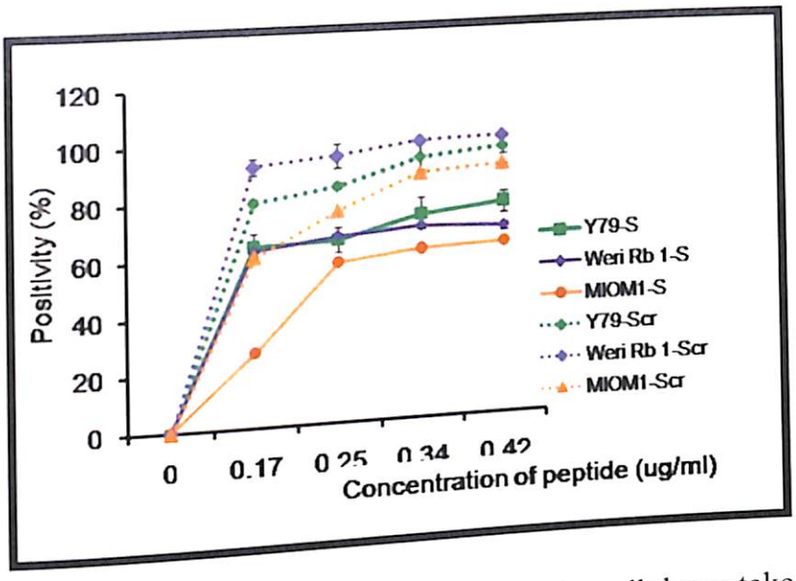

Figure 6.5: Cellular uptake assay. Line graph indicates the cellular uptake of peptides in RB cells and MIO-M1 cells. Error bars represent the SD of the triplicates.

6.2.5. Analysis of cytotoxic and cytostatic effect, of peptido-mimetic shepherdin molecules in RB cells

The anti-proliferative and toxic effect of shepherdin molecules was analyzed using CyQUANT assay and MTT assay. In cell viability assay (using MTT), a high percentage of cytotoxic activity of shepherdin in RB cells (in the order of 55.67% in Y79 cells; 49.85% in Weri Rb1 cells) was observed in 0.42 µg/ml concentration, while absence to low effect was observed in presence of scramble peptide (in the order of 92.21% in Y79 cells; 102.98% in Weri Rb1 cells) at the end of 4hrs, with peptide treatment. At the same concentration and time point, low cytotoxic effect was observed in the presence of scramble-peptide in RB cells [**Figure 6.6.A**]. Non- cytotoxic effect of shepherdin and scramble-peptide was confirmed in non-neoplastic cells (MIO-M1) at same concentration and time point [**Figure 6.6.B**].

By CyQUANT assay, the relative percentage of cell proliferation in Y79 cells was observed to be 96.5% in scramble peptide versus 59.6% in shepherdin peptide treated Y79 cells. Similar decrease in cell proliferation was observed in Weri Rb1 cells where the scramble treated showed 66.29% versus 17.83% of shepherdin treated Weri Rb1 cells compared to untreated RB control cells at the end of 4 hrs with 5% serum

supplementation. These results together indicate the cytotoxic and cytostatic effect of shepherdin in RB cells at 0.42µg/ml concentration at 4 h of 5% serum supplementation.

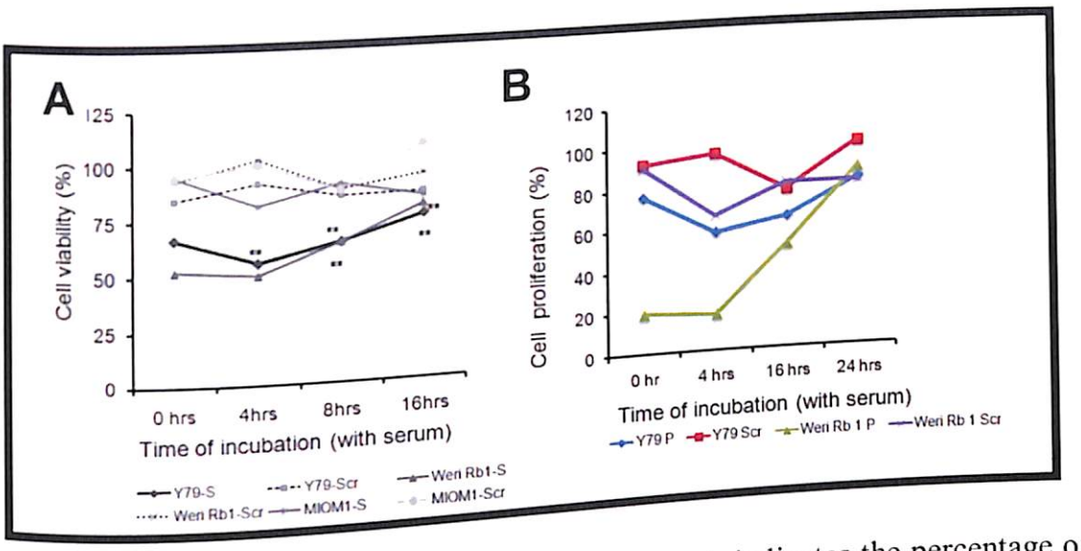

Figure 6.6: Cell viability / proliferation assay. Line graph indicates the percentage of cell death in the shepherdin and scramble treated RB cells, MIO-M1 cells. A. Cell viability analysis using MTT assay. B. Evaluation of Apoptosis using Annexin V FLUOS stain. Straight line indicates shepheridin treated Cells while the dotted lines indicate the scramble treated cells. Error bars represent the SD of the triplicates (** indicates $p<0.01$).

In 0.42 µg/ml of shepherdin treated RB cells, Annexin V PI stain showed 98.76 %; 90.27% of necrosis in Y79 and Weri Rb 1 at the end of 4 hrs of 5% serum supplementation compared to un-treated RB cells. Very low to low percentage of apoptosis was noted in the scramble-treated RB cells [**Figure 6.7**].

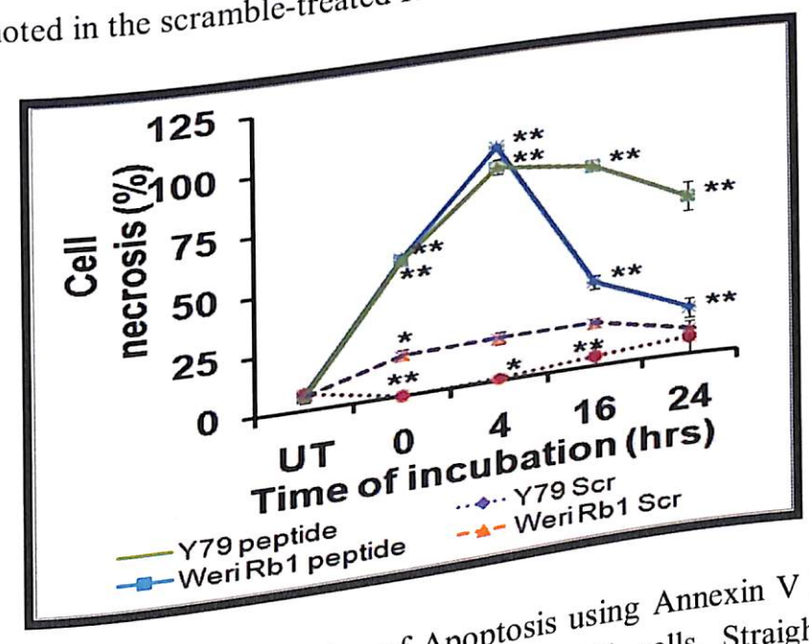

Figure 6.7: Apoptosis assay. Evaluation of Apoptosis using Annexin V FLUOS stain in the shepherdin, scramble treated RB cells and MIO-M1 cells. Straight line indicates

shepheridin treated Cells while the dotted lines indicate the scramble treated cells. Error bars represent the SD of the triplicates (** indicates $p<0.01$).

6.2.6. Suppression of MMPs activity in peptido-mimetic shepherdin treated RB cells

By zymography analysis, the relative percentage of MMPs activity in Y79 cells was observed to be 149.72% in scramble peptide versus 74.92 % in shepherdin treated cells. Similar decrease in MMPs activity was observed in Weri Rb1 cells where the scramble treated showed 70.91% MMPs activity versus 40.78% in shepherdin treated groups. Thus, both Y79 and Weri Rb1 cells showed decrease in MMPs activity with shepherdin peptide treatment (Figure 4). These results together indicate activity of MMP's, yet another client protein of HSP 90 in the presence of shepherdin molecules contributing to arrest of cellular invading property in RB cancerous cells.

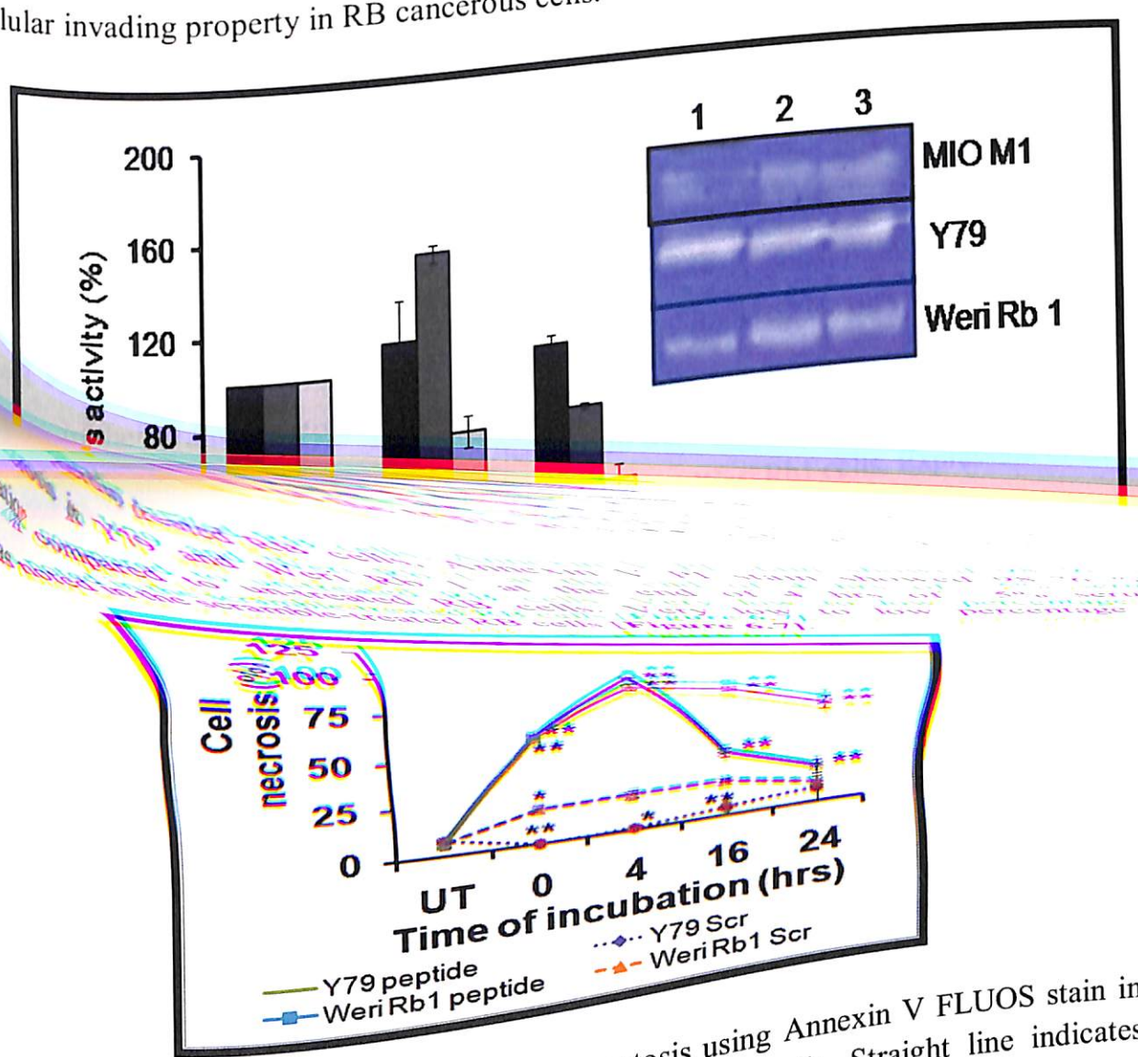

Figure 6.7: Apoptosis assay. Evaluation of Apoptosis using Annexin V FLUOS stain in the shepherdin, scramble treated RB cells and MIO-M1 cells. Straight line indicates

shepheridin treated Cells while the dotted lines indicate the scramble treated cells. Error bars represent the SD of the triplicates (** indicates $p<0.01$).

6.2.6. Suppression of MMPs activity in peptido-mimetic shepherdin treated RB cells

By zymography analysis, the relative percentage of MMPs activity in Y79 cells was observed to be 149.72% in scramble peptide versus 74.92 % in shepherdin treated cells. Similar decrease in MMPs activity was observed in Weri Rb1 cells where the scramble treated showed 70.91% MMPs activity versus 40.78% in shepherdin treated groups. Thus, both Y79 and Weri Rb1 cells showed decrease in MMPs activity with shepherdin peptide treatment (Figure 4). These results together indicate activity of MMP's, yet another client protein of HSP 90 in the presence of shepherdin molecules contributing to arrest of cellular invading property in RB cancerous cells.

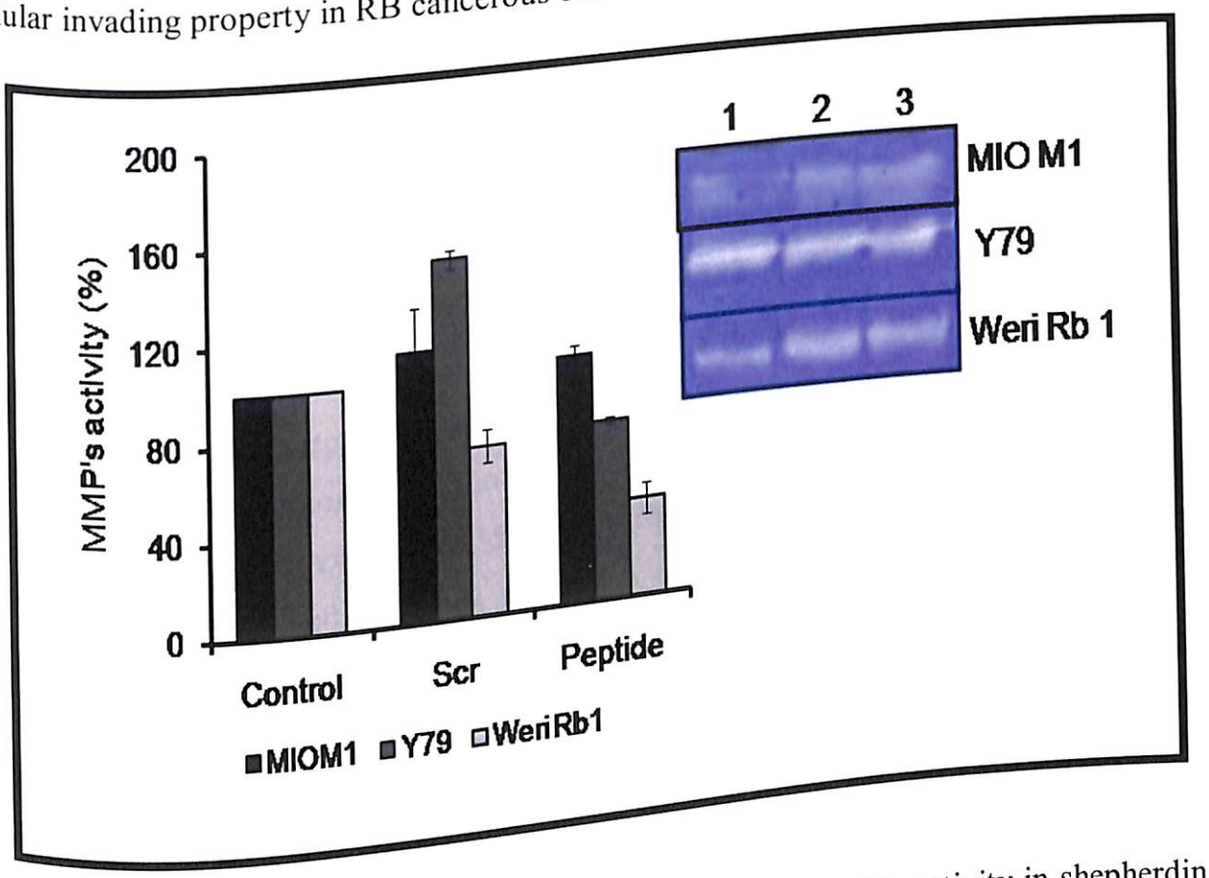

Figure 6.8: Zymogram of MMPs. Zymographic analysis of MMPs activity in shepherdin treated, scramble peptide treated, untreated control RB cells and MIO-M1 cells. The bar graph indicates the MMP's activity in the peptides treated RB cells and MIO-M1 cells. The insert represents the gelatin zymography picture of a single experiment. Error bars represent the SD of the triplicates.

6.3.5 Destabilization of survivin in peptido-mimetic shepherdin molecules treated RB cells

Destabilization of survivin, one of the client proteins of HSP90 was evaluated by flow cytometric analysis. In the presence of 0.42 mg/ml of shepherdin in RB cells, the decrease in survivin protein expression was 0.51% in Weri Rb1 cells compared to 41.79% of survivin in untreated cells at the end of 4 h of 5% serum supplementation. However, in scramble treated Weri Rb1 cells, survivin expression is 49.68% **[Figure 6.9]**. This result indicates the specific activity of shepherdin in inhibiting the physical interaction of HSP 90 and survivin, thereby destabilizing the anti-apoptotic protein, survivin, contributing to cytotoxicity in RB cells.

6.2.7. Induction of apoptosis mediated by down-regulation of Bcl-XL, up-regulation of BAX, BIM in peptido-mimetic shepherdin treated RB cells

As the result of cytotoxic and cytostatic effect of shepherdin treated RB cells were reported in section 6.3.3, we evaluated the functional pathway followed by shepherdin in inducing apoptosis, by studying the pro-apoptosis markers: Bax, Bim and anti-apoptotic markers Bcl2-XL by flow cytometric analysis in Weri Rb 1 cells. In the shepherdin treated Weri Rb1 cells, there is 40.12% elevation of Bax compared to very low expression of 1.91% in the scramble-peptide treated Weri Rb 1 cells and to 0.36% of Bax expression in un-treated cells. Expression of Bim in shepherdin treated RB cells showed an elevation of 30.14% in Weri Rb1 compared to 0.35% in un-treated Weri Rb1 cells. Expression of Bcl2-XL in shepherdin treated RB cells showed a decrease of 33.05% in Weri Rb1 cells compared to un-treated 50.08% in Weri Rb1). The scramble treated RB cells showed an elevation of 73.83% Bcl2-XL expression compared to the un-treated RB cells. This increase in Bcl2-XL in scramble treated RB cells might be due to mild stress induced due to nutrient deprivation (serum-free medium). Further, the activation of caspase 9 in shepherdin treated Weri Rb1 cells to 51.39% while no activation in untreated control (0.08%) and scramble peptide treated cells (0.21%). Elevation of Bax, Bim and suppression of Bcl2-XL together with activation of caspase 9 indicates the induction of mitochondria mediated apoptosis, due to the treatment of shepherdin in the RB cells **[Figure 6.9]**.

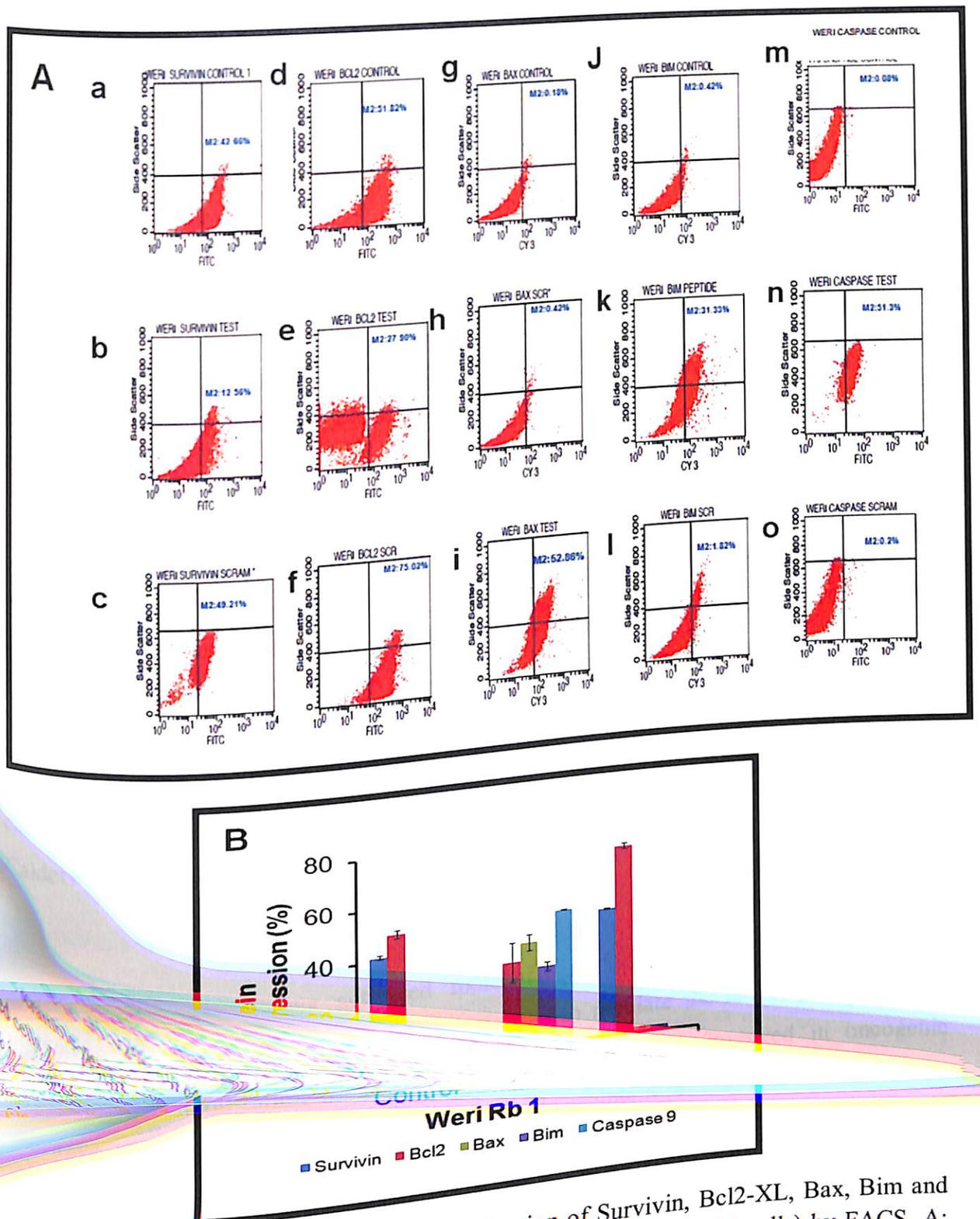

Figure 6.9: *Pro /anti-apoptotic proteins. Evaluation of* Survivin, Bcl2-XL, Bax, Bim and caspase 9 protein expressions in peptides treated *RB cells (Weri Rb1 cells)* by FACS. A: Scatter plot indicating the protein expressions in the order of untreated, shepheridin treated and scramble treated Weri Rb1 cells. a-c: Survivin protein expression; d-f: Bcl2-XL protein expression; g-i: Bax protein expression; j-l: Bim protein expression; m-o: caspase 9 expression. The bar graph represents the percentage of proteins (Survivin, Bcl2-XL, Bax, Bim and caspase 9) expression by FACS. Error bars represent the SD of the triplicates.

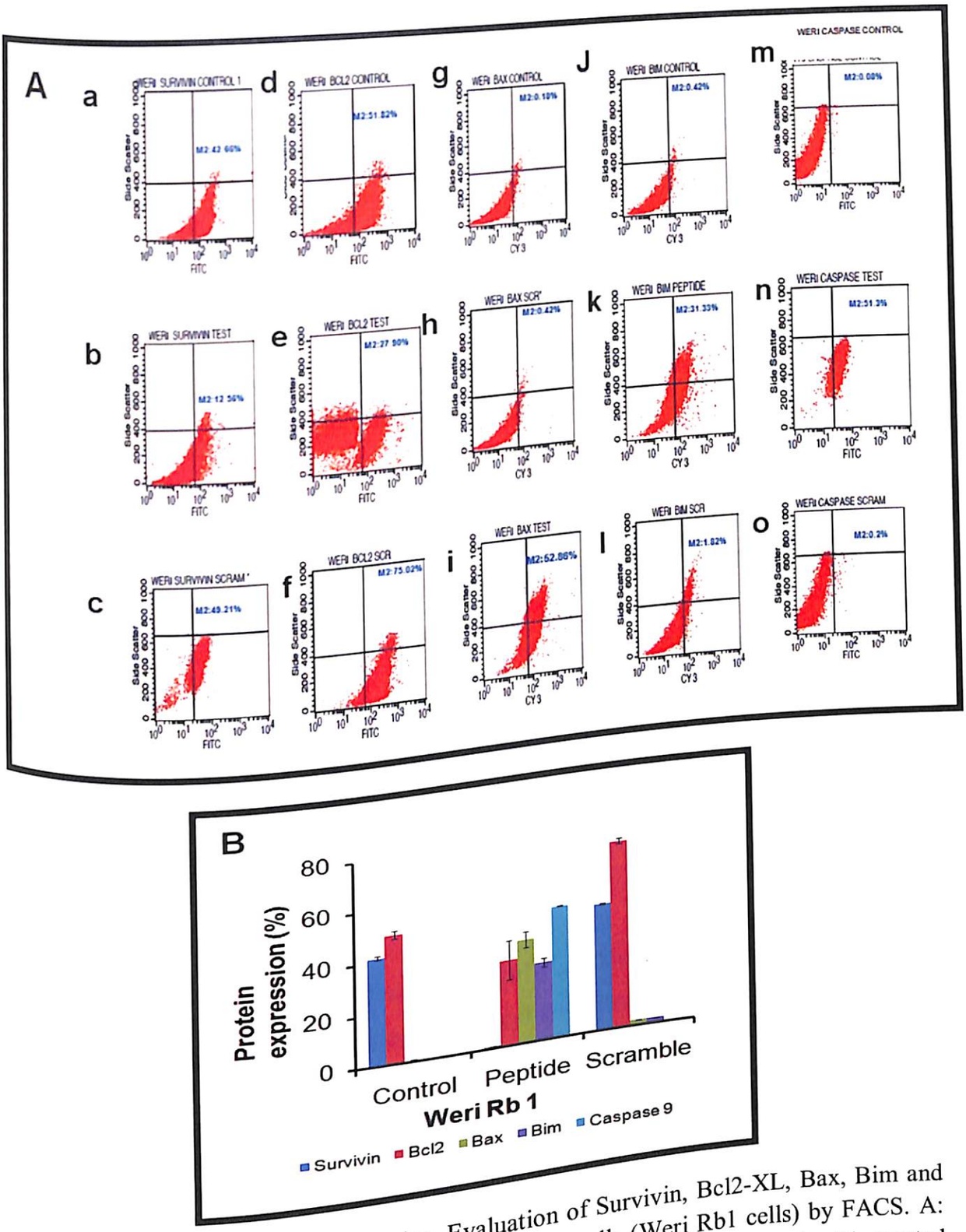

Figure 6.9: Pro /anti-apoptotic proteins. Evaluation of Survivin, Bcl2-XL, Bax, Bim and caspase 9 protein expressions in peptides treated RB cells (Weri Rb1 cells) by FACS. A: Scatter plot indicating the protein expressions in the order of untreated, shepheridin treated and scramble treated Weri Rb1 cells. a-c: Survivin protein expression; d-f: Bcl2-XL protein expression; g-i: Bax protein expression; j-l: Bim protein expression; m-o: caspase 9 expression. The bar graph represents the percentage of proteins (Survivin, Bcl2-XL, Bax, Bim and caspase 9) expression by FACS. Error bars represent the SD of the triplicates.

6.3. Discussion

Retinoblastoma, being a primary intraocular childhood malignancy is reported to occur in 11 cases per million children below the age of 5 years of age worldwide (Seregard et al. 2004). The historic treatments for the disease free survival includes enucleation (removal of eye), external beam radiation therapy resulting in loss of vision, mid-facial disfigurement and secondary cancers (Lin and O'Brien 2009). Improved survival rate and 90% retention of atleast one eye were attained by modified treatment modalities such as combination of systemic chemotherapy and focal consolidative therapy (Abraham, 2005). Modulating the susceptibility of cancer cells to apoptosis with the elucidation of molecular networks involved in this cascade may increase more efficient therapeutic approaches in RB management.

In this current study, we report the expression of HSP's (HSP70 and HSP90) and its correlation with one of its client protein survivin in advanced RB tumors. Here, we observed HSP90, HSP70 and survivin expression in 100% (29/29) of varying intensity in advanced primary retinoblastoma tumor tissues [**Figure 6.2; 6.3**]. These results corroborates with the earlier reports of HSPs expression on other cancers such as breast cancer (Sarto et al. 2000), lung cancer, prostate cancer and bladder cancer (Ciocca and Calderwood 2005).

Heat Shock Proteins, being activated molecular multi-chaperone complex are over expressed and well subjugated by malignant cells to regulate the late-stage maturation, activation and stabilization of wide range of client proteins involved in oncogenic pathways. High expression in normal cells helps to maintain protein homeostasis and its over-expression in malignant cells (Gyurkocza et al. 2006) is exploited mainly for 2 purposes (i) supporting the activated oncoproteins including cancer associated kinases, transcription factors, (ii) to manage the cellular stresses within malignant cells (Neckers 2007, Trepel et al. 2010, Workman et al. 2007). HSPs mediate anti-apoptosis by the Fas death receptor, JNK/SAPK and caspase activity. In particular, HSP70 blocks the apoptotic function of caspase 3 by its interaction with apoptosis protease activating factor-1(Apaf-1), whereas HSP 90 interacts with Apaf-1, RIP and Kinase domain of IKK alpha/beta for

the same function (Parcellier et al. 2003). In addition, HSP 90 can suppress TNFα mediated apoptosis (Li Z. and Srivastava 2004). Although, the expression of HSP's (HSP 70 and HSP 90) has been reported in primary RB tumors (Jiang et al. 2008) , its regulatory role along with its client proteins in anti-apoptosis needs to be investigated. At present, about 17 potential inhibitors (chemical derivatives and small molecules) of HSP 90 such as 17-AAG, novobiocin, geldanamycin (GA), tanespimycin, retaspimycin and HSP 90 are being tested in various levels of clinical trials in cancers (Trepel et al. 2010). Here, in the present study, we have used, a structure based molecules, which act as mimic of the unusual ATP structure adopted in N-terminal and C-terminal nucleotide binding pockets of HSP 90 resulting in the specific blocking of ATP binding and/or hydrolysis. Thus the inhibition of the molecular chaperones results in the suppression of other oncogenic client proteins and contributes to the anti-tumor property.

One of the recently discovered inhibitor of apoptosis proteins is Survivin a prime client protein of HSPs. Survivin is known to regulate cell division, maintains tissue homeostasis and differentiation (Johnson M. E. and Howerth 2004). Elevated expressions in less differentiated embryonic tissues and tumors with absence or negative expression in differentiated adult tissues were reported (Nakayama and Kamihira 2002). Survivin is reported as diagnostic (Lo Muzio et al. 2003) and prognostic markers in cancers (Yamashita et al. 2007). These earlier reports promise the multiple functions of Survivin in cell survival. So the report on Survivin together with HSPs in the current study states its contribution in RB tumor progression.

Despite Survivin not being an enzyme or a cell surface molecule, it acts as a drug target due to its various cellular functions, subtle expression and stability in interacting with associated proteins. Thus, the current report on Survivin, opens up the door for Survivin based targeted therapies (antagonist), especially suited for Retinoblastoma disease management. To exclude the limitations of using small molecules in therapy namely hepatotoxicity, low activity and instability (Banerji U 2003, Goetz et al. 2003, Soti et al. 2002), a cell permeable peptido-mimetic shepherdin was studied as an alternative molecule which binds with ATP pocket of HSP 90 and destabilizes Survivin by inhibiting ATP binding activity (Gyurkocza et al. 2006). The study reports the cytotoxic and

cytostatic concentrations of shepherdin in RB cancerous cells and non-neoplastic Muller glial cells (MIO-M1). In addition, the study also reports the functional characterization of peptido-mimetic in obstructing invading properties and induction of apoptosis due to the destabilization of HSP 90 and survivin proteins. In the current study, we have reported the cytotoxic dose of shepherdin, an antagonist of HSP 90-survivin RB cells and in non-neoplastic cells-MIO-M1.

Nutrient deprived RB cell model was used in the current study to evaluate the efficacy of cell permeable peptidomimetics. The nutritional deprived environment imitates one of the growth constrained conditions encountered during tumorigenic progression and also induces the levels of HSP 90 and Survivin (Trepel et al. 2010). This would aid to analyze the efficient cytotoxic dose of shepherdin. In the present study, increase of HSP 90 and survivin after 4 hrs of serum deprivation and at the end of 24 hrs of 5% serum supplementation [**Figure 6.1**] indicates the induction of molecular chaperones during the cellular stress. Thus, the advantage of using nutritionally deprived RB cell model was brought out in the current study.

Since HSP 90 localizes to the nucleus, the photomicrographs showed the nuclear localization of Shepherdin whereas scramble peptide localized only to cytoplasm (Salfity April,1996) [**Figure 6.4.B**]. Dose-dependent study of cell permeable peptidomimetics in RB cells revealed a maximum uptake of peptides at 0.34 μg/ml concentrations in RB cells and MIO-M1 cells at the end of 16 hrs of 5% serum addition [**Figure 6.4.B**].

On treatment of these peptido-mimetics, cell viability was altered only in RB cells; this is because of rapid destruction of chaperon complex with Survivin. Briefly, we investigated a few molecular alterations encountered in shepherdin treated RB cells. Initially, we analyzed the destabilization of survivin in shepherdin treated RB cells. Reduced percentage of survivin (Weri Rb1:0.51%) while untreated Weri Rb1 cells and scrambled treated Weri Rb1 cells showed 41.79% and 49.68% respectively [**Figure 6.9**]. This result points to the destabilization of survivin due to shepherdin treatment at the end of 4 hrs of 5% serum supplementation. At the end of 4 h of 5% serum supplementation, a massive

cytotoxic effect was observed in the presence of peptido-mimetics in RB cells while a meager effect was observed in scramble treatment. Toxicity of peptidomimetics was analyzed in the non-neoplastic MIO-M1 cells, where very minimal cytotoxicity (cell viability: 81.57%) was observed. This proves the site-specific target effect of sheperdin molecule on cancerous cells. Moreover, non-cancerous cells do not express Survivin, thereby no cytostatic effect was observed on MIO-MI cells when treated with sheperdin [**Figure 6.5.A, B**].

Further, we found that Shepherdin down-regulates anti-apoptotic protein Bcl2-XL and up-regulates pro-apoptotic proteins namely, Bax, Bim, Bcl2-XL and caspase 9 in RB cells (Weri Rb1) compared to scramble and untreated cell controls [**Figure 6.9**]. This is validated by annexin V PI staining of shepherdin treated cells that revealed an increased percentage of apoptosis in RB cells (please refer the results section 6.3.3) at the end of 4 hrs of 5% serum supplementation [**Figure 6.7**]. This suggests the induction of toxicity is due to molecular de-regulation of apoptotic proteins by shepherdin results in induction of mitochondrial mediated apoptosis in shepherdin treated RB cells.

In addition, based on an earlier report on the close correlation between MMPs and survivin contributing together in survival and invasiveness of other cancers namely endometrial cancers (Masatsugu Ueda 2003), we investigated the level of MMPs in shepherdin treated RB cells. Reduction in the matrix metallo proteinase activity of about 50% in shepherdin treated RB cells compared to the scramble and untreated control state the destabilization of another client protein MMPs due to the acute collapse of HSP 90 in RB cells [**Figure 6.8**] (Isaacs et al. 2003). These results include the effect of shepherdin competing for the ATP binding pockets resulting in the destabilization of its client proteins namely survivin and MMPs. Cytostatic analysis of shepherdin treated RB cells revealed less cell proliferation in the order of 59.6% in Y79 and 17.83% in Weri Rb1 cells. This is due to destabilization of HSP 90 client proteins such as Survivin and MMPs which are known for regulating Cell proliferation and apoptosis in various cancers. In addition, these results corroborate with the other reports that there do exists a co-existence between MMPs and survivin in the contribution to RB cell survival and invasiveness. Together, our study helps to understand

the molecular mechanism of retinoblastoma tumorigenesis and the alterations in them due to the specific action of shepherdin, structure based mimetic in RB cells.

In summary, this study revealed the co-expression of HSP 90, HSP 70 and survivin in advanced RB and their contribution in RB progression drug resistance. A brief exposure of cell-permeable variant of shepherdin resulted in the acute collapse of HSP 90, thereby destabilizing the client proteins, survivin and MMPs. Efficient intracellular penetration of shepherdin at 0.42 µg/ml concentration resulted in massive and complete killing of RB tumor cells while very meager cytotoxic effect was observed in normal cells. Elevation of Bax, Bim together with suppression of Bcl2-XL proves the ability of shepherdin to trigger the mitochondria mediated apoptosis in RB cells.

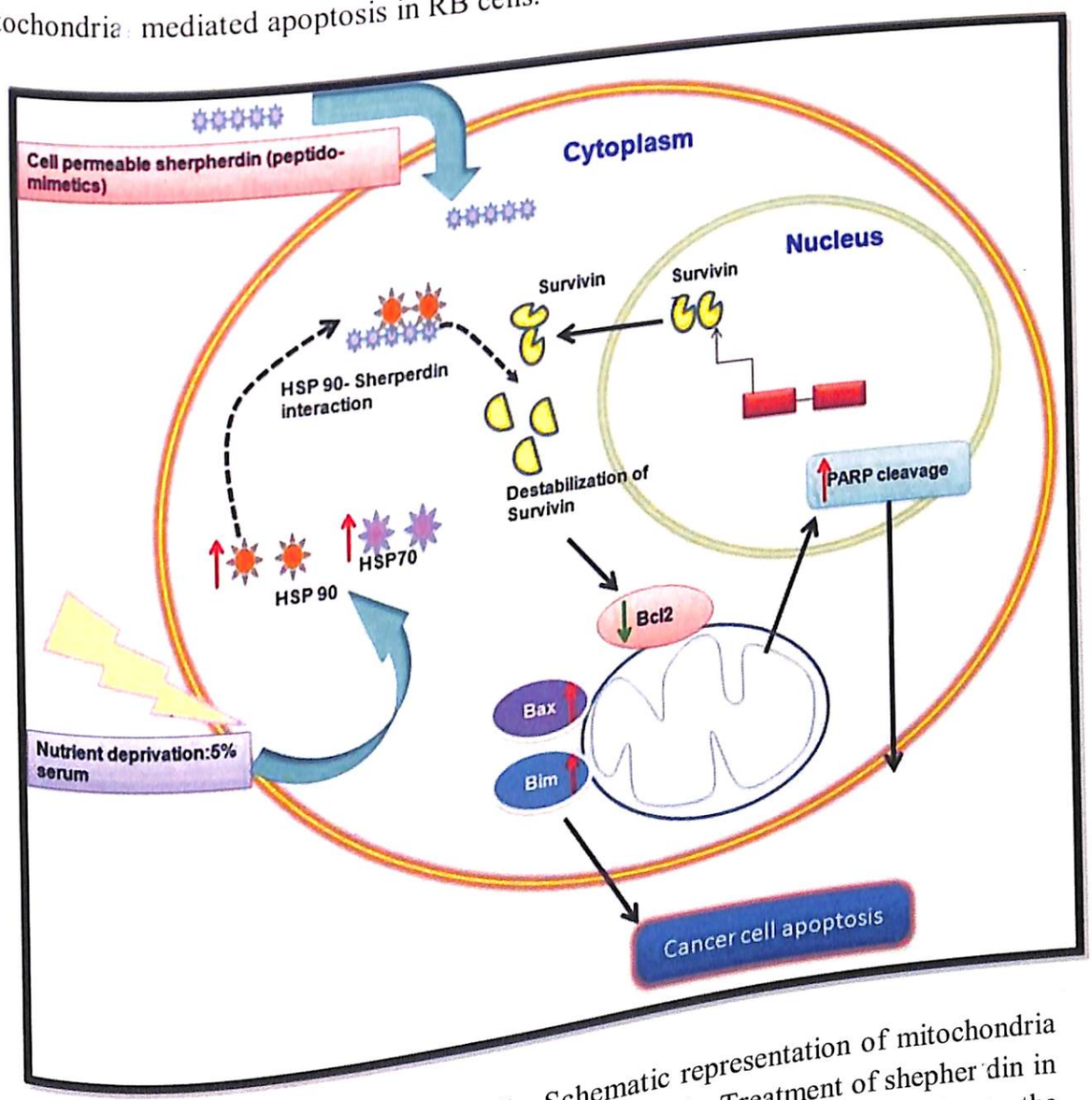

Figure 6.10: Molecular shuffling in RB cells. Schematic representation of mitochondria mediated cell death postulated in shepherdin treated RB cells. Treatment of shepherdin in nutrient deprived RB cells resulted in the destabilization of survivin contributing to the

suppression of Bcl2-XL. Taken together, with reduced levels of MMP's, increased Bax and Bim explains the molecular shuffling due to shepherdin treatment in RB cells contributing to the RB cell death.

6.4. Conclusion

Presence of HSPs (HSP 90 and HSP 70) together with anti-apoptotic protein survivin reveals the multiple cellular mechanisms adopted by the RB cancer cells during their cancer progression. Further, down-regulation of Bcl2-XL, destabilization of survivin together with reduced levels of MMP's and increased levels of Bax, Bim explains the molecular shuffling due to shepherdin treatment in RB cells. In addition, these studies conclude the mitochondria mediated cell death in shepherdin treated RB cells. The efficient concentration of peptido-mimetic (shepherdin) has been reported in RB cells. Overall, these findings strongly implicate the potential of targeting HSP 90-survivin interaction as an adjuvant therapy in RB management.

CHAPTER 7: COMPUTATIONAL AND *IN VITRO* INVESTIGATION OF miRNA-GENES IN RB PATHOGENESIS: miRNA MIMICS STRATEGY

7. Introduction

MicroRNAs (miRNAs) being small (~18-22 nucleotides) endogenous non-coding RNAs are involved in various biological roles by negatively regulating mRNA expression at both post-transcriptional and post translational level (Carthew and Sontheimer 2009, Guo et al. 2010, Huntzinger and Izaurralde 2011). Further, the gene expressions are suppressed by the interaction with their target messenger RNAs (mRNAs), either by blocking the translation process or initiating the cleavage. Thus, these small regulators have vital roles in numerous biological processes, such as cell differentiation and apoptosis (Frankel et al. 2008) and also in pathological processes including some of the cancers (Cho 2007, Hammond 2007, Voorhoeve et al. 2006). The abnormal expression of miRNAs may either contribute to cell progression (oncomirs) or to cell death (tumor suppressor) through miRNA-mRNA interactions (Reinhart et al. 2000). So determining the expression and the function of miRNAs in cancers would help to understand their pathogenesis and disease management.

In addition to the transcription factors (co-expressed genes), the dys-regulated miRNA-mRNA pairs play a crucial role in cancer formation. To this end, a number of predictive tools namely TargetScan (Friedman R. C. et al. 2009, Grimson et al. 2007), PicTar (Krek et al. 2005), miRanda (Betel et al. 2010, John et al. 2004) and PITA (Kertesz et al. 2007) are used to identify the miRNA-mRNA interactions based on the seed complementarity between miRNAs and the 3′UTRs of specific mRNA. In addition these tools also indicate the details of sequence conservation of adjacent bases together with thermodynamic properties of miRNA-mRNA interactions. Further, the availability of other methods are

based on the mRNA-miRNA expression profiles (data generated by microarray) and RNA seq and these methods are used to predict the functional miRNA-mRNA interactions (MMIs) (Li Y. et al. 2014). However, there exist high false discovery rate in determining the miRNA-target mRNA with these tools. This in turn, underscores the requirement of experimental validation tools including qRT-PCR and western analyses to indicate the functional miRNA and miRNA-mRNA interaction (Thomson et al. 2011).

In the current study, using a simple bio-informatics approach we have demonstrated two key miRNAs (miR-486-3p and miR-532-5p) regulating a panel of genes reported earlier in RB tumorigenesis (Balla et al. 2009, Castera et al. 2010, Felsher 2013, Li J. et al. 2012b, Mitra et al. 2012, Mohan et al. 2006, Vandhana et al. 2011, Venkatesan et al. 2009, Zhang J. et al. 2012a). In this approach, we have considered three groups of genes namely group1: oncogenes which include high mobility group –A2 (*HMGA2*) (Venkatesan et al. 2009), *N*-myc proto-oncogene protein (*MYCN*) (*Felsher 2013*), spleen tyrosine kinase (*SYK*) (*Zhang J. et al. 2012a*), Fatty acid synthase (*FASN*) (Vandhana et al. 2011), group 2: genes involved in cancer cell stemness which includes Epithelial cell adhesion molecule *TACSTD1* (*EpCAM*)(Mitra et al. 2012), ATP-binding cassette sub-family G member 2, *ABCCG2* (Mohan et al. 2006), cluster of differentiation 24 (*CD24*) (Li J. et al. 2012b), cluster of differentiation 133 (*CD133*) and cluster of differentiation 44 (*CD44*) (Balla et al. 2009), and group 3: cell cycle regulatory genes which includes cluster of differentiation (*p53*) and Mouse double minute 2 homolog (*MDM2*) (Castera et al. 2010). An *in silico* approach using the predictive tools including Microcosm, DIANALAB, miRBase v18, REFSEQ database and RNA Hybrid was used to determine the miRNA-mRNA interactions. Further, the identified miRNAs role in RB tumorigenesis has been addressed by *in vitro* experimental validations using RB cell lines (Y79 and Weri Rb1).

7.1. Material and Methods

7.1.3. In silico analysis to predict miRNAs regulating a panel of genes reported in RB

A comprehensive bio-informatic analysis was carried out to find the list of miRNA that could target and is likely to involve in post translational regulation of widely reported genes in RB progression. The select panel of genes are grouped into 3 groups based on the

functions namely Group 1: oncogenes (*HMGA2, MYCN, SYK, FASN*); Group 2: cancer stem cell markers (*TACSTD1 (EpCAM), ABCG2, CD133, CD44, CD24* and Group 3: cell cycle protein (*p53 and MDM2*). The known, predicted and validated miRNA that could target any of this group of genes in Groups 1, 2 and 3 were obtained from the following databases:

1. Microcosm (http://www.ebi.ac.uk/enright-srv/microcosm/htdocs/targets/v5/)
2. DIANALAB (http://diana.cslab.ece.ntua.gr/DianaToolsNew/index.php?r=tarbase)
3. miRBase v18 (http://www.mirbase.org/)
4. REFSEQ database (www.ncbi.nlm.nih.gov/RefSeq/).
5. RNA Hybrid

miRNA targeting the selected genes were considered based on their MFE (Minimal Free Energy of <= -30 and p-value of <=0.05). Further, using miRanda algorithm, the detailed complementary alignment between 5'seed sequence of differentially expressed miRNA's and the sequence of target genes were determined.

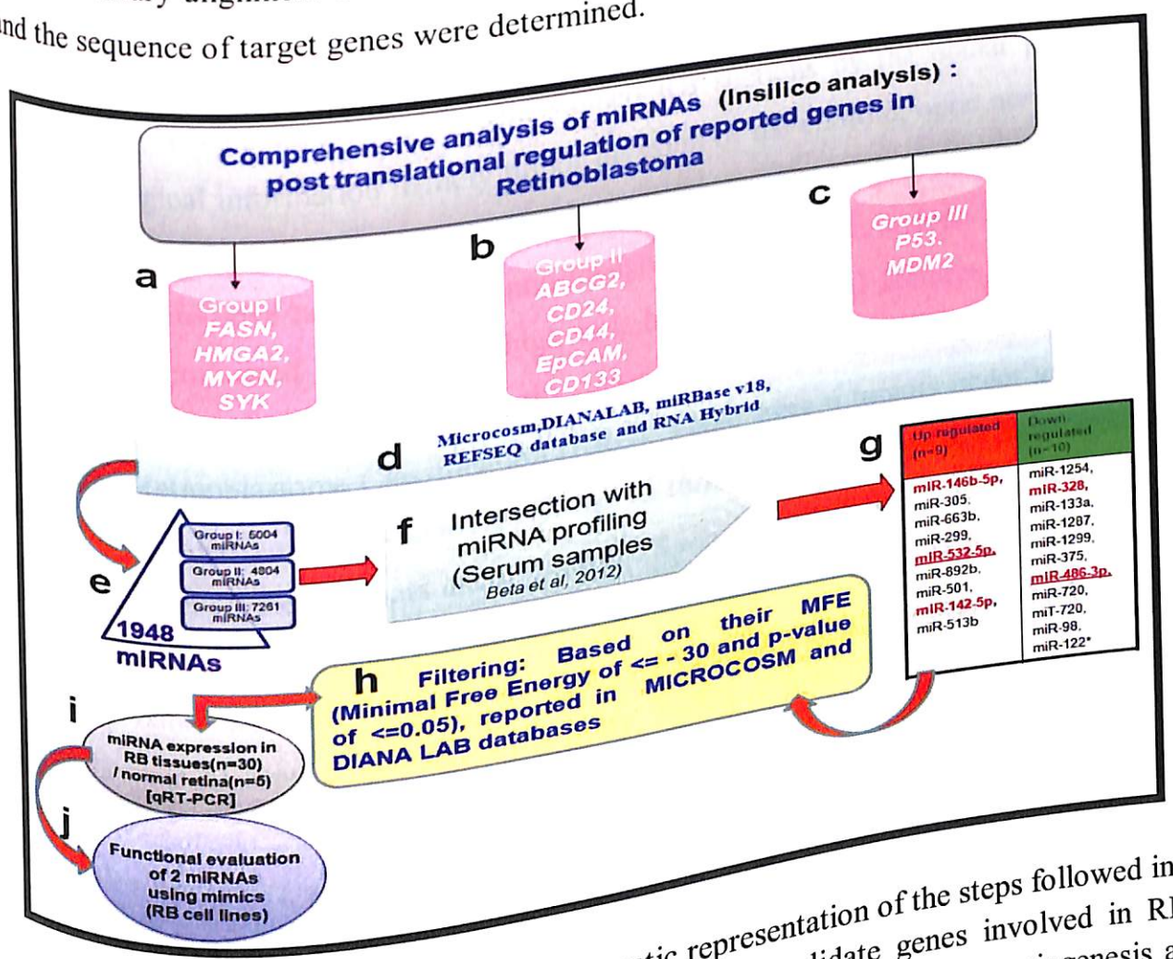

Figure 7.1: Steps followed in the study. Schematic representation of the steps followed in the identification of miRNAs regulating the panel of candidate genes involved in RB progression. a-c: classification of a panel of genes regulating the RB tumoriogenesis as Group 1: oncogenes (*HMGA2, MYCN, SYK, FASN*); Group 2: cancers stem cell marker

(*TACSTD1 (EpCAM), ABCG2, CD133, CD44, CD24* and Group 3: cell cycle protein (*p53 and MDM2*); d: Identification of the miRNA-mRNA targets using Microcosm, DIANALAB, miRBase v18, REFSEQ database and RNA Hybrid; e Reducing redundancy and filtering of 1948 miRNAs; f: Intersection with miRNA profiling (Serum samples) g: derived upregulated (n=9) and down-regulated miRNAs (n=10); h : Filtering: Based on their MFE (Minimal Free Energy of <= - 30 and p-value of <=0.05), reported in MICROCOSM and DIANA LAB databases; **i:** miRNA expression in RB tissues (n=30) / normal retina(n=5).[qRT-PCR]; **j:**Functional evaluation of 2 miRNAs using mimics (RB cell lines).

7.1.4. Primary RB tumor tissues

The institutional ethics committee of Vision Research Foundation, Sankara Nethralaya (Chennai, India) has reviewed and approved the study.

RB primary tumor samples were collected from 30 enucleated eyeballs of RB patients as part of RB management (2011 – 2012). The study includes 15 male and 15 female patients with median age of 2.5 years. Grading of tumors was performed from the microscopic observations of haematoxylin and eosin stained RB sections by the ocular pathologist. Histopathological information namely tumor invasion of the choroid, optic nerve, or orbit **Table 7.4** was obtained from surgical pathology reports. Among the tumors analyzed, there were 17 invasive tumors and 13 non-invasive tumors which include 8 differentiated and 22 undifferentiated tumors with high risk histopathological features. Based on the clinical presentation of the patients, the tumors were classified as per International Intraocular Retinoblastoma Classification (IIRC). There were 6 tumors under group B, in which 4 were invasive, 2 non-invasive. Of the 15 tumors under group D, 5 were invasive, 10 non-invasive. Of the 9 tumors under group E, 8 were invasive, 1 non-invasive (Sastre et al. 2009). Normal adult retina was collected from 5 cadaveric eyeballs (received at C.U. Shah eye bank, Sankara Nethralaya, http://www.sankaranethralaya.org/eye-bank.html) during the year 2012 were included in the study.

7.1.5. Cell lines

Human RB cancerous cell lines (Y79, Weri Rb1, Riken cell bank, Japan) were used in the study. The RB cell lines were cultured with supplementation of 10% heat-inactivated fetal

calf serum (Gibco- BRL, Rockville, MD, USA) in Rosewell Park Memorial Institute 1640 (Gibco-BRL Rockville, MD, USA) as described in the section 4.1.3.

7.1.6. miRNA mimics

The description of miRNA mimics used in the study is tabulated below.

Table 7.1: Details of miRNA mimics. Details of miRIDIAN microRNA mimics with the mature sequence and accession number.

S.No	miRIDIAN microRNA mimics, catalogue number (Dharmacon, Thermo Fisher Scientific-India)	Mature sequence and accession number
1.	Mimic Negative control (Based on cel-miR-67, as they have minimal identity with miRNAs in humans. CN-001000-01-20	5'UCACAACCUCCUAGAAAGAGUAGA3' (MIMAT0000039)
2.	Human hsa-miR-486-3p– Mimic, C-301211-01-0010	5'CGGGGCAGCUCAGUACAGGAU3' (MIMAT0004762)
3.	Human hsa-miR-532-5p – Mimic, C-300867-01-0010	5'CAUGCCUUGAGUGUAGGACCGU3' (MIMAT0002888)

Transfection of the mimics in the RB cells were carried out as described in the section 4.2.9.

7.1.7. miRNA expression analysis by qRT-PCR

The miRNA expression in the primary RB tumors and in cell lines was carried out as described in the section 4.7.2.2.2 and 4.7.3.2 using the LNA™ primers tabulated below.

Table 7.2: Details of miRNA primers (LNA). Details of miRIDIAN miRNA primers (LNA™, Exiqon, USA)

S.No	Product number	Product name, microRNA primer set.	Target sequence	Target sequence accession number
1.	202353	*hsa-miR-486-3p*	CGGGGCAGCUCAGUACAGGAU	MIMAT0004762
2.	202435	*hsa-miR-532-5p*	CAUGCCUUGAGUGUAGGACCGU	MIMAT0002888
3.	202074	*hsa-miR-328*	CUGGCCCUCUCUGCCCUUCCGU	MIMAT0000752
4.	202274	*hsa-miR-146b-5p*	UGAGAACUGAAUUCCAUAGGCU	MIMAT0002809
5.	204722	*hsa-miR-142-5p*	CAUAAAGUAGAAAGCACUACU	MIMAT0000433

7.1.8. Measurement of cell viability using MTT assay

The cell viability in the mimics transfected RB cells were analysed by MTT assay as described in section 4.11.3.

7.1.9. Measurement of apoptosis using Annexin-V-FLUOS stain

The percentage of apoptotic cells in mimics transfected cells were analysed using Annexin- V-FLUOS stain in flow cytometer as described in section 4.11.5

7.1.10. Measurement of change in cell cycle using propidium iodide stain

The percentage of cells at various cell cycle phases were determined using propidium iodide in flow cytometer as described in section 4.11.6.

7.1.11. Statistical analysis

One-way ANOVA, *post-hoc. Dunnet T test*, Independent't' test and Mann-whitney 'U' test was performed to compare the variables of *in vitro* experiments and of RB primary tumors.

7.2. Results

7.2.3. Identification of miRNAs regulating the most candidate genes involved in RB tumorigenesis

From the comprehensive bio-informatics analysis the number of miRNAs that are likely to involve in post translational regulation of group I genes (*HMGA2, MYCN, SYK, FASN*) is identified as 5004, group II genes (*TACSTD1 (EpCAM), ABCG2, CD133, CD44, CD24*) as 4804 miRNAs and that of group III genes (*p53 and MDM2*) as 7261 miRNAs. In order to remove the redundancy, filtration of all the identified miRNAs were carried out, by which we obtained 1948 miRNAs. Further, in order to determine the miRNAs relevant to RB tumoriogenesis, the identified 1948 miRNAs from the current study were intersected with that of the miRNAs involved in RB tumoriogenesis reported earlier in serum samples. From this intersection, we observed only 9 up-regulated miRNAs which include *miR-146b-5p, miR-305, miR-663b, miR-299, miR-532-5p, miR-892b, miR-501, miR-142-5p and miR-513b*. In addition, we again observed only 10 down-regulated miRNAs, which

includes *miR-1254, miR-328, miR-133a, miR-1287, miR-1299, miR-375, miR-486-3p, miR-720, miR-98,* and *miR-122**.

Further, from this list of miRNAs, the highly regulated miRNAs are filtered based on their MFE (Minimal Free Energy of <= - 30 and p-value of <=0.05) and those that are reported in MICROCOSM and DIANA LAB databases. Based on these results, we have selected three miRNAs namely *miR-146b-5p, miR-532-5p and miR-142-5p* from the up-regulated miRNAs panel while two miRNAs namely *miR-328 and miR-486-3p* from the down-regulated list for the validation in RB primary tumor tissues.

Table 7.3: miRNAs and post-translatory regulatory genes. miR-SVR scores and the position on the mRNA sequence for the select 5 miRNAs and their post translational regulatory genes.

S.No	Gene	miRNA showing hits on the gene	SVR score	Position on mRNA sequence
1.	FASN	*hsa-miR-532-5p*	-0.0013	137, 464
		hsa-miR-146b-3p	-0.0077	538
		hsa-miR- 328	-0.0004	498
		hsa-miR- 486-3p	-0.0008,-0.046, - 0.1287	1, 110, 393
2.	HMGA2	*hsa-miR-142-3p*	-0. 6633, -0.0281, -0.811, -0.5492- 0.0130	545, 1228, 1547, 2499
		hsa-miR-328		2093
3.	MYCN	*hsa-miR-532-3p*	-0.0006	239
4.	SYK	*hsa-miR-532-5p*	-0.0080	1574
		hsa-miR-146b-3p	-0.0005	2594
		hsa-miR-486-3p	-0.0283	2421
5.	ABCG2	*hsa-miR-532-5p*	-0.1924, -.0032	590, 659
		hsa-miR-146b-5p	-0.7574,-0.5036	910, 1819
		hsa-miR-142-5p	-0.5511, -.5931	361, 897
		hsa-miR-328	-0.0445	602
		hsa-miR-486-5p	-0.0083	1533
6.	CD24	*hsa-miR-532-5p*	-0.0076	711
		hsa-miR-142-5p	-0.0202	1677
		hsa-miR-146b-5p	-0.0027	543
		hsa-miR-486-5p	-0.0006,-0.0008	953,1090
7.	CD133	*hsa-miR-532-3p*	-0.0024	365
		has-miR-142-5p	-0.0098	503

		has-miR-146b-5p *hsa-miR-146b-3p* *has-miR-328*	-0.0030,-0.008, - 0.0109,-0.0249 - 0.0017,-0.0010 -0.1154	1355, 2166, 2433, 2800 975,1621 190
8.	CD133	*hsa-miR-532-5p* *hsa-miR-142-3p* *has-miR-142-5p* *hsa-miR-486-5p*	-0.0035 -0.9794 -0.8091 -0.0224	1076 272 604 392
9.	P53	*hsa-miR-532-3p* *has-miR-146b-5p* *hsa-miR-146b-3p*	-0.0687 -0.0017 -0.0016	235 88 176
10.	*MDM2*	*hsa-miR-532-5p* *hsa-miR-142-5p* *hsa-miR-146b-5p* *hsa-miR-486-5p*	-0.0057,-.0002, - 0.0006-0.0017,- .0014, -0.0011,- .0023, -0.0003,- .0005-0.0001,- .0001, -0.0003,- .0002, -0.0000	555, 783, 1122 1707,2868, 3158,4279,5297,4557 553, 778, 1119, 1510, 5177

7.2.4. miRNA expression in RB primary tumor tissues and in normal cadaveric adult donor retina

The miRNA expression analysis in RB primary tumor tissues (n=30) by qRT-PCR revealed a median fold change of miR-486-3p (in the order of I = -1.26, NI =-1.07); miR-532-5p (in the order of I = -0.69, NI =-1.00); miR-142 (in the order of I= -0.18, NI = -0.17); miR-146b (in the order of I = -0.73, NI=-0.87); and miR-382 (in the order of I = -0.70, NI= -0.59). Relative miRNA expression to normal cadaveric donor retina of RB primary tumor tissues with the clinico-pathological description has been stated in **Table 7.4**. The median fold change of all these 5 miRNAs in normal cadaveric adult donor retina is shown in **Table 7.5**. Interestingly, we observed down-regulation of all the validated miRNAs relative to the normal donor retina. No significant association of the miRNAs expression with that of normal retina was observed.

Table 7.4: miRNA expressionsin RB. miRNA expression (relative to normal cadaveric donor retina) of RB primary tumor tissues with the clinico-pathological description.

RB Tumor numbers	Age (Yrs) /sex	RB Group (IIRC) classification	Clinico-pathological descriptions	miR-142	miR-146b	miR-382	miR-486-3p	miR-582-5p
RB1	3Y/F	B	OS:WD, NI	-14.59	-8.11	-8.36	-14.85	-8.24
RB2	2Y/F	D	OS:PD, NI	-14.03	-8.52	-6.38	-14.75	-5.65
RB3	8mon/F	D	OD:PD, NI, necrotic	4.51	7.51	5.39	3.16	-3.77
RB4	1Y/M	D	OD:WD, RPE, No CI, Post-lam	5.01	5.44	4.80	2.67	-5.18
RB5	8mon/M	B	OS: WD, NI	-5.56	-4.00	-5.31	-8.86	-0.96
RB6	2Y/F	D	OD: PD,NI	-15.27	-13.14	-13.17	-14.18	-9.46
RB7	3Y/F	D	OD: WD focal RPE Inv, CI<3mm	0.30	0.14	0.12	-0.24	0.09
RB8	3Y/M	D	OD: MD, focal RPE, minimal ON inv	-0.17	-0.35	-0.39	-0.90	-0.58
RB9	7Y/F	D	OS: MD,NI	0.53	1.19	-0.42	0.17	0.22
RB10	2Y/F	D	OD: WD, RPE, CI<3mm	-1.19	-1.23	-1.21	-2.14	-0.83
RB11	2Y/M	B	OD: WD,NI	-0.11	-0.19	-0.48	-0.83	-0.50
RB12	2Y/F	D	OS: PD,NI	-0.64	-0.93	-1.34	-1.53	-1.38
RB13	2Y/M	D	OS: PD, NI	-1.44	-1.46	-2.14	-1.93	-2.01
RB14	2Y/F	E	OS: MD, CI>3mm, prelam inv	-12.69	-8.82	-8.30	-13.41	-4.90
RB15	6Y/F	E	OD:WD, focal CI< 3mm, prelam inv	-11.83	-8.17	-7.91	-10.97	-8.01
RB16	4Y/M	E	OS:PD, CI>3mm, prelam, scleral inv	-13.47	-7.36	-13.23	-13.10	-6.54
RB17	4Y/M	E	OD:PD, CI>3mm, post-lam ON	2.69	5.51	2.61	0.21	-8.22
RB18	11Y/F	D	OS: PD, diffuse CI <3mm, TC invading retinal vessels	-15.70	-13.32	-9.10	-15.81	-11.18

RB19	3Y/M	D	OS: PD, post-lam ON	-0.18	-0.34	-0.53	-1.00	-0.69
RB20	1Y/M	E	OS: MD, CI>3mm, prelam	0.23	0.04	0.01	-0.51	-0.14
RB21	3Y/M	E	OS: PD, CI >3mm, prelam and post-lam ON inv	0.02	-0.20	-0.30	-0.89	-0.51
RB22	9mon/M	E	OS: MD, CI<3mm, prelam	-0.16	-0.86	-0.38	-1.40	-0.57
RB23	2Y/F	E	OD: MD, CI>3mm	0.29	0.11	0.08	-0.44	-0.12
RB24	4Y/M	E	OS: PD, CI>3mm, prelam and post-lam inv	-0.49	-0.67	-0.71	-1.22	-0.90
RB25	4Y/F	D	OS: WD,CI<3mm	-0.57	-0.74	-0.90	-1.26	-0.69
RB26	4Y/F	D	OD: UD, CI>3mm, pre-lam ON inv	0.06	-0.12	-0.85	-2.12	-0.53
RB27	1Y/F	B	OD: MD, CI<3mm	-1.78	-1.75	-1.96	-2.65	-1.97
RB28	2Y/M	B	OS: MD, RPE, pre-lam and post- lam	-0.55	-0.53	-0.86	-1.43	-0.66
RB29	3Y/M	B	OS: MD,CI<3mm, pre-lam ON	2.21	-0.83	1.47	0.02	-0.24
RB30	4Y/M	D	OD: MD, Focal Choroid <3mm, pre-lam inv	0.79	-1.21	0.62	-0.77	-1.05

M: Male; F: Female; OD: Right eye;OS: Lefy eye; RPE: Retinal Pigment epithelium; CI: Choroidal invasion; pre-lam: Pre-laminar; post-lam: Post-laminar ; inv: Invasion; ON: optic nerve.

Table 7.5: Median miRNA expressions in RB (tumors, cell lines) and normal retina. Median fold change of select miRNAs (n=5) in RB cell lines (Y79 and Weri Rb1), RB primary tumors (Invasion / No invasion) and in normal cadaveric donor retinae.

miRNAs	Median fold change				
	Y79	Weri Rb 1	Invasion RB tumors (n=17)	No invasion RB tumors (n=13)	Retina(n=5)
miR-486-3p	-1.921	-1.868	-1.261	-1.079	-0.143
miR-532-5p	-1.765	-1.775	-0.694	-1.006	-0.014
miR-142-5p	-0.985	-0.870	-0.182	-0.176	0.244
miR-146-5p	-1.395	-1.877	-0.737	-0.877	0.143
miR-382	-2.090	-1.922	-0.705	-0.593	0.199

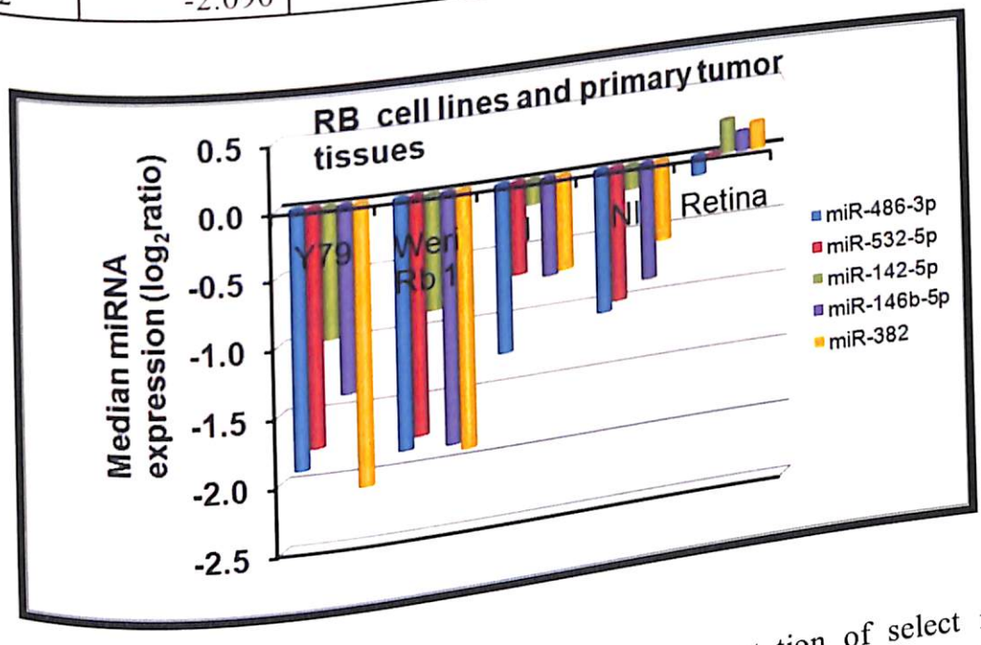

Figure 7.2: miRNA expression in RB. Graphical representation of select miRNA's median expression in RB cell lines (Y79 and Weri Rb1), RB primary tumors (Invasion, n=17 and No invasion=13) and in normal cadaveric adult retinae (n=5). Median fold change of the miRNAs is in the order of *miR-486-3p* (blue bar), *miR-532-5p* (red bar), *miR-142-5p* (green bar), *miR-146b-5p* (purple bar) and *miR-382* (yellow bar).

7.2.5. miRNA expression in RB cell lines (Y79 and Weri Rb1)

The median fold change of all these 5 miRNAs in Y79 is in the order of miR-486-3p: -1.92; miR-532-5p : -1.76; miR-142: -0.98; miR-146b: -1.39; and miR-382: -2.09 while in Weri Rb 1 is in the order of miR-486-3p: -1.86; miR-532-5p : -1.77; miR-142: -0.86; miR-146b: -1.87; and miR-382: -1.92. Taken together, based on the miRNA expressions in

primary RB tumor tissues and in cell lines, the two miRNAs with high fold decrease namely *miR-486-3p and miR-532-5p* was selected for the *in vitro* functional analysis using RB cell lines: Y79 and Weri Rb1. Based on the miRSVR scores, the gene targets of these 2 miRNAs namely *SYK* (*miR-532-5p*: miRSVR score is – 0.0080 and *miR-486-3p*: miRSVR score is - 0.0283) and FASN genes (*miR-532-5p*: miR-SVR score is – 0.0013 and *miR-486-3p*: miRSVR is -0.0008) were selected for further *in vitro* validations.

7.2.6. Functional analysis of the select miRNAs in RB cell lines

Since we observed, down-regulation of *miR-486-3p* and *miR-532-5p*, we have carried out the addition of miRNA mimics to the RB cells, which would enable us to better understand the mRNA-miRNA interaction. The non-targeting mimic was used as scramble control in miRNA mimic experiments.

7.2.7. Gene expression in mimic's transfected RB cells

The RB cells were transfected with 50 pmoles of mature miRNA sequences (mimics) - *miR-486-3p* and *miR-532-5p* and the scramble negative control. After 48 h of transfection, the levels of *SYK* and *FASN* mRNA were analyzed in comparison to the scramble transfected control. The mean expression level of *SYK* and *FASN* mRNA expression in mimics transfected Y79 and Weri Rb1 cells at the end of 24 h, 48 h and 72 h of incubation is stated in the table below.

Table 7.6: *SYK* and *FASN* mRNA expression in RB. Fold decrease in *SYK* and *FASN* mRNA in the miRNA mimics transfected RB cells.

Treatment with miRNA mimics	Y79-*SYK* (SD)	Y79-*FASN* (SD)	Weri Rb1-*SYK* (SD)	Weri Rb1-*FASN* (SD)
miR-486- 3p-24	-2.2(0.3)	-1.8(1.0)	-3.4(1.7)	0.8(2.0)
miR-532-5p-24	-0.6(0.3)	-0.6(0.2)	8.1(0.1)	4.9(0.1)
miR-486-3p-48	-2.2(1.1)	-2.6(0.3)	-3.4(1.0)	-0.3(0.5)
miR-532-5p-48	-4.7(2.1)	-1.2(0.4)	-8.7(1.0)	-1.7(2.2)
miR-486-3p-72	0.6 (0.1)	1.9(0.2)	3.9(0.8)	0.4(1.6)
miR-532-5p-72	0.1(0.1)	0.5(0.2)	3.3(1.3)	-0.7(1.1)

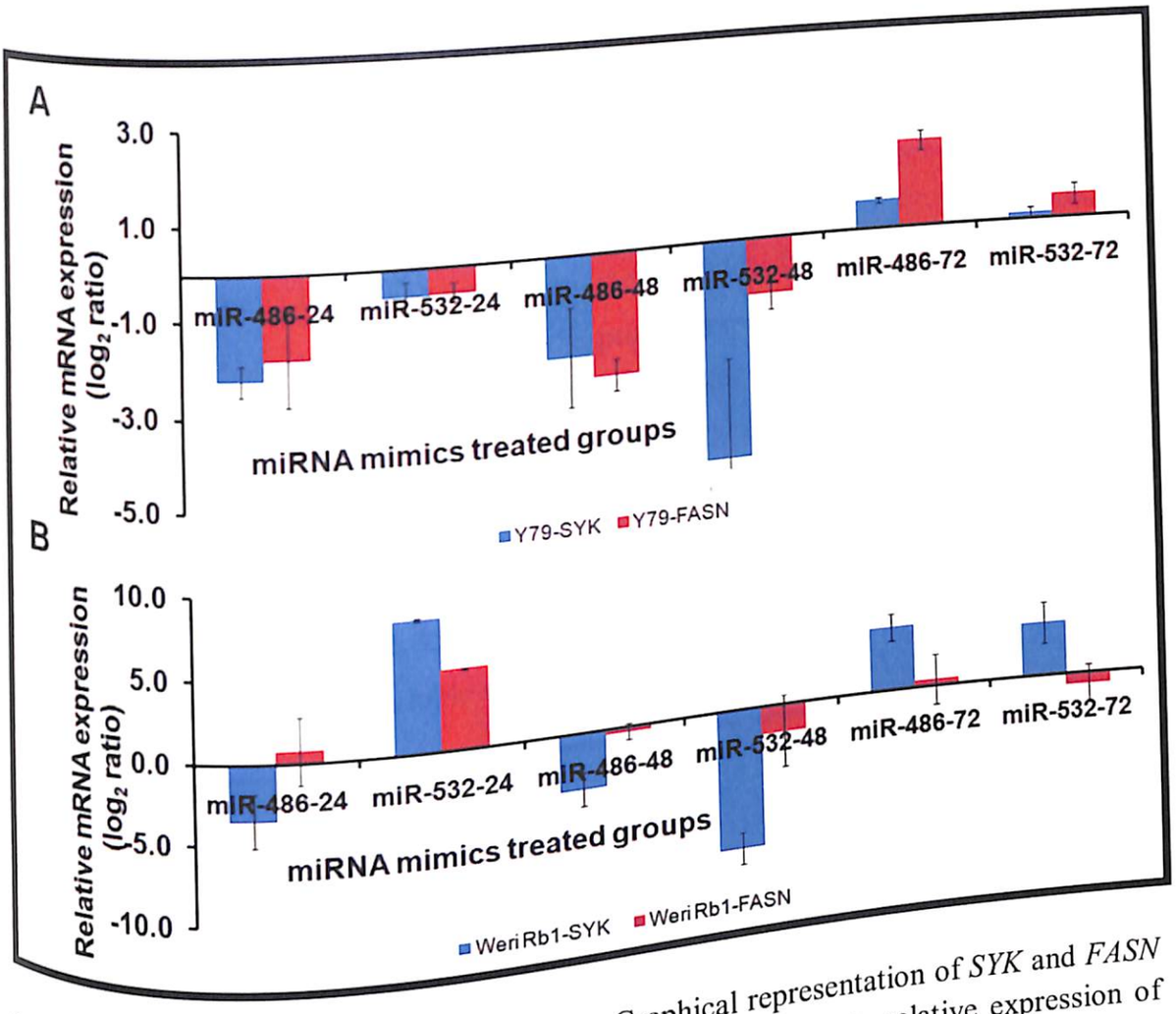

Figure 7.3: *SYK / FASN* mRNA expressions. Graphical representation of *SYK* and *FASN* mRNA in transfected RB cells mimics. The bar graph represents relative expression of *SYK* (blue) and *FASN* (red) in 50 pmoles of *miR-486-5p* and *miR-532-3p* mimics transfection. Fold change in transfected RB cells are derived in relative to scramble transfected control at the end of 24 h, 48 h and 72 h of incubation. Error bars represent the SD of the triplicates.A: Y79 and B: Weri Rb1.

These results indicate a significant decrease of *SYK* and *FASN* mRNA to -2.2 and -2.6 fold change in *miR-486-3p* mimics transfected Y79 cells at end of 48 h of incubation. Similarly a decrease of *SYK* and *FASN* mRNA to -4.7 and -1.2 fold change in *miR-532-5p* mimics transfected Y79 cells at the end of 48 h of incubation. In Weri Rb1, *miR-486-3p* mimics transfection resulted in the decrease of *SYK* and *FASN* mRNA to -3.4 and -0.3 fold change at the end of 48 h of incubation, while *miR-532-5p* mimics transfection resulted in the decrease of *SYK* and *FASN* mRNA to -8.7 and -1.7 fold change at the end of 48 h of incubation respectively. In addition, these results indicate the better down-regulation of the regulatory mRNAs (*SYK and FASN*) at the end of 48 h of incubation compared to other

time points (24 h and 72 h). Thus, 50 pmoles concentration of mimics and 48 h as the time of incubation was selected for the further experiments.

7.2.8. Change of *SYK* and *FASN* protein expression in miRNA mimics transfected RB cells

The decrease in *SYK* and *FASN* mRNA in the *miR-486-3p* and *miR-532-5p* mimics transfected RB cells were confirmed with the protein expression using western analysis. We observed a decrease of about 30% of *SYK* and 20% *FASN* protein in miR-486-3p transfected Y79 cells and 30 % of *SYK* and 20% *FASN* in *miR-532-5p* transfected Y79 cells compared to scramble transfected Y79 cells after 48 h of incubation. Similarly, we observed a decrease of about 35% of *SYK* and 25% *FASN* protein in miR-486-3p transfected Weri Rb1 cells and 35% of *SYK* and 25% *FASN* in *miR-532-5p* transfected Weri Rb1 cells compared to scramble transfected Weri Rb1 cells after 48 h of incubation.

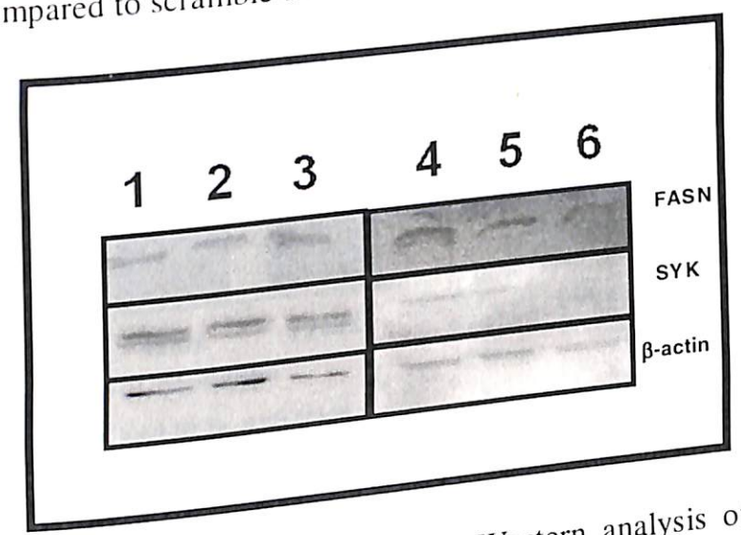

Figure 7.4: SYK / FASN proteins expression. Western analysis of *SYK* and FASN protein in miRNA mimics transfected RB cells. Lanes 1-3: Scramble control, *miR-486-5p* and *miR-532-3p* transfected Y79 cells. Lanes 4-6: Scramble control, *miR-486-5p* and *miR-532-3p* transfected Weri Rb1 cells.

7.2.9. Decrease of cell viability in mimics transfected RB cells

In Y79 cells, the treatment of *miR-486-3p* mimics has resulted in the respective reduction of cell viability to 86.08%, 58.42% and 66.86% at the end of 24 h, 48 h and 72 h of incubation. The treatment of *miR-532-5p* in Y79 cells have resulted in the decrease of cell viability to about 88.97%, 71.05%, 77.8% while the scramble transfected negative control

showed a cell viability of 94.2%, 82.2% and 80.84% at the end of 24 h, 48 h and 72 h of incubation compared to untransfected cell control.

Similarly in Weri Rb 1, the treatment of *miR-486-3p* mimics has resulted in the reduction of cell viability to 90.41%, 66.41%, and 51.74% at the end of 24 h, 48 h and 72 h of incubation respectively. The treatment of miR-532-5p in Weri Rb1 cells have resulted in the decrease of cell viability to about 87.63%, 72.47%, 56.39% while the scramble transfected negative control showed a cell viability of 96.51%, 86.51% and 89.78% at the end of 24 h, 48 h and 72 h of incubation compared to untransfected cell control.

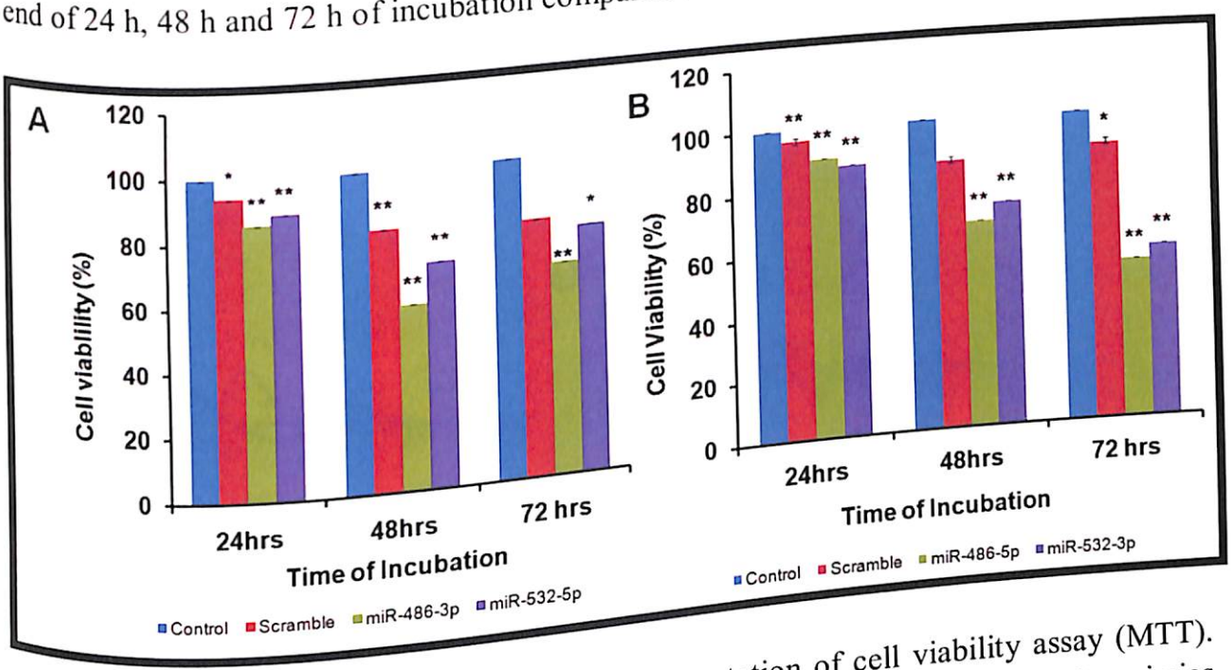

Figure 7.5: Cell viability assay. Graphical representation of cell viability assay (MTT). Percentage of cell viability in 50 pmoles of *miR-486-3p* and *miR-532-5p* mimics transfected RB cells A: Y79; B: Weri Rb1 at the end of 24 h, 48 h and 72 h of incubation. The four bars indicate in the order of untransfected control (blue), scramble control (red), *miR-486-3p* (green) and *miR-532-5p* (purple) respectively. Error bars represent the SD of the triplicates.

7.2.10. Increase of apoptosis in mimics transfected RB cells

In Y79 cells, the Annexin assay revealed the *miR-486-3p* and *miR-532-5p* mimics treatment resulted in the induction of late apoptotic cells to about 30.9% and 30.6% while the scramble mimics treatment has resulted in 2.62% compared to the untransfected cell control, at the end of 48 h of incubation. Similarly the miR-486-3p and miR-532-5p

mimics treatment in Weri Rb1 resulted in the induction of late apoptotic cells to about 19.6% and 21.8% while the scramble mimics treatment has resulted in 13.5% compared to the untransfected control cells, at the end of 48 h of incubation. A significant change (p-value <0.05) in the percentage of cell viability in *miR-486-3p* and *miR-532-5p* mimics treated Y79 cells was observed

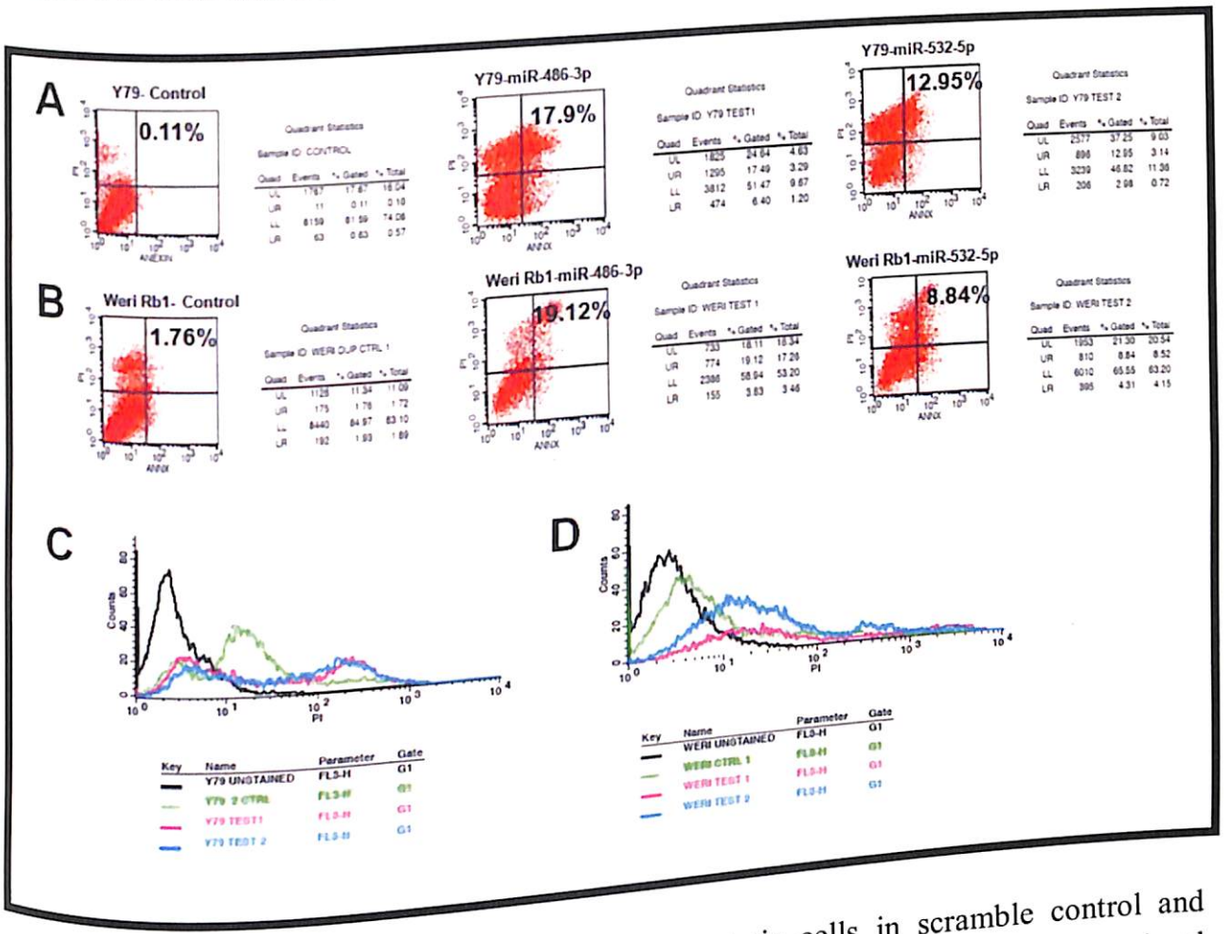

Figure 7.6: Apoptosis assay. Scatter plot of apoptotic cells in scramble control and mimics transfected RB cells. A: Y79; B: Weri Rb1. Overlay graph of scramble control and mimics transfected RB cells C: Y79; D: Weri Rb1. In the overlay graph, black line indicates unstained cells, green line indicates untransfected cells, pink line indicates miR-486-5p transfected cells and blue line indicates miR-532-3p transfected cells.

7.2.11. Alteration of cell cycle phases in the mimics transfected RB cells

In Y79 cells, the miR-486-3p and miR-532-5p mimics treatment resulted in altered percentage of G2/S phase cells percentage to about 48.7% and 48.7% respectively while the scramble mimics treatment resulted in 30.5% at the end of 48 h of incubation. Similarly the *miR-486-3p* and *miR-532-5p* mimics treatment in Weri Rb1 resulted in the alteration of G_2/S phase cells to about 53.1% and 54.9% respectively while the scramble

mimics treatment has resulted in 47.9% at the end of 48 h of incubation. Though a significant change of G_2/S phase cell percentage was observed in Y79 cell, no significant change was observed in Weri Rb1cells.

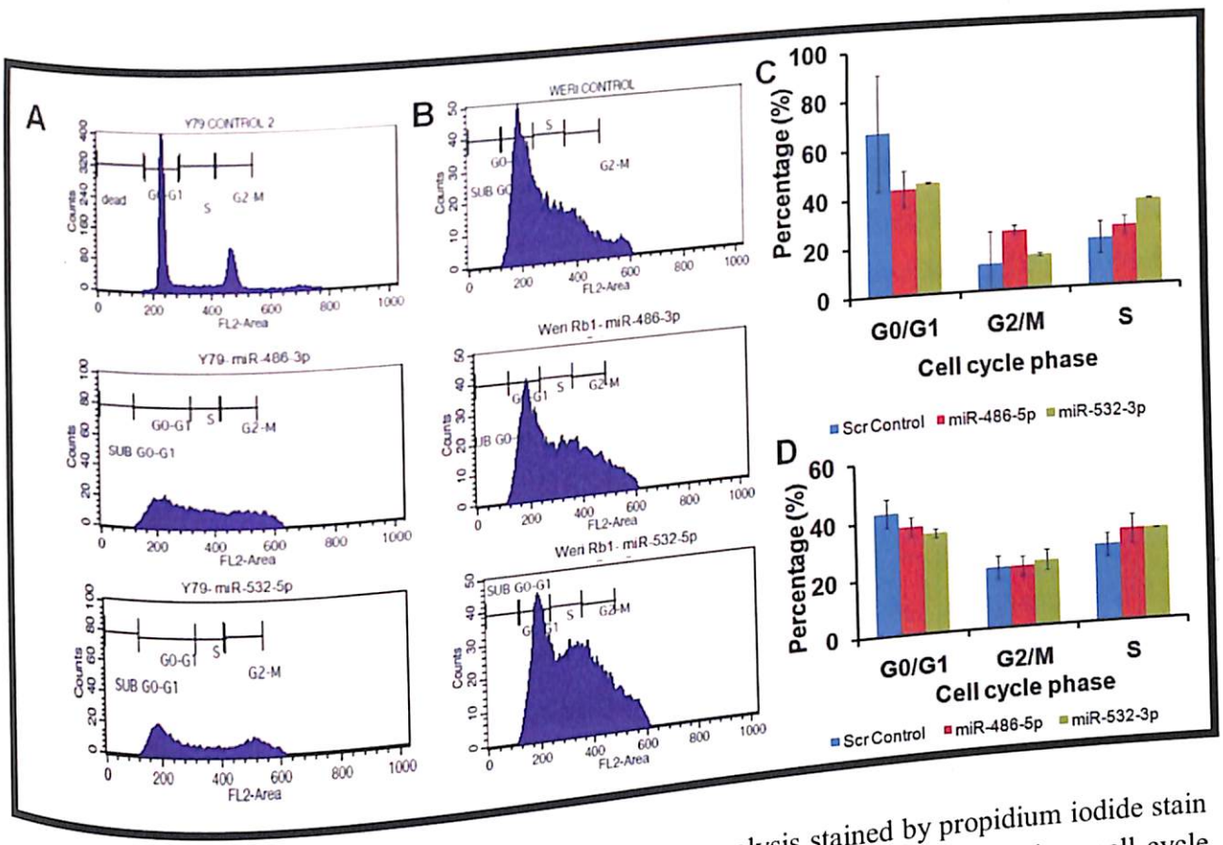

Figure7.7: Cell cycle assay. Scatter plot of cell cycle analysis stained by propidium iodide stain in 50pmoles of mimics at the end of 48 h of incubation. (A) Measurement of various cell cycle stages in mimics treated Y79 cells; (B) Measurement of various cell cycle stages in mimics treated Weri Rb 1 cells. The bar graph of RB cells at various stages of cell cycle in scramble and mimics treated RB cells. Error bars represent the SD of the triplicates.

7.3. Discussion

The standard methodology to perform the functional analysis of miRNA-mRNA interactions would require array based mRNA and miRNA global expressions or RNA – sequencing inputs. These approaches would require a large investment including a huge quantity of purified RNA and economic supports to perform 2 different arrays which in turn impedes the limited number of paired miRNA-mRNA datasets in the available public repositories (Stempor et al. 2012). Thus data mining from these repositories would provide

immediate information about the paired miRNA-mRNA networks and their gene target regulations.

Retinoblastoma, being a first disease to demonstrate the cancer development, good initial efforts has been achieved to identify the regulatory miRNAs, genes and their mechanisms contributing to RB gene therapy. This achievement is persuaded through the documentation of reports including gene expression, miRNA expression profiles and deep sequencing reports of RB tumors. In the current study, we have undertaken an comprehensive *in silico* approach to identify miRNAs regulating the panel of genes [categorised as group I genes (*HMGA2, MYCN, SYK, FASN*) group II genes (*TACSTD1 (EpCAM), ABCG2, CD133, CD44, CD24*) group III genes (*p53 and MDM2)]* involved in RB tumoriogenesis [**Figure 7.1**]. With the removal of redundancy, about 1948 common miRNAs were obtained from this insilico approach. Further, the interaction of these miRNAs with the reported RB serum expression profile revealed 9 up-regulated miRNAs (miR-146b-5p, miR-305, miR-663b, miR-299, miR-532-5p, miR-892b, miR-501, miR-142-5p and miR-513b) and 10 down-regulated miRNAs (*miR-1254, miR-328, miR-133a, miR-1287, miR-1299, miR-375, miR-486-3p, miR-720, miR-720, miR-98, and miR-122**). However, in order to rule out the false discovery rate of the current study, 5 miRNAs (up-regulated panel, n=3: *miR-146b-5p, miR-532-5p* and *miR-142-5p* and down- regulated panel, n=2*: miR-328 and miR-486-3p*) are selected for the *in vitro* experimental validation using qRT-PCR.

However, the miRNA expression analysis using qRT-PCR revealed a higher down-regulation of two miRNAs namely *miR-486-5p* (median fold change in the order of invasion = -1.26, no invasion = -1.07) and *miR-532-3p* (median fold change in the order of invasion = -0.69, no invasion of = -1.00) compared to the normal cadaveric donor retina. Finally these approaches has resulted to list out two key miRNAs namely miR-486-5p and miR-532-3p and their regulatory mRNAs as *SYK* and *FASN*. The mRNA filtration of these miRNAs was based on their MFE (Minimal Free Energy of <= - 30 and p-value of <=0.05) and those that are reported in MICROCOSM and DIANA LAB databases [**Table 7.3**]. Similarly, we observed the down-regulation of these miRNAs in two of the RB cell lines –Y79 and Weri Rb1 [**Table 7.4, 7.5 and Figure 7.2**]. Down-regulated miR-486-5p has been known to contribute aggressive lung cancer with lymphnode metastasis (Boeri et al. 2011, Seigler 1985, Shen J. et al. 2011) and also reported as biomarker in the primary

non-small cell lung carcinoma (NSCLC) tissues and plasma (Shen J. et al. 2011) and gastric cancer progression (Oh et al. 2011). Further, the lowered miR-486-5p and miR-532-3p has been reported in renal cell (Redova et al. 2013). These reports in other cancers together corroborates with the current results of lowered miR-486-5p and miR-532-3p expression in RB. However, interestingly higher expression of miR-532-3p is reported in the RB serum samples (n=14). Smaller sample size could be one of the contributing factors for the variation among these results.

In order to study the functional role of these two miRNAs in RB progression and their regulation of *SYK* and *FASN* as gene targets, *in vitro* experiments using miRNA mimics were performed. From these experiments, we observed an inverse correlation of SYK and *FASN* mRNA expression in mimics transfected RB cells especially at the end of 48 h of incubation [**Table7.5, Figure 7.3**]. The reduced *SYK* and *FASN* protein expression in mimics transfected RB cells compared to the scrambled control corroborates with the mRNA down regulation of mimics transfected RB cells [**Figure 7.4**]. Earlier reports have showed the significant role of these two genes in other cancers namely breast cancer (Coopman et al. 2000) and especially RB (Deepa et al. 2013, Vandhana et al. 2011, Zhang J. et al. 2012a). In a report, Zhang et al has elaborated the up-regulation of the proto-oncogene *SYK* with its importance in RB cell survival and has indicated *SYK* as a promising therapeutic target (Zhang J. et al. 2012a). Further, *FASN* was reported as an potential therapeutic target in RB management with its marked over-expression in invasive tumors (Vandhana et al. 2011). Further, the chemical inhibitors of FASN proteins in RB cells have resulted in apoptosis (Deepa et al. 2010, Vandhana et al. 2013). These earlier studies corroborates with the current results of reduced cell proliferation and increased apoptosis due to lowered *SYK* and *FASN* expression in mimics transfected RB cells relative to scramble treated control cells [**Figure 7.5 and 7.6**]. Taken together, the earlier reports along with current results of *SYK* and *FASN* down-regulation in mimics transfected RB cells indicates the role of these oncogenes in RB cell growth. Further, the cell cycle analysis in the mimics transfected RB cells stated a marked change in G_2/S phase of the Y79 cells (about 48.7% and 48.7% while the scramble mimics treatment has resulted in 30.5% of G_2/S phase of cell cycle) while no marked cell cycle phase was observed in mimics transfected Weri Rb 1 cells [**Figure 7.7**]. The difference in aggressive phenotype that exist between the two cell lines could be the contributing factor for the variation in this cell cycle results among the two mimics transfected RB cell lines.

7.4. Conclusion

The present report substantiates the identification of miRNAs regulating the panel of candidate genes involved in RB progression and continues the experimental validation of the identified miRNAs using miRNA mimics. Thus, the current study report on the down-regulation of *miR- 486-5p* and *miR-532-3p* in primary retinoblastoma implicates its role in RB tumorigenesis and implies its prognostic potential. The down-regulation of its gene targets: *SYK* and *FASN* at the transcript level and protein level were confirmed. In addition, miRNA over-expression resulted in the reduction of cell proliferation, through the induction of apoptosis (confirmed by Annexin V FLUOS assay) in RB cancer cells. The reduction in cancer cell viability by specific mimics suggests both *miR-486-3p* and *miR-532-5p*, a potential target for RB therapy.

CHAPTER 8: GENE DEREGULATION IN RB TUMORS POST-CHEMOTHERAPY: WHOLE GENOME MICROARRAY ANALYSIS

8. Introduction

[#] RB, a pediatric intraocular malignancy is fatal when left untreated. Enucleation is the treatment of choice, and is curative in more than 90% of cases but results in adverse physiological and psychological effects (Anteby et al. 1998, Dhar et al. 2011, Friedman D. L. et al. 2000). Chemotherapy in combination with cyclosporin has also been used in management of intraocular RB (Chan H. S. et al. 1996). Previous studies on drug resistance in RB are based on proteins playing a role in drug resistance reported in other cancers. Some examples are P-glycoprotein (P-gp) / multidrug resistance-associated protein (MRP) and lung resistance protein (LRP) (Chan H. S. et al. 1991, Krishnakumar et al. 2004b), Crystallin alpha A, alpha B (Kase et al. 2009a), heat shock proteins (HSP 27) (Kase et al. 2009b), cancer stem cell markers (ABCG2, MCM2) (Mohan et al. 2006), serine/arginine-rich protein-specific kinase 1 (SRPK1) (Krishnakumar et al. 2008), Hypoxia inducible factors-alpha (HIF1a) and survivin (Job Sudhakar 2013) and stathmin (Mitra et al. 2011b) gene and protein expressions. These studies have analysed the protein expression mainly by various techniques such as immunohistochemistry and western analysis. Other studies on gene expression in RB are in primary RB samples prior to chemotherapy (Chakraborty et al. 2007, Ganguly and Shields 2010). Molecular understanding of drug resistance in post chemotherapy RB microarray is limited.

Tumor aggressiveness and/or late diagnosis (Schultz K. R. et al. 1993) of RB has prompted development of therapeutic strategies, such as chemo thermotherapy (Murphree

[4] # *The results presented in this chapter have been published: Nalini V, Segu R, Deepa PR, Khetan V, Vasudevan M, Krishnakumar S. Molecular Insights on Post-chemotherapy Retinoblastoma by Microarray Gene Expression Analysis.Bioinform Biol Insights. 2013 Sep 18; 7: 289-306.*

et al. 1996), cryotherapy (Rodriguez-Galindo et al. 2003), chemotherapy (high-dose chemo), laser therapy (Gallie et al. 1996), brachytherapy, adjuvant therapy or various combinations of these therapies (Schueler et al. 2003, Uusitalo et al. 2001). However even these sometimes fail to prevent tumor recurrence owing to several factors such as larger tumor size, vitreous seedings, age of onset, and family history of RB (Kingston et al. 1996, Shields et al. 2003, Shields et al. 2002b). In this context, insights on molecular mechanisms of anti-tumor agents and their relationship with the drug resistant states would provide effective options for chemo prevention (Goldie 2001, Wilson M. W. et al. 2009). Hence, here cDNA microarray analysis of various deregulated genes was performed in tumor tissues obtained from RB patients who had undergone chemotherapy. The present study also evaluates the possible role of two genes, namely *PRAME* (Preferentially expressed Antigen in Melanoma) and *Ect2* (Epithelial cell transforming sequence 2) in chemotherapeutic drug response modulation in primary RB tissues.

8.1. Materials and Methods

The snap frozen RB tumors (n=3) and snap frozen retinal samples (n=2) collected from 2 cadaveric eyeball (received at C.U Shah eye bank, Sankara Nethralaya) during 2009-2010 were included for the gene expression studies. **Table 8.3** shows the clinico-pathological descriptions of the RB tumors included in the microarray gene expression profiling. From the microarray analyses, the differentially expressed genes were validated in RB tumors (n=21) by Real-Time PCR (qRT-PCR) and immunohistochemistry. Paraffin embedded tissue blocks from 21 patients with RB between 2009 and 2011 with median age of 2.6 years were retrieved for PRAME protein expression studies by immunohistochemistry. Clinical and pathological information was obtained from medical records and surgical pathology reports respectively.

8.1.3. Histopathology

All the tumors were grouped into A-E groups following International Intraocular Retinoblastoma Classification (IIRC) (Linn Murphree 2005). The clinico-pathological description of the RB included in the validation studies has been described in **[Table 8.3]**.

et al. 1996), cryotherapy (Rodriguez-Galindo et al. 2003), chemotherapy (high-dose chemo), laser therapy (Gallie et al. 1996), brachytherapy, adjuvant therapy or various combinations of

were subjected

oarray

analysis, the 3 RB tumour tissues were processed in triplicate using Affymetrix Human Gene 1.0 ST Genechip following the detailed protocol discussed in the section 4.8. Following hybridization, the arrays were washed and stained using the GeneChip Fluidics Station 450 and scanned using the GeneChip® Scanner 3000 7G as recommended by the manufacturer (Affymetrix Technologies, Santa Clara, CA).

8.1.5. Microarray Data Acquisition and Pre-processing

Raw data was obtained as .CEL and .CHP format using GCOS software. Agilent Technologies GeneSpring GX v 12.0 was used to process the raw data Probeset summarization was done using ExonRMA16 algorithm with confidence level set at 100%. Intra sample normalization was done by Quantile method and baseline transformation was calculated taking median of all samples. The HuGene 1.0 ST Genechip comprises of 28,869 well-annotated genes with 764,885 distinct probes. The design of the Human Gene 1.0 ST Array was based on the March 2006 human genome sequence assembly (UCSC Hg18, NCBI build 36) with comprehensive coverage of RefSeq, Ensembl and putative complete CDS GenBank transcripts. The Human Gene 1.0 ST Array has greater than 99 percent coverage of NM sequences present in the November 3, 2006, RefSeq database.

8.1.6. Differential gene expression analysis

Volcano plot based method was used to find out genes that are differentially expressed between two conditions. Volcano plots allow easy comparison between the "double filtering"gene selection criteria and "single filtering" or "joint filtering" criteria (http://www.ncbi.nlm.nih.gov/pubmed/23075208). Genes whose log fold change is +2 and

8.1.4. Oligonucleotide microarray analysis

Three RB fresh tumor tissues (n=3,) and two normal adult retina samples were subjected to oligonucleotide microarray using U133 Affymetrix gene platform. For the microarray analysis, the 3 RB tumour tissues were processed in triplicate using Affymetrix Human Gene 1.0 ST Genechip following the detailed protocol discussed in the section 4.8. Following hybridization, the arrays were washed and stained using the GeneChip Fluidics Station 450 and scanned using the GeneChip® Scanner 3000 7G as recommended by the manufacturer (Affymetrix Technologies, Santa Clara, CA).

8.1.5. Microarray Data Acquisition and Pre-processing

Raw data was obtained as .CEL and .CHP format using GCOS software. Agilent Technologies GeneSpring GX v 12.0 was used to process the raw data Probeset summarization was done using ExonRMA16 algorithm with confidence level set at 100%. Intra sample normalization was done by Quantile method and baseline transformation was calculated taking median of all samples. The HuGene 1.0 ST Genechip comprises of 28,869 well-annotated genes with 764,885 distinct probes. The design of the Human Gene 1.0 ST Array was based on the March 2006 human genome sequence assembly (UCSC Hg18, NCBI build 36) with comprehensive coverage of RefSeq, Ensembl and putative complete CDS GenBank transcripts. The Human Gene 1.0 ST Array has greater than 99 percent coverage of NM sequences present in the November 3, 2006, RefSeq database.

8.1.6. Differential gene expression analysis

Volcano plot based method was used to find out genes that are differentially expressed between two conditions. Volcano plots allow easy comparison between the "double filtering"gene selection criteria and "single filtering" or "joint filtering" criteria (http://www.ncbi.nlm.nih.gov/pubmed/23075208). Genes whose log fold change is +2 and

above is considered as up regulated and -2 and below as down regulated. Applying unpaired student t-test with a p-value cutoff of <0.05 did filtering of differentially expressed genes. To the filtered list of differentially expressed genes, Benjamini Hocheberg method was applied to calculate FDR (False Discovery Rate). Differentially expressed genes in RB tumors were identified in comparison to normal retina and for post-chemo treated tumor it was done in comparison to pre-chemo treated RB tumor. Further unsupervised hierarchical clustering of differentially expressed genes was done by applying Pearson uncentered algorithm with average linkage rule.

8.1.6.1. *Gene Ontology, Phenotype, Biomarkers and Pathway Enrichment analysis*

GOElite tool (www.genmapp.org/go_elite) was used for enrichment analysis of biological processes dysregulated by differentially expressed genes. Significant biological processes were filtered out based on categories with a p-value of <0.05 along with one or more of the following criteria: Z score (>2.0) / q-value (<0.1).

8.1.6.2. *Biological Analysis Network modeling*

Information pertaining to protein-protein interaction along with biological processes involved for the differentially expressed genes was collated to identify key genes which can act as biomarker for treatment response and tumor profile. Protein-protein interaction data for gene list in each group was obtained from MiMi database (mimi.ncibi.org). Further Cytoscape V 8 was used to model the biological network with emphasis to proteins that are significantly connected to the network (>10 edges) to understand their role and significance.

8.1.7. PRAME / Ect2 mRNA quantification using quantitative Real-Time polymerase chain reaction (qRT-PCR)

Total RNA was isolated using RNeasy Mini Kit and total RNA was transcribed into cDNA using Omniscript (Qiagen, Hilden, Germany) following the protocol discussed in section 4.2.5. Quantitative PCR was performed using the ABI Prism 7500 Sequence

Detector (Applied Biosystems, Lab India, and Chennai, India). Primers and Taq-Man probes for *GAPDH, MRP1 and PRAME* were used in accordance with the manufacturer's instructions following the protocol discussed in section 4.7.3.1. The expression of each gene in each sample was analyzed in triplicates for statistical comparisons.

8.1.8. Immunohistochemistry

Immunohistochemistry was performed as explained in section 4.2.1.

8.1.8.1. *Immunoreactivity scoring*

Two observers without knowledge of the clinical data independently assessed the expression of PRAME. The distribution of PRAME expression was semi quantitatively assessed by estimating the percentage of positively stained cells. Randomly 10 tumor fields were scanned for protein expression under 40% and percentage of positive tumor cells were noted for each field. Then the average expression was calculated from the 10 values for the entire slide. Depending on the percentage of positive cells, 4 categories were established: 0, no positive cells; 1+, positive cells in less than one third; 2+, positive cells in 33% to 67%; and 3+, positive cells in more than two thirds of total tumor cell population (Detre et al. 1995).

8.1.9. Transient transfection

Human RB cell line (Y79, ATCC, USA) cultured in RPMI 1640 medium (Rosewell Park Memorial Institute; Gibco-BRL) with 10% heat-inactivated fetal bovine serum [FBS, Gibco- BRL (Rockville, MD)], 0.1% ciprofloxacin, 2 mM L-glutamine, 1 mM sodium pyruvate, and 4.5% dextrose (Sigma Aldrich, St. Louis, MD, USA) as supplements were used in the study. The cultures were grown as suspension at 37 °C with 5% CO_2. Transient over expression of PRAME gene (PRAME cDNA (NM_206955.1) cloned into the pcDNA3.1 vector was purchased from OriGene Technologies, Inc, U.S.A) was established as per the manufacturer's protocol explained in section 4.2.9. The transfected cells were collected after 48 h of incubation for the further experiments.

8.1.10. IC_{50} determination of three chemotherapeutic drugs

After 48 h of transfection, the cell proliferation assay using 3-(4,5- Dimethylthiazol-2-yl)-2,5-diphenyltetrazolium bromide (MTT; Sigma, St Louis, MO) was performed in triplicates with 8000 cells per well in 96-well plate in complete growth medium containing concentrations of 25, 30, 35, 40, 45µg/ml for carboplatin, 0.5, 1.0, 1.5, 2.0 µg/ml for vincristine and 2.5, 5.0, 7.5, 10.0 µg/ml for etoposide and incubated further for 48 h. The complete growth medium was replaced by 100 µl of MTT reagent (5mg/ml). After the 4hrs of incubation at 37°C the reagent was replaced by 100µl of dimethyl sulphoxide (DMSO) and incubated for 10 minutes at 37°C. The absorbance was determined at 570 nm.

8.1.11. Statistical analysis

For microarray analysis, Benjamini and Hochberg algorithm was used to derive statistical t-test and p-value based on Volcano Plot. P-value ≤ 0.05 was considered significant for change in gene expression. Log_2 transformed values of gene expression changes showing $\geq$1.0 fold were considered as up-regulation, while $\leq$1.0 fold change in gene expression was considered down-regulation.

For **immunohistochemistry analysis**, paired samples t-test was used to derive the statistical significance. Statistical analysis was performed to correlate PRAME expression with invasion and differentiation of tumors. For statistical analysis, moderately differentiated and well-differentiated tumors were compared with poorly differentiated tumors. Mann-Whitney U-test revealed statistically non-significant association of PRAME protein expression with respect to tumor invasiveness (p-value = 0.715) and tumor differentiation (p-value = 0.201). For the comparison of the chemotherapeutics (IC_{50}) in PRAME transfected and un-transfected RB (Y79) cells, student's t-test was used to derive the p-value.

Table 8.1: Detail of RB tumors. Clinico-pathological features of retinoblastoma tumor tissues included in the whole genome expression studies by cDNA microarray.

S.No	Age/Sex	Clinicopathological features	Chemotherapy
1.	3Y/ Male	OD: UD, no invasion into the choroid and ON	11 cycles
2.	2.5 Y/M	OS: UD, no invasion of choroid, sclera and ON	9 cycles
3.	1 Y/F	OD: UD, endophytic, No choroidal invasion	No Chemotherapy

UD: Undifferentiated, ON: optic nerve, OD: Right eye, OS: Left eye, M: Male, F: Female, Y: Years.

8.2. Results

8.2.3. Oligonucleotide microarray analysis in primary (pre-chemotherapy and post-chemotherapy) RB tumor tissues.

8.2.3.1. *Differentially expressed genes in pre-chemotherapy and post-chemo treated RB tissues normalized to normal retina.*

PCA (Principal Component Analysis) showed replicate samples under each condition were grouped together. Normal retina, pre-chemotherapy RB tumor samples are distinctively different from post-chemo therapy RB tumor tissues **[Figure 8. A, B]**. A fold change above 2.0 was considered as up-regulation in gene expression; while a log fold changes below 2.0 was considered as down-regulation. Volcano plot based method to identify differentially expressed genes showed that 2538 genes were down regulated and 1672 genes were up regulated in RB tumors in comparison to normal retina. We observed a down-regulation of 821 genes and up-regulation of 1011 genes in post-chemotherapy RB tumor tissues relative to pre-chemotherapy RB tumor tissues **[Figure 8.B and 8.C]**.

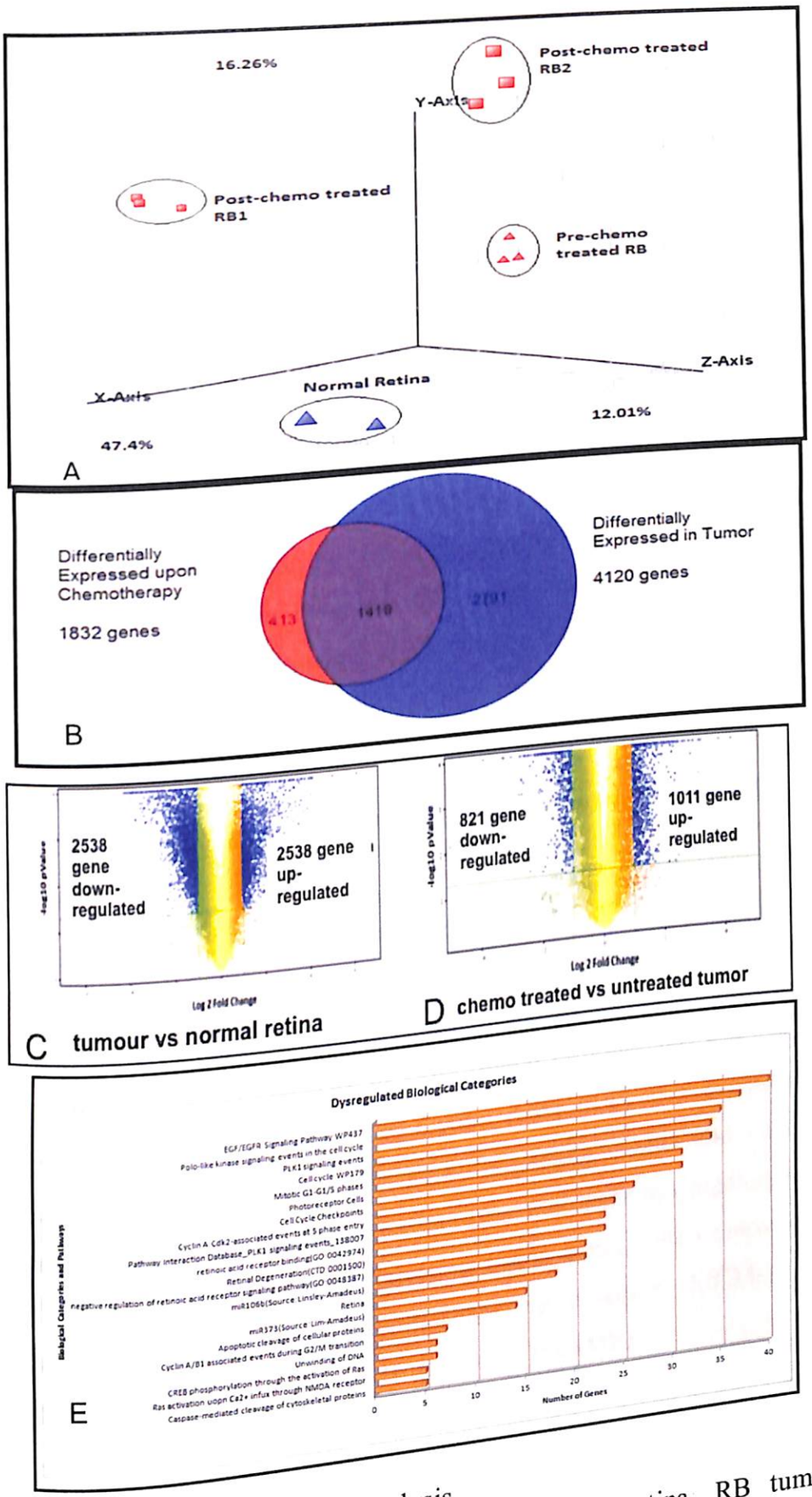

Figure 8.1: Whole genome microarray analysis.

A. PCA (Principal Component Analysis) of normal retina, RB tumor (pre – chemotherapy RB tumor tissue) and post-chemotherapy RB tumor tissues (RB1 and RB2). The PCA shows clustering of the gene profiles in groups respectively.

B. Venn diagram representing distribution of differentially expressed genes upon chemo treatment and in tumor sample compared to normal retina.

C. The volcano plot showing differentially expressed 4210 genes (includes 1672 up-regulated genes and 2538 down – regulated genes) in number identified in the gene expression profiling of RB tumors compared with normal retina.

D. The volcano plot showing differentially expressed 1832 genes (includes 1011 up-regulated genes and 821 down – regulated genes) in number identified in the gene expression profiling of post- chemotherapy RB tumors compared with pre-chemotherapy RB.

E. Key biological categories and pathways that was dys-regulated in the RB tumors.

8.2.3.2. *Comparison of differentially expressed genes between pre-chemotherapy RB tumor tissue and post- chemotherapy RB tumor tissues*

Unsupervised hierarchical clustering of differentially expressed gene sets in pre-chemotherapy RB tumor tissue revealed 2791 genes de-regulated relative to normal retinae. Out of this, 1419 gene expressions overlapped with post-chemotherapy group. In addition, 413 genes were differently de-regulated only in post-chemotherapy RB tumor tissues **[Figure 8.D]**.

8.2.3.3. *Significantly dysregulated biological categories and pathways*

GoElite analysis of merged differentially expressed genes resulted in identification of 21 key gene ontology categories, pathways, biomarkers and phenotype groups dys-regulated, harbouring 250 differentially expressed genes. Some of the key biological categories include (i) Caspase-mediated cleavage of cytoskeletal proteins, (ii) Ras activation uopn Ca2+ infux through NMDA receptor, (iii) Cyclin A/B1 associated events during G2/M transition, (iv) Retinal degeneration, (v) PLK1 signaling events and (vi) EGF/EGFR Signaling Pathway **[Figure 8.E].** Key gene families that were dys regulated included (i) Aurora Kinases, (ii) Cyclins, (iii) Cell Division Cycle genes, (iii) Centromere Proteins, (iv) Guanylate Cyclases, (v) Mini-chromosome maintenance (MCMs), (vi) Origin recognition complex (ORCs), (vii) PRAME Families (PRAMEF).

Table 8.2: *De-regulated genes in RB. Significantly dys- regulated genes determined by Microarray analysis*

Gene description	Gene symbol	Accession number	Chromosomal location	Mean fold change (log_2 ratio)	
				Post-chemotherapy treated RB tumors	Pre-chemotherapy treated RB tumor
Modulator of apoptosis 1	MOAP1	NM_022151	chr14	2.75	2.81
Programmed cell death 4 (neoplastic transformation inhibitor)	PDCD4	NM_145341,NM_014456	chr10	2.11	2.66
TCDD-inducible poly(ADP-ribose) polymerase	TIPARP	NM_015508	chr3	2.71	1.599
Poly (ADP-ribose) polymerase family, member 9	PARP9	NM_031458	chr3	2.64	1.35
Signal transducer and activator of transcription 1,	STAT1	NM_007315,NM_139266	chr2	2.22	1.41
Signal transducer and activator of transcription 3	STAT3	NC_000017	chr17	1.60	2.39
Prune homolog 2 (Drosophila)	PRUNE2	NM_138818	chr9	6.52	2.24
Stathmin1	STMN1	NC_000001	chr1	1.51	2.27
EGF epidermal growth factor	EGF	NC_000004	Chr4	1.16	2.05
Interferon, alpha-inducible protein 6	IFI6	NM_002038,NM_022872	chr1	4.33	1.94

Transcription factor 4	*TCF4*	*NM_003199*	*chr18*	*1.80*	*3.11*
Serine/Threonine kinase 35	*STK35*	*NM_080836*	*chr20*	*2.29*	*4.98*
ATP-binding cassette, sub-family C(CFTR/MRP), member 4	ABCC4	NM_005845	chr13	2.17	1.75
BCL2-like 1	BCL2L1	NM_138578,NM_001191	chr20	3.80	2.25
Preferentially expressed antigen in melanoma	PRAME	NM_206953,NM_006115	chr22	5.57	5.78
ATP-binding cassette, sub-family A (ABC1), member 4	ABCA4	NM_000350	chr1	3.42	8.32
Interleukin 13 receptor, alpha 1	IL13RA1	NM_001560	chrX		
Epithelial cell transforming sequence 2 oncogene	ECT2	NM_018098	chr3	1.16	2.05
Thyroid hormone receptor, beta (erythroblastic leukemia viral (verb-a) oncogene homolog 2, avian)	THRB	NM_000461	chr3	2.89	4.64
Tumor necrosis factor receptor superfamily, member 10b	TNFRSF10B	NM_003842,NM_147187	chr8	1.31	3.07
Spleen tyrosine kinase	SYK	NM_003177	chr9	1.05	3.97
RB1 retinoblastoma 1	RB1	NC_000013	Chr13	1.97	2.77
v-myb myeloblastosis viral oncogene homolog (avian)-like 2	MYBL2	NC_000020	Chr 20	1.27	3.24
Nuclear receptor corepressor 1	NCoR1	NC_000017	Chr 17	1.28	2.04
Phosphatase and tensin homolog	PTEN	NC_000010	Chr 10	1.57	2.27

Figure 8.2 represents the heat map of the gene expression profile of 28 dys-regulated genes in RB tumors compared to normal retina. Green and red indicates increased and decreased expression respectively, in relation to normal expression (yellow). Significantly dys-regulated biological processes were grouped as cell cycle process, Retina specific gene expression, and Signal transduction. Protein: Protein interactions were classified as Binding. Differentially expressed genes were considered as nodes and processes and binding were considered as edges that connect the nodes. Clustering using Cytoscape V 8.0 showed distinct gene and biological process clusters where all the PRAMEFs were clustered together and MCMs and CCNs clustered in one group. **[Figures 8.2A and 8.2B]** present the key regulatory networks that underlie the differential gene expression between pre-chemo and post chemo RB tumour tissues. The data discussed here have been deposited in NCBI's Gene Expression Omnibus and are accessible through GEO Series accession number GSE24673.

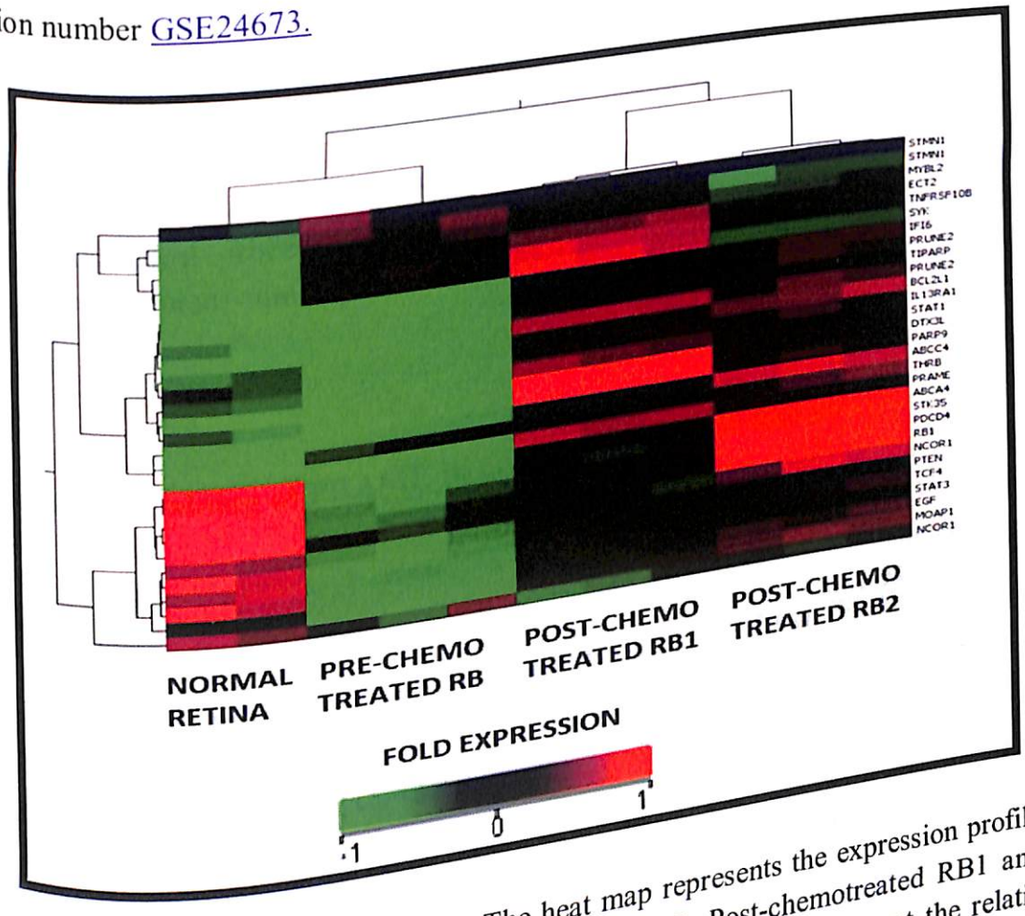

Figure 8.2: Heat map of RB and retina. The heat map represents the expression profile of 15 differentially expressed genes in RB (Pre-chemotreated RB, Post-chemotreated RB1 and Post-chemo treated RB2) compared to normal retina. The horizontal lines represent the relative fold change in the expression of individual genes. Green and red indicates increased and decreased gene expression respectively, while yellow represents normal expression.

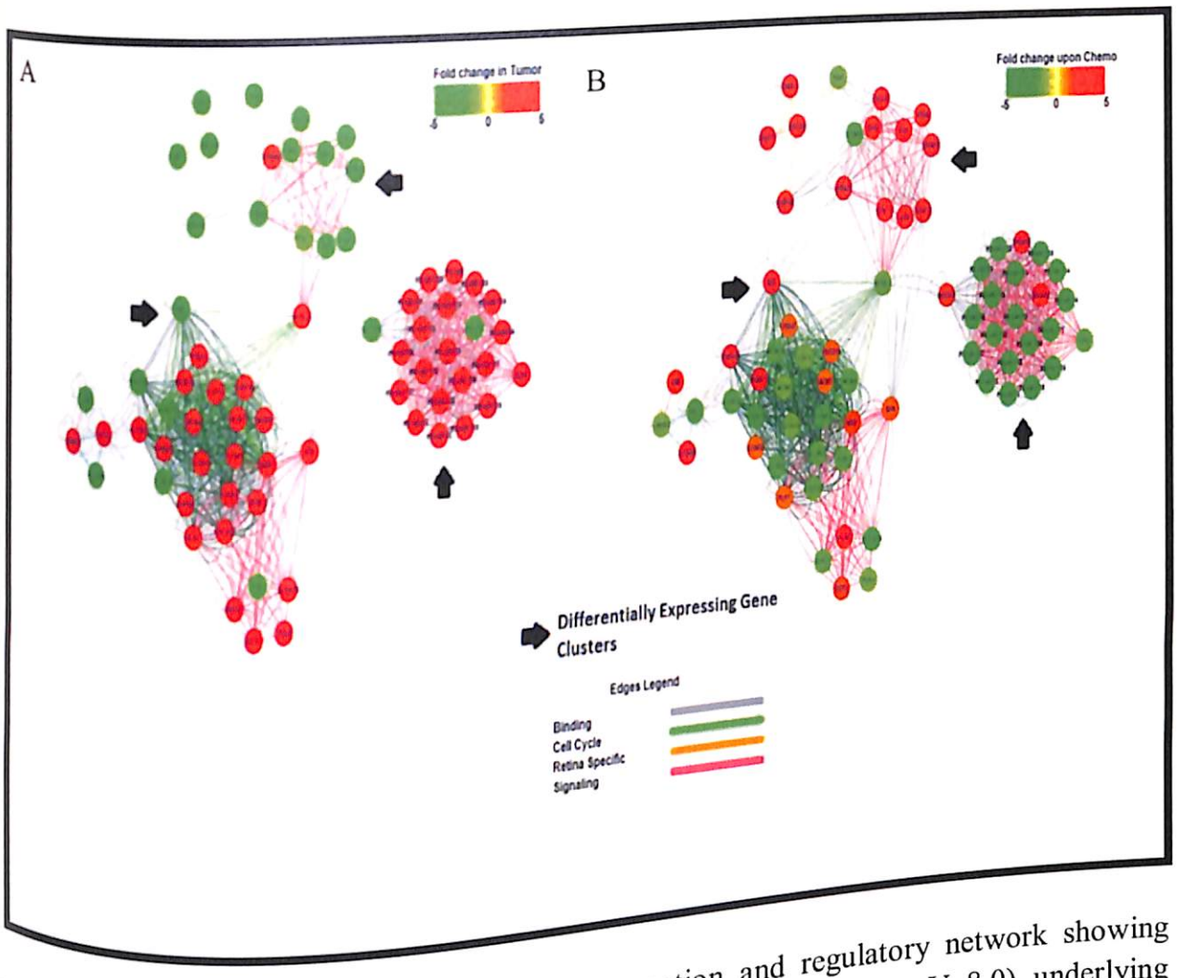

Figure 8.3: Regulatory networks. Protein interaction and regulatory network showing genes and biological process clustering (obtained using cytoscape V 8.0) underlying chemo treatment versus tumor profile A: post-chemotherapy, B: pre – chemo treated RB tumors.

8.2.4. Immuno-staining of PRAME in primary RB tumor tissues

Nucleo-cytoplasmic positivity of PRAME protein in 19 out of 21 RB tumors was in the order: higher expression in 5 tumors (5 out of 21 corresponding to 23.80%), moderate expression in 4 tumors (4 out of 21 corresponding to 19.04%), less expression in 9 (9 out of 21 RB tumors corresponding to 42.85%) and absent in 3 RB tumors **[Figure 7.4]**. There was neither any correlation between PRAME protein expression and tumor invasion, nor was there any correlation with chemotherapy status.

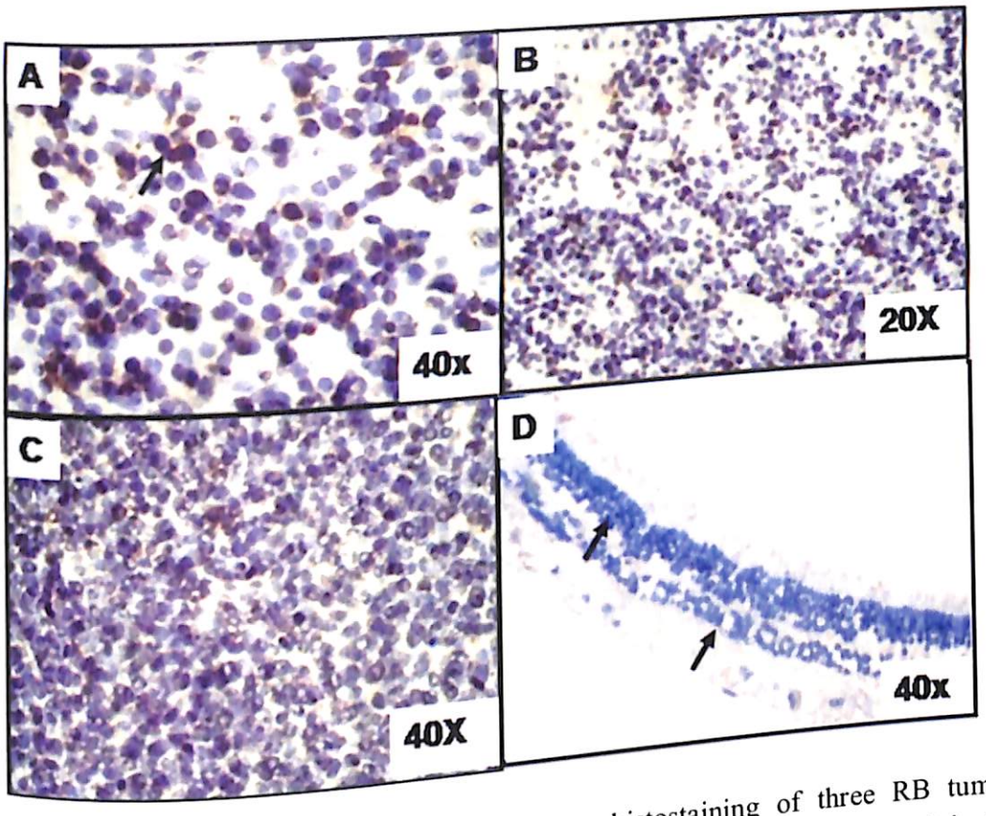

Figure 8.4: PRAME expression in RB. Immunohistostaining of three RB tumor tissues compared with non-neoplastic retina (DAB staining with hematoxylin counter staining). (A) The photomicrograph shows the strong nuclear expression of PRAME (arrows show positivity) in a RB tumor (40x magnification); (B) The photomicrograph shows the strong nuclear expression of PRAME (arrows show positivity) in a RB tumor (20x magnification); (C) The photomicrograph shows lesser percentage of nuclear of PRAME (arrows show positivity) in a RB tumor (40x magnification); (D) The photomicrograph shows the negative expression of PRAME (arrows show negativity) in the retinal layers (40x magnification).

8.2.5. Ect2 mRNA expression analyzed by qRT-PCR in primary RB tumor tissues

Ect2 mRNA expression was detected in 9 out of 21 (42.87%) tumors. Out of this cohort, 7 out of 9 post-chemo treated RB showed a marked positivity (77.77 %) while the remaining pre-chemo group showed low to high positivity, 2 out of 12 (corresponding to16.66 %). The down regulation of Ect2 mRNA was observed in 6 out of 12 pre-chemo treated RB tumors (corresponding to 50%). No significant fold-change in expression was observed in 6 RB tumors (which includes 4 out of 12 pre-chemo treated RB tumors (33.33%) and 2 out of 9 post-chemo treated RB tumors (22.22%)) **[Figure 8.4]**.

Figure 8.5: PRAME/Ect2 mRNA expression in RB. The mRNA expression of *PRAME* (Grey bar) and *Ect2* (Black bar) analyzed by real time quantitative reverse transcriptase PCR (qRT– PCR) relative to normal adult retina. Values are expressed as mean+/- SD of triplicate analyses.* indicates the post-chemotherapy RB tumor tissues.

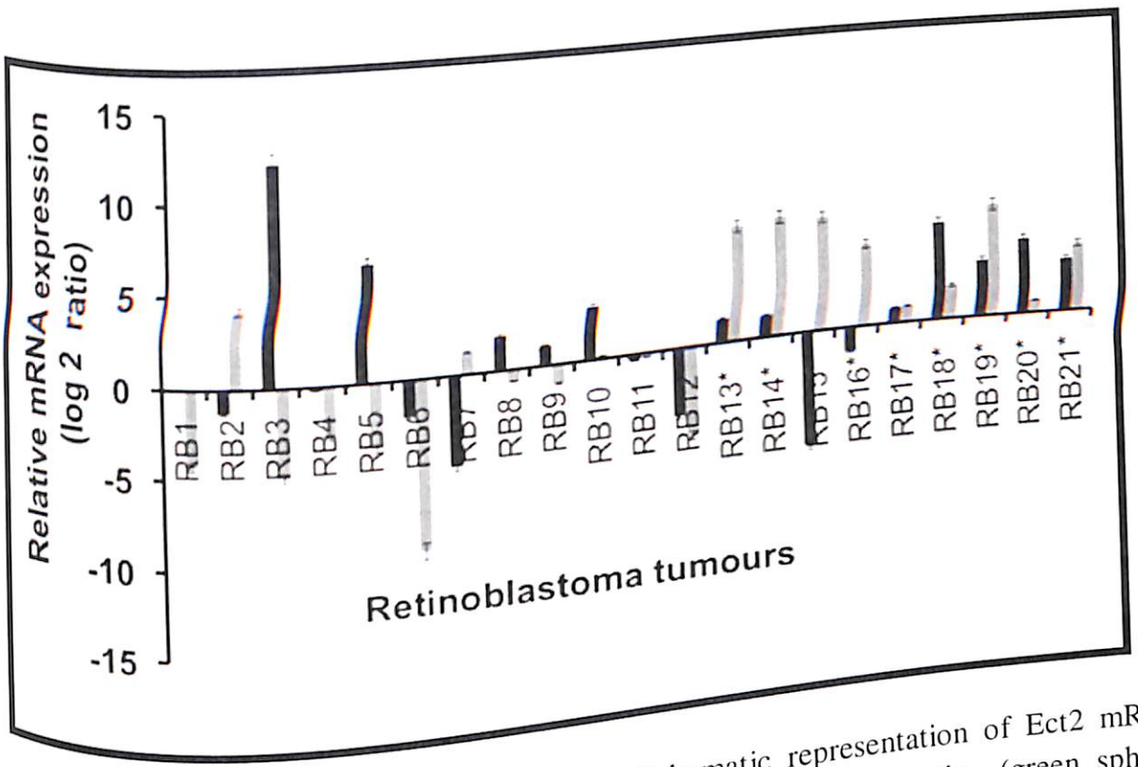

Figure 8.6: Ect2 mRNA expression in RB. Schematic representation of Ect2 mRNA levels in retinoblastoma tumor tissues relative to normal adult retina (green spheres represent post-chemotherapy RB tumor tissues, red spheres represent pre-chemotherapy RB tissues).

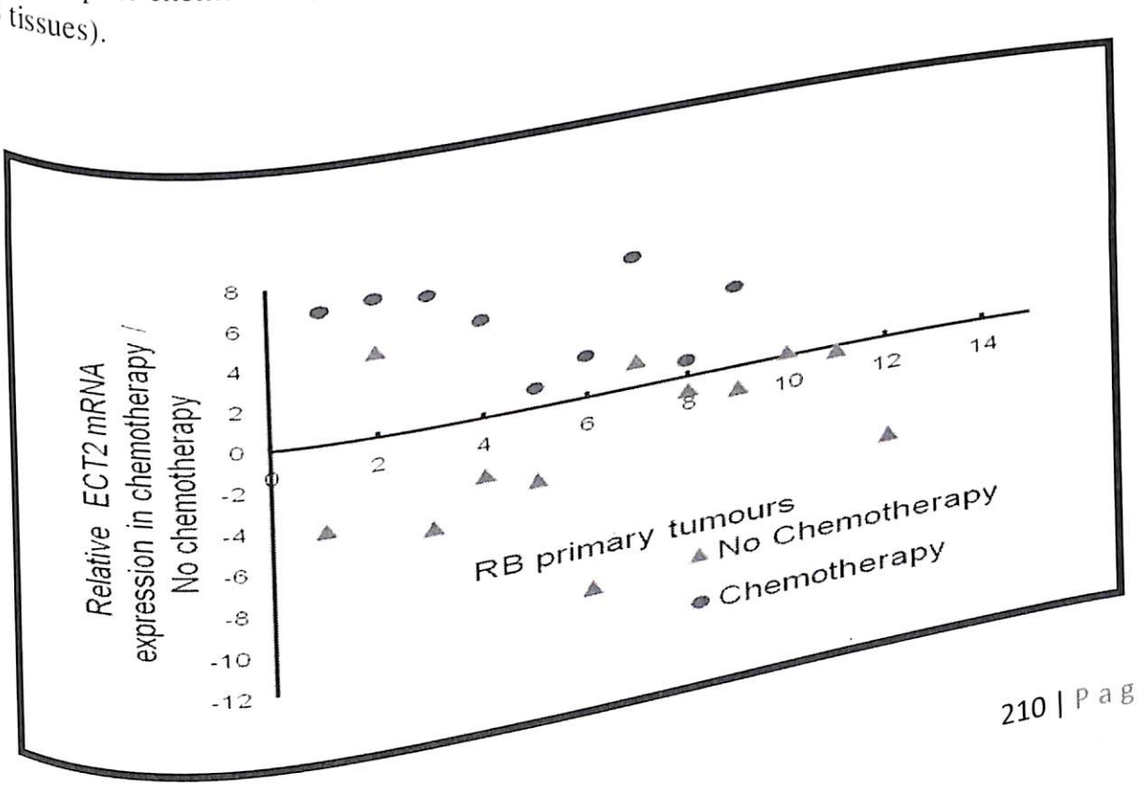

Table 8.3: PRAME/ ECT2 mRNA expression in RB. Clinico-pathological features of retinoblastoma tumor tissues, the percentage positivity of PRAME expressions (IHC), PRAME mRNA (black bar) expressions and ECT2 mRNA (Gray bar) expressions relative to normal adult retina (qRT-PCR).

S.No	Age (Yrs)/ sex	Post-chemotherapy /Pre-chemotherapy	Clinicopathological features	PRAME protein Percentage of Positivity	PRAME mRNA expression	ECT2 mRNA expression
1.	3/M	NC	OS: UD, Focal CI, pre-lam inv	20%	-5.11	1.25
2.	2/M	C (7 cycles)	OU:UD, Focal CI <3mm	40%	3.42	6.59
3.	3/F	NC	OD:WD, Focal CI<3mm, pre- lam	20%	-1.34	4.22
4.	3/M	NC	OS:UD, NI	80%	12.21	-5.00
5.	2/M	C (8 cycles)	OD:UD, Full thickness CI>3mm,prelam	80%	5.77	2.08
6.	2/M	NC	OS:PD, CI >3mm.	20%	-0.21	-2.91
7.	7.6/M	NC	OD:WD, Focal CI	70%	6.50	-3.70
8.	10/F	C(9 cycles)	OU:UD, CI<3mm	80%	3.19	4.04
9.	3/F	C(10cycles)	OU:WD,NI	0	-6.46	6.62
10.	3/M	NC	OD: PD, Diffuse CI>3mm tumor cells invading pre-lam , post laminar portion of ON	10%	-3.87	-5.08
11.	2.6/F	NC	OS:WD, focal CI	70%	2.90	0.19
12.	1/M	NC	OS: PD ,NI	10%	-2.07	-9.57
13.	3/F	C (17 cycles)	OU: UD ,NI	0	-1.34	4.87
14.	1/F	NC	OS: PD ,focal CI <3mm full thickness pre-lam ON	60%	1.9	-0.67
15.	1.8/M	NC	OD: UD full thickness CI>3mm pre-lam lam of ON	40%	1.09	-1.12
16.	2/M	C(9 cycles)	OD: PD, focal CI<3mm tumor cells invading pre- lam, post lam of ON	60%	4.50	0.78
17.	5months/F	NC	OS:MD, CI>3mm pre-lam of ON,	30%	-0.34	-0.23

18.	1/F	NC	OS:WD.Focal CI<3mm	20%	-0.05	-4.27
19.	4/F	C(5 cycles)	OS:UD.Focal RPE invasion	30%	1.32	6.60
20.	4/F	C (7 cycles)	OD:PD.NI	20%	1.24	6.88
21.	4/M	C(20 cycles)	OD:PD.Focal CI>3mm, tumor cells invading pre-lam and post laminar region of ON	0	0.93	0.98

C: post-chemotherapy RB tumor tissues, NC: pre-chemotherapy RB tumor tissues, WD: Well differentiated, PD: Poorly differentiated, UD: Undifferentiated, ON: optic nerve; OD: Right eye, OS: Left eye, OU: Both eyes, M: Male, F: Female, Y: Years; pre-lam: prelaminar; post-lam: post-laminar; CI: choroidal invasion

8.2.6. PRAME expression analysed by qRT-PCR in primary RB tumors and in PRAME over expressed RB cells

The present cohort of RB primary tumors showed PRAME mRNA expression in 11 tumors (52.38%), down-regulation in 6 tumors (28.57%) while there was no significant fold change in 4 RB tumors (19.04%). In the transfected cells, PRAME gene expression was estimated to be 14.67 log_2 fold change, while MRP1 showed 1.538 log_2 fold changes, which was non-significant when compared to PRAME by qRT-PCR **[Figure 8.6]**. **Table 8.3** shows the clinico-pathological features, percentage of positivity, and log_2 fold-change of PRAME expression in RB tumors.

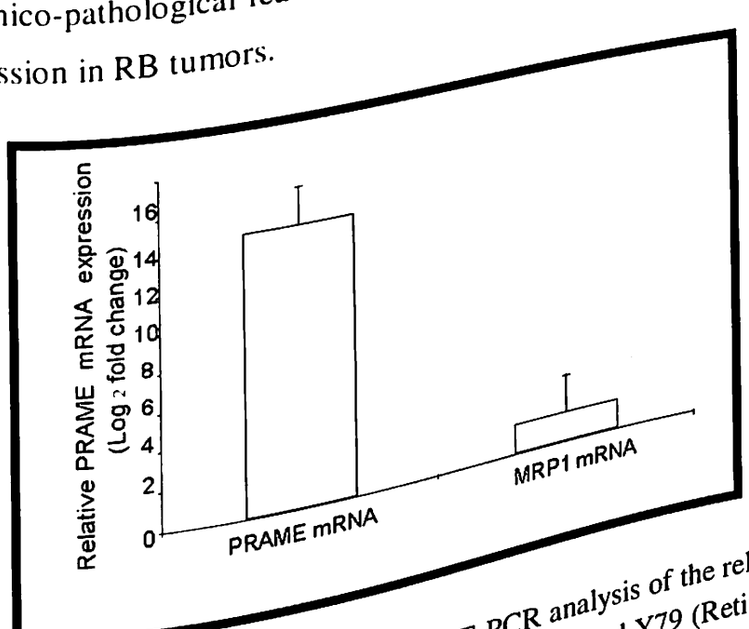

Figure 8.7: PRAME/ MRP expressions in RB. qRT-PCR analysis of the relative mRNA expression of *PRAME* and *MRP 1* gene in *PRAME* vector transfected Y79 (Retinoblastoma cell line) normalized with un-transfected Y79 cells.

8.2.7. Comparison of IC_{50} of chemotherapeutics in PRAME transfected vs un-transfected RB cells

By polynomial regression analysis, the IC_{50} of three anti-cancer drugs were computed in both PRAME transfected and un-transfected RB (Y79) cells. The IC_{50} of the carboplatin, vincristine, and etoposide in the transfected cells was 31.93µg/ml, 0.86µM/ml, and 4.13 µg/ml respectively. In un-transfected cells, the respective IC_{50} was 34.53 µg/ml, 0.97µM/ml, and 5.23µg/ml respectively. The transfected and un-transfected cells showed no significant change in the percentage of cell survival upon the three anti cancer drugs treatment groups (vincristine: p-value >0.05, and etoposide: p-value >0.05 and carboplatin: p-value >0.05).

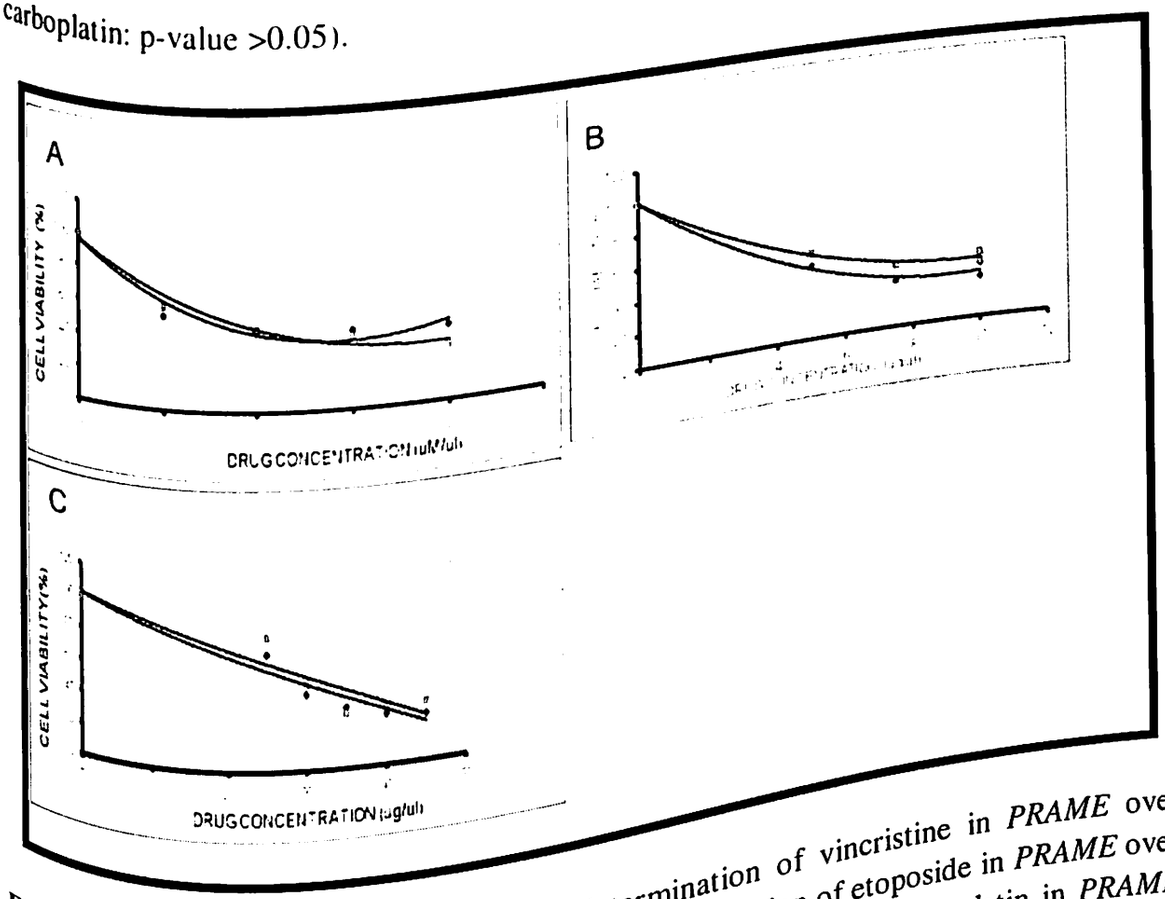

Figure 8.8: IC_{50} determination. A: IC_{50} determination of vincristine in *PRAME* over expressed and control RB (Y79) cells, B: IC_{50} determination of etoposide in *PRAME* over expressed and control RB (Y79) cells. C: IC_{50} determination of carboplatin in *PRAME* over expressed and control RB (Y79) cells.

8.3. Discussion

8.3.3. Drug resistance in tumor is a complex phenomenon

Tumors can be intrinsically resistant to chemotherapy (even before treatment), or some chemo-sensitive tumors turn resistant due to chemotherapy (acquired chemo resistance) (Kerbel et al. 1994, Longley and Johnston 2005). This reflects the existence of some multi-factorial components involving drug sensitivity, acceleration of drug efflux, activation or inactivation of drugs; modification in drug targets and DNA methylation which contribute to drug resistance property (Wilson T. R. et al. 2006b). In order to address the drug resistance challenge observed in the clinical management of RB, there is an urgent need to identify the responsible genes in order to aid the prognostic stratification. The microarray assay, being a high throughput screening technology was used here to understand the various gene alterations in post chemo RB.

The present study included the gene expression analysis of 2 RB tumor samples corresponding to two children who were subjected to 11 and 9 cycles of chemotherapy respectively (to represent the lack of chemo sensitivity), and one RB tumor sample of a child who was not subjected to pre-operative chemotherapy. These two experimental groups were compared with normal retinal gene expression to identify genes, which could play a role in drug resistance in RB. Genes with p value of ≤ 0.05 and log fold change of at least 2.0 and more for up-regulation and log fold change of 2.0 and below for down-regulation were considered for differential expression analysis.

8.3.4. Key regulatory genes in post chemotherapy RB tumors

After normalization with donor retina, we observed 1419 genes in common between pre-chemotherapy and post-chemotherapy RB tumor tissues. In addition, we observed about 413 differentially expressed genes specific to post chemotherapy RB tumors **[Figure 8.1C]**. By following a stringent criteria of statistical significance (p value ≤ 0.05, q value ≤ 0.05, z-score = >2) the biological pathway analysis revealed major cellular functions

namely apoptotic pathways, cell cycle check points, negative regulation of retinoic acid receptor signaling pathway, PLK1 signaling events, EGF/EGFR Signaling Pathway, Ras mediated pathway were dys-regulated and chosen for further analysis. These pathways were known to be regulating by about 239 genes (determined by using the gene ontology database). From this gene list, the BAN (Biological Analysis Network) was modeled by mapping the key pathways and intra molecular interaction data involving 75 genes was derived using cytoscape V 8.0 **[Figure 8.3.A and 8.3.B]**. **Table 8.2** gives the list of few dys-regulated genes significantly in the pre-chemotherapy and post- chemotherapy RB tumor tissues.

Earlier studies on differential gene expression between the normal retina and RB, and their canonical pathways, have implicated numerous genes as potential anti-cancer targets (Chakraborty et al. 2007, Ganguly and Shields 2010). Deregulation of PI3K/AKT/mTOR (insulin signaling) pathways has been reported (Chakraborty et al. 2007). However, at present, not much information is available on drug resistance genes in post-chemotherapy RB tumors using cDNA gene expression analysis. Here, we observed the de-regulation of the key genes involved in cell cycle: *CCNA1, CCNA2, CCNB1, CCNB2, CCND2, CCNE2, CDC25C, CDC6, CDC25A, CDC25C*; cell cycle regulators: *PLK1, PLK2, PLK4, PTEN*; pro-apoptosis: survivin (*BIRC5*), tumour suppressors: *BUB1*, oncogenes: *SYK, MYBL2, STMN1* and *KRAS*. **Figure 8.3A and 8.3B** (derived using cytoscape v 8.0) demonstrates the interacting nodes of all the above-mentioned genes in both non-chemo treated and chemo treated RB. Taken together, the activation of cell cycle and inhibition of apoptotic cell death may form the basis for the cancer cell survival in resistant RB.

8.3.5. Multidrug resistance genes in RB

Previous studies have shown the expression of various drug resistant proteins such as P-gp, MRP1 and LRP in RB primary tumors (Krishnakumar et al. 2004b). Reports indicate the expression of SRPK1 (a cisplatin-sensitivity-related protein), ABCG2 and MCM2 in RB chemo resistance (Krishnakumar et al. 2008, Mohan et al. 2006). In this context, various therapeutic approaches have been attempted by oncologists including the use of cyclosporine A (CSA), a drug resistance modulator in their chemotherapy protocols for

RB(Friedman D. L. et al. 2000). Among the up regulated genes in the present study, the genes with reported role in regulating drug resistance include *ABCC4* (Wilson M. W. et al. 2006a), spleen tyrosine kinase (*SYK*) (Zhang J. et al. 2012a), PRAME (Goellner et al. 2006) and *Ect2* (Srougi and Burridge 2011).

While *ABCC4* and *SYK* have reported implications in RB, there is no current evidence for the roles of *PRAME* and *Ect2* in RB. The *ABCC4* gene encodes for the protein which is a member of the super family of ATP-binding cassette (ABC) transporters. These ABC proteins transport various molecules across extra and intra cellular membranes. ABC genes are divided into three distinct sub families (*ABC1, MDR/TAP, MRP, ALD, OABP, GCN20* and *WHITE*) and this protein is a member of MRP family, which is involved, in multi-drug resistance. *ABCC4* gene expression in RB has been reported earlier (Wilson M. W. et al. 2009). The *SYK*, a proto-oncogene has been reported as one of the most up-regulated kinase gene by the integrative analysis in RB by Zhang et al (Zhang J. et al. 2012a). In their study, strong expression of *SYK* (100%) in RB primary tumors was reported. Further, the treatment of RB cell lines (Weri Rb 1 and RB 355) with *SYK* inhibitors (BAY 61-3606 or R406) had resulted in the caspase mediated cell death, suggesting that the *SYK* could be a target for chemotherapeutic interventions in RB management (Murphree and Triche 2012, Zhang J. et al. 2012a).

In the present study, response of *Ect2* and *PRAME* was validated by qRT-PCR in the primary RB tumors (n=9 post-chemotherapy and n=12 pre- chemotherapy) [**Figure 8.5**]. Surprisingly, there was no significant association of PRAME expression with chemotherapy status as observed in other childhood cancers such as leukemia (Goellner et al. 2006). In order to rule out any direct effect of PRAME in drug response, comparative IC_{50} studies were carried out. Here again, the IC_{50} in PRAME over-expressed (transfected) RB cells was not significantly different from non-transfected RB cells [**Figure8.8**]. Following this confirmation, we set out to explore the interactive pathways associated with PRAME in order to identify any other role of PRAME, as it was localized in the cell nucleus [**Figure 8.4**].

8.3.6. Association of Ect2 and chemotherapy

Briefly, Epithelial cell transforming sequence 2 (*Ect2*) functions as a guanine nucleotide exchange factor (*GEF*) 3 for Rho family (*RhoA, Rac1, and Cdc42*) regulating the cytokinesis (Hara et al. 2006, Niiya et al. 2006, Niiya et al. 2005, Tatsumoto et al. 1999). In normal cells, Ect2 is inactive and it is activated during mitosis and cytokinesis by the presence of N-terminal regulatory domain that modulates its functional activity (Cook et al. 2011, Justilien et al. 2011, Kim J. E. et al. 2005, Niiya et al. 2006). Recent reports showed the over expression of Ect2 among several human tumors and their differential role in cellular transformation and cytokinesis (Salhia et al. 2008, Sano et al. 2006). In the current study, we observed an up-regulation of Ect2 in the chemo-treated RB. Further, on validation of *Ect2* expression, the study revealed 42.87% *Ect2* expression in 9/21 RB tumor samples. There are reports that indicate the activation of *Ect2* by genotoxic stress in other cancer types. Srougi et al (Srougi and Burridge 2011) have reported the increase in Rho B activity along with *Ect2* after genotoxic stress in breast cancer cell lines, which have resulted in cell death. Further, Srougi et al (Srougi and Burridge 2011) have also reported that despite the presence of genotoxic stress, when there is loss of *Ect2* expression along with reduced Rho B activity, there is a reduction in apoptosis. This confirms the pivotal role of *Ect2* in accelerating the cell death after cellular stress (induced by therapy). So the existence of higher expression of *Ect2* (77%) in the RB tumor tissues (n=9 post chemo treated) suggests the activation of *Ect2* in these tumors, which may contribute to the chemotherapy, induced cell death. In contrast, the pre-chemotherapy RB tumor tissue revealed *Ect2* over expression in 2 out of 12 tumors only (16.66%) as shown in **[Figure 8.6]**. Thus, these results prompt further study of *Ect2*'s role in mediating chemo sensitivity in RB.

8.3.7. PRAME expression and RB

PRAME (Preferentially expressed Antigen in Melanoma) was first detected as a tumor antigen in cells isolated from melanoma. High PRAME expression has been detected in 88–95% of primary melanomas (Ikeda et al. 1997). Previous studies have reported *PRAME* gene expression and its role in drug resistance in various tumors such as non

small cell cancer (Bankovic et al. 2010), breast cancer (Epping et al. 2008), leukemia (Goellner et al. 2006). and melanoma (Ikeda et al. 1997), but its role in RB was not known. In the present study, *PRAME* gene was found to be up regulated in the RB tumor samples (pre-chemotherapy and post-chemotherapy RB tumor tissues) as revealed by microarray and qRT- PCR analysis. Immunohistochemistry revealed PRAME protein over expression that was variable / heterogeneous in the primary tumor samples between the chemo-treated and non-chemo treated groups. The expression of PRAME has been reported to be low or absent in normal tissues (Szczepanski et al. 2013). We also observed lack of PRAME expression in normal cadaveric retina **[Figure 8.4D]**. No significant association of PRAME protein expression with respect to tumor invasion and chemotherapy status was observed.

Wilson et al. (Wilson M. W. et al. 2009) showed 50% expression of MRP1 in RB sample. *MRP1* is one of the MDR related genes. The present study revealed no significant correlation between PRAME and MRP1 expression **[Figure 8.7]**. To clearly define the role (if any) of PRAME in drug resistance, we determined IC_{50} of vincristine, etoposide and carboplatin, in RB cells over-expressed with *PRAME* gene. There was no marked change in the IC_{50} values in the PRAME over expressed versus control RB cells (Y79), suggesting that PRAME does not have a direct role in drug resistance in RB. However nuclear localization of the PRAME protein suggests that they could act as a transcription factor. To evaluate this, BAN analysis was performed as discussed below.

8.3.8. Network regulation of *PRAME* involving *MYBL2* gene

8.3.8.1. Interaction of MYBL2 with RB1, and NCOR1

The biological process clustering **[Figure 8.3. A and B]** revealed that there exists a binding interaction between the *PRAME, PRAME* family with *NCoR1* (Nuclear Receptor Co-Repressor 1). The level of *NCoR1* expression was increased in the post-chemotherapy RB compared to the pre-chemotherapy RB. The translocation of *NCoR1* from nucleus to cytoplasm resulted in the transcriptional repression of its target genes in RB and human retinal progenitor cells (hRPCs) was discussed earlier by Nazha et al (Nazha et al. 2013). Its role in cellular differentiation and tumorigenesis has been deciphered in few of the

earlier studies (Nazha et al. 2013);(Jepsen et al. 2000). Earlier studies have reported the co-repressor interaction between *MYBL2* (B-Myb) and *N-CoR1*.

In the present study, we could observe the down-regulation of *MYBL2* which may have resulted due to the activation of *N-CoR1* in the chemo treated RB (Li X. and McDonnell 2002). Interestingly, we could observe the activation of RB1 in the absence / low levels of *MYBL2* in the post- chemotherapy RB tumor tissues. In this linearity, the suppression of *MYBL2* with activation of RB1 could be one of the molecular targets to be established. Our results corroborate with an earlier study on the *MYBL2* inhibition contributing it as an important adjuvant to treatment of human hepato cellular carcinoma (Calvisi et al. 2011). Further studies on these molecules *NCoR1*, *MYBL2* and *RB1* could explain their role at cellular level and its interaction with each other molecules contributing to RB tumorigenesis. Network analysis **[Figure 8.3. A and B]** also reveals a signaling interlinking between *MYBL2* and *JAK /STAT (JAK1, JAK2, STAT1 and STAT3). STAT1* and *3* are known for their dual role in tumorigenesis (Sara Pensa 2009).

8.3.8.2. *Signaling interaction between PRAME family and EZH2 in retinoic acid receptors mediated pathway*

EZH2 is known to be over expressed in various cancers such as prostrate and breast and for its interaction with *PRAME* and *TRAIL* enhancing the imatinib sensibility in CML (De Carvalho et al. 2011). The silencing of *EZH2* in uveal melanoma had resulted in the arrest of cell migration and invasion (Chen X. et al. 2013). In the current study, we observed the down regulation of *EZH2*, which acts as a key signaling regulator of *PRAME* and *PRAME* family **[Figure 8.3 – A and B]**. So the down-regulation of *EZH2* and *PRAME* family but not of *PRAME* in the post-chemotherapy RB tumor tissues strongly point towards further research on the role of *PRAME* in sensitizing the RB cells to chemotherapy.

8.4. Conclusion

Differential gene analysis between post-chemo and pre chemo treated RB tumors revealed several anti-apoptotic and pro-cell survival gene expressions. The expressions of key genes namely *MYBL2, NCoR1, STAMN, CHD9, CRY2, RHOC, STAT1/STAT3* in the post-chemotherapy RB tissues are reported. These results would widen the area of research in these gene regulations contributing either to chemo resistance or to RB tumorigenesis. Further, the positive correlation between Ect2 and drug response modulation in RB reported here offers potential for further explorations at the molecular level. The over-expressed *PRAME* does not directly influence response of RB tumors to chemotherapy, which is substantiated by the lack of marked up-regulation of *MRP1* in *PRAME* over-expressed RB cell line, and also by the lack of a substantial change in IC_{50} doses of standard chemotherapeutic drugs. The nuclear localization of over-expressed PRAME protein possibly implicates its role in gene regulation. The network analysis performed here presents some evidence for the regulatory role of *PRAME* in RB.

CHAPTER 9: DELINEATION OF DYSREGULATED MIRNAS BETWEEN MONOSOMY 3 AND DISOMY 3 AND THEIR CLINICAL CORRELATION WITH UVEAL MELANOMA

9. Introduction

Uveal Melanoma (UM also referred to as choroidal melanoma), primary intraocular neoplasm of adults that arise from choroidal melanocytes and represents about 5% of all types of melanomas (Woll et al. 1999). UM has been observed with 3 fold higher incidences in white races compared to dark pigmented races and is rare in Indian populations (1998b, Biswas et al. 2004, Kuo et al. 1982, Manohar et al. 1991, Margo C. E. and McLean 1984). The incidence of UM is 0.02% in Indian population (Dhupper et al. 2012, Le Thi Huong et al. 1991).

Improvements in diagnostics and therapeutics have resulted in better eye preservations (1990, Augsburger et al. 1990, Finger 1997), however, the median survival rate of UM Patients remains alarmingly high (Kujala et al. 2003, Singh and Topham 2003a). Early metastasis could be the possible underlying mechanism irrespective of tumor size (Callejo et al. 2007). Liver metastasis occurs in approximately 40-50% of melanoma patients within the period of 10 years from the onset of primary disease with median survival rate of 2-7 months, and less than a year in 10% (2001, Shields et al: 1991b). Genetically uveal melanoma tumours varies from cutaneous type with respect to the aberrations in chromosomes 1, 3, 8 (Singh et al. 2012) and varied expressions of heat shock protein 27 (HSP27) (Jmor et al. 2012) as these factors are considered as valuable prognostic indicators in UM.

Recent research in UM focuses on the identification of the prognostic factors to pre-determine hepatic metastasis at the earliest for better management of the disease. Initially these prognostic factors include clinical parameters (such as tumour size, location),

histopathological parameters (cell types, Tumor Infiltrating Lymphocytes (TIL, vascular patterns and nuclear grade) extra-ocular extension, immune-markers (HSP27, nm23, IGFR1), and chromosomal aberrations (loss of chromosome 3,1p, 6q, 13q, 8p, gain chromosome1q, 6, 8q, 16p) and gene expression profiles (Aalto et al. 2001),(Biswas et al. 2004). Here, in this chapter, we have categorised UM as monosomy 3 and disomy 3 based on the chromosome 3 abberrations. Further, the classified group of UM has been considered for the miRNA/mRNA expression studies detailed in the next chapter 10.

9.1. Materials and Methods

9.1.3. Sample Collection

Formalin – fixed paraffin embedded (FFPE) tissue samples (n=86) were utilized for the study. Enucleated eyeballs received at L&T Ocular Pathology Laboratory, Medical Research foundation, Sankara Nethralaya, during the year 2009 – 2013 were processed and included in the study. Duly signed consent forms from the patient/guardian as a part of clinical management was obtained from enrolled patients who were treated in Mahavir vitreo-retina department. Normal melanocytes (n=5) were collected from the human cadaveric eyeballs received at CU Shah Eye bank (http://www.sankaranethralaya.org/eye-bank.html) during 2011-2012, Medical Research Foundation, Sankara Nethralaya. The study was reviewed and approved by the local ethics committee at Vision Research Foundation, and the committee deemed that it conformed to the generally accepted principles of research, in accordance with the Helsinki Declaration.

9.1.4. Specimen Selection

9.1.4.1. Clinico-pathological Features

Study cohort includes 58 male and 28 female with the median age of 48.5. The study group consists of 12 patients diagnosed with ciliary body involvement and 74 with choroidal melanoma. Mean of largest tumor diameter (LTD) was 13.7mm X 9.6mm. Haematoxylin and Eosin slides were reviewed and 1-2 representative tumor tissue blocks

9.1.6.1. *Evaluation of the immunostain*

The slides were examined by 2 observers using conventional light microscopy. The levels of immuno-reactivity and the cell types that exhibited HSP 27 immuno-reactivity was recorded for each slide. Ten tumor fields on each tumor section were randomly scanned and the average percentage positivity (0% to 100%) of the tumor cells was calculated. The percentage of positivity were scored based on the percentage of the positive cells and the intensity of the positivity as reported earlier (Jmor et al. 2012) and indicated in detail under the section 4.4.1. Thus immune-score ranges from 0-12.

9.1.7. Statistical analysis

Pearson's correlation and chi-square test was used to derive the association between monosomy 3 group, HSP 27 expression and clinico-pathological features of UM tumours.

9.2. Results

9.2.3. Grouping of monosomy and disomy in uveal melanoma tumours

9.2.3.1. *Insitu Hybridisation*

CISH was performed to group the tumors based on the level of alterations in chromosome 3. Partial deletion of chromosome 3 (monosomy) was detected in 60.46% (52/86), and the presence of both the copies of chromosome 3 (disomy) was detected in 39.53% (34/86) of melanoma tumors (n=86). Among metastasis group (n=17), monosomy 3 was detected in 52.94% (9/17) and disomy was detected in 47.06% (8/17) [**Figure 9**].

9.2.3.2. *Immunohistochemistry*

Among the monosomy 3 tumors (n=52), moderate to high percentage of HSP 27 was detected in 19.23% of samples (10/52), negative to low percentage of HSP 27 was detected in 80.76% of Monosomy 3 tumors (42/52). Among the disomy 3 tumors (n=34), moderate to high percentage of HSP 27 was detected in 73.52 % of samples (25/34), low

percentage of HSP 27 was detected in 26.47% of disomy 3 tumors (9/34). The photomicrographs [**Figure 9.2.A-E**] reveal the cytoplasmic positivity of HSP27 in the uveal melanoma tumors and in the positive control - breast cancer cell line (MCF-7).

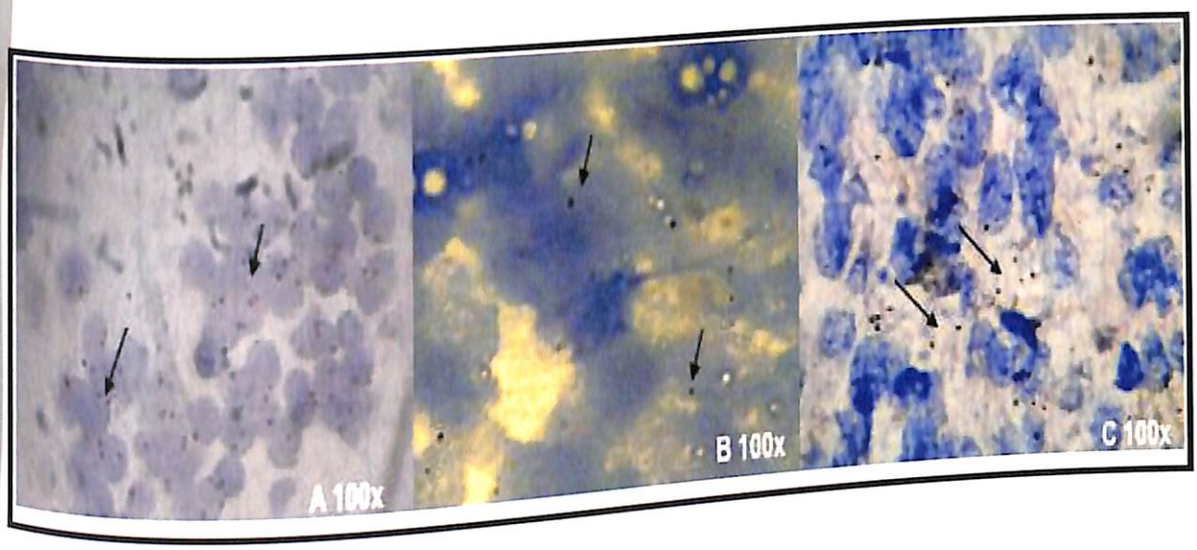

Figure 9.1: Insitu hybridization. Photomicrographs of chromosomal aberrations (Chromosome 3) by chromogenic insitu hybridization (CISH). A: Normal retina with disomy 18 (control). B: Uveal melanoma tumour with partial deletion / monosomy 3, C: Uveal melanoma tumour with disomy 3. The arrow heads indicates the hybridized spots

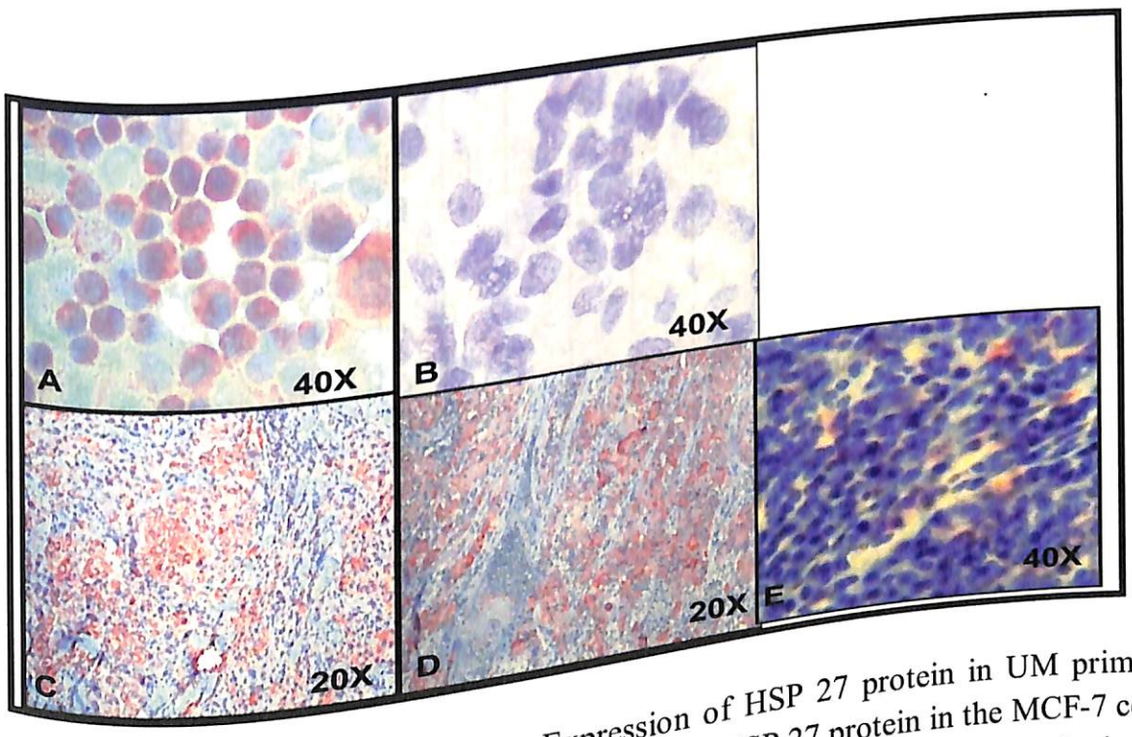

Figure 9.2: HSP 27 protein expression. Expression of HSP 27 protein in UM primary tumor samples: A: Positive control: High expression of HSP 27 protein in the MCF-7 cells (Breast carcinoma cell line). B: Negative control (performed by the exclusion of primary antibody) Absence of HSP 27 protein in the MCF-7 cells (Breast carcinoma cell line). C & D: High to Moderate expression of HSP 27 in the disomy 3 melanoma tumors. E: Low to Negative expression of HSP 27 in the monosomy 3 melanoma tumors.

Table 9.1: *Chromosomal 3 abberration / HSP27 expression in UM. Clinico-pathological descriptions, results of the In-situ hybridization and HSP 27 expressions for uveal melanoma tumor tissues.*

Patient ID	Age/ sex	Ciliay body	Tumor Base (mm)	Tumor thickness (mm)	Specimen	Cell type	Chromosomal adderation (CISH)	Hsp 27 expression (IHC)		
								Positivity	Intensity	Immuno-score
M1	36/F	NO	16.5	14	OS:EB	M	M	2	2	4
M2	57/M	NO	9	9.5	OD:EB	M	D	2	2	4
M3	36/F	NO	10	11	OD:EB	M	D	1	1	1
M4	73/M	NO	11.5	17	OD:EB	M	D	2	1	2
M5	47/M	NO	14	9	OS:EB	S	D	3	3	9
M6	48/F	NO	13.5	13.5	OS:EB	E	M	1	1	1
M7	57/M	NO	13.4	14.9	OD:EB	S	M	1	1	1
M8	48/F	NO	12.1	9.5	OS:EB	M	M	4	3	12
M9	51/M	YES	1	2	OD:EB	S	D	2	2	4
M10	65/M	NO	5.5	11.5	OS:EB	E	M	3	3	9
M11	21/M	NO	155	15	OS:orbit	E	M	3	3	9
M12	54/M	YES	9	9.5	OS:EB	S	D	3	3	9
M13	38/M	NO	14.5	13.5	OD:EB	S	M	1	1	1
M14	61/M	YES	10	10	OS:EB	M	M	1	1	1
M15	46/M	NO	10.5	12.9	OS:EB	M	D	2	1	2
M16	60/F	NO	12	9	OD:EB	M	M	0	0	0

M17	*43/F*	*NO*	*7*	*4*	*OD:EB*	*S*	*M*	*1*	*1*	*1*
M18	*17/M*	*NO*	*15*	*15*	*OS:EB*	*M*	*D*	*1*	*1*	*1*
M19	*63/M*	*NO*	*9*	*8.5*	*OD:EB*	M	D	2	2	4
M20	35/F	NO	7	8	OS:EB	M	D	1	1	1
M21	46/M	NO	11.5	15	OD:EB	M	D	2	2	4
M22	32/F	YES	20	11.5	OS:EB	M	M	1	0	0
M23	60/M	NO	11.5	7	OD:EB	M	M	1	1	1
M24	62/F	NO	13	4	OD:EB	E	D	3	3	9
M25	50/M	NO	10	8	OD:EB	S	M	3	3	9
M26	23/F	NO	14	9	OD:EB	S	D	3	3	9
M27	58/M	NO	9	9.5	OD : Ex	M	D	3	3	9
M28	36/M	NO	16.5	15	OD:EB	E	M	4	3	12
M29	51/M	NO	9.5	14	OD:EB	M	M	1	1	1
M30	58/M	NO	7	7	OS:EB	M	D	4	3	12
M31	65/F	NO	6	10	OS:EB	M	M	1	1	1
M32	70/M	NO	20	12	OS:EB	M	D	1	1	1
M33	43/M	NO	5	8	OD:EB	M	D	3	3	9
M34	53/F	NO	12	10	OD:EB	S	M	4	3	12
M35	37/F	NO	12	8	OS:EB	S	D	1	1	1
M36	33/M	NO	12	7	OS:EB	S	D	2	2	4

M38	*76/M*	*YES*	*12*	*10*	*OS:EB*	*E*	*M*		2	0
M39	*46/F*	*NO*	*7*	*4*	OD:EB	S	D	2	2	4
M40	63/M	NO	14	16	OD:EB	M	D	2	2	4
M41	45/F	NO	20	20	OS:EB	M	D	2	2	4
M42	41/F	NO	16.5	12	OS:EB	S	M	1	1	1
M43	21/M	NO	12	7	OS:EB	S	M	3	3	9
M44	56/M	YES	14.5	3.5	OS:EB	S	D	3	3	9
M45	30/M	NO	5.5	11	OS:EB	S	M	3	3	9
M46	38/M	NO	15	1	OS: Ex	E	M	0	0	0
M47	56/F	NO	15	1	OS: Ex	M	M	1	1	1
M48	34/M	NO	15	1	OS: Ex	E	M	2	1	2
M49	55/M	NO	5	12	OD:EB	E	D	3	2	6
M50	48/M	NO	15	1	OD:orbit	E	M	2	1	2
M51	28/M	NO	15	17	OS:EB	E	M	2	2	4
M52	32/M	NO	10	0.1	OS:Ex	E	D	2	3	6
M53	26/M	NO	14	10	OD:EB	S	M	1	1	1
M54	37/F	NO	9	9.5	OS:EB	M	M	2	2	4
M55	74/M	YES	15	12	OD:EB	M	M	2	2	4
M56	34/M	NO	15	7	OD:Ex	M	M	1	2	2

M57	58/F	NO	12.5	8	OD:EB	S	M	1	2	2
M58	28/M	NO	11	20	OS:EB	E	M	1	1	1
M59	68/M	NO	17	14	OS:EB	S	M	2	2	4
M60	54/M	NO	10	7	OD:Ex	E	M	2	2	4
M61	35/F	NO	15	7	OD:orbit	M	M	3	3	9
M62	70/M	NO	12	7	OS:EB	M	M	2	2	4
M63	44/F	NO	14	13	OS:EB	S	M	3	3	9
M64	43/M	NO	15	7	OS;Ex	M	M	1	1	1
M65	34/M	NO	9	9.5	OD:orbit	E	D	1	1	1
M66	55/F	YES	9	8	OS:EB	S	M	3	2	6
M67	62/M	NO	11	7	OD:EB	M	D	2	2	4
M68	52/M	NO	6	5	OD:EB	S	M	3	2	6
M69	62/M	NO	15	10	OS:EB	M	M	1	1	1
M70	49/F	NO	7	4	OD:EB	M	M	1	1	1
M71	48/M	NO	15	8	OS:EB	S	D	3	3	9
M72	74/M	NO	10	12	OS:EB	M	M	1	1	1
M73	49/F	YES	17	19	OS:EB	M	M	1	1	1
M74	2/F	NO	10.0 , 20.0	5.0 , 10.0	OS:EB	M	M	2	2	4
M75	36/F	NO	14	11.5	OS:EB	M	D	3	3	9
M76	60/M	NO	11.5	15	OS:EB	S	M	0	0	0

M77	*40/F*	*NO*	*10*	*9*	*OS:EB*	*S*	*M*	*0*	*0*	*0*
M78	*65/M*	*NO*	*11*	*8*	*OS:EB*	*E*	*M*	*1*	*1*	*1*
M79	*63/F*	*NO*	*15*	*10*	OS:EB	M	D	2	1	2
M80	52/M	NO	12	8	OD:EB	M	M	2	1	2
M81	21/M	NO	9	9.5	OS:Orbit	E	D	4	3	12
M82	54/M	YES	16	10	OS:EB	M	D	3	2	6
M83	60/M	NO	9.5	4	OD:EB	M	D	3	2	6
M84	51/M	NO	15	7	OD:EB	E	M	1	1	1
M85	54/M	YES	9	9.5	OS:EB	S	D	3	3	9
M86	38/M	NO	14.5	13.5	OD:EB	S	M	1	1	1

M: Male; F:Female, OS: Left eye, OD: Right eye, EB: Eneucleated eyeball; Ex: Exenterated tissue.

M77	*40/F*	*NO*	*10*	*9*	*OS:EB*	*S*	*M*	*0*	*0*	*0*
M78	*65/M*	*NO*	*11*	*8*	*OS:EB*	*E*	*M*	*1*	*1*	*1*
M79	*63/F*	*NO*	*15*	*10*	OS:EB	M	D	2	1	2
M80	52/M	NO	12	8	OD:EB	M	M	2	1	2
M81	21/M	NO	9	9.5	OS:Orbit	E	D	4	3	12
M82	54/M	YES	16	10	OS:EB	M	D	3	2	6
M83	60/M	NO	9.5	4	OD:EB	M	D	3	2	6
M84	51/M	NO	15	7	OD:EB	E	M	1	1	1
M85	54/M	YES	9	9.5	OS:EB	S	D	3	3	9
M86	38/M	NO	14.5	13.5	OD:EB	S	M	1	1	1

M: Male; F:Female, OS: Left eye, OD: Right eye, EB: Eneucleated eyeball; Ex: Exenterated tissue.

9.2.3.3. *Association of monosomy 3/ disomy3 with the clinico-pathological factors and HSP 27 expression*

A significant association (p value=0.021) was observed between HSP 27 expression and monosomy 3 in uveal melanomas. This result corroborates with the study published by Jmor et al, 2010, where significant association of monosomy 3 to tumor base (p=0.002) was observed. **Table 9** gives the clinico-pathological description of the tumors, in-situ hybridization scores, immunostaining scores of HSP 27 expression for the individual melanoma tumors. Statistical analysis performed between the clinico-pathological parameters and monosomy 3 / disomy 3 has been tabulated (**Table 9.1**).

Table 9.2: Association of liver metastasis with clinico-pathological features. Correlation analysis of liver metastasis with clinico pathological parameters in UM patients under study

Clinico pathological parameters	p-value
Chromosome 3 aberration	0.282
HSP27	0.90
Age	0.166
Sex	0.532
Ciliarybody involvement	0.185
Tumor base	0.70
Tumour width	0.111
Cell type	0.165

Table 9.3: Association of Chromosome 3 aberration with clinico-pathological features. Correlation analysis of Chromosome 3 aberration with clinico pathological parameters in UM patients under study.

Clinico pathological parameters	p-value
(Independent-t –test)	0.021
HSP27	0.17
Age	0.39
Sex	0.64
Ciliarybody involvement	0.002
Tumor base	0.73
Tumour width	0.94
Cell type	0.03
Metastais	

9.3. Discussion

Uveal melanoma usually occurs in elderly men (Egan et al. 1988), rare in children/teenagers and less predominant in women. The pre-existing benign nevi, oculo-dermal melanocytosis and congenital melanosis occuli may result in malignant melanoma (Carreno et al. 2012). According to Collaborative Ocular Melanoma study group (COMS, 2001), about 50% of uveal melanoma harbouring patients result in metastasis within 10-15 years of enucleation.

Earlier diagnosis of UM and prediction of hepatic lesions has significant consequences in planning the therapeutic regimes and prognostic determinations (Field and Harbour 2014, Harbour and Chen 2013, Onken et al. 2012). At present, the diagnosis of UM is purely based on the clinical observation and histopathological evaluation of eye tissues. Among these observations, a few of the best indicators studied earlier to predict the metastasis is cell type (especially epitheliod cell type), largest tumor diameter, scleral extension and chromosomal aberrations. However, intra-tumoral heterogeneity existing in UM and the accuracy of methods used to determine the cytogenetic abnormalities together have proven difficulty in early predictions of hepatic lesions. This in turn has limited them to be used for diagnostic purpose. In the present study, among 86 UMs, we observed about 60.46% of monosomy 3 tumours and among 17 liver metastasis UMs, 50.96% are of monosomy 3 tumours [**Figure 9.1**]. In addition, a significant association of monosomy 3 with that of tumor base and scleral extension was observed. However, 47.06% of disomy 3 was observed among the liver metastasis group of UMs. This indicates the reduced sensitivity of CISH to determine the metastasis. Further, these results indicate the need of more precise methods for determining the high risk group of tumours at the earliest.

9.4. Conclusion

This study has aided to classify the UM tumors as monosomy 3 and disomy 3. A significant association of the monosmy 3 tumours with Hsp 27 protein expression, tumor base and with the scleral extension indicates the aggressiveness of monosomy 3 tumours. Thus, the current classification of tumors has been considered as the basis to predict the miRNAs associated with monosomy 3 tumours in the following chapter 10.

CHAPTER 10: MOLECULAR DEREGULATION IN UM: MIRNA AND GENE EXPRESSION ANALYSIS

10. Introduction

#Currently, clinicians are able to differentiate the patients with higher risk of choroidal, ciliary body melanoma through molecular signatures specific to the tumor types that has a strong tendency to metastasize (Singh et al. 2004). Earlier studies on UM, stated the strong association of monosomy 3 with liver metastasis (Radhakrishnan et al. 2009). Earlier study by Worley, et al, (2007) stated the molecular classification of UM tumors (Class 1: low risk and Class 2: High risk tumors) using microarray gene expression profiling (Worley et al. 2007). This study also reported the sensitivity and the specificity of gene expression profiling as 84.6% and 92.9%, respectively, compared to monosomy detection by an array comparative genomic hybridization (aCGH) (58.3% and 85.7%, respectively) and fluorescence in situ hybridization (FISH) (50.0% and 72.7%, respectively). The study concluded gene expression profiling as superior tool than other prognostic indicators. However, the data inconsistency and micro-deletion of genes observed in the tumours could contribute in misdiagnosis of the disease state.

Current knowledge on miRNAs role in UM carcinogenesis is limited. A few earlier reports discuss the miRNA profiles in the primary uncultured melanoma cells and melanoma cell lines normalized to non-cancerous cells (Worley et al. 2008, Yang C. and Wei 2011). Worley, et al, (2008) has reported 6 miRNAs discriminating the two classes (class1 and 2) of UM (Worley et al. 2008). Our study deviates from these reports, as it reveals the

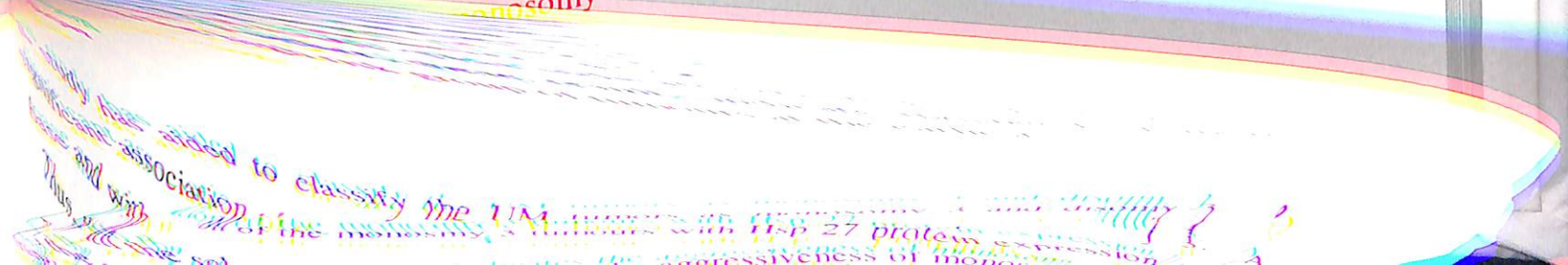

CHAPTER 10: MOLECULAR DEREGULATION IN UM: MIRNA AND GENE EXPRESSION ANALYSIS

10. Introduction

#Currently, clinicians are able to differentiate the patients with higher risk of choroidal, ciliary body melanoma through molecular signatures specific to the tumor types that has a strong tendency to metastasize (Singh et al. 2004). Earlier studies on UM, stated the strong association of monosomy 3 with liver metastasis (Radhakrishnan et al. 2009). Earlier study by Worley, et al, (2007) stated the molecular classification of UM tumors (Class 1: low risk and Class 2: High risk tumors) using microarray gene expression profiling (Worley et al. 2007). This study also reported the sensitivity and the specificity of gene expression profiling as 84.6% and 92.9%, respectively, compared to monosomy detection by an array comparative genomic hybridization (aCGH) (58.3% and 85.7%, respectively) and fluorescence in situ hybridization (FISH) (50.0% and 72.7%, respectively). The study concluded gene expression profiling as superior tool than other prognostic indicators. However, the data inconsistency and micro-deletion of genes observed in the tumours could contribute in misdiagnosis of the disease state.

Current knowledge on miRNAs role in UM carcinogenesis is limited. A few earlier reports discuss the miRNA profiles in the primary uncultured melanoma cells and melanoma cell lines normalized to non-cancerous cells (Worley et al. 2008, Yang C. and Wei 2011). Worley, et al, (2008) has reported 6 miRNAs discriminating the two classes (class1 and 2) of UM (Worley et al. 2008). Our study deviates from these reports, as it reveals the miRNAs associated with monosomy 3 from the FFPE blocks. FFPE samples are also

Since the stability of the *RNU48* was better than *RNU6B, RNU48* miRNA was used as an endogenous control to normalize differences in total RNA levels in each sample. Commercial software (SDS version 1.3; ABI) was used to calculate $^{\Delta\Delta Ct}$ (Livak and Schmittgen 2001). The relative amount of each miRNA to *RNU48* miRNA was expressed using equation 2^{-DDCt}, where DDCt = (Ct (miRNA) - Ct (RNU48)). The value of each control sample was set at 1 and was used to calculate the fold change in target genes and up regulation of miRNA expression was calculated based on the $\log_2$ transformed ratio of fold change.

10.1.4. miRNA profiling

10.1.4.1. Specimen Processing and miRNA extraction for qRT-PCR

Five to eight sections of 20 µm thickness were used for the miRNA profiling. Total RNA was isolated from formalin-tumor tissues using Recover All ™ total nucleic acid isolation (Ambion, Life technologies, USA) as per the manufacture's protocol. The quality and the quantity of the total RNA was assessed spectrometrically using Nano Drop spectrophotometer (ND 1000, Thermo scientific, USA).

10.1.5. Microarray profiling of the formalin fixed tumor tissues of Monosomy 3 and Disomy 3

Three tumours harbouring monosomy 3 and three tumours with disomy 3 were taken for expression studies using Human miRNA V3, 8x15k Agilent arrays. The study was carried out using biological and technical triplicates.

10.1.5.1. Protocol for miRNA profiling

The small RNA was extracted from the formalin fixed tissues using miRVANA kit (Ambion, Life Technologies, USA) following protocol indicated in the section 4.9 using Human_miRNA_version 3,8x15k array. The microarray slide was scanned using Agilent Scanner (Agilent Technologies, Part Number G2565CA).

10.1.6. Statistical analysis

10.1.6.1. qRT- PCR data analysis

Cut off used for up and down-regulation: Greater than 1(log_2 ratio) as positive expression and less than - 0.5(log_2 ratio) as negative. Independent student't' test was performed to calculate the statistical significance between the miRNAs expression and the cilinico-pathological parameters. ANOVA was used to derive the significance between the miRNA association with tumour base and width. Kaplen-Meier test was used to assess the rate of survival in the presence of the respective miRNAs.

10.1.6.2. Microarray data

Cut off used for up and down-regulation: Greater than 1(log_2 transformed value) in Monosomy 3 detected tumors and less than 1(log_2 transformed value) in chromosome 3 balanced tumors and vice versa.

Unsupervised analysis: The outliers identified by the Principal Component Analysis (PCA) were eliminated from further analysis. Target sites were predicted using – miRANDA algorithm. ANOVA was used to identify the highly expressed miRNA in the monosomy 3 tumors compared with disomy 3 tumors.

Supervised analysis: Significance Analysis of Microarray (SAM) was performed to derive the significant miRNAs that are differentially expressed between the monosomy and disomy groups. The false discovery rate (FDR) of Q= 0.78 was set as the threshold for the predicting the miRNAs that are associated with monosomy-3 group of tumors. The list of miRNAs with the Q= 0.0 is considered for the further validation.

10.2. Results

10.2.3. Quantitative analysis of miRNAs in UM

Based on the earlier reports on uveal melanoma and in other cancers, eight miRNAs namely *miR-214, miR-149*, miR-143, miR146b, miR-199a* and *let7b, hsa-miR-1238* and *hsa-miR-134* were selected to analyse the expressions and its association with monosomy 3 and disomy 3 of UM (Balaguer et al. 2011, Liu C. J. et al. 2014, Worley et al. 2008).

10.2.1.1 Expression of miRNAs in monosomy 3 group of tumors

In the present cohort of monosomy 3 tumors, the mean fold change in the select miRNAs were as follows: *miR-134: 2.63; miR-1238: 9.31; miR-214: 1.69; miR-149*: 5.75; miR-143: 0.24; miR146b: 1.99; miR-199a: 8.11 and let7b: -2.33* (**Table 10.1, Figure 10.1**). The miRNA expressions are derived after normalizing with the mean expression of normal melanocytes (n=5). Upon validation, the expression of *miR-134, miR-214, miR-143, miR-146b and miR-199a* showed a significant association with the groups of chromosome 3 loss. Among monosomy 3 group with metastasis, higher expressions of *miR-134* [100% (9/9)], *miR-1238* [100% (9/9)], *miR-199a* [88.88% (8/9)], *miR-214* [77.77% (7/9), *miR-149** [77.77% (7/9)] and *miR-146b* [66.66% (6/9)] was observed. Moderate to negative expressions miR-143* [44.44% (4/9)] and let-7b was observed.

Table 10.1: *Clinico-pathological features of UM. Clinico-pathological descriptions of the tumors with Mean and median fold change of individual miRNAs; statistical significance (p-value) derived between the clinico-pathological parameters and mean fold change of miRNAs expression.*

Clinico-pathological parameter	No. of samples	miR-214			miR-let 7b			miR-149*			miR-143*		
		Median RQ (IQR)	Mean RQ (S.D)	P-value	Median RQ (IQR)	Mean RQ (s.d.)	P-value	Median RQ (IQR)	Mean RQ (s.d.)	P-value	Median RQ (IQR)	Mean RQ (s.d.)	P-value
Gender Male	58	1.21(5.28)	0.94(4.38)	0.63	2.32(5.75)	-3.04(4.50)	0.67	4.62(6.16)	4.91(6.18)	0.25	-0.80(7.30)	-1.27(6.06)	0.80
Female	27	0.60(6.68)	0.48 (3.61)		-2.27(7.85)	-2.57 (5.40)		4.81(10.34)	6.60 (6.48)		-0.22(6.44)	0.91(6.03)	
Chromosome 3 aberration													
Monosomy	52	1.97(5.15)	1.69(3.46)	0.01	-2.46(5.56)	-2.33(4.47)	0.21	5.08(6.11)	5.75(6.69)	0.52	0.377(5.91)	-0.24(5.93)	0.009
Disomy	34	-0.07(4.75)	-0.54(4.7)		-1.80(7.21)	-3.64(5.15)		4.13(5.81)	4.86(5.60)		-2.64(9.71)	-3.18(5.59)	
CB Yes	12	2.06(3.11)	0.96(2.40)	0.88	-132(5.36)	-1.79(3.70)	0.40	4.79(6.23)	4.423(7.51)	0.56	0.08(7.40)	-0.66(4.13)	0.78
No	74	1.11(6.08)	0.78(4.34)		-2.78(6.05)	-0.30(4.91)		4.69(6.11)	5.565(6.08)		-0.54(7.44)	-1.179 (6.28)	
Tumour base (mm) <5mm	3	0.93(0)	1.13(1.46)	0.55	-1.40(0)	-1.40(0.42)	0.92	3.97(0)	4.19(3.0)	0.78	0.60(0)	0.12(3.81)	0.85
6-8mm	7	1.18(6.91)	0.89(5.27)		-2.27(7.85)	-3.11(4.53)		1.32(14.3)	3.18(9.3)		-0.22(2.95)	-0.36(2.60)	
9-12mm	34	0.11(3.75)	0.03(4.35)		-2.83(6.35)	-3.14(4.48)		5.20(6.75)	7.97(6.63)		0.74(10.44)	-0.67(8.10)	
>12mm	42	1.81(6.5)	1.40(3.85)		-2.47(6.99)	-2.68(5.25)		4.72(5.15)	5.65(5.63)		-.83(6.38)	-1.67(4.42)	
Tumour width (mm) <5mm	12	2.30(6.80)	1.27(5.01)	0.77	-3.17(7.22)	3.68(4.96)	0.50	1.74(6.43)	1.22(5.02)	0.01	-0.26(4.61	-0.87(4.63)	0.84
6-8mm	21	1.95(5.79)	1.49(3.26)		-2.27(6.35)	-3.23(4.60)		6.67(11.22)	7.90(7.70)		-2.02(8.87)	-1.28(8.78)	
9-12mm	32	1.27(4.68)	0.43(4.43)		-2.32(6.48)	-2.84(5.01)		4.53(7.54)	6.13(5.99)		0.92(7.71)	-0.48(5.47)	
>12mm	21	1.02(5.49)	0.44(4.02)		-1.68(5.86)	-2.01(4.64)		4.46(4.93)	6.15(4.30)		-0.98(6.37)	-2.01(4.06)	
Cell type Spindle	27	1.43(5.08)	1.19(3.33)	0.844	-1.59(6.38)	-2.41(5.02)	0.22	4.51(5.46)	6.03(5.51)	0.804	0.73(5.11)	-0.09(5.19)	0.560
Epitheliod	15	1.25(6.88)	0.62(4.01)		-2.94(6.11)	-4.14(4.57)		4.46(5.47)	4.80(5.43)		-0.82(8.48)	-1.88(5.55)	
Mixed	44	1.03(5.88)	0.64(4.63)		-2.30(5.83)	-2.68(4.70)		5.20(8.56)	5.22(7.01)		-2.27(7.50)	-1.46(6.64)	
Liver metastasis		2.06(6.55)	0.3928 (4.241)	0.17	-3.05(5.14)	-2.7259 (4.806)	0.44	6.49(10.88)	4.7321 (6.053)	0.04	-1.72(8.36)	-0.9035 (6.384)	0.37
Yes	17												
No	66	1.02(4.96)	1.94(3.59)		-2.28(6.31)	-3.73(5.00)		4.51(5.88)	8.16(6.98)		-0.30(7.61)	-2.37(4.75)	
KM (2-5 years)	52	22%			71%			5%			39%		

Y: Years, CB: Ciliary body involvement, KM : Kaplan-Meier metastasis –free survival analysis (Follow-up duration:2-5 years)

Clinico-pathological parameter	*No. of samples*	*miR-134*			*miR-146b*			*miR-1238*			*miR-199a*		
		Median RQ (IQR)	*Mean RQ (s.d.)*	*P-value*	*Median RQ (IQR)*	*Mean RQ (s.d.)*	*P-value*	*Median RQ (IQR)*	*Mean RQ (s.d.)*	*P-value*	*Median RQ (IQR)*	*Mean RQ (s.d.)*	*P-value*
Gender Male	58	1.34(5.53)	1.64(4.41)	0.74	1.27(3.55)	0.60(5.35)	0.64	9.66(6.47)	9.301(4.59)	0.46	6.60(5.24)	6.59(5.59)	0.65
Female	27	2.01(5.86)	2.02(5.85)		2.10(5.76)	1.18(5.20)		7.46(6.65)	8.472(5.38)		7.10(8.52)	7.20 (6.32)	
Chromosome 3 aberration													
Monosomy	52	2.15(5.22)	2.63(4.27)	0.04	1.92(3.96)	1.99(3.63)	0.009	9.32(6.35)	9.31(4.78)	0.45	7.34(5.58)	8.11(5.19)	0.009
Disomy	34	0.61(7.46)	0.45(5.38)		0.79(7.64)	-1.00(6.70)		7.61(6.66)	8.5(4.93)		5.70(7.15)	4.78(6.14)	
Ciliarybody Involvement													
Yes	12	2.21(4.17)	1.75(5.02)	0.98	2.77(2.78)	2.38(2.07)	0.26	7.04(8.63)	10.00(5.79)	0.44	6.19(6.78)	8.04(4.98)	0.43
No	74	1.58(5.77)	1.77 (4.84)		1.43(4.96)	0.55(5.56)		9.04(5.82)	8.83 (4.67)	0.20	7.23(2.55)	6.61(5.90)	0.24
Tumour base (mm)													
<5mm	3	-2.90(0)	-2.37(1.81)	0.28	0.60(0)	-3.50(8.2)	0.47	0.26(0)	2.35(4.12)	0.08	7.29(0)	7.27(5.96)	0.53
6-8mm	7	2.20(6.03)	2.22(3.44)		4.94(10.53)	2.10(7.90)		6.20(8.39)	7.70(4.74)		5.93(10.84)	3.71(10.31)	
9-12mm	34	0.99(5.66)	1.13(5.41)		1.37(3.33)	1.07(4.17)		8.20(6.57)	9.44(4.52)		6.19(4.67)	6.93(4.81)	
>12mm	42	2.52(4.83)	2.51(4.56)		1.71(5.46)	0.69(5.39)		10.08(6.45)	9.33(4.88)		7.13(6.58)	7.21(5.58)	
Tumour width													
<5mm	12	-1.24(7.23)	-0.65(5.62)	0.44	0.57(7.75)	0.42(6.40)	0.41	7.44(6.43)	8.32(3.59)	0.90	9.2(10.36)	6.58(3.88)	0.44
6-8mm	21	1.23(7.06)	1.52(5.33)		2.10(2.62)	1.79(4.18)		7.89(6.54)	9.12(4.45)		6.04(5.76)	6.86(4.74)	
9-12mm	32	2.48(5.20)	2.75(4.59)		2.39(5.25)	1.11(4.05)		9.36(5.38)	8.80(5.13)		7.69(5.35)	7.89(5.86)	
>12mm	21	1.24(4.94)	1.90(3.96)		0.69(7.12)	-0.42(6.99)		10.5(10.1)	9.58(5.51)		4.89(5.03)	7.13(4.17)	
Cell type													
Spindle	27	2.20(5.35)	2.19(4.73)	0.44	1.85(2.91)	1.79(4.07)	0.41	8.52(4052)	8.27(3.88)	0.22	6.95(6.41)	7.67(5.35)	0.59
Epitheliod	15	0.015(4.04)	0.32(5.07)		0.07(4.05)	0.36(3.90)		7.61(6.0)	7.74(4.73)		6.96(7.0)	7.06(5.27)	
Mixed	44	2.05(5.95)	2.00(4.83)		2.29(5.77)	0.60(6.19)		10.1(7.21)	9.85(5.27)		6.39(6.0)	6.81(5.78)	
Liver metastasis													
Yes	17	2.93(3.7)	1.18(5.07)	0.03	2.27(4.93)	0.58(5.56)	0.78	7.74(5.07)	5.16 (0.64)	0.65	8.34 (6.17)	6.07(0. .75)	0.53
No	66	1.14(5.4)	4.03(3.5)		1.46(4.3)	0.99(4.1)		9.31(7.16)	3.61(0.87)		6.40(5.58)	5.13(1.24)	
KM (2-5 years)	52	13%			13%			2%			7%		

Y: Years, CB: Ciliary body involvement, KM : Kaplan-Meier metastasis –free survival analysis (Follow-up duration:2-5 years)

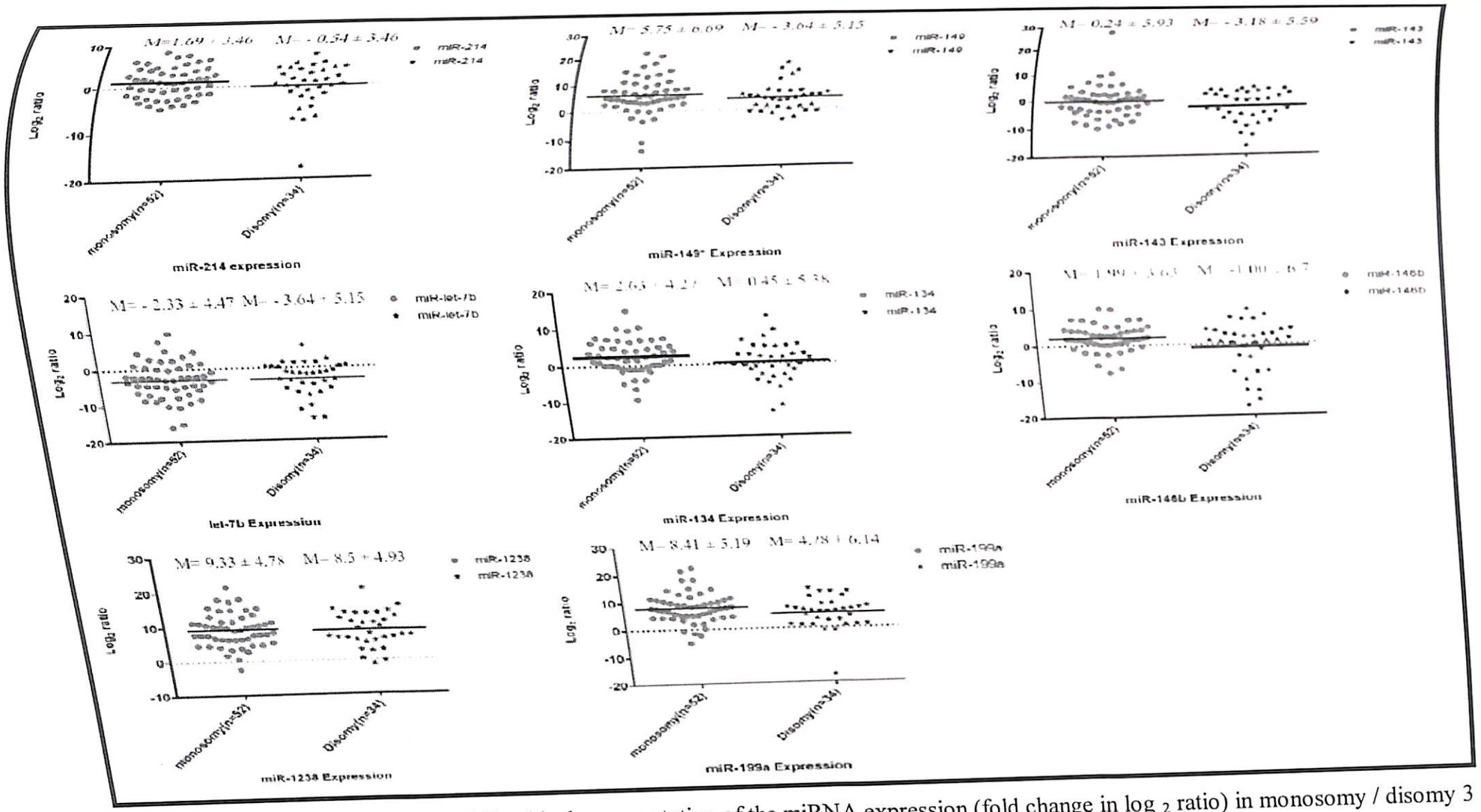

Figure 10.1: miRNA expressions in UM.Graphical representation of the miRNA expression (fold change in log $_2$ ratio) in monosomy / disomy 3 uveal melanomas derived using Graph pad Prism. The line represents the mean fold change of the respective miRNAs in uveal melanoma groups. "M" denotes the mean fold change of the respective miRNA expression.

10.2.1.2. Expression of miRNAs in disomy 3 group of tumors

In the present cohort of disomy 3 tumors, the mean fold change in the select miRNAs were as follows: *miR-134*: 0.45; *miR-1238*:8.5; *miR-214*:-0.54; *miR-149**:4.86; *miR-143*:-3.18; *miR146b*: -1.00; *miR-199a*: 4.78 and *let7b*: -3.64 [**Table 10.1, Figure 10.1**]. The miRNA expressions are derived after normalizing with the mean expression of normal melanocytes (n=5). Among the disomy 3 group with metastasis, higher expressions of *miR-134* [87.5% (7/8)], *miR-1238* [100% (8/8)], *miR-149** [87.5% (7/8)] and *miR-199a* [100% (8/8)] was observed. To the moderate to lower end, *miR-214* [50.0% (4/8)], *miR-143**[12.5% (1/8)], *miR-146b* [62.5% (5/8)] and *let-7b* [25% (2/8)] was observed.

10.2.1.3. Association of miRNAs with clinico-pathological parameters

Clinico-pathological characteristics of the independent sample sets with their median and mean values as well as p-values are summarized in **Table 10.1**. It is clear that *miR-134* and *miR-149** showed statistically significant association with liver metastasis. An elevated level of *miR-1238* expression was observed in all the tumors irrespective of monosomy / disomy 3. *let -7b* did not show any significant association with any of the clinico-pathological parameters.

10.2.2. Determination of miRNAs through High throughput analysis

10.2.2.1. Unsupervised data analysis of miRNA profiling

Further, to elaborate the list of miRNAs involved in UM tumor progression, Principal Component Analysis (PCA) of miRNA profiling demonstrated the clustering of the tumors into two distinct groups [**Figure 10.2**]. The tumor classification identified by PCA analysis correlated exactly with the CISH based classification as monosomy and disomy

The miRNA profiling of the melanoma tumors (n=5) revealed a total of 585 differentially expressed miRNAs between monosomy 3 (n=3) and disomy 3 (n=3) samples. **Figure 10.3** shows the hierarchical cluster for the top 100 differentially expressed miRNAs with $p<0.05$. The lists of miRNAs were further filtered using ANOVA and the top 10 miRNAs identified by ANOVA is tabulated [**Table 10.2**]. Consequently 25 miRNA's were found to be significantly up-regulated, while 26 miRNAs were down-regulated in the monosomy 3 group relative disomy 3 UM case..

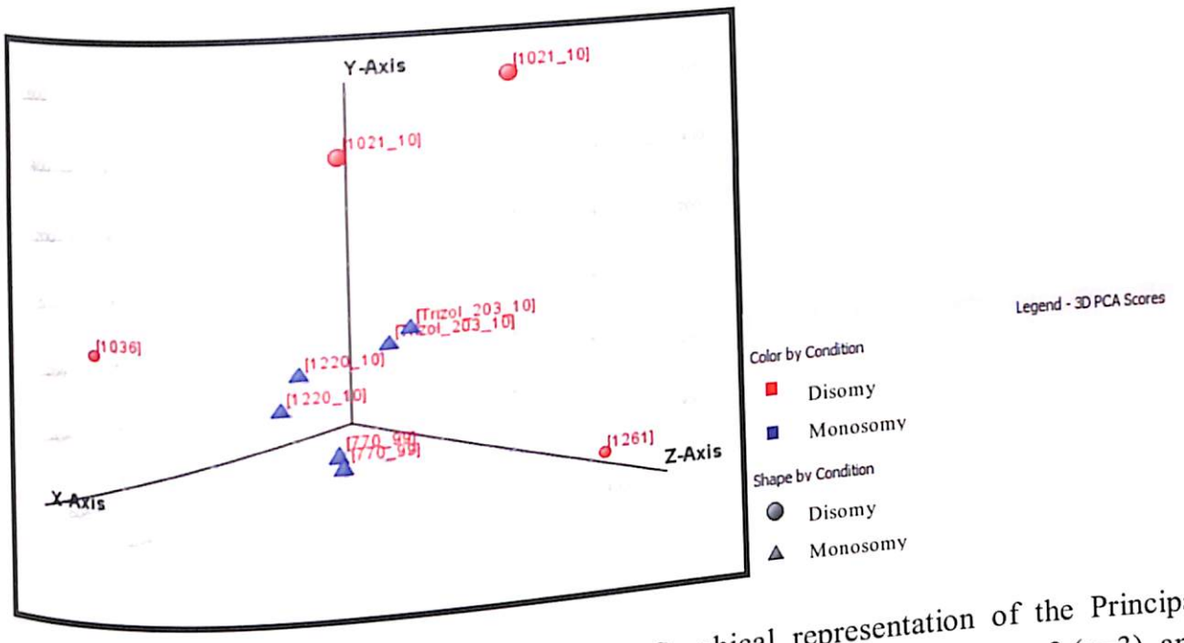

Figure 10.2: Principle Component Analysis.Graphical representation of the Principal component analysis (PCA) for the uveal melanoma tumor tissues: monosomy 3 (n=3), and disomy 3 (n=3) showing the clustering of samples correspondingly into two distinct groups (monosomy and disomy 3. Blue colored triangle indicates the monosomy 3 tumors, while red color circle indicates disomy UM tumors.

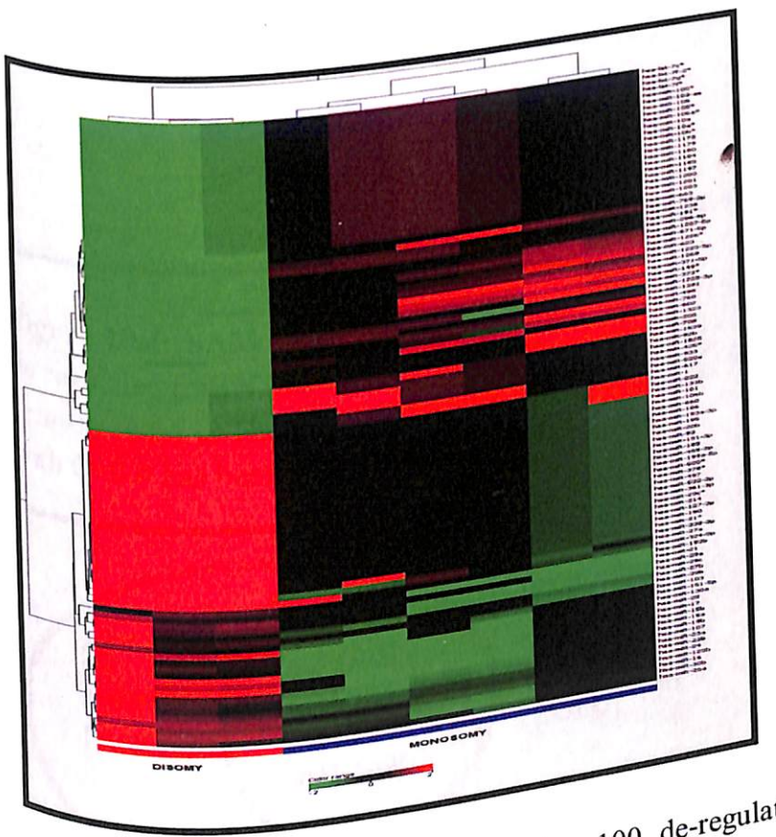

Figure 10.3: Hierarchical cluster. Top 100 de-regulated miRNA's that are differentially expressed between monosomy and disomy formalin fixed uveal melanoma primary tumours are shown. The green colour indicates the down-regulated miRNA's and the red colour indicates the up-regulated miRNAs. The range of the significant de-regulation is -2.0 to +2.0 $\log_2$ ratio).

10.2.2.2. *Supervised analysis of miRNA profiling*

Significance Analysis of Microarray (SAM) was performed to determine the differentially expressed miRNAs associated with monosomy 3 group of tumors. In this analysis, we observed 82 differentially expressed miRNA's with the false discovery rate (FDR) set to Q = 0.0 **[Figure 10.4]**. Further, the top 10 up-regulated miRNA's with maximum score and high fold change are: *hsa- miR-317-5p, hsa- miR- 373, hsa- miR- 1268, hsa- miR-191*, hsa- miR-150, hsa- miR-1275, hsa- miR-188-5p, hsa- miR- 1238, hsa- miR-134, hsa- miR-296-5p* **[Table 10.2]**. On intersection of miRNAs detected in both ANOVA and SAM analysis, we observed 14 up-regulated miRNAs, of which two of the select miRNAs: *hsa-miR-1238* and *hsa-miR-134* are present **[Figure 10.5].**

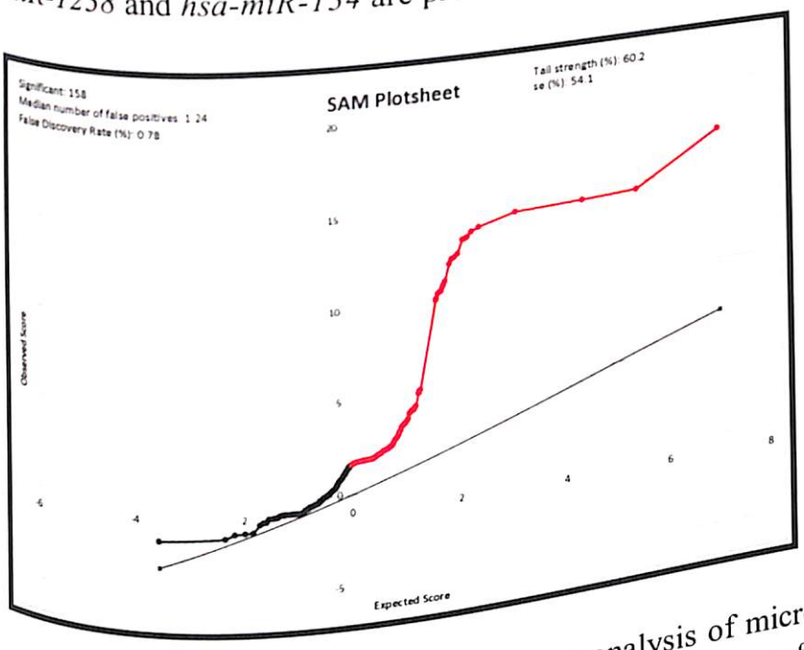

Figure 10.4: SAM plot. The Significance analysis of microarray (SAM) plot reveals the de regulated miRNAs between the monosomy and disomy formalin fixed uveal melanoma primary tumors. The false discovery rate (FDR) has set at Q=0.78%. The list of miRNA's with Q=0.0 has been considered for the validation.

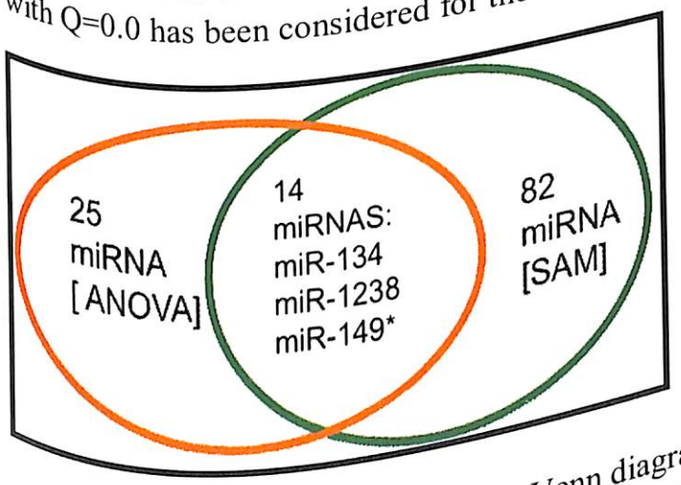

Figure 10.5: Intersection of miRNAs. Venn diagram on intersection of miRNAs obtained from ANOVA and SAM. *miR-134, miR-1238, miR-149** are the common select miRNAs observed from this study.

Table 110.2: Up-regulated miRNAs in UM. List of top 10 up-regulated miRNAs obtained by ANOVA and SAM.

S.No	List of top 10 up-regulated miRNAs obtained by ANOVA		List of top 10 up-regulated miRNAs obtained by SAM		
	miRNAs	Fold change (Transformed ratio)	miRNAs	Score (d)	Fold change (Arbitrary units)
1.	*hsa-miR-1238*	7.8	*hsa-miR-206*	17.23	826.66
2.	*hsa-miR-191**	7.7	*hsa-miR-21**	14.55	370.09
3.	*hsa-miR-498*	6.4	*hsa-miR-361-3p*	14.44	137.55
4.	*hsa-miR-602*	5.2	*hsa-miR-378**	14.33	263.02
5.	*hsa-miR-149**	4.05	*hsa-miR-101*	13.80	314.705
6.	*hsa-miR-371-5p*	3.9	*hsa-miR-29c**	13.60	250.02
7.	*hsa-miR-373**	3.7	*hsa-miR-532-3p*	13.33	294.92
8.	*hsa-miR-623*	3.7	*hsa-miR-199a-5p*	13.25	135.19
9.	*hsa-miR-296-5p*	3.5	*hsa-miR-497*	13.23	248.17
10.	*hsa-miR-1268*	3.26	*hsa-miR-20b*	12.46	141.35

10.2.3. Gene expression analysis of mRNAs regulated by differentially expressed genes in UM

The mRNA expression levels of the target genes (*WISP1, HDAC8, SMAD4, c-KIT, HIPK1*) regulated by the differentially expressed miRNAs (section 10.3.2) analyzed by using qRT-PCR are indicated in the **Table 10.3**. The network connecting these miRNAs and their respective gene targets are indicated in the **Figure 10.6.**

Table 10.3: Gene expression in UM. mRNA expression analysis using qRT-PCR.

S.NO	Genes	Gene expression : Fold change in log $_2$ ratio (S.D)	
		Monosomy (N=5)	Disomy (N=5)
1.	*WISP1*	-1.16 (3.12)	0.5 (2.32)
2.	*HDAC8*	3.81(2.34)	3.52 (2.92)
3.	*SMAD4*	-0.29(1.87)	-0.64(2.26)
4.	*c-KIT*	2.70(2.95)	1.82(3.42)
5.	*HIPK1*	2.53(1.43)	3.80(1.12)

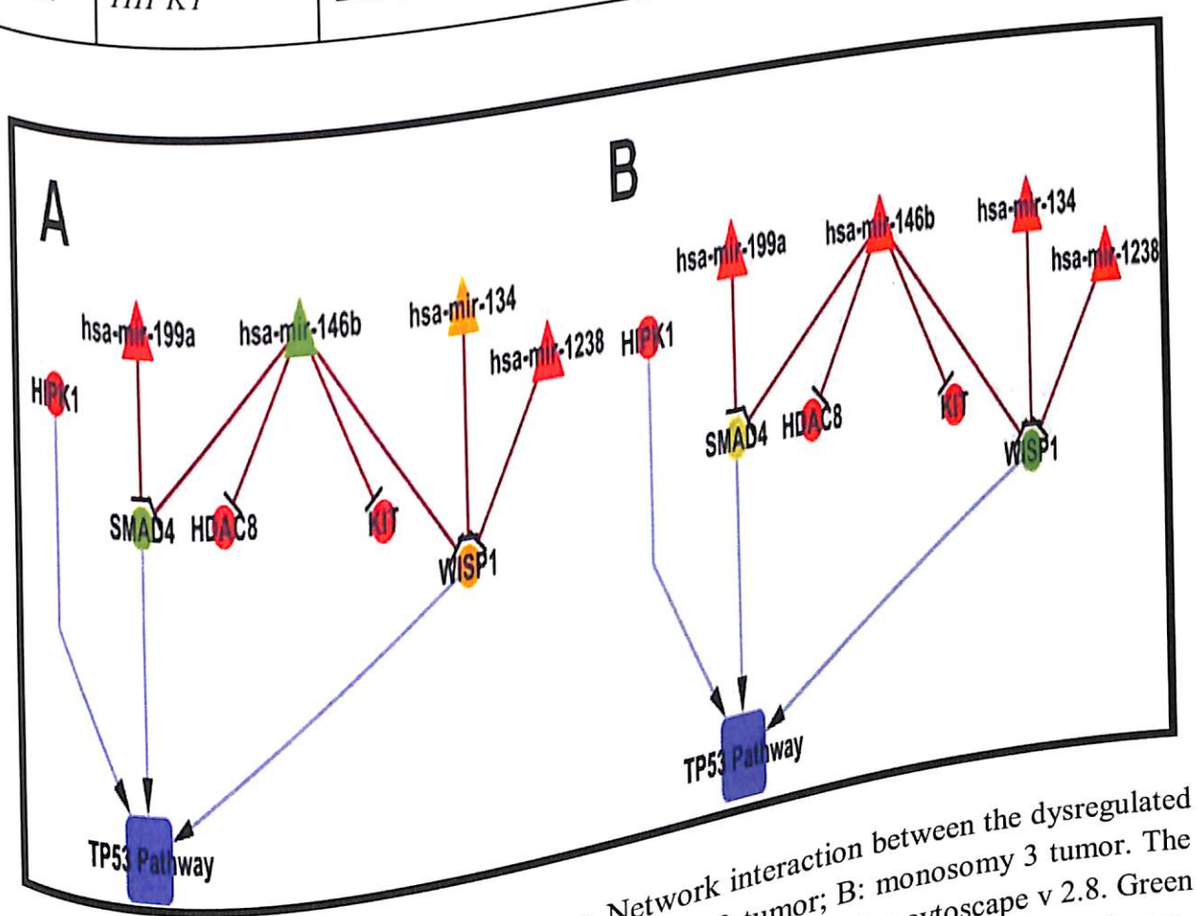

Figure 10.6: miRNA / mRNA interactions. Network interaction between the dysregulated miRNAs and their gene targets in UM – A: disomy 3 tumor; B: monosomy 3 tumor. The network is drawn with the expressions obtained by qRT-PCR using cytoscape v 2.8. Green colour indicates the down-regulation of miRNAs/ genes; red colour indicates the up-regulation of miRNAs/ genes; Yellow colour indicates varied miRNA / gene expression.

10.3. Discussion

Based on the gene expression profiling UM is classified in to two classes - Class 1 with low risk of metastasis, associated with disomy 3 and have better prognosis, while class 2 with high risk of metastasis, associated with monosomy 3 (Onken et al. 2004). Recent reports on germ line mutations in *BRCA1* associated protein 1(*BAP1*) (Njauw et al. 2012), *GNAQ* (Van Raamsdonk et al. 2010) adds to the list of indicators, predetermining the metastasizing UM lesions. Unfortunately, the lack of accuracy in the molecular genetic testing due to intra-tumoral heterogeneity (Mensink et al. 2009), micro-deletions of genes prevailing in UM decreases the precision of identifying the micro-metasizes (Damato 2012). Since miRNAs regulate the gene expression at post-transcriptional stage, they can be regarded as key indicators to predetermine the hepatic metastasis. In addition, the need to determine, the patients with high risk of metastasize is of utmost importance, for monitoring chemotherapy regimen.

10.3.1. miRNA expression in UM

To address if the select miRNAs could differentiate the monosomy 3 from disomy 3 group, qRT-PCR analysis was performed on formalin fixed paraffin embedded eye tissues. **Figure 10.1** shows the expression levels of each individual miRNA in all the samples under study divided in to experimental groups based on the chromosomal aberration, mean expression of individual miRNAs varied among the 2 groups **[Table 10.1]**.

10.3.1.1. Expression of miR-134 in UM

miR-134 is well studied in other cancers such as squamous cell carcinoma of tongue (Wong et al. 2008), colorectal cancer (CRC) (Ahmed et al. 2013). Up-regulated *miR-134* expression was associated with the Head and neck squamous cell carcinoma (HNSCC) tumor invasiveness abrogating the ectopic expression of *WWOX1* gene expression (Liu C. J. et al. 2014). In yet another study, Li., et al, (2012) have reported the significant inhibition of EMT pathway in Non-small-cell lung carcinoma (NSCLC) cells by *miR-134*

regulating *FOXM1* (Li J. et al. 2012c). In the current study, up-regulation of *miR-134* in the monosomy 3 (mean fold change=2.63) corroborates with the earlier reports. This indicates, *miR-134* could contribute to the invasive properties of the UM.

10.3.1.2. *Expression of miR-1238 in UM*

From earlier report in CRC, *miR-1238* was known to differentiate the tumor cells from normal cells (Balaguer et al. 2011). However, in the current study, we observed no significant difference of *miR-1238* expression among the two groups (monosomy 3/disomy 3) of tumors. Thus, up-regulation of *miR-1238* expression observed in monosomy 3 and disomy 3 reveals indicates that it might contribute to the melanoma tumoriogenesis rather than contributing to invasive property.

10.3.1.3. *Expression of miR-149* in UM*

Elevated levels of miR-149* especially in monosomy 3 group (mean fold change= 5.75) than in disomy group (mean fold change=4.86) was observed in the current study. This result suggests that *miR-149** contributes to the aggressiveness of the melanoma tumor. This study is supported by other studies, in which over-expression of *miR-149** has been reported in other cancers like pituitary adenomas (Bottoni et al. 2007), primary serous papillary ovarian caricinoma (Laios et al. 2008). An association with decreased glycogen synthase kinase-3α level (target gene), increased Mcl-1 together regulating the p53 mediated pro-survival pathway suppressing the melanoma cell growth have been reported in fresh human metastatic melanoma isolates. Further *in vitro* studies may conclude its functional role in UM to classify them as a biomaker or a therapeutic target.

10.3.1.4. *Expression of miR-214 in UM*

Earlier report states that over-expression of miR-214 contributes to the malignant features of non-small-cell lung cancer (NSCLC) suppressing *CADM1* expression (M. Ishimura 2012). Further, in few other studies of ovarian cancer cells, the gene targets of *miR-214* namely *PTEN* (Yang H. et al. 2008), AP2, p53 (Xu C. X. et al. 2012) and *TWIST1* (Yin et al. 2010) has resulted in acquiring the chemo resistance. In addition, Penna., et al (2011)

has reported the melanoma tumour progression with elevated levels of *miR-214* together with suppression of *TFAP2C* (as gene target) (Penna et al. 2011) using an *in vivo* model. These studies, together state the implication of *miR-214* in cell proliferation, invasion and cancer progression. These studies substantiates the results on differential expression levels of *miR-214* among 2 groups of UM (pvalue=0.01). Thus *miR-214*, an oncomir can be further tested and validated as the diagnostic and / or therapeutic marker in larger sample size.

10.3.1.5. *Expression of miR-143* in UM*

Another significantly de-regulated miRNA in the current study includes miR-143. In the present study, we have observed the presence of *miR-143* expression (mean fold change monosomy 3 group=0.24/ disomy 3 group= -3.18), a significant association with the chromosome 3 aberrations, but insignificant association with the liver metastasis. These results indicate significance of *miR-143* in cancer progression but not in metastasis. In previous studies, it is reported as oncomir in prostate cancer by negatively regulating *KRAS* (Xu B. et al. 2011a). Further, elevation of *miR-143* during differentiation of cancer stem cells promotes metastasis by modulating *FNDC3B* gene expression in prostate cancer (Fan et al. 2013). Yet another supports the role of miR-143 in promoting hepatocellular carcinoma metastasis in an athymic nude mouse model by regulating nuclear factor kappa B (NF-kB) (Zhang X. et al. 2009). However, Hu Y., et al, (2012) have reported the antimetastatic and antitumoriogenic role of miR-143 in liver metastasis model and xenograft Panc-1 tumor model of pancreatic cancer by dysregulating the target genes namely *MMP 2, MMP 9, KRAS* and E-Cadherin (Hu et al. 2012). Taken together, these reports substantiates further studies on its gene target (KRAS, NF-kB) regulation in UM which would address the role of miR-143 in UM tumor progression.

10.3.1.6. *Expression of miR-146b in UM*

Up-regulation of *miR-146b* has been observed in other cancers such as prostate cancer, ovarian carcinoma cell lines and tissues (Dahiya et al. 2008). The current study reveals a significant association of *miR-146b* with monosomy 3 group and insignificant correlation with liver metastasis. Role of *miR-146b* in regulating TGF-Beta pathway by repressing the *SMAD4* has been reported in thyroid cancer (Geraldo et al. 2012). In yet another study, its over-expression has resulted in reversal of the malignant phenotype in lung carcinoma cell

line (A548)(Patnaik et al. 2011). This result indicates the various roles of miR-146b in cancer progression.

Further, Hurst, et al. (2009) has reported the suppression of breast cancer metastasis regulated by elevated levels of Breast cancer metastasis suppressor 1 (*BRMS1*) together with up-regulation of *miR-146b* (Hurst et al. 2009). In a recent report of UM, expression of *BRMS1* and its statistical insignificance with prognostic parameters have been reported (Ventura et al. 2014). Also, our present results of elevated *miR-146b* (mean fold change: monosomy 3 group=1.99; disomy group = -1.00) is supported by yet another report in UM, where de-regulation of NF-KB pathway (a known gene target of *miR-146b*) regulates metastasis (Dror et al. 2010). Thus, these reports points to the role of miR-146b in melanoma progression and metastasis suppression. These findings can be further justified using knock-down studies (RNAi) in *in vitro/in vivo* models.

10.3.1.7. *Expression of miR-199a in UM*

miR-199a, an another delineated miRNA identified in the current study (mean fold change: monosomy group 3=8.11; disomy 3=4.78) has been known for its diverse role as oncomir or tumor suppressor miRNA in different cancers. It has been reported to be elevated in gastric cancers (He X. J. et al. 2014) and ovarian cancers (He J. et al. 2013) including uveal melanoma (Worley et al. 2008). In a previous report, *miR-199a* suppresses *SMAD4*, de-regulates TGF-β pathway implicating its role in gastric tumorigenesis (Zhang Y. et al. 2012b). These reports support the present result and state the role of *miR-199a* as an oncomir in UM. The significant association of *miR-199a* with the monosomy 3 aberration indicates that it can be one of the indicators to differentiate the high risk group of melanomas.

10.3.1.8. *Expression of let7b in UM*

In the present study, the down-regulation of *let-7b* (mean fold change: monosomy group = -2.33, disomy group= -3.64) was observed in UM. Suppression of *let 7b* has been reported in various cancers namely acute lymphoblastic leukaemia (Mi et al. 2007), bladder cancer (Nam et al. 2008), malignant melanoma (Schultz J. et al. 2008). Earlier reports suggest the restoration of *let-7b* is potential therapeutic option in cancers (Li Y. et al. 2009b). Up-regulation of *let-7b* has been reported in other cancers such as UM (Worley

et al. 2008), lymphoma (Lawrie et al. 2009), breast cancer and retinoblastoma (Nam et al. 2008) suggesting it as a good prognostic marker to differentiate the high grade tumors. These studies were supported by an earlier report by Garzon etal, where *let-7b* over-expression is found to regulate NF-KB pathway contributing aggressiveness of acute promyelocytic leukemia (Garzon et al. 2007). So these reports state the existing diversified role of *let-7b* in cancer progression. But, in the current study, we observed the decreased level of *let-7b*, along with insignificant association with the monosomy 3 group and liver metastasis which differs with the Worley, et al, (2008) reports on let-7b in uveal melanoma. Further studies to explore *let-7b* related gene targets namely NF-KB, RB1, CCND1 could reveal its role in promoting UM.

10.3.2. miRNAs associated with metastasis-free survival in UM

Association of miRNAs with metastasis free survival is essential for the better understanding of how miRNAs are involved in micro metastasis of uveal melanoma. Kaplen-meier metastasis free survival analysis was carried out with the clinical follow-up of 52 patients under study (60.46% corresponding to 52/86). We observed metastasis free survival percentage in less than 10% in the presence of *miR-1238, miR-149* and miR-199a*; less than 25% in *miR-214, miR-134,miR-146b*; less than 40 % in *miR-143* and less than 75% in presence of *let-7b* (**Table 10.1; Figure 10.6**). These results suggests that the expression of *miR-1238, miR-149*, miR-199a, miR-214, miR-134 and miR-146b* could be assessed to evaluate the metastasis status in UM patients.

10.3.3. Expression levels of delineated miRNAs detected using miRNA profiling

Further, in the current study, PCA (unsupervised data analysis) revealed the diverse clustering of the two groups of UM. The 3 samples of the monosomy 3 group tumours cluster together to form a single group. The slight difference among the tumours within the group could be due to the heterogenous tumor in-filtrating lymphocyte population. The three samples of disomy 3 group shows a separation within the group. This separation might be due to difference in phenotype with in groups namely the cell type of UM tumors.

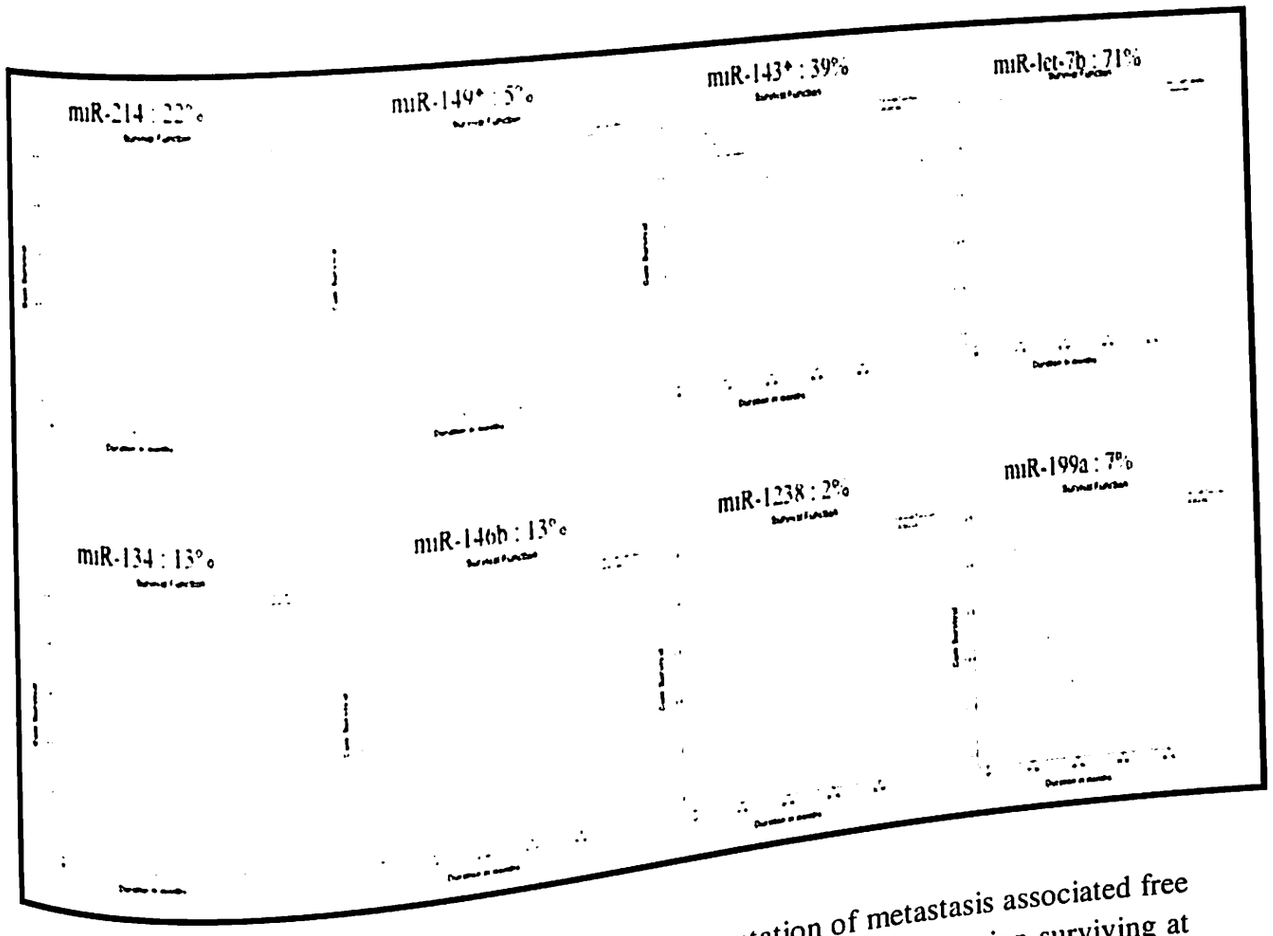

Figure 10.7: Kaplan-Meier analysis.Graphical representation of metastasis associated free survival was analysed by Kaplan-Meier analysis. The cumulative proportion surviving at end of the interval (60 months) is represented in percentage. Follow up of 52 patients with a period of 2-5 years of duration were enrolled in the study.

Among 585 differentially expressed miRNAs between two groups of UM, we observed the significant levels of *hsa- miR-317-5p, hsa- miR- 373, hsa- miR- 1268, hsa- miR-191*, hsa- miR-150, hsa- miR-1275, hsa- miR-188-5p, hsa- miR- 1238, hsa- miR-134, hsa- miR-296-5p* **[Table 10.2]**. These results widens up the list of miRNAs to be screened for diagnostic implication. Among the delineated miRNAs studied by qRT-PCR, *miR-134, miR-1238, miR-214, miR-199a, let7b* were detected by miRNA profiling while *miR-146b and miR-143* were not identified **[Table 10.1 and 10.2]**. Difference in the expression levels obtained from these two techniques might be due to the cross hybridisation or the presence of pre-miRNAs, which would mask the signal of mature miRNAs (Ralfkiaer et al. 2011). Though miRNA profiling is one of the high-throughput techniques, the sensitivity, specificity of qRT-PCR makes it more applicable as a diagnostic tool. Thus, from the current study, the list of delineated miRNAs studied by qRT-PCR can be

considered to have a diagnostic implication, while the other panel of miRNAs detected by miRNA profiling needs further validation.

10.3.4. Gene target validation of differentially expressed miRNAs

Prediction of miRNA targets using Target scan (human), of the differentially expressed miRNAs revealed the negative regulation of genes namely *SMAD4, WISP1, HDAC8 and c-KIT* by *miR-146b*, negative regulation of *WISP1* by *miR-134, miR-1238* and negative regulation of *SMAD4* by *miR-199a* [**Figure 10.5**]. Among these interactions, we observed *SMAD4 and WISP1* as the common regulators.

10.3.4.1. Role of SMAD4, WISP1 in UM

In UM, down-regulation of *SMAD4* gene (in order of monosomy 3 -0.29 and disomy 3 -0.64) was observed. As miRNA negatively regulates the 3' UTR of mRNA, differential expression of miR-146b (monosomy 3 tumors: 1.99; disomy 3 tumors: -1.00) and over-expression of miR-199a monosomy 3 tumors: 8.11, disomy 3 tumors: 4.78 in UM substantiates the down-regulation of *SMAD4* gene in UM tumors. Further, varied expression of *WISP1*gene in UM tumors (monosomy 3 tumors: -1.16; disomy 3 tumors: 0.5) corroborates with the over-expression of *miR-146b* in monosomy 3 UM. In addition, varied expression of *WISP1* gene together with over expression of *miR-134* (monosomy 3 tumors: 2.63; disomy 3 tumors: 0.45) and *miR-1238* (monosomy 3 tumors: 9.31; disomy 3 tumors: 8.5) substantiates the negative regulation between them.

SMAD4 and WISP1 are known to regulate p53 pathway (Su et al. 2002, Wang C. L. et al. 2006). Earlier reports state the infrequent mutation of p53 pathway (Brantley and Harbour 2000). Thus, the down-regulation of *SMAD4* gene and varied expression of WISP1 gene substantiates the varied activation of p53 pathway in UM. In the current study, inactivation of p53 pathway in UM was further supported by the over-expression of *HIPK1* gene (monosomy 3: 2.53; disomy 3: 3.8) which corroborates with an earlier report on colorectal cancer (Rey et al. 2013).

10.3.4.2. *Expression of HDAC8 and C-KIT in UM*

Irrespective of chromosome 3 aberrations, over-expression of *HDAC8* gene in UM substantiates, with an earlier study of its association with advanced neuroblastoma (Witt et al. 2009). However, there do exist a differential expression of miR-146b in UM, a negative regulator of *HDAC8* gene. In addition, a similar association of differential expression of miR-146b and over-expression of *c-KIT* mRNA was observed. Taken together, these results widen the future scope of the study to determine the role of *HDAC8* and *c-KIT* in [illegible] *miR-146b*.

[illegible] of miRNA targets using Target [illegible] of the [illegible] revealed the negative regulation of genes namely *SMAD4*, *WISP1*, *HDAC8* and *c-KIT* by miR-146b, negative regulation of *WISP1* by *miR-134*, *miR-1338* and negative regulation of *SMAD4* by miR-199a (**Figure 10.5**). Among these interactions, we observed [illegible]

10.3.4.1. *Role of SMAD4* [illegible]

In [illegible] *miR-146b and miR-199a* to be associated with [illegible]

[illegible]ge of miRNA namely *miR-134* and *miR-149** levels are [illegible] metastasis of UM in Indian population. Further, this study has [illegible]vel of *SMAD4*, *WISP1*, *HDAC8*, *c-KIT and HIPK1* as the targets of [illegible] expressed miRNAs in UM. This study has explored the role of miRNAs/mRNAs in UM tumor progression and their implication in predetermining the hepatic lesions. Further, this study has provided the qRT-PCR based miRNA detection as the diagnostic tool that can differentiate the two groups of UM.

10.3.4.2. *Expression of HDAC8 and C-KIT in UM*

Irrespective of chromosome 3 aberrations, over-expression of *HDAC8* gene in UM substantiates, with an earlier study of its association with advanced neuroblastoma (Witt et al. 2009). However, there do exist a differential expression of miR-146b in UM, a negative regulator of *HDAC8* gene. In addition, a similar association of differential expression of miR-146b and over-expression of *c-KIT* mRNA was observed. Taken together, these results widen the future scope of the study to determine the role of *HDAC8* and *c-KIT* in UM progression and its association with *miR-146b*.

10.4. Conclusion

Among, the panel of 8 miRNAs (*miR-214, miR-149*, miR-143, miR146b, miR-199a and let7b, hsa-miR-1238 and hsa-miR-134*), the current study has identified 5 key miRNAs *miR-134, miR-214, miR-143*, miR-146b and miR-199a* to be associated with monosomy 3. Especially high percentage of miRNA namely *miR-134* and *miR-149** levels are associated with liver metastasis of UM in Indian population. Further, this study has indicated the level of *SMAD4, WISP1, HDAC8, c-KIT and HIPK1* as the targets of differentially expressed miRNAs in UM. This study has explored the role of miRNAs/mRNAs in UM tumor progression and their implication in predetermining the hepatic lesions. Further, this study has provided the qRT-PCR based miRNA detection as the diagnostic tool that can differentiate the two groups of UM.

CHAPTER 11: SUMMARY AND CONCLUSION

The current dissertation outlines the present understanding of the molecular dysregulation, highlighting genome-wide analyses resulting in the identification of exciting candidate genes implicating them as potential prognostic and therapeutic targets in RB and UM. Further these data highlight the cohesive molecular complexity existing within RB and UM which in turn aids, to better understand the patho-biology in these two ocular cancers.

Retinoblastoma (RB), the common primary intraocular tumour manifests in infants and children with a relative incidence of 3% of all paediatric tumours worldwide. RB occurs as either unilateral sporadic tumors or bilateral hereditary tumors (less frequent). Mainly the RB is grouped as genetic-heritable and non-genetic-non-heritable type (predominant). If untreated, children with bilateral hereditary tumors have a high risk of developing secondary cancers through intracranial extension and metastasis resulting in mortality [1]. The pattern of invasion and metastasis exhibited by RB tumors are through the optic nerve to the brain and also gets disseminated in the orbital tissue and adjacent bone (Chevez-Barrios et al. 2000). Current disease management includes enucleation, external beam radiotherapy, cryotherapy, photocoagulation, and chemotherapy (Vemuganti et al. 2001). Inspite of these advanced methods achieving a survival rate of over 95%, there remains a need for better treatment alternatives to improve visual impairment and to avoid eye salvage especially in hereditary retinoblastoma. Therefore, effective chemopreventive treatment including adjuvant therapy and gene therapy for metastasis would have a major impact on retinoblastoma mortality rates.

a) HMGA2 as potential therapeutic target in RB

Newer molecules and pathways have to be identified for designing novel targeted therapies. In this context, in the current dissertation **[chapter 5]**, we have reported one of

the High Mobility group (HMG) proteins: *HMGA2* as a target molecule in RB. HMGA family consists of *HMGA1a, HMGA1b, HMGA1c* and *HMGA2*. The high mobility group A (HMGA) proteins are small non-histone chromosomal proteins that are characterized by 3 highly conserved DNA-binding motifs called "AT-hooks" on the N- terminal and an acidic tail on c- terminal. They preferentially bind to the minor groove of AT-rich B form DNA by recognizing a particular DNA structure rather than a specific nucleotide sequence. Members of the HMGA protein family are often referred to as "architectural transcription factors " because of their ability to regulate expression of a large number of target genes through alteration of chromatin structure. These multifunctional proteins are involved in many fundamental cellular processes, including gene regulation, cell cycle, differentiation, and viral integration. *HMGA* mutations contribute to many diseases, including benign and malignant tumours, obesity, diabetes, and atherosclerosis. *HMGA1 (HMGA-1/Y)* and *HMGA2 (HMG1-C)* have similar functions. These proteins are relatively abundant in the early embryo, where cells are proliferating rapidly, whereas they are undetectable in terminally differentiated cells.

Primarily, the study **[chapter 5.1]** was initiated by evaluating the HMGA2 expression and its correlation with clinico-pathologic features in a larger cohort of RB primary tumors (n=64). In 64 primary RB tumours, HMGA2 protein was strongly positive (++) in 16 (25%) tumors, moderately positive (+) in 17 (26%) tumors, and faint/absent in 31 (48%) tumors. Among tumors without invasion (n=35), HMGA2 protein was strongly positive (++) in 6 tumors, moderately positive (+) in 6 tumors, and faint/absent (±) in 23 tumors. Among tumors with invasion (n=29), HMGA2 protein was strongly positive (++) in 10 tumors, moderately positive (+) in 11 tumors, and faint/absent (±) in 8 tumors. We observed significantly higher expression of HMGA2 protein in tumors with invasion compared with tumors without invasion ($P<0.01$). Chau et al' (2003), report of de-repression of HMGA2 gene expression in RB suggests that this protein might contribute to neoplastic transformation of retinal cells. This corroborates with the present study. We have observed positive expression of HMGA2 protein in the tumor-affected retinal nuclear layers and ganglion cells. However, HMGA2 protein was negative in the non-neoplastic donor retina. The ectopic expression of HMGA2 in RB and the clinico-pathological correlations of HMGA2 protein in primary RB tissues suggest its role in the genesis and maintenance of the transformed phenotypes. So, understanding the role that HMGA2

protein plays in patho-biology and molecular mechanisms of RB occurrence becomes biologically and clinically significant.

The strong correlation between HMGA2 protein expression and tumour invasiveness has prompted to further research on this molecule and related pathways. However, molecular understanding of *HMGA2* mediated cell signalling is limited. We have established the suppression of cell proliferation in cultured RB cells of differing tumour aggressiveness (Y79 and Weri Rb1) using *HMGA2* gene silencing technique (RNAi). Here, in **chapter 5.2** we analysed the molecular effects of *HMGA2* gene silencing in cell signalling, apoptotic, and cell adhesion regulation in RB, using high throughput technique, cDNA microarray (Agilent Technologies, Human Whole Genome 44K Oligo Microarray). The de-regulated genes (*ELK1, CDK6, E2F4, GTSE1, DRAM, CDH1, and SNAI1, MMP2, MMP9*) in the post-silenced RB cells were compared with the primary tumours for their expression levels. This study revealed the molecular regulatory changes induced by *HMGA2* silencing in RB cancer cells, offering mechanistic insights on its anti- cancer potential and mechanisms. Further, the current data indicated *HMGA2*, may be considered a promising candidate for gene silencing therapy in RB.

In continuation, we studied other molecular de-regulations using a post-*HMGA2* silenced RB cell line model by an integrated miRNA-mRNA analysis, to reconstruct miRNA-gene (post-transcriptional regulatory) networks involved in post-*HMGA2* silenced RB cells **[chapter 5.3]**. The de-regulated miRNAs in post-*HMGA2* RB cells (Y79) were identified using Agilent chip (Human_miRNA_version 3,8x15K array). Key miRNA that targets differentially expressed genes were identified and modelled using Cytarget linker, plugin of Cytoscape v 2.8. The integration between transcription factor and the de-regulated miRNAs were analysed by feed forward loop network analysis. Loop network analysis revealed a regulatory association between the transcription factor (*SOX5*) and the deregulated miRNAs (*miR-29a, miR-9*, miR-9-3*). The differentially regulated miRNAs includes 102 down-regulated miRNAs and 86 up-regulated miRNAs. The cluster classification using TAM tool revealed three main clusters: *hsa-miR-let7e clusters [miR-99b, miR125a]* ($p \leq 0.02$), *hsa-miR-506 cluster [miR-513a, miR-513b, miR-513c]* ($p \leq 0.04$), and *hsa-miR-1283 cluster* ($p \leq 0.008$) have been determined from the up-regulated miRNAs list. The filtered 82 up-regulated miRNAs were found to be involved in the following functional annotations ($p \leq 0.05$): activation of caspase cascade *[miR-150, miR-*

155], angiogenesis *[miR-150]*, activation of apoptosis, cell cycle regulation *[miR-494, miR-150 and miR-155]*, cell proliferation *[miR-150]*, and tumour suppressors *[miR-125a, miR-150, and miR-155]*. The down – regulated 106 miRNAs were categorized in to 15 families which include *miR-17* ~ 92 clusters and *miR-106b* ~ 25 clusters. The functional annotations of these de-regulated miRNAs are found to be involved in angiogenesis, apoptosis (p-value < 0.001), regulating cell cycle, cell differentiation, cell proliferation, tumour suppressors and oncomirs. The study also revealed the down regulation of AKT pathway (p-value < 0.001). The miRNA involved in this pathway was determined as *miR-20a, miR-18a, miR-7, miR- 17, miR-19a, miR-331, miR-19b, miR-26a, miR-92a, and miR-221.*

From these observations, the role of selected miRNA cluster: *miR-106b ~25* was analysed in post *HMGA2* silenced RB cells, for possible therapeutic targeting in RB. The miRNA cluster (*miR-106b, miR-93, miR-25*) regulating the major list of genes in integrated array were confirmed by quantitative Reverse Transcriptase PCR (qRT–PCR) in primary retinoblastoma tissues (n=20). Functional role of these miRNA cluster have been studied by using antagomirs in cultured RB (Y79, Weri Rb-1) cells in vitro. The expression of gene targets - p21 / Bim regulated by *miR-106b* family, was confirmed by western analysis. Cell proliferation and apoptotic studies have been performed using cell viability assay (MTT), and Annexin V FLUOS assay, in the antagomirs-treated RB cells (Y79 and Weri Rb-1). Thus, i*n vitro* silencing of these upstream miRNAs and *HMGA2* in RB cells resulted in the reduction of cell proliferation and in reduced invasion, through the induction of apoptosis (confirmed by Annexin V FLUOS assay) suggesting them as a potential targets for RB therapy. Taken together, *HMGA2* mediated anti-tumour effect in RB is, in part, mediated through the *miR-106b ~ 25 cluster.*

In addition, in order to suppress the function of the translated DNA-binding HMGA2 protein, we have used an 'aptamer' strategy **[chapter 5.4]**. The DNA binding sites in *HMGA2* gene are currently being identified with possible implications for developing DNA based therapeutics (aptamer). The stable sequence was selected and synthesized using phosphorothioate modification for the better stability of DNA aptamers (HMGA2-aptamer and mix-aptamer (scramble)) within the cells. The internalisation of the DNA

aptamer in RB cells (Y79, Weri Rb1 and non-neoplastic cell line, MIO-M1) was evaluated. At 1.0μM of aptamer for a period 24-48 h, the cellular cytotoxicity (LDH activity), cell proliferation (CyQUANT assay) and cell viability (MTT assay) revealed a significant decrease RB cell growth. At the moderate concentration of 0.5 μM of aptamer, for a period of 48 h of incubation, compromised cell proliferation [G2/M and S phase: Y79 (31.75%) and Weri Rb1 (27.94%)] while the mix-aptamer treated RB cells synchronised at S-phase [Y79: 58.29% and Weri Rb1: 31.76%] was observed in HMGA2-aptamer treated RB cells. However, in 1.0 μM mix-aptamer treated RB cells, mild to moderate regulation of cell viability was observed and thus attention need to be paid in using them in further *in vivo* studies. Further, in the current dissertation, down-stream regulators of the HMGA2 protein namely *SNAI1, CDH1, SMAD4* were de-regulated in the aptamer treated RB cells. In addition, activation of *TGFß-SMAD4* mediated apoptosis in HMGA2-aptamer mediated RB cells were validated at mRNA level using qRT-PCR. The incidence of apoptosis in HMGA2-aptamer treated RB cells was further confirmed by measuring the transcripts of apoptotic genes namely *Bcl2, BAX, PARP, and CASP 3.* Further, the role of *SMAD4* in increasing the efficacy of chemotherapy in HMGA2-aptamer treated RB cells were evaluated by treating the aptamer transfected cells with various concentrations of etoposide (chemotherapeutic drug). We could observe a significant shift in the drug modulation in HMGA2-aptamer treated RB cells in comparison with the mix-aptamer treated RB cells as control. Taken together, these results of inverse molecular changes (TGFß-SMAD4 induced apoptosis) in HMGA2-aptamer treated RB cells relative to mix-aptamer treated RB cells and MIO-M1 cells resulting in compromised RB cell proliferation indicates the implication of these synthetic DNA oligos (HMGA2-aptamer), as suitable adjuvant therapeutic intervention in RB management.

b) Heat shock proteins as therapeutic target in RB

The expressions of heat shock proteins (HSP-70, 90) and survivin is well reported in other cancers and its association with the proliferative index (Ki67) is documented in RB. The present study **[chapter 6.0]** was carried out to understand the association between these HSP proteins and survivin in RB primary tumors (n=30, spearman correlation, r^2=, p value=), we have used a peptido-mimetic, a structure based peptide (TAT-conjugated Shepheridin) to inhibit the physical interaction of Hsp90 and survivin in *in vitro* RB cell

line (Y79 and Weri Rb-1). The addition of these peptides in serum deficient condition has resulted in the destabilisation of survivin protein, suppression of Bcl2 protein and induction of apoptotic proteins namely Bim, Bax and caspase 9. Further, shepheridin treatment has resulted increase in cellular apoptosis (Annexin V FLUOS stain) and reduction in the cell proliferation (CyQUANT assay) and cell viability (MTT assay). These data together, is a good indication of using these molecules as one of the future therapeutic interventions in RB management.

c) miRNAs regulating post-transcriptional genes, as therapeutic targets in RB management

At present, the study on the dys-regulation of genes by miRNA contributes a novel therapeutic approach for the cancer management. miRNAs being a class of endogenous small RNA molecules elicits their effects on the target genes either by repressing their translation or by mRNA degradation. So identification of various miRNAs, regulating a panel of oncogenes involved in the RB tumorigenesis would enable a better understanding of RB pathobiology in tumor progression. In the current study **[chapter 7.0]**, using a comprehensive bio-informatics approach, we have demonstrated two key miRNAs (*miR-486-3p and miR-532-5p*) regulating a panel of genes reported earlier in RB tumorigenesis (Balla et al. 2009, Castera et al. 2010, Felsher 2013, Li J. et al. 2012b, Mitra et al. 2012, Mohan et al. 2006, Vandhana et al. 2011, Venkatesan et al. 2009, Zhang J. et al. 2012a). In this approach, we have considered three groups of genes namely group1: oncogenes which include high mobility group –A2 (*HMGA2*) *(Venkatesan et al. 2009)*, *N*-myc proto-oncogene protein *(MYCN) (Felsher 2013)*, spleen tyrosine kinase (*SYK*) *(Zhang J. et al. 2012a)*, Fatty acid synthase *(FASN) (Vandhana et al. 2011)*, group 2: genes involved in cancer cell stemness which includes Epithelial cell adhesion molecule *TACSTD1 (EpCAM)(Mitra et al. 2012)*, ATP-binding cassette sub-family G member 2, *ABCCG2 (Mohan et al. 2006)*, cluster of differentiation 24 *(CD24) (Li J. et al. 2012b)*, cluster of differentiation 133 (*CD133)* and cluster of differentiation 44 (*CD44) (Balla et al. 2009)*, and group 3: cell cycle regulatory genes which includes cluster of differentiation (*p53)* and Mouse double minute 2 homolog *(MDM2) (Castera et al. 2010)*. An *in silico* approach using the predictive tools including Microcosm, DIANALAB, miRBase v18, REFSEQ database and RNA Hybrid was used to determine the miRNA-mRNA interactions. Further, from this list of miRNAs, the highly regulated miRNAs are filtered

based on their MFE (Minimal Free Energy of <= - 30 and p-value of <=0.05) and those that are reported in MICROCOSM and DIANA LAB databases.

Based on these results, we have selected three miRNAs namely *miR-146b-5p, miR-532-5p and miR-142-5p* from the up-regulated miRNAs panel while two miRNAs namely *miR-328 and miR-486-3p* from the down-regulated list for the validation in RB primary tumor tissues. Relative to normal cadaveric donor retina, the miRNA expression analysis in RB primary tumor tissues (n=30) by qRT-PCR revealed a median fold change of *miR-486-3p* (in the order of invasion = -1.26, no invasion = -1.07); *miR-532-5p* (in the order of invasion = -0.69, no invasion of =-1.00); *miR-142* (in the order of invasion= -0.18, no invasion = -0.17); *miR-146b* (in the order of invasion = -0.73, no invasion=-0.87); and *miR-382* (in the order of invasion =-0.70, no invasion= -0.59). The median fold change of all these 5 miRNAs in normal cadaveric adult donor retina is in the order of *miR-486-3p*: -0.14; *miR-532-5p*: -0.01; *miR-142*: 0.24; *miR-146b*: 0.14; and *miR-382*: 0.19. Interestingly, we observed down-regulation of all the validated miRNAs relative to the normal donor retina. In addition, the identified miRNAs (*miR-486-5p, miR-532-3p*) regulatory role along with its target genes (*SYK and FASN*) in RB tumorigenesis has been addressed by *in vitro* experimental validations using RB cell lines (Y79 and Weri Rb1) using mimics. Interestingly, mimics of *miR-486-5p* and *miR-532-3p* resulted in the reduction of RB cell growth but no significant change was observed in cell cycle phase compared to the scramble transfected RB cells as negative control. Taken together, these results indicate that *miR-486-5p* and *miR-532-3p* regulating the oncogenes *SYK* and *FASN*, as potential therapeutic targets in RB management.

d) Identification of genes involved in chemo-modulation of RB

Chemotherapy plays a major role in RB management however, drug resistance and drug dosage related side effects are some of the current clinical limitations. There is a need for molecular information on drug resistance genes in RB [**chapter 8.0**]. Here, we have analyzed differential gene expression (two post-chemotherapy tumors and one pre chemotherapy RB tumor tissues) using Affymetrix Human Genome U133 plus 2.0 array chips and identified the genes which are influenced by chemotherapy. PCA (Principle Component Analysis), Gene ontology, phenotype, Bio markers, Pathway Enrichment

analysis and Biological Analysis Network (BAN) modeling was carried out to identify the significantly regulated genes in post-chemo treated RB primary tumor tissues. RB tumor tissues revealed an up -regulation of 1672 genes and 2538 down-regulated genes. Unsupervised hierarchical clustering of differentially expressed gene sets showed 1419 genes as common between pre-chemotherapy RB and post-chemotherapy RB primary tumor tissues. GoElite analysis of merged differentially expressed genes revealed 21 key gene ontology categories, pathways, biomarkers and phenotype groups dys-regulated, harbouring 250 differentially expressed genes. We observed there is deregulation of key genes namely *EZH2, NCoR1, MYBL2, RB1, STAMN1, SYK, JAK1/2, STAT1/2, PLK2/4, BIRC5, LAMN1*. We observed 3 significant genes associated with drug resistance - Ect2, *PRAME* and a well known drug resistant gene *ABCC4*.

We validated the expression of two significantly up-regulated genes — Epithelial cell transforming sequence 2 (Ect2), and preferentially expressed Antigen in Melanoma (PRAME) ($p \leq 0.05$) using qRT-PCR in primary RB tumor tissues [n=21] and by immunohistochemistry for PRAME protein expression [n=21]. Vector mediated PRAME over-expression in cultured RB cells (Y79) were used to test the association between *PRAME* and drug resistance gene *MRP1*. However, there was no up regulation of *MRP1* in *PRAME* over expressed RB cells. Further, in these PRAME over-expressed cells, the IC_{50} of vincristine, etoposide and carboplatin were 0.86µM/ml, 4.13 µg/ml, and 31.93µg/ml respectively and these values were close to the corresponding IC_{50} values in untransfected cells (0.97µM/ml, 5.23µg/ml, and 34.53µg/ml respectively.

In post-chemotherapy RB tumor tissues (which did not respond to chemotherapy), Ect2 gene is expressed in response to stress induced due to chemotherapy. Thus, PRAME does not contribute to drug resistance in RB. These results would widen the area of research in these gene regulations contributing either to chemo resistance or to RB tumoriogenesis. Further, the positive correlation between Ect2 and drug response modulation in RB reported here offers a potential for further explorations at the molecular level. The over-expressed PRAME does not directly influence response of RB tumors to chemotherapy, which is substantiated by the lack of marked up-regulation of *MRP1* in PRAME over-expressed RB cell line, and also by the lack of a substantial change in IC_{50} doses of standard chemotherapeutic drugs. However, the nuclear localization of over-expressed PRAME protein possibly implicates its role in gene regulation. The network analysis performed here presents some evidence for the regulatory role of PRAME in RB.

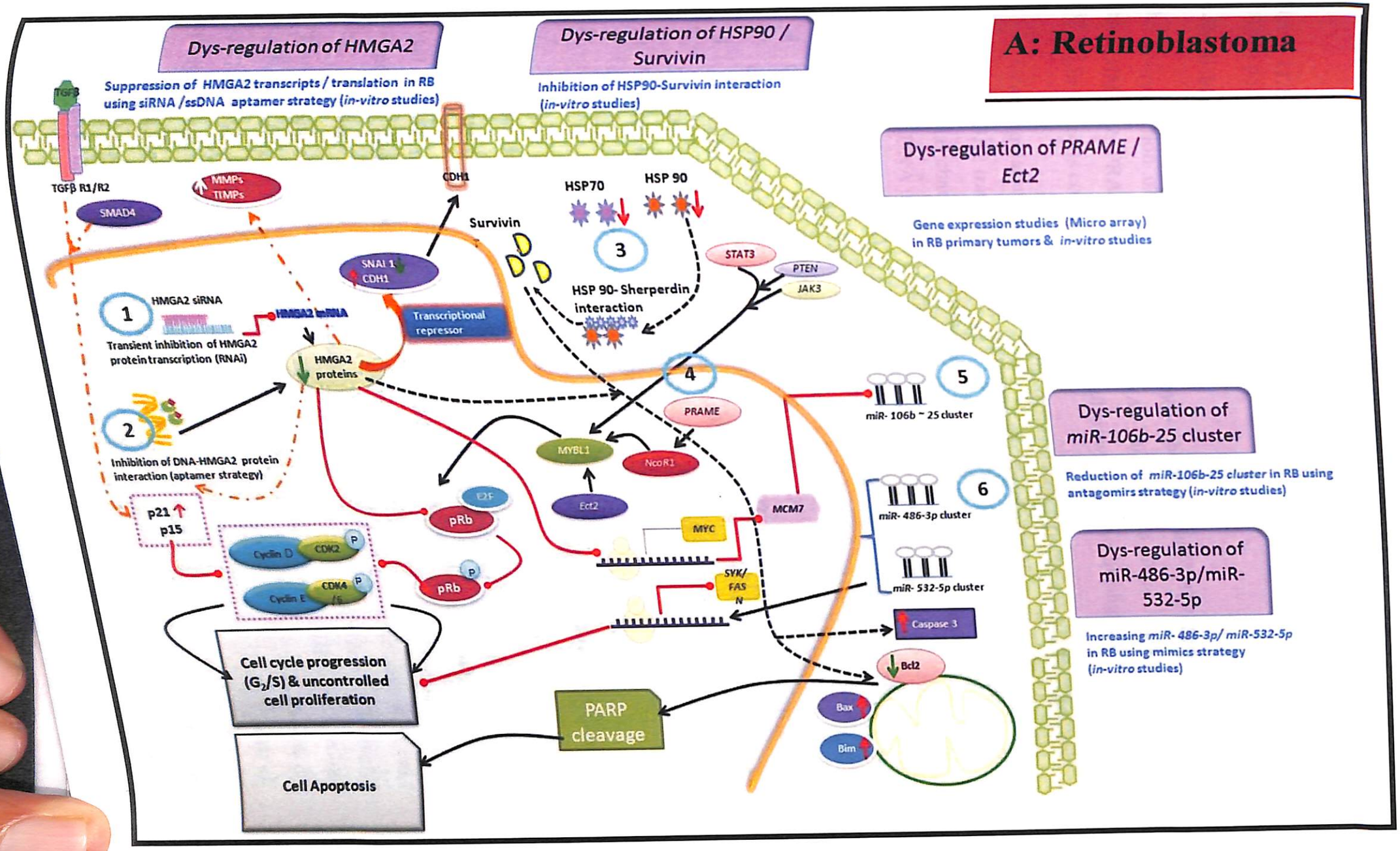
A: Retinoblastoma
Dys-regulation of HMGA2
Suppression of HMGA2 transcripts / translation in RB using siRNA /ssDNA aptamer strategy (in-vitro studies)
Dys-regulation of HSP90 / Survivin
Inhibition of HSP90-Survivin interaction (in-vitro studies)
Dys-regulation of PRAME / Ect2
Gene expression studies (Micro array) in RB primary tumors & in-vitro studies
Dys-regulation of miR-106b-25 cluster
Reduction of miR-106b-25 cluster in RB using antagomirs strategy (in-vitro studies)
Dys-regulation of miR-486-3p/miR-532-5p
Increasing miR- 486-3p/ miR-532-5p in RB using mimics strategy (in-vitro studies)
TGFβ
TGFβ R1/R2
SMAD4
MMPs
TIMPs
CDH1
Survivin
HSP70
HSP 90
HSP 90- Sherperdin interaction
STAT3
PTEN
JAK3
SNAI 1
CDH1
Transcriptional repressor
HMGA2 siRNA
Transient inhibition of HMGA2 protein transcription (RNAi)
HMGA2 proteins
Inhibition of DNA-HMGA2 protein interaction (aptamer strategy)
PRAME
MYBL1
NcoR1
Ect2
MCM7
MYC
E2F
pRb
p21
p15
Cyclin D
CDK2
Cyclin E
CDK4 /6
SYK/ FAS N
miR- 106b ~ 25 cluster
miR- 486-3p cluster
miR- 532-5p cluster
Caspase 3
Bcl2
Bax
Bim
Cell cycle progression (G2/S) & uncontrolled cell proliferation
PARP cleavage
Cell Apoptosis

Figure 11.1: Molecular dys-regulations in RB. Schematic representation of the molecular insights postulated in the current thesis.

A.Retinoblastoma

The dys-regulation of proteins [HMGA2, heat shock proteins (HSP 70/90, Survivin], genes [HMGA2, PRAME, and Ect2], miRNAs [*miR-106b-25 cluster, miR-486-3p, miR-532-5p*] in RB cells contributing to the RB cell growth arrest are highlighted.

1. Gene regulatory network shows the dysregulation resulted due to the suppression of HMGA2 transcripts in RB cells using RNAi technology.
2. Molecular changes due to the inhibition of the HMGA2 protein interaction with B-form of DNA using phosphorothioate modified DNA aptamer strategy.
3. Inhibition of heat shock protein (HSP90) and Survivin physical interaction using structure based peptido-mimetic shepheridin resulting in the RB cell death.
4. Contribution of *PRAME, Ect2, NcoR1* and *MYBl1* to RB tumorigenesis in chemotherapy non-responding RB primary tumors.
5. Molecular changes due to *miR-106b-25 cluster* dys-regulation in RB cells in the presence of *HMGA2* siRNA and *miR-106b-25* cluster antagomirs.
6. Suppression of *SYK/ FASN* oncogenes in the presence of *miR-486-3p* and *miR-532-5p* endogenous copies (mimics strategy).

e) **Delineation of dysregulated miRNAs, a prognostic implication of uveal melanoma**

Uveal Melanoma has been observed with 3 fold higher incidences in white races compared to dark pigmented races and is rare in Indian populations (1998b, Kuo et al. 1982, Manohar et al. 1991, Margo C. E. and McLean 1984). Despite accuracy in diagnostic and therapeutic modulations resulted in better eye preservations (1990, Augsburger et al. 1990, Finger 1997), but the median survival rate remains alarmingly high (Kujala et al. 2003, Singh and Topham 2003a). Early metastasis could be the possible underlying mechanism irrespective of tumor size (Callejo et al. 2007). About 40-50% of melanoma patients result in liver metastasis within the period of 10 years from the onset of primary disease, with median survival rate is of 2-7 months, and less than a year in 10% (2001, Shields et al. 1991b). Hepatic metastasis is the most common cause for the

mortality of UM patients. The current molecular prognostic indicators in UM includes aberrations in chromosomes 1, 3, 8 (Singh et al. 2012) and varied expressions of heat shock protein 27 (HSP27) (Jmor et al. 2012).

One of the main objectives in the current dissertation [**chapter 9 and 10**], is to predict the differentially expressed miRNAs between monosomy 3 and disomy, and to associate these miRNAs with the clinico-pathological parameters in Indian population with uveal melanoma. The study [**chapter 9**] includes formalin fixed paraffin embedded (FFPE) eyeballs harbouring the uveal melanoma (n=86), normal melanocytes (cadaveric eye balls n=5). The expression profile of miRNAs was obtained in three monosomy and two disomy samples. These expression profiles were analysed by unsupervised analysis (Principal Component Analysis) and supervised analysis (Significance analysis of microarray). The expression of 8 miRNAs: *miR-214, miR-143, miR-146b, miR-149, miR-134, miR-1238, miR-199a* and *let7b* were validated using qRT-PCR. Univariate and multivariate analyses was used to analyse the association between these miRNAs and clinico-pathological parameters. Partial deletion of chromosome 3 (monosomy) was detected in 60.46% (52/86) and the presence of both the copies of chromosome 3 (disomy) was detected in 39.53% (34/86) of melanoma tumors (n=86). In the metastasis group (n=17), monosomy 3 was detected in 52.94% (9/17) and disomy was detected in 47.05% (8/17). A significant correlation of the monosomy 3 detection was with respect to HSP 27 expression (p=0.021), tumor base (p value=0.002). Unsupervised, cluster analysis revealed a total of 585 differentially expressed miRNAs. Filtering of miRNA expression using ANOVA demonstrated 25 up-regulated miRNAs in monosomy 3 and 26 miRNA's in disomy 3 tumors. Significance Analysis of Microarray (SAM) demonstrated 82 differentially expressed miRNA's with the false discovery rate set to Q = 0.0. *miR-134, miR-214, miR146b, miR-143 and miR-199a* expressions were discriminating monosomy and disomy 3 tumors. *miR-134 and miR-149** showed statistically significant association with liver metastasis. Finally, the current study has identified five key miRNAs associated with monosomy 3 and two miRNAs associated with liver metastasis among Indian population with uveal melanoma.

f) Gene targets of select miRNAs, a prognostic and therapeutic implications in UM

In **chapter 10,** mRNA expression of the gene targets namely *SMAD4, HDAC8, KIT, WISP1* and *HIPK1* of the select miRNAs were analysed using qRT-PCR.

To conclude, the present dissertation states the implication of various molecules in the prognostic and therapeutic application of RB (childhood cancer) and UM (adult cancer). The salient conclusions of this study are as follows

1. High mobility group of (HMG) A2 (transcripts and proteins) as a potential therapeutic target molecule in RB management
2. miRNAs namely *miR 106b~25 cluster, miR-486-5p* and *miR-532-3p* as potential targets in RB gene therapy
3. Blockade of physical interaction of HSP 90 and survivin using a peptido-mimetic, could serve as adjuvant therapy in RB management.
4. Functional role of *PRAME, ECT2* (chemo-sensitizer) in chemo treated RB patients.
5. Implication of eight miRNAs in UM tissues, which includes *miR-214, miR-143, miR-146b, miR-149, miR-134, miR-1238, miR-199a* and *let7b* as prognostic indicator discriminating the metastasis free survival of UM tumors.
6. Reporting the gene expression levels of *SMAD4, HDAC8, KIT, WISP1* and *HIPK1* (predicted gene targets of the reported miRNAs in the current dissertation) in UM tumors.

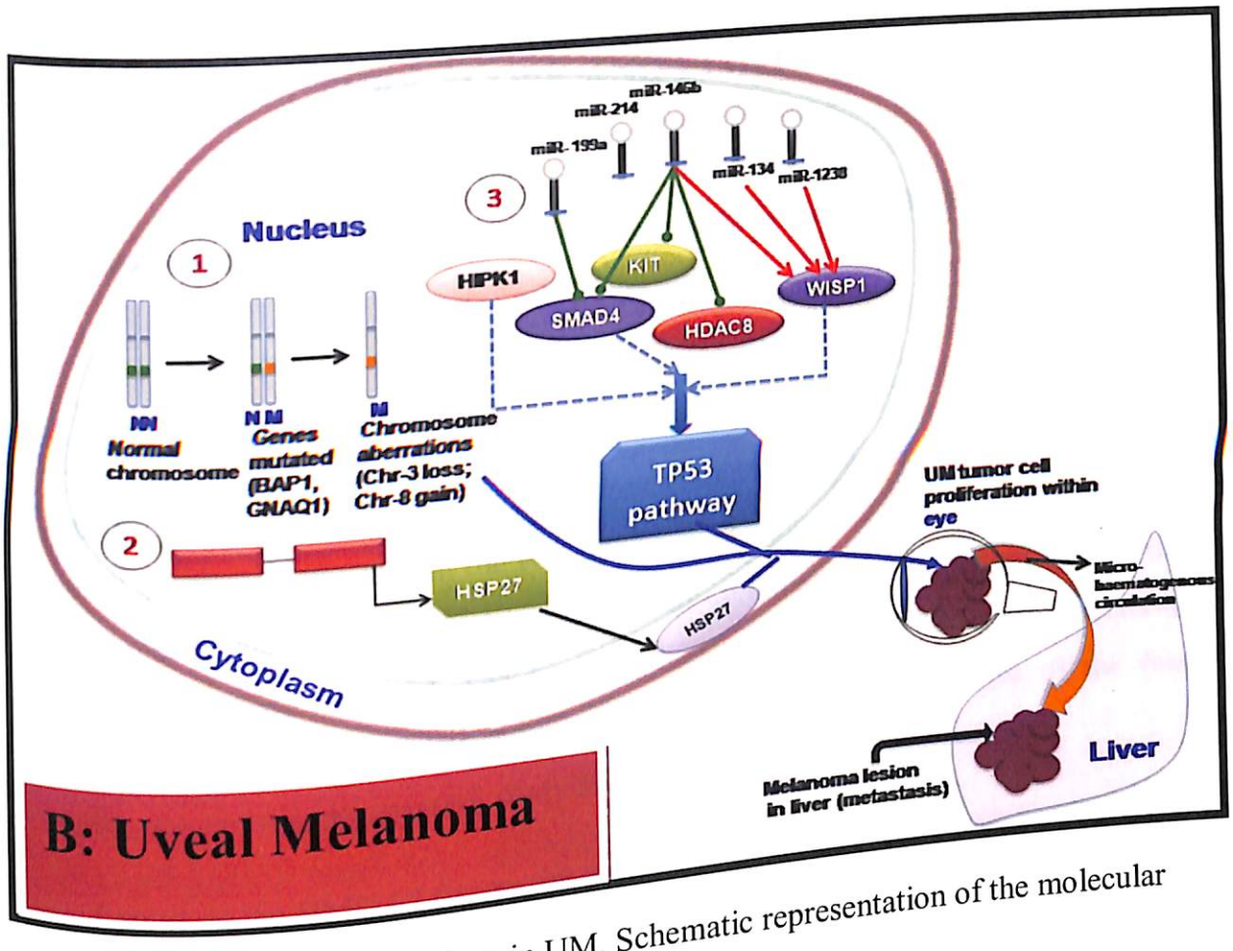

Figure 11.2: Molecular regulations in UM. Schematic representation of the molecular regulations postulated in the current thesis.

B. Uveal melanoma

Study on the molecular changes contributing to the risk factor of liver metastasis in uveal melanoma through micro-haematogenous route

1. Presence of Chromosomal aberrations: Partial or complete deletion of chromosome 3
2. Presence of proteins: heat shock proteins (HSP27)
3. Presence of miRNAs/ regulatory gene targets: *miR-214, miR-199a, miR-146b, miR-134 and miR-1238* in the progression of uveal melanoma cells.

The black arrow headed lines and red coloured arrow headed dotted lines indicate the positive regulation of the pathway. The red and green lines with blunt head indicate the suppression of the pathway. The green coloured arrow indicates down-regulation of molecules while red coloured arrow indicates up-regulation of the molecules.

CHAPTER 12: FUTURE SCOPE AND LIMITATION OF THE STUDY

FUTURE SCOPE:

This dissertation has detailed the mechanistic signatures of some candidate molecules (miRNAs, genes, proteins) in the two main ocular cancers – Retinoblastoma (RB) and Uveal melanoma (UM). A number of networks contributing to the progression of these cancers have been analysed. These studies have paved way for further exploration of the associated pathways that need to be addressed in future. Some of the future implications of this dissertation study are:

1. Report on the HMGA2 (transcript and protein), a potential therapeutic target in RB management has opened a wide area of research to work on the **delivery systems** of nucleic acids (RNA and DNA) to suppress its function. The present advancement of gene therapy with the **use of chimeras** (integrating the complementary RNA sequence of HMGA2 transcript and DNA aptamers of HMGA2 proteins) would be a better choice to improve the efficacy of silencing HMGA2 both at transcription and translation level. Further, the addition of ***in vivo* studies** with the chimeras tagged with the liposomal delivery systems would provide us the better scope of targeting HMGA2 in RB disease management.

2. Further studies such as *in silico* molecular docking of HMGA2 protein with the DNA aptamers (simulations) can be attempted which would reveal a better understanding of the interaction of the protein ('AT hooks') with that of the complementary DNA aptamers.

3. Report on the structure based peptide, shepherdin to block the physical interaction of HSP 90 and survivin can be taken forward for ***in vivo* studies** to know the low toxicity and low immunogenic property of this peptido-mimetic molecule.

4. The current dissertation has revealed a list of miRNAs regulating the known candidate genes in RB tumoriogenesis (*HMGA2, FASN, SYK, MCYN, TACSTD1,*

ABCCG2, CD24, CD133, CD44, p53, MDM2). However, the functional evaluation of only two (spleen tyrosine kinase, *SYK* and fatty acid synthase, *FASN*) of these **post-transcriptional regulators** has been indicated in the current dissertation. Further studies on the other miRNAs can be established which would contribute for the better understanding of their role in RB tumoriogenesis.

5. Gene expression analysis on chemo-treated RB versus non-chemo RB has revealed a list of gene networks namely NcoR1, MYBL2, STAMN1, and PLK2/4, which can be elaborated further for the **functional studies using *STAMN1* and *PLK2/4* RNAi**. These studies would implicate the gene regulatory role contributing to the chemo resistance of the RB.

6. List of dysregulated miRNAs (n=5) indicated in the current dissertation showed a significant association between the high risk and low risk UMs in a cohort size of 86 tumors under study. A qRT-PCR based study on this panel of miRNA in a larger sample size would implicate a **diagnostic tool** for the higher precision of high risk UM tumors.

7. Further studies, by investigating these de-regulated miRNAs (*miR-214, miR-149*, miR-143, miR146b, miR-199a and let7b, hsa-miR-1238 and hsa-miR-134*), using a smaller quantity of samples such as fine needle aspiration biopsy (FNAB) would **facilitate the clinicians to plan for the diagnostic investigation**

8. **Bio-informatic analysis** of the de-regulated miRNAs including its location, mapping of its promoter regions, its post-transcriptional regulators would add up the list of miRNA-mRNA networks. Attention to these networks would aid us to better understand the patho-biology of UM.

9. Study on the delineated miRNAs stating the prognostic implication of UM has widened the **futuristic scope of *in vitro* studies using primary cultures** to understand the role of these miRNAs in UM tumor progression.

10. miRNA-mRNA regulatory networks of UM has revealed the significance of genes which includes *SMAD4, HDAC8,c-KIT, WISP1,* and *HIPK1* in UM progression. Functional evaluation of these genes and its regulators using RNAi in primary cultures would indicate more significant results contributing to the **therapeutic strategies in UM**.

LIMITATION OF THE STUDY:

The current study reveals the implication of various therapeutic molecules using nucleic acid and peptide based strategy in the clinical management of retinoblastoma. This in turn needs further confirmation on the stability and cytotoxicity studies at *in vivo* level using respective experimental models. *In silico* analysis carried over in the study to derive the mRNA-miRNA interactions may be addressed by the other competitive assays such as luciferase reporter assay. Validation of miRNAs associated with monosomy 3 in uveal melanoma in larger sample size with clinical follow-up would implicate them as furistic prognostic and or therapeutic biomarkers.

BIOGRAPHY OF Ms. NALINI VENKATESAN

I, **Ms. Nalini Venkatesan** (Ph.D. student, Dept. of Biological Sciences, BITS Pilani in collaboration with Sankara Nethralaya) have completed Master of Science in Medical Laboratory Technology (MSMLT) programme and CGPA-9.6 in May 2010, at Medical Research Foundation, Sankara Nethralaya, and an off-campus centre of BITS Pilani. I have completed my undergraduate (B.Sc., Microbiology) at University of Madras, in 1999, and certificate course of Medical laboratory Technology (CMLT), in 2001.

From 2001- 2007, I served as technologists in various research projects approved by ICMR in Vision Research Foundation, Sankara Nethralaya. From 2010, I am serving as Senior Research Fellow, in Department of Science and Technology (DST) and Department of Bio-technology sanctioned projects in Vision Research Foundation, Sankara Nethralaya.

My research areas of interest are in understanding Retinoblastoma and Uveal melanoma tumor biology, diagnostic and therapeutic implications of miRNA-mRNA interactions.

Awards and/or other recognitions received:

- Dr.H.N.Madhavan Endowment Award for Best Outgoing student in Master of Science (Medical Laboratory Technology, Year 2007-2010).
- Sankara Nethralaya Silver Jubilee Award for best performance in Microbiology (2010).
- Hi-Media performance Private Limited Endowment Award for best performance in Clinical Microbiology (2010).
- Sankara Nethralaya Silver Jubilee Endowment Award for Best Performance in Biochemistry Research Department (2010).

Peer-Review journals published:

2010-till date

1. **# Nalini Venkatesan** P. R. Deepa, Madavan Vasudevan, Vikas Khetan, Ashwin M. Reddy, Subramanian Krishnakumar, Integrated analysis of dysregulated miRNA-gene expression in HMGA2-silenced retinoblastoma cells, Bioinform Biol Insights. 2014 Sep 4;8:177-91

2. **# Nalini V**, Segu R, Deepa PR, Khetan V, Vasudevan M, Krishnakumar S. Molecular Insights on Post-chemotherapy Retinoblastoma by Microarray Gene Expression Analysis.Bioinform Biol Insights. 2013 Sep 18;7: 289-306.

3. Sudhakar J, **Venkatesan N**, Lakshmanan S, Khetan V, Krishnakumar S, Biswas. Hypoxic tumor microenvironment in advanced retinoblastoma. J.Pediatr Blood Cancer. 2013 Oct; 60(10):1598-601

4. Beta M*, **Venkatesan N***, Vasudevan M, Vetrivel U, Khetan V, Krishnakumar S. Identification and Insilico Analysis of Retinoblastoma Serum microRNA Profile and Gene Targets Towards Prediction of Novel Serum Biomarkers. Bioinform Biol Insights. 2013; 7:21-34 (* Authors share equal contribution)

5. **# Nalini Venkatesan**, Dr. S. Krishnakumar, Role of molecular genetic testing in choroidal melanomas; Journal of TamilNadu Ophtalmic Association (TNOA) Volume: 51, Issue 1 January 2013

6. **# Nalini Venkatesan,** Subramanian Krishnakumar, Perinkulam Ravi Deepa, Murali Deepa, Vikas Khetan, M. Ashwin Reddy, Molecular deregulation induced by silencing of the high mobility group protein A2 gene in retinoblastoma cells, Molecular Vision 2012; 18:2420-2437.

2004- 2009

1. Krishnakumar S, Mallikarjuna K, Desai N, Muthialu, A, **Venkatesan N**, Sundaram A, Khetan V, Shanmugam MP. Multidrug-Resistant Proteins: - P- glycoprotein and Lung Resistance Protein Expression in Retinoblastoma. Br J Ophthalmol. 2004 Dec; 88(12): 1521-6.
2. Krishnakumar S, Mallikarjuna K, Mohan A, Iyer A, **Venkatesan N**, Shanmugam MP, Gopal L, Biswas J. Expression of Fas ligand in Retinoblastoma: Contribution to Tumor Escape Mechanisms. Cancer. 2004 Oct 1; 101(7): 1672-6
3. Krishnakumar S, Mohan A, Mallikarjuna K, **Venkatesan N**, Shanmugam MP, Heidenreich LR. EpCAM Expression in Retinoblastoma: A Novel Molecular Target for Therapy. Invest Ophthalmol Vis Sci. 2004 Dec; 45(12): 4247-50.
4. **S.** Krishnakumar, M. Adithi, **Venkatesan N**. Role of Nitric Oxide Synthases and Nitrotyrosine in Retinoblastoma Cancer 2005 Apr 15; 103(8): 1-11.
5. Mohan A, Mallikarjuna K, **Venkatesan N,** Abhyankar D, Parikh PM, Krishnakumar S. The study of c-Src kinase and pStat3 protein expression in retinoblastoma. Exp Eye Res. 2006 May 19;
6. Mohan A, Mallikarjuna K, **Venkatesan N,** Hema Ramkumar, Ishwarya, Krishnakumar S. Retinoblastoma- Expression of HLA-G. Ocul Immunol Inflamm. 2006 Aug; 14(4):207-13.
7. Adithi M, **Venkatesan N,** Mallikarjuna K, Gopal L, Krishnakumar S. Expressions of Rac1, Tiam1 and Cdc42 in Retinoblastoma. Experimental Eye Research, 2006 Dec; 83(6):1446-52.
8. Adithi M, **Venkatesan N,** Mallikarjuna K, Biswas J, Krishnakumar S. Expression of Motility-Related Protein MRP1/CD9, N-Cadherin, E-Cadherin, Alpha-Catenin and Beta-Catenin in Retinoblastoma. Experimental Eye Research Exp Eye Res. 2007 Apr; 84(4):781-9. Epub 2007 Jan 9.
9. Adithi M, **Nalini V**, Kandalam M, Krishnakumar S. Expression of matrix metalloproteinases and their inhibitors in retinoblastoma. J Pediatr Hematol Oncol. 2007 Jun; 29(6):399-405.
10. Krishnakumar S, Mohan A, Kandalam M, Ramkumar HL, **Venkatesan N**, Das RR SRPK1: a cisplatin sensitive protein expressed in retinoblastoma. Pediatr Blood Cancer. 2008 Feb; 50(2):402-6.

11. Adithi M, **Nalini V**, Kandalam M, Krishnakumar S. Expression of p63 and p73 in retinoblastoma: a clinicopathological correlation study. Exp Eye Res. 2008 Oct; 87(4):312-8.

12. Mohan A, **Venkatesan N**, Kandalam M, Pasricha G, Acharya P, Khetan V, Gopal L, Sharma T, Biswas J, Krishnakumar S. Detection of human papillomavirus DNA in retinoblastoma samples: a preliminary study. J Pediatr Hematol Oncol. 2009 Jan; 31(1):8-1.

13. Deepa PR, **Nalini V**, Mallikarjuna K, Vandhana S, Krishnakumar S. Oxidative stress in retinoblastoma: correlations with clinicopathologic features and tumor invasiveness. Curr Eye Res. 2009 Dec; 34(12):1011-8.

14. Mohan A, **Venkatesan N**, Kandalam M, Pasricha G, Acharya P, Khetan V, Gopal L, Sharma T, Biswas J, Krishnakumar S Detection of human papillomavirus DNA in retinoblastoma samples: a preliminary study.J Pediatr Hematol Oncol. 2009 Jan; 31(1):8-13.

15. **# Venkatesan N**, Kandalam M, Pasricha G, Sumantran V, Manfioletti G, Ono SJ, Reddy MA, Krishnakumar S. Expression of high mobility group A2 protein in retinoblastoma and its association with clinicopathologic features. J Pediatr Hematol Oncol. 2009 Mar;31(3):209-14

Participation in Conferences:

1. Presented the **poster** titled " *Identification Of Oncomirs In Uveal Melanoma : A Biomarker Tool In Predicting The Metastasis*" **Nalini Venkatesan*** , Abirami Radhakrishnan, Nirmala BadhriNarayanan, Vikas Khetan, Lingam Gopal, Jyothirmay Biswas, Amit Nagpal , Subramanian Krishnakumar,* MSMLT student, BITS, Pilani. in RNAi conference held at CCMB Hyderabad from December 4th – 6th 2009.
2. Presented the **poster** titled " *Differential gene expression induced by High Mobility Group Proteins (HMG) A2 gene silencing in Retinoblastoma cancer cells*" **Nalini Venkatesan**, P.R.Deepa, Ashwin M Reddy, Subramanian Krishnakumar1in The XXXV All India Cell Biology conference and symposium on Membrane dynamics and disease conference held, from 16 - 18 December 2011 at National Institute of Science Education and Research (NISER), Bhuvaneswar, India.

3. Presented an **oral presentation** titled *"Expression of select miRNAs in retinoblastoma cancer tissues: in vitro analysis of their functions using antagomirs"* **NaliniVenkatesan**, Dr.S.Krishnakumar, P.R.Deepa, M.Ashwin Reddy, in the 20th Annual Meeting , Indian Eye Research Group (IERG-ARVO India Chapter) held from July 28 - 29, 2012 at LVPE institute, Hyderabad, India.
4. Presented the **poster** titled "Down- regulation of *miR-532-5p* and *miR- 486-3p* contributes to Retinoblastoma tumorigenesis: *in vitro* analysis of their functions using miRNA mimics", Nalini Venkatesan, Dr. P. R. Deepa, Dr. M. Yamuna, Dr.S.Krishnakumar conducted by Society of Biological Chemists (SBCI) held from December 3-5, 2013 at University of Hyderabad, India.

[1]Participation in Workshops

1. Attended the "Next generation Deep sequencing for the whole human exons, Illumina platform" conducted by Genotypic technologies, Bangalore (2011).
2. Attended the "National level Bioinformatic workshop" conducted at Loyola College, Chennai, India (2012).

 # Indicates the publications, presentations and participation of workshops relevant to the current Ph.D. dissertation.

BIOGRAPHY OF Dr. S.KRISHNA KUMAR

BIOGRAPHY OF Dr. P.R.DEEPA

Dr. P. R. Deepa (Associate Professor, Dept. of Biological Sciences, BITS Pilani) has been involved (since 2005) in teaching and co-ordination at off-campus collaborative programmes of *BITS Pilani — Chennai Centre*. She also serves as Course Instructor for students from BITS, Pilani during their internship (Practice School – *I and II*) at several industries and research organizations in Chennai, Hyderabad and Bangalore.

Dr. Deepa has been collaborating with the Department of Ocular Pathology, Sankara Nethralaya (Chennai) for ongoing research in the evaluation of molecular targets for diagnosis and therapy of retinoblastoma. Her other collaborative research efforts are in the areas of bio-mathematical modelling, bioinformatics, and bio-chemical engineering. She earned her doctoral degree in 2005 for her research titled *"Biochemical Evaluation of a Low-Molecular Weight Heparin (certoparin sodium) in Experimental Atherogenic and Cytotoxic Conditions"* (Dept. of Medical Biochemistry, University of Madras, 2005). Her first Ph.D. student graduated in June 2013 where the dissertation focused on lipogenic target in RB. Presently she is supervising three Ph.D. research scholars and a DBT-Senior Research Fellow in the broad areas of retinoblastoma, cancer biology, lipogenic targets, bioinformatics, and protein biochemistry.

1990. Accuracy of diagnosis of choroidal melanomas in the Collaborative Ocular Melanoma Study. COMS report no. 1. Arch Ophthalmol 108: 1268-1273.

1998a. Histopathologic characteristics of uveal melanomas in eyes enucleated from the Collaborative Ocular Melanoma Study. COMS report no. 6. Am J Ophthalmol 125: 745-766.

1998b. The Collaborative Ocular Melanoma Study (COMS) randomized trial of pre-enucleation radiation of large choroidal melanoma I: characteristics of patients enrolled and not enrolled. COMS report no. 9. Am J Ophthalmol 125: 767-778.

2001. Assessment of metastatic disease status at death in 435 patients with large choroidal melanoma in the Collaborative Ocular Melanoma Study (COMS): COMS report no. 15. Arch Ophthalmol 119: 670-676.

Aalto Y, Eriksson L, Seregard S, Larsson O, Knuutila S. 2001. Concomitant loss of chromosome 3 and whole arm losses and gains of chromosome 1, 6, or 8 in metastasizing primary uveal melanoma. Invest Ophthalmol Vis Sci 42: 313-317.

Abe N, Watanabe T, Suzuki Y, Matsumoto N, Masaki T, Mori T, Sugiyama M, Chiappetta G, Fusco A, Atomi Y. 2003. An increased high-mobility group A2 expression level is associated with malignant phenotype in pancreatic exocrine tissue. Br J Cancer 89: 2104-2109.

Abramson DH, Gombos DS. 1996. The topography of bilateral retinoblastoma lesions. Retina 16: 232-239.

Adithi M, Nalini V, Kandalam M, Krishnakumar S. 2007. Expression of matrix metalloproteinases and their inhibitors in retinoblastoma. J Pediatr Hematol Oncol 29: 399-405.

Ahmed FE, et al. 2013. Diagnostic microRNA markers to screen for sporadic human colon cancer in stool: I. Proof of principle. Cancer Genomics Proteomics 10: 93-113.

Albert DM KA, ed. 2011. Intraocular melanoma. 9th ed. Philadelphia, Pa: Lippincott Williams & Wilkins

Altieri DC. 2003. Validating survivin as a cancer therapeutic target. Nat Rev Cancer 3: 46-54.

Amaral FC, Torres N, Saggioro F, Neder L, Machado HR, Silva WA, Jr., Moreira AC, Castro M. 2009. MicroRNAs differentially expressed in ACTH-secreting pituitary tumors. J Clin Endocrinol Metab 94: 320-323.

Anand A, Chada K. 2000. In vivo modulation of Hmgic reduces obesity. Nat Genet 24: 377-380.

Andersen MH, thor SP. 2002. Survivin--a universal tumor antigen. Histol Histopathol 17: 669-675.

Andrieux J, Demory JL, Dupriez B, Quief S, Plantier I, Roumier C, Bauters F, Lai JL, Kerckaert JP. 2004. Dysregulation and overexpression of HMGA2 in myelofibrosis with myeloid metaplasia. Genes Chromosomes Cancer 39: 82-87.

Angel P, Karin M. 1991. The role of Jun, Fos and the AP-1 complex in cell-proliferation and transformation. Biochim Biophys Acta 1072: 129-157.

Anteby I, Ramu N, Gradstein L, Miskin H, Pe'er J, Benezra D. 1998. Ocular and orbital complications following the treatment of retinoblastoma. Eur J Ophthalmol 8: 106-111.

Augsburger JJ. 1993. Is observation really appropriate for small choroidal melanomas. Trans Am Ophthalmol Soc 91: 147-168; discussion 169-175.

Augsburger JJ, Gamel JW, Lauritzen K, Brady LW. 1990. Cobalt-60 plaque radiotherapy vs enucleation for posterior uveal melanoma. Am J Ophthalmol 109: 585-592.

Bakhshi S BR. 2007. Genetics and management of retinoblastoma. J Indian Assoc Pediatr Surg 12: 109-111.

Bakri MM, Rich AM, Cannon RD, Holmes AR. 2014. In vitro expression of Candida albicans alcohol dehydrogenase genes involved in acetaldehyde metabolism. Mol Oral Microbiol.

Balaguer F, et al. 2011. Colorectal cancers with microsatellite instability display unique miRNA profiles. Clin Cancer Res 17: 6239-6249.

Balla MM, Vemuganti GK, Kannabiran C, Honavar SG, Murthy R. 2009. Phenotypic characterization of retinoblastoma for the presence of putative cancer stem-like cell markers by flow cytometry. Invest Ophthalmol Vis Sci 50: 1506-1514.

Balmer A, Munier F, Gailloud C. 1991. Retinoma. Case studies. Ophthalmic Paediatr Genet 12: 131-137.

Balmer A MF. 2000a. Rétinoblastome: diagnostic. In: Zografos L, editor. Tumeurs intraoculaires. Paris: Société Française d'Ophtalmologie et Masson. pp. 485–533.

Balmer MF. 2002b. Rétinoblastome: Epidémiologie. In: Zografos L, editor. Tumeurs intraoculaires. Paris: Société Française d'Ophtalmologie et Masso. pp. 481–485.

Banerji U ODA, and Scurr M. 2003. A pharmacokinetically (PK)—pharmacodynamically (PD) guided phase I trial of the heat shock protein 90 (HSP90) inhibitor 17-allylamino, 17-demethoxy-geldanamycin (17AAG). Proc ASCO 22.

Bankovic J, Stojsic J, Jovanovic D, Andjelkovic T, Milinkovic V, Ruzdijic S, Tanic N. 2010. Identification of genes associated with non-small-cell lung cancer promotion and progression. Lung Cancer 67: 151-159.

Barrallo-Gimeno A, Nieto MA. 2005. The Snail genes as inducers of cell movement and survival: implications in development and cancer. Development 132: 3151-3161.

Bartel DP. 2004. MicroRNAs: genomics, biogenesis, mechanism, and function. Cell 116: 281-297.

Beaverson K AD, Lee TC, Hochberg HM,, Kirszrot J SPea. 2001. In: Keunen JEE, Imhof SM, de Keizer RJW, Moll AC (eds). Xth International Congress of Ocular Oncology.Amsterdam, Conference Proceedings, published by the eds 202.

Bein K, Simons M. 2000. Thrombospondin type 1 repeats interact with matrix metalloproteinase 2. Regulation of metalloproteinase activity. J Biol Chem 275: 32167-32173.

Berlingieri MT, Manfioletti G, Santoro M, Bandiera A, Visconti R, Giancotti V, Fusco A. 1995. Inhibition of HMGI-C protein synthesis suppresses retrovirally induced neoplastic transformation of rat thyroid cells. Mol Cell Biol 15: 1545-1553.

Beta M, Venkatesan N, Vasudevan M, Vetrivel U, Khetan V, Krishnakumar S. 2013. Identification and Insilico Analysis of Retinoblastoma Serum microRNA Profile and Gene Targets Towards Prediction of Novel Serum Biomarkers. Bioinform Biol Insights 7: 21-34.

Betel D, Koppal A, Agius P, Sander C, Leslie C. 2010. Comprehensive modeling of microRNA targets predicts functional non-conserved and non-canonical sites. Genome Biol 11: R90.

Biswas J, Das D, Krishnakumar S, Shanmugam MP. 2003. Histopathologic analysis of 232 eyes with retinoblastoma conducted in an Indian tertiary-care ophthalmic center. J Pediatr Ophthalmol Strabismus 40: 265-267.

Biswas J, Kabra S, Krishnakumar S, Shanmugam MP. 2004. Clinical and histopathological characteristics of uveal melanoma in Asian Indians. A study of 103 patients. Indian J Ophthalmol 52: 41-44.

Blanco MJ, Moreno-Bueno G, Sarrio D, Locascio A, Cano A, Palacios J, Nieto MA. 2002. Correlation of Snail expression with histological grade and lymph node status in breast carcinomas. Oncogene 21: 3241-3246.

Blow JJ, Hodgson B. 2002. Replication licensing--defining the proliferative state? Trends Cell Biol 12: 72-78.

Blum R, Jacob-Hirsch J, Rechavi G, Kloog Y. 2006. Suppression of survivin expression in glioblastoma cells by the Ras inhibitor farnesylthiosalicylic acid promotes caspase-dependent apoptosis. Mol Cancer Ther 5: 2337-2347.

Boeri M, Verri C, Conte D, Roz L, Modena P, Facchinetti F, Calabro E, Croce CM, Pastorino U, Sozzi G. 2011. MicroRNA signatures in tissues and plasma predict development and prognosis of computed tomography detected lung cancer. Proc Natl Acad Sci U S A 108: 3713-3718.

Boo LM, Lin HH, Chung V, Zhou B, Louie SG, O'Reilly MA, Yen Y, Ann DK. 2005. High mobility group A2 potentiates genotoxic stress in part through the modulation of basal and DNA damage-dependent phosphatidylinositol 3-kinase-related protein kinase activation. Cancer Res 65: 6622-6630.

Bottoni A, Zatelli MC, Ferracin M, Tagliati F, Piccin D, Vignali C, Calin GA, Negrini M, Croce CM, Degli Uberti EC. 2007. Identification of differentially expressed microRNAs by microarray: a possible role for microRNA genes in pituitary adenomas. J Cell Physiol 210: 370-377.

Boutrid H, Jockovich ME, Murray TG, Pina Y, Feuer WJ, Lampidis TJ, Cebulla CM. 2008. Targeting hypoxia, a novel treatment for advanced retinoblastoma. Invest Ophthalmol Vis Sci 49: 2799-2805.

Boxrud REC. 1995. Retinoblastoma. In: Jaeger EA, Montzka DT, Tasman W (ed.).Duane's Ophthalmology.Philadelphia. J.B. Lippincott: 3–35.

Brantley MA, Jr., Harbour JW. 2000. Deregulation of the Rb and p53 pathways in uveal melanoma. Am J Pathol 157: 1795-1801.

Brisse HJ, et al. 2007. Relevance of CT and MRI in retinoblastoma for the diagnosis of postlaminar invasion with normal-size optic nerve: a retrospective study of 150 patients with histological comparison. Pediatr Radiol 37: 649-656.

Brody EN, Gold L. 2000. Aptamers as therapeutic and diagnostic agents. J Biotechnol 74: 5-13.

Biswas J, Kabra S, Krishnakumar S, Shanmugam MP. 2004. Clinical and histopathological characteristics of uveal melanoma in Asian Indians. A study of 103 patients. Indian J Ophthalmol 52: 41-44.

Blanco MJ, Moreno-Bueno G, Sarrio D, Locascio A, Cano A, Palacios J, Nieto MA. 2002. Correlation of Snail expression with histological grade and lymph node status in breast carcinomas. Oncogene 21: 3241-3246.

Blow JJ, Hodgson B. 2002. Replication licensing--defining the proliferative state? Trends Cell Biol 12: 72-78.

Blum R, Jacob-Hirsch J, Rechavi G, Kloog Y. 2006. Suppression of survivin expression in glioblastoma cells by the Ras inhibitor farnesylthiosalicylic acid promotes caspase-dependent apoptosis. Mol Cancer Ther 5: 2337-2347.

Boeri M, Verri C, Conte D, Roz L, Modena P, Facchinetti F, Calabro E, Croce CM, Pastorino U, Sozzi G. 2011. MicroRNA signatures in tissues and plasma predict development and prognosis of computed tomography detected lung cancer. Proc Natl Acad Sci U S A 108: 3713-3718.

Boo LM, Lin HH, Chung V, Zhou B, Louie SG, O'Reilly MA, Yen Y, Ann DK. 2005. High mobility group A2 potentiates genotoxic stress in part through the modulation of basal and DNA damage-dependent phosphatidylinositol 3-kinase-related protein kinase activation. Cancer Res 65: 6622-6630.

Bottoni A, Zatelli MC, Ferracin M, Tagliati F, Piccin D, Vignali C, Calin GA, Negrini M, Croce CM, Degli Uberti EC. 2007. Identification of differentially expressed microRNAs by microarray: a possible role for microRNA genes in pituitary adenomas. J Cell Physiol 210: 370-377.

Boutrid H, Jockovich ME, Murray TG, Pina Y, Feuer WJ, Lampidis TJ, Cebulla CM. 2008. Targeting hypoxia, a novel treatment for advanced retinoblastoma. Invest Ophthalmol Vis Sci 49: 2799-2805.

Boxrud REC. 1995. Retinoblastoma. In: Jaeger EA, Montzka DT, Tasman W (ed.).Duane's Ophthalmology.Philadelphia. J.B. Lippincott: 3–35.

Brantley MA, Jr., Harbour JW. 2000. Deregulation of the Rb and p53 pathways in uveal melanoma. Am J Pathol 157: 1795-1801.

Brisse HJ, et al. 2007. Relevance of CT and MRI in retinoblastoma for the diagnosis of postlaminar invasion with normal-size optic nerve: a retrospective study of 150 patients with histological comparison. Pediatr Radiol 37: 649-656.

Brody EN, Gold L. 2000. Aptamers as therapeutic and diagnostic agents. J Biotechnol 74: 5-13.

Brooks H, Lebleu B, Vives E. 2005. Tat peptide-mediated cellular delivery: back to basics. Adv Drug Deliv Rev 57: 559-577.

Bunin GR, Petrakova A, Meadows AT, Emanuel BS, Buckley JD, Woods WG, Hammond GD. 1990. Occupations of parents of children with retinoblastoma: a report from the Children's Cancer Study Group. Cancer Res 50: 7129-7133.

Burr DB, Molina SA, Banerjee D, Low DM, Takemoto DJ. 2011. Treatment with connexin 46 siRNA suppresses the growth of human Y79 retinoblastoma cell xenografts in vivo. Exp Eye Res 92: 251-259.

Bustin M, Reeves R. 1996. High-mobility-group chromosomal proteins: architectural components that facilitate chromatin function. Prog Nucleic Acid Res Mol Biol 54: 35-100.

Cai K, Wang Y, Bao X. 2011. MiR-106b promotes cell proliferation via targeting RB in laryngeal carcinoma. J Exp Clin Cancer Res 30: 73.

Calin GA, et al. 2004. Human microRNA genes are frequently located at fragile sites and genomic regions involved in cancers. Proc Natl Acad Sci U S A 101: 2999-3004.

Callejo SA, Antecka E, Blanco PL, Edelstein C, Burnier MN, Jr. 2007. Identification of circulating malignant cells and its correlation with prognostic factors and treatment in uveal melanoma. A prospective longitudinal study. Eye (Lond) 21: 752-759.

Calvisi DF, et al. 2011. Activation of v-Myb avian myeloblastosis viral oncogene homolog-like2 (MYBL2)-LIN9 complex contributes to human hepatocarcinogenesis and identifies a subset of hepatocellular carcinoma with mutant p53. Hepatology 53: 1226-1236.

Carlsson E, et al. 2012. Potential role of a navigator gene NAV3 in colorectal cancer. Br J Cancer 106: 517-524.

Carreno E, Saornil MA, Garcia-Alvarez C, Lopez-Lara F, De Frutos-Baraja JM, Almaraz A. 2012. Prevalence of ocular and oculodermal melanocytosis in Spanish population with uveal melanoma. Eye (Lond) 26: 159-162.

Carthew RW, Sontheimer EJ. 2009. Origins and Mechanisms of miRNAs and siRNAs. Cell 136: 642-655.

Castera L, et al. 2010. MDM2 as a modifier gene in retinoblastoma. J Natl Cancer Inst 102: 1805-1808.

Ch'ng S, Sullivan M, Yuan L, Davis P, Tan ST. 2006. Mast cells dysregulate apoptotic and cell cycle genes in mucosal squamous cell carcinoma. Cancer Cell Int 6: 28.

Chakraborty S, Khare S, Dorairaj SK, Prabhakaran VC, Prakash DR, Kumar A. 2007. Identification of genes associated with tumorigenesis of retinoblastoma by microarray analysis. Genomics 90: 344-353.

Chan HS, Thorner PS, Haddad G, Gallie BL. 1991. Multidrug-resistant phenotype in retinoblastoma correlates with P-glycoprotein expression. Ophthalmology 98: 1425-1431.

Chan HS, et al. 1996. Combining cyclosporin with chemotherapy controls intraocular retinoblastoma without requiring radiation. Clin Cancer Res 2: 1499-1508.

Chan JA, Krichevsky AM, Kosik KS. 2005. MicroRNA-21 is an antiapoptotic factor in human glioblastoma cells. Cancer Res 65: 6029-6033.

Chantada G, Fandino A, Casak S, Manzitti J, Raslawski E, Schvartzman E. 2003. Treatment of overt extraocular retinoblastoma. Med Pediatr Oncol 40: 158-161.

Char DH, Kroll S, Phillips TL, Quivey JM. 2002. Late radiation failures after iodine 125 brachytherapy for uveal melanoma compared with charged-particle (proton or helium ion) therapy. Ophthalmology 109: 1850-1854.

Chau KY, Manfioletti G, Cheung-Chau KW, Fusco A, Dhomen N, Sowden JC, Sasabe T, Mukai S, Ono SJ. 2003. Derepression of HMGA2 gene expression in retinoblastoma is associated with cell proliferation. Mol Med 9: 154-165.

Chen D, Law ME, Theis JD, Gamez JD, Caron LB, Vrana JA, Dogan A. 2009. Clinicopathologic features of CDK6 translocation-associated B-cell lymphoproliferative disorders. Am J Surg Pathol 33: 720-729.

Chen X, He D, Dong XD, Dong F, Wang J, Wang L, Tang J, Hu DN, Yan D, Tu L. 2013. MicroRNA-124a is epigenetically regulated and acts as a tumor suppressor by controlling multiple targets in uveal melanoma. Invest Ophthalmol Vis Sci 54: 2248-2256.

Chen Y, Liu W, Chao T, Zhang Y, Yan X, Gong Y, Qiang B, Yuan J, Sun M, Peng X. 2008. MicroRNA-21 down-regulates the expression of tumor suppressor PDCD4 in human glioblastoma cell T98G. Cancer Lett 272: 197-205.

Chevez-Barrios P, Hurwitz MY, Louie K, Marcus KT, Holcombe VN, Schafer P, Aguilar-Cordova CE, Hurwitz RL. 2000. Metastatic and nonmetastatic models of retinoblastoma. Am J Pathol 157: 1405-1412.

Chieffi P, Battista S, Barchi M, Di Agostino S, Pierantoni GM, Fedele M, Chiariotti L, Tramontano D, Fusco A. 2002. HMGA1 and HMGA2 protein expression in mouse spermatogenesis. Oncogene 21: 3644-3650.

Chintagumpala M, Chevez-Barrios P, Paysse EA, Plon SE, Hurwitz R. 2007. Retinoblastoma: review of current management. Oncologist 12: 1237-1246.

Cho WC. 2007. OncomiRs: the discovery and progress of microRNAs in cancers. Mol Cancer 6: 60.

Cintron NS, Toft D. 2006. Defining the requirements for Hsp40 and Hsp70 in the Hsp90 chaperone pathway. J Biol Chem 281: 26235-26244.

Ciocca DR, Calderwood SK. 2005. Heat shock proteins in cancer: diagnostic, prognostic, predictive, and treatment implications. Cell Stress Chaperones 10: 86-103.

Ciocca DR, Rozados VR, Cuello Carrion FD, Gervasoni SI, Matar P, Scharovsky OG. 2003. Hsp25 and Hsp70 in rodent tumors treated with doxorubicin and lovastatin. Cell Stress Chaperones 8: 26-36.

Conkrite K, Sundby M, Mukai S, Thomson JM, Mu D, Hammond SM, MacPherson D. 2011. miR-17~92 cooperates with RB pathway mutations to promote retinoblastoma. Genes Dev 25: 1734-1745.

Cook DR, et al. 2011. The ect2 rho Guanine nucleotide exchange factor is essential for early mouse development and normal cell cytokinesis and migration. Genes Cancer 2: 932-942.

Coopman PJ, et al. 2000. The Syk tyrosine kinase suppresses malignant growth of human breast cancer cells. Nature 406: 742-747.

Corson TW, Gallie BL. 2007. One hit, two hits, three hits, more? Genomic changes in the development of retinoblastoma. Genes Chromosomes Cancer 46: 617-634.

Creighton CJ, Nagaraja AK, Hanash SM, Matzuk MM, Gunaratne PH. 2008. A bioinformatics tool for linking gene expression profiling results with public databases of microRNA target predictions. RNA 14: 2290-2296.

Crighton D, Wilkinson S, O'Prey J, Syed N, Smith P, Harrison PR, Gasco M, Garrone O, Crook T, Ryan KM. 2006. DRAM, a p53-induced modulator of autophagy, is critical for apoptosis. Cell 126: 121-134.

Cui T, Leng F. 2007. Specific recognition of AT-rich DNA sequences by the mammalian high mobility group protein AT-hook 2: a SELEX study. Biochemistry 46: 13059-13066.

Dahiya N, Sherman-Baust CA, Wang TL, Davidson B, Shih Ie M, Zhang Y, Wood W, 3rd, Becker KG, Morin PJ. 2008. MicroRNA expression and identification of putative miRNA targets in ovarian cancer. PLoS One 3: e2436.

Dalgard CL, Van Quill KR, O'Brien JM. 2008. Evaluation of the in vitro and in vivo antitumor activity of histone deacetylase inhibitors for the therapy of retinoblastoma. Clin Cancer Res 14: 3113-3123.

Dalgard CL, Gonzalez M, deNiro JE, O'Brien JM. 2009. Differential microRNA-34a expression and tumor suppressor function in retinoblastoma cells. Invest Ophthalmol Vis Sci 50: 4542-4551.

Damato B. 2012. Progress in the management of patients with uveal melanoma. The 2012 Ashton Lecture. Eye (Lond) 26: 1157-1172.

De Carvalho DD, et al. 2011. BCR-ABL-mediated upregulation of PRAME is responsible for knocking down TRAIL in CML patients. Oncogene 30: 223-233.

De Martino I, Visone R, Fedele M, Petrocca F, Palmieri D, Martinez Hoyos J, Forzati F, Croce CM, Fusco A. 2009. Regulation of microRNA expression by HMGA1 proteins. Oncogene 28: 1432-1442.

De Potter P, Shields CL, Shields JA. 1996. New treatment modalities for uveal melanoma. Curr Opin Ophthalmol 7: 27-32.

de Winter JP, Roelen BA, ten Dijke P, van der Burg B, van den Eijnden-van Raaij AJ. 1997. DPC4 (SMAD4) mediates transforming growth factor-beta1 (TGF-beta1) induced growth inhibition and transcriptional response in breast tumour cells. Oncogene 14: 1891-1899.

Debatin KM. 1997. Cytotoxic drugs, programmed cell death, and the immune system: defining new roles in an old play. J Natl Cancer Inst 89: 750-751.

Deepa PR, Vandhana S, Krishnakumar S. 2013. Fatty acid synthase inhibition induces differential expression of genes involved in apoptosis and cell proliferation in ocular cancer cells. Nutr Cancer 65: 311-316.

Deepa PR, Vandhana S, Muthukumaran S, Umashankar V, Jayanthi U, Krishnakumar S. 2010. Chemical inhibition of fatty acid synthase: molecular docking analysis and biochemical validation in ocular cancer cells. J Ocul Biol Dis Infor 3: 117-128.

DerKinderen DJ, Koten JW, Tan KE, Beemer FA, Van Romunde LK, Den Otter W. 1990. Parental age in sporadic hereditary retinoblastoma. Am J Ophthalmol 110: 605-609.

Derynck R, Akhurst RJ, Balmain A. 2001. TGF-beta signaling in tumor suppression and cancer progression. Nat Genet 29: 117-129.

Detre S, Saclani Jotti G, Dowsett M. 1995. A "quickscore" method for immunohistochemical semiquantitation: validation for oestrogen receptor in breast carcinomas. J Clin Pathol 48: 876-878.

Dhar SU, Chintagumpala M, Noll C, Chevez-Barrios P, Paysse EA, Plon SE. 2011. Outcomes of integrating genetics in management of patients with retinoblastoma. Arch Ophthalmol 129: 1428-1434.

Dhupper M, Biswas J, Gopal L, Kumar SK, Khetan V. 2012. Clinicopathological correlation of choroidal melanoma in Indian population: A study of 113 cases. Oman J Ophthalmol 5: 42-45.

Diener-West M, Earle JD, Fine SL, Hawkins BS, Moy CS, Reynolds SM, Schachat AP, Straatsma BR. 2001. The COMS randomized trial of iodine 125 brachytherapy for choroidal melanoma, III: initial mortality findings. COMS Report No. 18. Arch Ophthalmol 119: 969-982.

Dimaras H, Kimani K, Dimba EA, Gronsdahl P, White A, Chan HS, Gallie BL. 2012. Retinoblastoma. Lancet 379: 1436-1446.

Dror R, Lederman M, Umezawa K, Barak V, Pe'er J, Chowers I. 2010. Characterizing the involvement of the nuclear factor-kappa B (NF kappa B) transcription factor in uveal melanoma. Invest Ophthalmol Vis Sci 51: 1811-1816.

Dunkel IJ, Aledo A, Kernan NA, Kushner B, Bayer L, Gollamudi SV, Finlay JL, Abramson DH. 2000. Successful treatment of metastatic retinoblastoma. Cancer 89: 2117-2121.

Dyer MA, Rodriguez-Galindo C, Wilson MW. 2005. Use of preclinical models to improve treatment of retinoblastoma. PLoS Med 2: e332.

Eagle R. 2000. Retinoblastoma and simulating lesions. In: Duane TD. editor. Duane's Clinical Ophthalmology, Foundations. 3: 429–483.

Edge SB BD, Compton CC, et al., ed. 2010. Malignant melanoma of the uvea. 7th ed. New York, NY: Springer.

Edwards SK, Desai A, Liu Y, Moore CR, Xie P. 2014. Expression and function of a novel isoform of Sox5 in malignant B cells. Leuk Res 38: 393-401.

Egan KM, Seddon JM, Glynn RJ, Gragoudas ES, Albert DM. 1988. Epidemiologic aspects of uveal melanoma. Surv Ophthalmol 32: 239-251.

Elison JR, Cobrinik D, Claros N, Abramson DH, Lee TC. 2006. Small molecule inhibition of HDM2 leads to p53-mediated cell death in retinoblastoma cells. Arch Ophthalmol 124: 1269-1275.

Enerly E, et al. 2011. miRNA-mRNA integrated analysis reveals roles for miRNAs in primary breast tumors. PLoS One 6: e16915.

Eng C, Li FP, Abramson DH, Ellsworth RM, Wong FL, Goldman MB, Seddon J, Tarbell N, Boice JD, Jr. 1993. Mortality from second tumors among long-term survivors of retinoblastoma. J Natl Cancer Inst 85: 1121-1128.

Epping MT, Hart AA, Glas AM, Krijgsman O, Bernards R. 2008. PRAME expression and clinical outcome of breast cancer. Br J Cancer 99: 398-403.

Eshkoor SA, Ismail P, Rahman SA, Mirinargesi M, Oshkour SA. 2009. Increased protein expression of p16 and cyclin D1 in squamous cell carcinoma tissues. Biosci Trends 3: 105-109.

Fan X, Chen X, Deng W, Zhong G, Cai Q, Lin T. 2013. Up-regulated microRNA-143 in cancer stem cells differentiation promotes prostate cancer cells metastasis by modulating FNDC3B expression. BMC Cancer 13: 61.

Friard O, Re A, Taverna D, De Bortoli M, Cora D. 2010. CircuitsDB: a database of mixed microRNA/transcription factor feed-forward regulatory circuits in human and mouse. BMC Bioinformatics 11: 435.

Friedman DL, Himelstein B, Shields CL, Shields JA, Needle M, Miller D,

Friard O, Re A, Taverna D, De Bortoli M, Cora D. 2010. CircuitsDB: a database of mixed microRNA/transcription factor feed-forward regulatory circuits in human and mouse. BMC Bioinformatics 11: 435.

Friedman DL, Himelstein B, Shields CL, Shields JA, Needle M, Miller D, Bunin GR, Meadows AT. 2000. Chemoreduction and local ophthalmic therapy for intraocular retinoblastoma. J Clin Oncol 18: 12-17.

Friedman RC, Farh KK, Burge CB, Bartel DP. 2009. Most mammalian mRNAs are conserved targets of microRNAs. Genome Res 19: 92-105.

Fusco A, Fedele M. 2007. Roles of HMGA proteins in cancer. Nat Rev Cancer 7: 899-910.

Gallie BL, Ellsworth RM, Abramson DH, Phillips RA. 1982. Retinoma: spontaneous regression of retinoblastoma or benign manifestation of the mutation? Br J Cancer 45: 513-521.

Gallie BL, Budning A, DeBoer G, Thiessen JJ, Koren G, Verjee Z, Ling V, Chan HS. 1996. Chemotherapy with focal therapy can cure intraocular retinoblastoma without radiotherapy. Arch Ophthalmol 114: 1321-1328.

Ganguly A, Shields CL. 2010. Differential gene expression profile of retinoblastoma compared to normal retina. Mol Vis 16: 1292-1303.

Garzon R, et al. 2007. MicroRNA gene expression during retinoic acid-induced differentiation of human acute promyelocytic leukemia. Oncogene 26: 4148-4157.

Gattas GJ, Quade BJ, Nowak RA, Morton CC. 1999. HMGIC expression in human adult and fetal tissues and in uterine leiomyomata. Genes Chromosomes Cancer 25: 316-322.

Geraldo MV, Yamashita AS, Kimura ET. 2012. MicroRNA miR-146b-5p regulates signal transduction of TGF-beta by repressing SMAD4 in thyroid cancer. Oncogene 31: 1910-1922.

Girard B, Le Hoang P, D'Hermies F, Quere MA, Rousselie F. 1989. [Diffuse infiltrating retinoblastoma]. J Fr Ophtalmol 12: 369-381.

Glud M, Klausen M, Gniadecki R, Rossing M, Hastrup N, Nielsen FC, Drzewiecki KT. 2009. MicroRNA expression in melanocytic nevi: the usefulness of formalin-fixed, paraffin-embedded material for miRNA microarray profiling. J Invest Dermatol 129: 1219-1224.

Goellner S, Steinbach D, Schenk T, Gruhn B, Zintl F, Ramsay E, Saluz HP. 2006. Childhood acute myelogenous leukaemia: association between PRAME, apoptosis- and MDR-related gene expression. Eur J Cancer 42: 2807-2814.

Goetz MP, Toft DO, Ames MM, Erlichman C. 2003. The Hsp90 chaperone complex as a novel target for cancer therapy. Ann Oncol 14: 1169-1176.

Goldie JH. 2001. Drug resistance in cancer: a perspective. Cancer Metastasis Rev 20: 63-68.

Gragoudas ES, Egan KM, Seddon JM, Glynn RJ, Walsh SM, Finn SM, Munzenrider JE, Spar MD. 1991. Survival of patients with metastases from uveal melanoma. Ophthalmology 98: 383-389; discussion 390.

Graner MW, Cumming RI, Bigner DD. 2007. The heat shock response and chaperones/heat shock proteins in brain tumors: surface expression, release, and possible immune consequences. J Neurosci 27: 11214-11227.

Grimson A, Farh KK, Johnston WK, Garrett-Engele P, Lim LP, Bartel DP. 2007. MicroRNA targeting specificity in mammals: determinants beyond seed pairing. Mol Cell 27: 91-105.

Grossniklaus HE GW, ed. 1994. Uveal tumors. 2nd ed. New York, NY: M. Dekker.

Gunduz K, Muftuoglu O, Gunalp I, Unal E, Tacyildiz N. 2006. Metastatic retinoblastoma clinical features, treatment, and prognosis. Ophthalmology 113: 1558-1566.

Guo H, Ingolia NT, Weissman JS, Bartel DP. 2010. Mammalian microRNAs predominantly act to decrease target mRNA levels. Nature 466: 835-840.

Gyrd-Hansen M, Nylandsted J, Jaattela M. 2004. Heat shock protein 70 promotes cancer cell viability by safeguarding lysosomal integrity. Cell Cycle 3: 1484-1485.

Gyurkocza B, Plescia J, Raskett CM, Garlick DS, Lowry PA, Carter BZ, Andreeff M, Meli M, Colombo G, Altieri DC. 2006. Antileukemic activity of shepherdin and molecular diversity of hsp90 inhibitors. J Natl Cancer Inst 98: 1068-1077.

Hahn SA, et al. 1996. DPC4, a candidate tumor suppressor gene at human chromosome 18q21.1. Science 271: 350-353.

Hammond SM. 2007. MicroRNAs as tumor suppressors. Nat Genet 39: 582-583.

Hanahan D, Weinberg RA. 2000. The hallmarks of cancer. Cell 100: 57-70.

Hanahan D, Weinberg RA. 2011. Hallmarks of cancer: the next generation. Cell 144: 646-674.

Hara T, Abe M, Inoue H, Yu LR, Veenstra TD, Kang YH, Lee KS, Miki T. 2006. Cytokinesis regulator ECT2 changes its conformation through phosphorylation at Thr-341 in G2/M phase. Oncogene 25: 566-578.

Haraguchi M. 2009. The role of the transcriptional regulator snail in cell detachment, reattachment and migration. Cell Adh Migr 3: 259-263.

Haraguchi M, Okubo T, Miyashita Y, Miyamoto Y, Hayashi M, Crotti TN, McHugh KP, Ozawa M. 2008. Snail regulates cell-matrix adhesion by regulation of the expression of integrins and basement membrane proteins. J Biol Chem 283: 23514-23523.

Harbour JW, Chen R. 2013. The DecisionDx-UM Gene Expression Profile Test Provides Risk Stratification and Individualized Patient Care in Uveal Melanoma. PLoS Curr 5.

Harbour JW, Onken MD, Roberson ED, Duan S, Cao L, Worley LA, Council ML, Matatall KA, Helms C, Bowcock AM. 2010. Frequent mutation of BAP1 in metastasizing uveal melanomas. Science 330: 1410-1413.

Harris RB, Griffith K, Moon TE. 2001. Trends in the incidence of nonmelanoma skin cancers in southeastern Arizona, 1985-1996. J Am Acad Dermatol 45: 528-536.

Hawkes SP, Li H, Taniguchi GT. 2010. Zymography and reverse zymography for detecting MMPs and TIMPs. Methods Mol Biol 622: 257-269.

He J, Jing Y, Li W, Qian X, Xu Q, Li FS, Liu LZ, Jiang BH, Jiang Y. 2013. Roles and mechanism of miR-199a and miR-125b in tumor angiogenesis. PLoS One 8: e56647.

He L, He X, Lowe SW, Hannon GJ. 2007. microRNAs join the p53 network--another piece in the tumour-suppression puzzle. Nat Rev Cancer 7: 819-822.

He L, et al. 2005. A microRNA polycistron as a potential human oncogene. Nature 435: 828-833.

He XJ, Ma YY, Yu S, Jiang XT, Lu YD, Tao L, Wang HP, Hu ZM, Tao HQ. 2014. Up-regulated miR-199a-5p in gastric cancer functions as an oncogene and targets klotho. BMC Cancer 14: 218.

Hebert C, Norris K, Scheper MA, Nikitakis N, Sauk JJ. 2007. High mobility group A2 is a target for miRNA-98 in head and neck squamous cell carcinoma. Mol Cancer 6: 5.

Hicks N, Zack M, Caldwell GG, Fernbach DJ, Falletta JM. 1984. Childhood cancer and occupational radiation exposure in parents. Cancer 53: 1637-1643.

Hirning-Folz U, Wilda M, Rippe V, Bullerdiek J, Hameister H. 1998. The expression pattern of the Hmgic gene during development. Genes Chromosomes Cancer 23: 350-357.

Honavar SG, Singh AD. 2005. Management of advanced retinoblastoma. Ophthalmol Clin North Am 18: 65-73, viii.

Honavar SG, Singh AD, Shields CL, Meadows AT, Demirci H, Cater J, Shields JA. 2002. Postenucleation adjuvant therapy in high-risk retinoblastoma. Arch Ophthalmol 120: 923-931.

Hristov AC, Cope L, Reyes MD, Singh M, Iacobuzio-Donahue C, Maitra A, Resar LM. 2009. HMGA2 protein expression correlates with lymph node metastasis and increased tumor grade in pancreatic ductal adenocarcinoma. Mod Pathol 22: 43-49.

Hsueh EC, Essner R, Foshag LJ, Ye X, Wang HJ, Morton DL. 2004. Prolonged survival after complete resection of metastases from intraocular melanoma. Cancer 100: 122-129.

Hu Y, Ou Y, Wu K, Chen Y, Sun W. 2012. miR-143 inhibits the metastasis of pancreatic cancer and an associated signaling pathway. Tumour Biol 33: 1863-1870.

Huang JC, Babak T, Corson TW, Chua G, Khan S, Gallie BL, Hughes TR, Blencowe BJ, Frey BJ, Morris QD. 2007. Using expression profiling data to identify human microRNA targets. Nat Methods 4: 1045-1049.

Huntzinger E, Izaurralde E. 2011. Gene silencing by microRNAs: contributions of translational repression and mRNA decay. Nat Rev Genet 12: 99-110.

Huppertz B, Frank HG, Reister F, Kingdom J, Korr H, Kaufmann P. 1999. Apoptosis cascade progresses during turnover of human trophoblast: analysis of villous cytotrophoblast and syncytial fragments in vitro. Lab Invest 79: 1687-1702.

Hurst DR, Edmonds MD, Scott GK, Benz CC, Vaidya KS, Welch DR. 2009. Breast cancer metastasis suppressor 1 up-regulates miR-146, which suppresses breast cancer metastasis. Cancer Res 69: 1279-1283.

Ikeda H, et al. 1997. Characterization of an antigen that is recognized on a melanoma showing partial HLA loss by CTL expressing an NK inhibitory receptor. Immunity 6: 199-208.

Inskip PD, Devesa SS, Fraumeni JF, Jr. 2003. Trends in the incidence of ocular melanoma in the United States, 1974-1998. Cancer Causes Control 14: 251-257.

Isaacs JS, Xu W, Neckers L. 2003. Heat shock protein 90 as a molecular target for cancer therapeutics. Cancer Cell 3: 213-217.

Ivanovska I, et al. 2008. MicroRNAs in the miR-106b family regulate p21/CDKN1A and promote cell cycle progression. Mol Cell Biol 28: 2167-2174.

Jayasena SD. 1999. Aptamers: an emerging class of molecules that rival antibodies in diagnostics. Clin Chem 45: 1628-1650.

Jazag A, et al. 2005. Smad4 silencing in pancreatic cancer cell lines using stable RNA interference and gene expression profiles induced by transforming growth factor-beta. Oncogene 24: 662-671.

Jeffers JR, et al. 2003. Puma is an essential mediator of p53-dependent and -independent apoptotic pathways. Cancer Cell 4: 321-328.

Jepsen K, et al. 2000. Combinatorial roles of the nuclear receptor corepressor in transcription and development. Cell 102: 753-763.

Jiang LB, Liu XQ, Li B, He XJ, Jin YL, Li LQ, Gao F, Wang NL. 2008. Heat shock proteins and survivin: relationship and effects on proliferation index of retinoblastoma cells. Histol Histopathol 23: 827-831.

Jiao W, Miyazaki K, Kitajima Y. 2002. Inverse correlation between E-cadherin and Snail expression in hepatocellular carcinoma cell lines in vitro and in vivo. Br J Cancer 86: 98-101.

Jmor F, Kalirai H, Taktak A, Damato B, Coupland SE. 2012. HSP-27 protein expression in uveal melanoma: correlation with predicted survival. Acta Ophthalmol 90: 534-539.

Jo DH, Kim JH, Park WY, Kim KW, Yu YS. 2011. Differential profiles of microRNAs in retinoblastoma cell lines of different proliferation and adherence patterns. J Pediatr Hematol Oncol 33: 529-533.

Job Sudhakar NV, Shruthi Lakshmanan,Vikas Khetan, Subramanian Krishnakumar and Jyotirmay Biswas. 2013. Hypoxic tumor environment in advanced retinoblastoma. Journal of Pediatric Blood and cancer (in press).

John B, Sander C, Marks DS. 2006. Prediction of human microRNA targets. Methods Mol Biol 342: 101-113.

John B, Enright AJ, Aravin A, Tuschl T, Sander C, Marks DS. 2004. Human MicroRNA targets. PLoS Biol 2: e363.

Johnson BD, Schumacher RJ, Ross ED, Toft DO. 1998. Hop modulates Hsp70/Hsp90 interactions in protein folding. J Biol Chem 273: 3679-3686.

Johnson DA, Zhang J, Frase S, Wilson M, Rodriguez-Galindo C, Dyer MA. 2007. Neuronal differentiation and synaptogenesis in retinoblastoma. Cancer Res 67: 2701-2711.

Johnson ME, Howerth EW. 2004. Survivin: a bifunctional inhibitor of apoptosis protein. Vet Pathol 41: 599-607.

Jolly C, Morimoto RI. 2000. Role of the heat shock response and molecular chaperones in oncogenesis and cell death. J Natl Cancer Inst 92: 1564-1572.

Justilien V, Jameison L, Der CJ, Rossman KL, Fields AP. 2011. Oncogenic activity of Ect2 is regulated through protein kinase C iota-mediated phosphorylation. J Biol Chem 286: 8149-8157.

Kaddar T, Rouault JP, Chien WW, Chebel A, Gadoux M, Salles G, Ffrench M, Magaud JP. 2009. Two new miR-16 targets: caprin-1 and HMGA1, proteins implicated in cell proliferation. Biol Cell 101: 511-524.

Kan T, et al. 2009. The miR-106b-25 polycistron, activated by genomic amplification, functions as an oncogene by suppressing p21 and Bim. Gastroenterology 136: 1689-1700.

Kandalam MM, Beta M, Maheswari UK, Swaminathan S, Krishnakumar S. 2012. Oncogenic microRNA 17-92 cluster is regulated by epithelial cell adhesion molecule and could be a potential therapeutic target in retinoblastoma. Mol Vis 18: 2279-2287.

Karasawa Y, Okisaka S. 2004. Inhibition of histone deacetylation by butyrate induces morphological changes in Y79 retinoblastoma cells. Jpn J Ophthalmol 48: 542-551.

Karcioglu ZA, al-Mesfer SA, Abboud E, Jabak MH, Mullaney PB. 1997. Workup for metastatic retinoblastoma. A review of 261 patients. Ophthalmology 104: 307-312.

Karin M, Liu Z, Zandi E. 1997. AP-1 function and regulation. Curr Opin Cell Biol 9: 240-246.

Kase S, Parikh JG, Rao NA. 2009a. Expression of alpha-crystallin in retinoblastoma. Arch Ophthalmol 127: 187-192.

Kase S, Parikh JG, Rao NA. 2009b. Expression of heat shock protein 27 and alpha-crystallins in human retinoblastoma after chemoreduction. Br J Ophthalmol 93: 541-544.

Kelly DL, Rizzino A. 1999. Growth regulatory factors and carcinogenesis: the roles played by transforming growth factor beta, its receptors and signaling pathways. Anticancer Res 19: 4791-4807.

Kerbel RS, Kobayashi H, Graham CH. 1994. Intrinsic or acquired drug resistance and metastasis: are they linked phenotypes? J Cell Biochem 56: 37-47.

Kertesz M, Iovino N, Unnerstall U, Gaul U, Segal E. 2007. The role of site accessibility in microRNA target recognition. Nat Genet 39: 1278-1284.

Khelfaoui F, et al. 1996. Histopathologic risk factors in retinoblastoma: a retrospective study of 172 patients treated in a single institution. Cancer 77: 1206-1213.

Kim JE, Billadeau DD, Chen J. 2005. The tandem BRCT domains of Ect2 are required for both negative and positive regulation of Ect2 in cytokinesis. J Biol Chem 280: 5733-5739.

Kim PK, Armstrong M, Liu Y, Yan P, Bucher B, Zuckerbraun BS, Gambotto A, Billiar TR, Yim JH. 2004. IRF-1 expression induces apoptosis and inhibits tumor growth in mouse mammary cancer cells in vitro and in vivo. Oncogene 23: 1125-1135.

Kingston JE, Hungerford JL, Madreperla SA, Plowman PN. 1996. Results of combined chemotherapy and radiotherapy for advanced intraocular retinoblastoma. Arch Ophthalmol 114: 1339-1343.

Kivela T. 1999. Trilateral retinoblastoma: a meta-analysis of hereditary retinoblastoma associated with primary ectopic intracranial retinoblastoma. J Clin Oncol 17: 1829-1837.

Klintworth GK SM, ed. 1999. The eye and ocular adnexa. Philadelphia, Pa: Lippincott Williams & Wilkins.

Knudson AG, Jr. 1971. Mutation and cancer: statistical study of retinoblastoma. Proc Natl Acad Sci U S A 68: 820-823.

Krek A, et al. 2005. Combinatorial microRNA target predictions. Nat Genet 37: 495-500.

Krishnakumar S, Mohan A, Kandalam M, Ramkumar HL, Venkatesan N, Das RR. 2008. SRPK1: a cisplatin sensitive protein expressed in retinoblastoma. Pediatr Blood Cancer 50: 402-406.

Krishnakumar S, Mohan A, Mallikarjuna K, Venkatesan N, Biswas J, Shanmugam MP, Ren-Heidenreich L. 2004a. EpCAM expression in retinoblastoma: a novel molecular target for therapy. Invest Ophthalmol Vis Sci 45: 4247-4250.

Krishnakumar S, Mallikarjuna K, Desai N, Muthialu A, Venkatesan N, Sundaram A, Khetan V, Shanmugam MP. 2004b. Multidrug resistant proteins: P-glycoprotein and lung resistance protein expression in retinoblastoma. Br J Ophthalmol 88: 1521-1526.

Kujala E, Makitie T, Kivela T. 2003. Very long-term prognosis of patients with malignant uveal melanoma. Invest Ophthalmol Vis Sci 44: 4651-4659.

Kuo PK, Puliafito CA, Wang KM, Liu HS, Wu BF. 1982. Uveal melanoma in China. Int Ophthalmol Clin 22: 57-71.

Laios A, et al. 2008. Potential role of miR-9 and miR-223 in recurrent ovarian cancer. Mol Cancer 7: 35.

Lambertini E, Lolli A, Vezzali F, Penolazzi L, Gambari R, Piva R. 2012. Correlation between Slug transcription factor and miR-221 in MDA-MB-231 breast cancer cells. BMC Cancer 12: 445.

Lassalle HP, Marchal S, Guillemin F, Reinhard A, Bezdetnaya L. 2012. Aptamers as remarkable diagnostic and therapeutic agents in cancer treatment. Curr Drug Metab 13: 1130-1144.

Laurie NA, et al. 2006. Inactivation of the p53 pathway in retinoblastoma. Nature 444: 61-66.

Lawrie CH, et al. 2009. Expression of microRNAs in diffuse large B cell lymphoma is associated with immunophenotype, survival and transformation from follicular lymphoma. J Cell Mol Med 13: 1248-1260.

Le Thi Huong D, Wechsler B, Merillon H, Sauvaget F, De Gennes C, Piette JC, Godeau P. 1991. [Wegener's granulomatosis disclosed by clinical symptoms of Horton's disease]. Rev Med Interne 12: 380-382.

Leal-Leal CA, Rivera-Luna R, Flores-Rojo M, Juarez-Echenique JC, Ordaz JC, Amador-Zarco J. 2006. Survival in extra-orbital metastatic retinoblastoma:treatment results. Clin Transl Oncol 8: 39-44.

Leal-Leal., et al. 2004. A multicentre report from the Mexican Retinoblastoma Group. Br J Ophthalmol 88: 1074-1077.

Lee YS, Dutta A. 2007. The tumor suppressor microRNA let-7 represses the HMGA2 oncogene. Genes Dev 21: 1025-1030.

Lefebvre V. 2010. The SoxD transcription factors--Sox5, Sox6, and Sox13--are key cell fate modulators. Int J Biochem Cell Biol 42: 429-432.

Lei C, Wang Y, Huang Y, Yu H, Wu L, Huang L. 2012. Up-regulated miR155 reverses the epithelial-mesenchymal transition induced by EGF and increases chemo-sensitivity to cisplatin in human Caski cervical cancer cells. PLoS One 7: e52310.

Levy L, Hill CS. 2005. Smad4 dependency defines two classes of transforming growth factor {beta} (TGF-{beta}) target genes and distinguishes TGF-{beta}-induced epithelial-mesenchymal transition from its antiproliferative and migratory responses. Mol Cell Biol 25: 8108-8125.

Lewis BP, Shih IH, Jones-Rhoades MW, Bartel DP, Burge CB. 2003. Prediction of mammalian microRNA targets. Cell 115: 787-798.

Li AY, Boo LM, Wang SY, Lin HH, Wang CC, Yen Y, Chen BP, Chen DJ, Ann DK. 2009a. Suppression of nonhomologous end joining repair by overexpression of HMGA2. Cancer Res 69: 5699-5706.

Li BQ, Zhang J, Huang T, Zhang L, Cai YD. 2012a. Identification of retinoblastoma related genes with shortest path in a protein-protein interaction network. Biochimie 94: 1910-1917.

Li J, Li C, Yuan H, Gong F. 2012b. Clinical value of CD24 expression in retinoblastoma. J Biomed Biotechnol 2012: 158084.

Li J, Wang Y, Luo J, Fu Z, Ying J, Yu Y, Yu W. 2012c. miR-134 inhibits epithelial to mesenchymal transition by targeting FOXM1 in non-small cell lung cancer cells. FEBS Lett 586: 3761-3765.

Li JT, Liu W, Kuang ZH, Chen HK, Li DJ, Feng QS, Liu QC, Hu B. 2003. [Amplification of RIT1 in hepatocellular carcinoma and its clinical significance]. Ai Zheng 22: 695-699.

Li Q, Wu L, Oelschlager DK, Wan M, Stockard CR, Grizzle WE, Wang N, Chen H, Sun Y, Cao X. 2005. Smad4 inhibits tumor growth by inducing apoptosis in estrogen receptor-alpha-positive breast cancer cells. J Biol Chem 280: 27022-27028.

Li X, McDonnell DP. 2002. The transcription factor B-Myb is maintained in an inhibited state in target cells through its interaction with the nuclear corepressors N-CoR and SMRT. Mol Cell Biol 22: 3663-3673.

Li Y, Liang C, Wong KC, Jin K, Zhang Z. 2014. Inferring probabilistic miRNA-mRNA interaction signatures in cancers: a role-switch approach. Nucleic Acids Res 42: e76.

Li Y, VandenBoom TG, 2nd, Kong D, Wang Z, Ali S, Philip PA, Sarkar FH. 2009b. Up-regulation of miR-200 and let-7 by natural agents leads to the reversal of epithelial-to-mesenchymal transition in gemcitabine-resistant pancreatic cancer cells. Cancer Res 69: 6704-6712.

Li Z, Srivastava P. 2004. Heat-shock proteins. Curr Protoc Immunol Appendix 1: Appendix 1T.

Liang CC, Park AY, Guan JL. 2007. In vitro scratch assay: a convenient and inexpensive method for analysis of cell migration in vitro. Nat Protoc 2: 329-333.

Lidegaard O, Pinborg A, Andersen AN. 2005. Imprinting diseases and IVF: Danish National IVF cohort study. Hum Reprod 20: 950-954.

Linn Murphree A. 2005. Intraocular retinoblastoma: the case for a new group classification. Ophthalmol Clin North Am 18: 41-53, viii.

Liu CJ, Shen WG, Peng SY, Cheng HW, Kao SY, Lin SC, Chang KW. 2014. miR-134 induces oncogenicity and metastasis in head and neck carcinoma through targeting WWOX gene. Int J Cancer 134: 811-821.

Liu X, Gao R, Dong Y, Gao L, Zhao Y, Zhao L, Zhao X, Zhang H. 2010. Survivin gene silencing sensitizes prostate cancer cells to selenium growth inhibition. BMC Cancer 10: 418.

Liu Y, Yan X, Liu N, Zhou J, Liu J, Pang H, Cao J, Wang Y, Liu L, Zhang H. 2012. Lentivirus-delivered ZEB-1 small interfering RNA inhibits lung adenocarcinoma cell growth in vitro and in vivo. J Cancer Res Clin Oncol 138: 1329-1338.

Livak KJ, Schmittgen TD. 2001. Analysis of relative gene expression data using real-time quantitative PCR and the 2(-Delta Delta C(T)) Method. Methods 25: 402-408.

Lo Muzio L, Pannone G, Leonardi R, Staibano S, Mignogna MD, De Rosa G, Kudo Y, Takata T, Altieri DC. 2003. Survivin, a potential early predictor of tumor progression in the oral mucosa. J Dent Res 82: 923-928.

Longley DB, Johnston PG. 2005. Molecular mechanisms of drug resistance. J Pathol 205: 275-292.

Lu M, Shi B, Wang J, Cao Q, Cui Q. 2010. TAM: a method for enrichment and depletion analysis of a microRNA category in a list of microRNAs. BMC Bioinformatics 11: 419.

M. Ishimura MS-Y, T. Maruyama, T. Ando, M. Fukayama, A. Goto and Y. Murakami. 2012. Involvement of miR-214 and miR-375 in Malignant Features of Non-Small-Cell Lung Cancer by Down-Regulating CADM1. Journal of Cancer Therapy 3: 379-387.

Ma L, et al. 2010. miR-9, a MYC/MYCN-activated microRNA, regulates E-cadherin and cancer metastasis. Nat Cell Biol 12: 247-256.

Ma W, Xie S, Ni M, Huang X, Hu S, Liu Q, Liu A, Zhang J, Zhang Y. 2012. MicroRNA-29a inhibited epididymal epithelial cell proliferation by targeting nuclear autoantigenic sperm protein (NASP). J Biol Chem 287: 10189-10199.

Maat-Kievit JA, Oepkes D, Hartwig NG, Vermeij-Keers C, van Kamp IL, van de Kamp JJ. 1993. A large retinoblastoma detected in a fetus at 21 weeks of gestation. Prenat Diagn 13: 377-384.

Manohar S, Ramakrishnan R, Das TP, Namperumalsamy P. 1991. Malignant melanoma of choroid. Indian J Ophthalmol 39: 70-73.

Maragkakis M, et al. 2009. Accurate microRNA target prediction correlates with protein repression levels. BMC Bioinformatics 10: 295.

Margo C, Hidayat A, Kopelman J, Zimmerman LE. 1983. Retinocytoma. A benign variant of retinoblastoma. Arch Ophthalmol 101: 1519-1531.

Margo CE, McLean IW. 1984. Malignant melanoma of the choroid and ciliary body in black patients. Arch Ophthalmol 102: 77-79.

Martin J, et al. 2013. Differentially expressed miRNAs in retinoblastoma. Gene 512: 294-299.

Masatsugu Ueda YY, Mikio Takehara, Yoshito Terai, Koji Kumagai, Ken Ueki, Koji Kanda, Hiroyuki Yamaguchi, Daisuke Akise, Hikari Yamashita, Yao-Ching Hung, Minoru Ueki. 2003. Biological Implications of Survivin Gene Expression in the Development of Endometriosis and Endometrial Carcinoma. Cell and Molecular Biology of Endometrial Carcinoma: pp 252-263.

Mashiah M, Barishak YR. 1977. Photoreceptor differentiation in retinoblastomas and its significance in prognosis. Br J Ophthalmol 61: 417-422.

Mclean IWea. 1994. Tumors of the retina Atlas of Tumor Pathology:Tumors of the EyeandOcular Adnexa. Washington, DC Armed Forces Institute of pathology.

Medina PP, Nolde M, Slack FJ. 2010. OncomiR addiction in an in vivo model of microRNA-21-induced pre-B-cell lymphoma. Nature 467: 86-90.

Meli M, Pennati M, Curto M, Daidone MG, Plescia J, Toba S, Altieri DC, Zaffaroni N, Colombo G. 2006. Small-molecule targeting of heat shock protein 90 chaperone function: rational identification of a new anticancer lead. J Med Chem 49: 7721-7730.

Mensink HW, Vaarwater J, Kilic E, Naus NC, Mooy N, Luyten G, Bruggenwirth HT, Paridaens D, de Klein A. 2009. Chromosome 3 intratumor heterogeneity in uveal melanoma. Invest Ophthalmol Vis Sci 50: 500-504.

Meyer B, Loeschke S, Schultze A, Weigel T, Sandkamp M, Goldmann T, Vollmer E, Bullerdiek J. 2007. HMGA2 overexpression in non-small cell lung cancer. Mol Carcinog 46: 503-511.

Mi S, et al. 2007. MicroRNA expression signatures accurately discriminate acute lymphoblastic leukemia from acute myeloid leukemia. Proc Natl Acad Sci U S A 104: 19971-19976.

Mi S, et al. 2010. Aberrant overexpression and function of the miR-17-92 cluster in MLL-rearranged acute leukemia. Proc Natl Acad Sci U S A 107: 3710-3715.

Minucci S, Pelicci PG. 2006. Histone deacetylase inhibitors and the promise of epigenetic (and more) treatments for cancer. Nat Rev Cancer 6: 38-51.

Mitra M, Kandalam M, Verma RS, UmaMaheswari K, Krishnakumar S. 2010. Genome-wide changes accompanying the knockdown of Ep-CAM in retinoblastoma. Mol Vis 16: 828-842.

Mitra M, Misra R, Harilal A, Sahoo SK, Krishnakumar S. 2011a. Enhanced in vitro antiproliferative effects of EpCAM antibody-functionalized paclitaxel-loaded PLGA nanoparticles in retinoblastoma cells. Mol Vis 17: 2724-2737.

Mitra M, Kandalam M, Sundaram CS, Verma RS, Maheswari UK, Swaminathan S, Krishnakumar S. 2011b. Reversal of stathmin-mediated microtubule destabilization sensitizes retinoblastoma cells to a low dose of antimicrotubule agents: a novel synergistic therapeutic intervention. Invest Ophthalmol Vis Sci 52: 5441-5448.

Mitra M, Kandalam M, Harilal A, Verma RS, Krishnan UM, Swaminathan S, Krishnakumar S. 2012. EpCAM is a putative stem marker in retinoblastoma and an effective target for T-cell-mediated immunotherapy. Mol Vis 18: 290-308.

Miyazawa J, Mitoro A, Kawashiri S, Chada KK, Imai K. 2004. Expression of mesenchyme-specific gene HMGA2 in squamous cell carcinomas of the oral cavity. Cancer Res 64: 2024-2029.

Mohan A, Kandalam M, Ramkumar HL, Gopal L, Krishnakumar S. 2006. Stem cell markers: ABCG2 and MCM2 expression in retinoblastoma. Br J Ophthalmol 90: 889-893.

Mohan A, Venkatesan N, Kandalam M, Pasricha G, Acharya P, Khetan V, Gopal L, Sharma T, Biswas J, Krishnakumar S. 2009. Detection of human papillomavirus DNA in retinoblastoma samples: a preliminary study. J Pediatr Hematol Oncol 31: 8-13.

Moll AC, Imhof SM, Kuik DJ, Bouter LM, Den Otter W, Bezemer PD, Koten JW, Tan KE. 1996. High parental age is associated with sporadic hereditary retinoblastoma: the Dutch retinoblastoma register 1862-1994. Hum Genet 98: 109-112.

Monte M, Benetti R, Buscemi G, Sandy P, Del Sal G, Schneider C. 2003. The cell cycle-regulated protein human GTSE-1 controls DNA damage-induced apoptosis by affecting p53 function. J Biol Chem 278: 30356-30364.

Moolmuang B, Tainsky MA. 2011. CREG1 enhances p16(INK4a) -induced cellular senescence. Cell Cycle 10: 518-530.

Morgan G. 1971. Diffuse infiltrating retinoblastoma. Br J Ophthalmol 55: 600-606.

Moser JJ, Fritzler MJ. 2010. The microRNA and messengerRNA profile of the RNA-induced silencing complex in human primary astrocyte and astrocytoma cells. PLoS One 5: e13445.

Mosser DD, Morimoto RI. 2004. Molecular chaperones and the stress of oncogenesis. Oncogene 23: 2907-2918.

Mu G, Liu H, Zhou F, Xu X, Jiang H, Wang Y, Qu Y. 2010. Correlation of overexpression of HMGA1 and HMGA2 with poor tumor differentiation, invasion, and proliferation associated with let-7 down-regulation in retinoblastomas. Hum Pathol 41: 493-502.

Munier F BA. 2002. Rétinoblastome: génétique. In: Zografos L, editor. Tumeurs intraoculaires. Paris: Société Française d'Ophtalmologie et Masson. pp. 467–480.

Murphree AL, Triche TJ. 2012. An epigenomic mechanism in retinoblastoma: the end of the story? Genome Med 4: 15.

Murphree AL, Villablanca JG, Deegan WF, 3rd, Sato JK, Malogolowkin M, Fisher A, Parker R, Reed E, Gomer CJ. 1996. Chemotherapy plus local treatment in the management of intraocular retinoblastoma. Arch Ophthalmol 114: 1348-1356.

Nakamura Y, Ishiguro A, Miyakawa S. 2012. RNA plasticity and selectivity applicable to therapeutics and novel biosensor development. Genes Cells 17: 344-364.

Nakayama K, Kamihira S. 2002. Survivin an important determinant for prognosis in adult T-cell leukemia: a novel biomarker in practical hemato-oncology. Leuk Lymphoma 43: 2249-2255.

Nalini V, Segu R, Deepa PR, Khetan V, Vasudevan M, Krishnakumar S. 2013. Molecular Insights on Post-chemotherapy Retinoblastoma by Microarray Gene Expression Analysis. Bioinform Biol Insights 7: 289-306.

Nam S, Kim B, Shin S, Lee S. 2008. miRGator: an integrated system for functional annotation of microRNAs. Nucleic Acids Res 36: D159-164.

Nazha B, Granner T, Maloney S, Odashiro AN, Antecka E, Burnier Jr MN. 2013. Aberrant Nuclear Repressor Coreceptor 1 Localization in Human Retinoblastoma. Ophthalmic Res 49: 171-176.

Neckers L. 2007. Heat shock protein 90: the cancer chaperone. J Biosci 32: 517-530.

Negrini M, Calin GA. 2008. Breast cancer metastasis: a microRNA story. Breast Cancer Res 10: 203.

Ni X, Castanares M, Mukherjee A, Lupold SE. 2011. Nucleic acid aptamers: clinical applications and promising new horizons. Curr Med Chem 18: 4206-4214.

Niiya F, Tatsumoto T, Lee KS, Miki T. 2006. Phosphorylation of the cytokinesis regulator ECT2 at G2/M phase stimulates association of the mitotic kinase Plk1 and accumulation of GTP-bound RhoA. Oncogene 25: 827-837.

Niiya F, Xie X, Lee KS, Inoue H, Miki T. 2005. Inhibition of cyclin-dependent kinase 1 induces cytokinesis without chromosome segregation in an ECT2 and MgcRacGAP-dependent manner. J Biol Chem 280: 36502-36509.

Nishida N, Mimori K, Fabbri M, Yokobori T, Sudo T, Tanaka F, Shibata K, Ishii H, Doki Y, Mori M. 2011. MicroRNA-125a-5p is an independent prognostic factor in gastric cancer and inhibits the proliferation of human gastric cancer cells in combination with trastuzumab. Clin Cancer Res 17: 2725-2733.

Nishino J, Kim I, Chada K, Morrison SJ. 2008. Hmga2 promotes neural stem cell self-renewal in young but not old mice by reducing p16Ink4a and p19Arf Expression. Cell 135: 227-239.

Nittner D, et al. 2012. Synthetic lethality between Rb, p53 and Dicer or miR-17-92 in retinal progenitors suppresses retinoblastoma formation. Nat Cell Biol 14: 958-965.

Njauw CN, Kim I, Piris A, Gabree M, Taylor M, Lane AM, DeAngelis MM, Gragoudas E, Duncan LM, Tsao H. 2012. Germline BAP1 inactivation is preferentially associated with metastatic ocular melanoma and cutaneous-ocular melanoma families. PLoS One 7: e35295.

Nylandsted J, Brand K, Jaattela M. 2000. Heat shock protein 70 is required for the survival of cancer cells. Ann N Y Acad Sci 926: 122-125.

O'Donnell KA, Wentzel EA, Zeller KI, Dang CV, Mendell JT. 2005. c-Myc-regulated microRNAs modulate E2F1 expression. Nature 435: 839-843.

Oehme I, et al. 2009. Histone deacetylase 8 in neuroblastoma tumorigenesis. Clin Cancer Res 15: 91-99.

Oh HK, et al. 2011. Genomic loss of miR-486 regulates tumor progression and the OLFM4 antiapoptotic factor in gastric cancer. Clin Cancer Res 17: 2657-2667.

Ohdaira H, Sekiguchi M, Miyata K, Yoshida K. 2012. MicroRNA-494 suppresses cell proliferation and induces senescence in A549 lung cancer cells. Cell Prolif 45: 32-38.

Olmeda D, Moreno-Bueno G, Flores JM, Fabra A, Portillo F, Cano A. 2007. SNAI1 is required for tumor growth and lymph node metastasis of human breast carcinoma MDA-MB-231 cells. Cancer Res 67: 11721-11731.

Olmeda D, Montes A, Moreno-Bueno G, Flores JM, Portillo F, Cano A. 2008. Snai1 and Snai2 collaborate on tumor growth and metastasis properties of mouse skin carcinoma cell lines. Oncogene 27: 4690-4701.

Onken MD, Worley LA, Ehlers JP, Harbour JW. 2004. Gene expression profiling in uveal melanoma reveals two molecular classes and predicts metastatic death. Cancer Res 64: 7205-7209.

Onken MD, et al. 2012. Collaborative Ocular Oncology Group report number 1: prospective validation of a multi-gene prognostic assay in uveal melanoma. Ophthalmology 119: 1596-1603.

Orjuela M, Castaneda VP, Ridaura C, Lecona E, Leal C, Abramson DH, Orlow I, Gerald W, Cordon-Cardo C. 2000. Presence of human papilloma virus in tumor tissue from children with retinoblastoma: an alternative mechanism for tumor development. Clin Cancer Res 6: 4010-4016.

Orjuela MA, Titievsky L, Liu X, Ramirez-Ortiz M, Ponce-Castaneda V, Lecona E, Molina E, Beaverson K, Abramson DH, Mueller NE. 2005. Fruit and vegetable intake during pregnancy and risk for development of sporadic retinoblastoma. Cancer Epidemiol Biomarkers Prev 14: 1433-1440.

Orlic M, Spencer CE, Wang L, Gallie BL. 2006. Expression analysis of 6p22 genomic gain in retinoblastoma. Genes Chromosomes Cancer 45: 72-82.

Ota A, Tagawa H, Karnan S, Tsuzuki S, Karpas A, Kira S, Yoshida Y, Seto M. 2004. Identification and characterization of a novel gene, C13orf25, as a target for 13q31-q32 amplification in malignant lymphoma. Cancer Res 64: 3087-3095.

Pan RMC, L. Fine, J. Hwang, K.R. Van Quill, and J.M. O'Brien. 2005. Socioeconomic Predictors of Outcome in Hereditary Retinoblastoma Invest. Ophthalmol. Vis. Sci. 46: E-Abstract 3396.

Parcellier A, Gurbuxani S, Schmitt E, Solary E, Garrido C. 2003. Heat shock proteins, cellular chaperones that modulate mitochondrial cell death pathways. Biochem Biophys Res Commun 304: 505-512.

Park SM, Shell S, Radjabi AR, Schickel R, Feig C, Boyerinas B, Dinulescu DM, Lengyel E, Peter ME. 2007. Let-7 prevents early cancer progression by suppressing expression of the embryonic gene HMGA2. Cell Cycle 6: 2585-2590.

Patnaik SK, Kannisto E, Mallick R, Yendamuri S. 2011. Overexpression of the lung cancer-prognostic miR-146b microRNAs has a minimal and negative effect on the malignant phenotype of A549 lung cancer cells. PLoS One 6: e22379.

Pearl LH, Prodromou C. 2000. Structure and in vivo function of Hsp90. Curr Opin Struct Biol 10: 46-51.

Peng Y, Laser J, Shi G, Mittal K, Melamed J, Lee P, Wei JJ. 2008. Antiproliferative effects by Let-7 repression of high-mobility group A2 in uterine leiomyoma. Mol Cancer Res 6: 663-673.

Penna E, et al. 2011. microRNA-214 contributes to melanoma tumour progression through suppression of TFAP2C. EMBO J 30: 1990-2007.

Pentimalli F, Dentice M, Fedele M, Pierantoni GM, Cito L, Pallante P, Santoro M, Viglietto G, Dal Cin P, Fusco A. 2003. Suppression of HMGA2 protein synthesis could be a tool for the therapy of well differentiated liposarcomas overexpressing HMGA2. Cancer Res 63: 7423-7427.

Petrocca F, et al. 2008. E2F1-regulated microRNAs impair TGFbeta-dependent cell-cycle arrest and apoptosis in gastric cancer. Cancer Cell 13: 272-286.

Philiponnet A, Grange JD, Baggetto LG. 2014. [Application of gene therapy to oncologic ophthalmology]. J Fr Ophtalmol 37: 155-165.

Piboonniyom SO, Timmermann S, Hinds P, Munger K. 2002. Aberrations in the MTS1 tumor suppressor locus in oral squamous cell carcinoma lines preferentially affect the INK4A gene and result in increased cdk6 activity. Oral Oncol 38: 179-186.

Poser I, Dominguez D, de Herreros AG, Varnai A, Buettner R, Bosserhoff AK. 2001. Loss of E-cadherin expression in melanoma cells involves up-regulation of the transcriptional repressor Snail. J Biol Chem 276: 24661-24666.

Pratt WB, Toft DO. 2003. Regulation of signaling protein function and trafficking by the hsp90/hsp70-based chaperone machinery. Exp Biol Med (Maywood) 228: 111-133.

Qi L, Bart J, Tan LP, Platteel I, Sluis T, Huitema S, Harms G, Fu L, Hollema H, Berg A. 2009. Expression of miR-21 and its targets (PTEN, PDCD4, TM1) in flat epithelial atypia of the breast in relation to ductal carcinoma in situ and invasive carcinoma. BMC Cancer 9: 163.

Radhakrishnan A, Badhrinarayanan N, Biswas J, Krishnakumar S. 2009. Analysis of chromosomal aberration (1, 3, and 8) and association of microRNAs in uveal melanoma. Mol Vis 15: 2146-2154.

Ralfkiaer U, et al. 2011. Diagnostic microRNA profiling in cutaneous T-cell lymphoma (CTCL). Blood 118: 5891-5900.

Redova M, et al. 2013. MiR-210 expression in tumor tissue and in vitro effects of its silencing in renal cell carcinoma. Tumour Biol 34: 481-491.

Reese AB, Ellsworth RM. 1963. The evaluation and current concept of retinoblastoma therapy. Trans Am Acad Ophthalmol Otolaryngol 67: 164-172.

Reeves R. 2001. Molecular biology of HMGA proteins: hubs of nuclear function. Gene 277: 63-81.

Reeves R, Nissen MS. 1990. The A.T-DNA-binding domain of mammalian high mobility group I chromosomal proteins. A novel peptide motif for recognizing DNA structure. J Biol Chem 265: 8573-8582.

Rehmsmeier M, Steffen P, Hochsmann M, Giegerich R. 2004. Fast and effective prediction of microRNA/target duplexes. RNA 10: 1507-1517.

Reinhart BJ, Slack FJ, Basson M, Pasquinelli AE, Bettinger JC, Rougvie AE, Horvitz HR, Ruvkun G. 2000. The 21-nucleotide let-7 RNA regulates developmental timing in Caenorhabditis elegans. Nature 403: 901-906.

Reis AH, Vargas FR, Lemos B. 2012a. More epigenetic hits than meets the eye: microRNAs and genes associated with the tumorigenesis of retinoblastoma. Front Genet 3: 284.

Reis ST, et al. 2012b. miR-21 may acts as an oncomir by targeting RECK, a matrix metalloproteinase regulator, in prostate cancer. BMC Urol 12: 14.

Ren B, Yu G, Tseng GC, Cieply K, Gavel T, Nelson J, Michalopoulos G, Yu YP, Luo JH. 2006. MCM7 amplification and overexpression are associated with prostate cancer progression. Oncogene 25: 1090-1098.

Rey C, Soubeyran I, Mahouche I, Pedeboscq S, Bessede A, Ichas F, De Giorgi F, Lartigue L. 2013. HIPK1 drives p53 activation to limit colorectal cancer cell growth. Cell Cycle 12: 1879-1891.

Robertson DM, Buettner H, Bennett SR. 1999. Transpupillary thermotherapy as primary treatment for small choroidal melanomas. Arch Ophthalmol 117: 1512-1519.

Rodriguez-Galindo C, Chantada GL, Haik BG, Wilson MW. 2007. Treatment of retinoblastoma: current status and future perspectives. Curr Treat Options Neurol 9: 294-307.

Rodriguez-Galindo C, Wilson MW, Haik BG, Lipson MJ, Cain A, Merchant TE, Kaste S, Pratt CB. 2003. Treatment of metastatic retinoblastoma. Ophthalmology 110: 1237-1240.

Rodriguez-Manzaneque JC, Lane TF, Ortega MA, Hynes RO, Lawler J, Iruela-Arispe ML. 2001. Thrombospondin-1 suppresses spontaneous tumor growth and inhibits activation of matrix metalloproteinase-9 and mobilization of vascular endothelial growth factor. Proc Natl Acad Sci U S A 98: 12485-12490.

Rogalla P, Drechsler K, Schroder-Babo W, Eberhardt K, Bullerdiek J. 1998. HMGIC expression patterns in non-small lung cancer and surrounding tissue. Anticancer Res 18: 3327-3330.

Rogalla P, Drechsler K, Kazmierczak B, Rippe V, Bonk U, Bullerdiek J. 1997. Expression of HMGI-C, a member of the high mobility group protein family, in a subset of breast cancers: relationship to histologic grade. Mol Carcinog 19: 153-156.

Rogalla P, Drechsler K, Frey G, Hennig Y, Helmke B, Bonk U, Bullerdiek J. 1996. HMGI-C expression patterns in human tissues. Implications for the genesis of frequent mesenchymal tumors. Am J Pathol 149: 775-779.

Rommel B, Rogalla P, Jox A, Kalle CV, Kazmierczak B, Wolf J, Bullerdiek J. 1997. HMGI-C, a member of the high mobility group family of proteins, is expressed in hematopoietic stem cells and in leukemic cells. Leuk Lymphoma 26: 603-607.

Rosai J, ed. 1996 Eye and ocular adnexa. 8th ed ed.: St. Louis, Mo: Mosby.

Roubelakis MG, Zotos P, Papachristoudis G, Michalopoulos I, Pappa KI, Anagnou NP, Kossida S. 2009. Human microRNA target analysis and gene ontology clustering by GOmir, a novel stand-alone application. BMC Bioinformatics 10 Suppl 6: S20.

Rushlow D, Piovesan B, Zhang K, Prigoda-Lee NL, Marchong MN, Clark RD, Gallie BL. 2009. Detection of mosaic RB1 mutations in families with retinoblastoma. Hum Mutat 30: 842-851.

Rushlow DE, et al. 2013. Characterisation of retinoblastomas without RB1 mutations: genomic, gene expression, and clinical studies. Lancet Oncol 14: 327-334.

Sachdeva UM, O'Brien JM. 2012. Understanding pRb: toward the necessary development of targeted treatments for retinoblastoma. J Clin Invest 122: 425-434.

Salfity AAKaM. April,1996. Nuclear localization and the heat shock proteins. Nuclear localization and the heat shock proteins 21.

Salhia B, et al. 2008. The guanine nucleotide exchange factors trio, Ect2, and Vav3 mediate the invasive behavior of glioblastoma. Am J Pathol 173: 1828-1838.

Sano M, Genkai N, Yajima N, Tsuchiya N, Homma J, Tanaka R, Miki T, Yamanaka R. 2006. Expression level of ECT2 proto-oncogene correlates with prognosis in glioma patients. Oncol Rep 16: 1093-1098.

Sara Pensa GR, Daniela Boselli, Francesco Novelli and Valeria Polianou. . 2009. STAT1 and STAT3 in Tumorigenesis: Two Sides of the Same Coin?: Landes Bioscience.

Sarto C, Binz PA, Mocarelli P. 2000. Heat shock proteins in human cancer. Electrophoresis 21: 1218-1226.

Sastre X, Chantada GL, Doz F, Wilson MW, de Davila MT, Rodriguez-Galindo C, Chintagumpala M, Chevez-Barrios P. 2009. Proceedings of the consensus meetings from the International Retinoblastoma Staging Working Group on the pathology guidelines for the examination of enucleated eyes and evaluation of prognostic risk factors in retinoblastoma. Arch Pathol Lab Med 133: 1199-1202.

Sausville EA, Tomaszewski JE, Ivy P. 2003. Clinical development of 17-allylamino, 17-demethoxygeldanamycin. Curr Cancer Drug Targets 3: 377-383.

Scat Y, Liotet S, Carre F. 1996. [Epidemiological study of 1705 malignant tumors of the eye and adnexa]. J Fr Ophtalmol 19: 83-88.

Schlueter C, Hauke S, Loeschke S, Wenk HH, Bullerdiek J. 2005. HMGA1 proteins in human atherosclerotic plaques. Pathol Res Pract 201: 101-107.

Schueler AO, Jurklies C, Heimann H, Wieland R, Havers W, Bornfeld N. 2003. Thermochemotherapy in hereditary retinoblastoma. Br J Ophthalmol 87: 90-95.

Schultz J, Lorenz P, Gross G, Ibrahim S, Kunz M. 2008. MicroRNA let-7b targets important cell cycle molecules in malignant melanoma cells and interferes with anchorage-independent growth. Cell Res 18: 549-557.

Schultz KR, Ranade S, Neglia JP, Ravindranath Y. 1993. An increased relative frequency of retinoblastoma at a rural regional referral hospital in Miraj, Maharashtra, India. Cancer 72: 282-286.

Scott GK, Goga A, Bhaumik D, Berger CE, Sullivan CS, Benz CC. 2007. Coordinate suppression of ERBB2 and ERBB3 by enforced expression of micro-RNA miR-125a or miR-125b. J Biol Chem 282: 1479-1486.

Seigler HF. 1985. Immunodiagnosis of human malignancy. Ann Surg 201: 415-422.

Seregard S, Lundell G, Svedberg H, Kivela T. 2004. Incidence of retinoblastoma from 1958 to 1998 in Northern Europe: advantages of birth cohort analysis. Ophthalmology 111: 1228-1232.

Sevel D, Rohm GF, Sealy R. 1974. Clinical significance of the fleurette in retinoblastoma. Br J Ophthalmol 58: 687-693.

Sgarra R, Rustighi A, Tessari MA, Di Bernardo J, Altamura S, Fusco A, Manfioletti G, Giancotti V. 2004. Nuclear phosphoproteins HMGA and their relationship with chromatin structure and cancer. FEBS Lett 574: 1-8.

Shah MY, Calin GA. 2011. MicroRNAs miR-221 and miR-222: a new level of regulation in aggressive breast cancer. Genome Med 3: 56.

Shell S, Park SM, Radjabi AR, Schickel R, Kistner EO, Jewell DA, Feig C, Lengyel E, Peter ME. 2007. Let-7 expression defines two differentiation stages of cancer. Proc Natl Acad Sci U S A 104: 11400-11405.

Shen J, et al. 2011. Diagnosis of lung cancer in individuals with solitary pulmonary nodules by plasma microRNA biomarkers. BMC Cancer 11: 374.

Shen SM, Yu Y, Wu YL, Cheng JK, Wang LS, Chen GQ. 2010. Downregulation of ANP32B, a novel substrate of caspase-3, enhances caspase-3 activation and apoptosis induction in myeloid leukemic cells. Carcinogenesis 31: 419-426.

Sherman M, Multhoff G. 2007. Heat shock proteins in cancer. Ann N Y Acad Sci 1113: 192-201.

Shields CL, Shields JA, Baez KA, Cater J, De Potter PV. 1993. Choroidal invasion of retinoblastoma: metastatic potential and clinical risk factors. Br J Ophthalmol 77: 544-548.

Shields CL, Shields JA, Perez N, Singh AD, Cater J. 2002a. Primary transpupillary thermotherapy for small choroidal melanoma in 256 consecutive cases: outcomes and limitations. Ophthalmology 109: 225-234.

Shields CL, Shelil A, Cater J, Meadows AT, Shields JA. 2003. Development of new retinoblastomas after 6 cycles of chemoreduction for retinoblastoma in 162 eyes of 106 consecutive patients. Arch Ophthalmol 121: 1571-1576.

Shields CL, Manalac J, Das C, Ferguson K, Shields JA. 2014. Choroidal melanoma: clinical features, classification, and top 10 pseudomelanomas. Curr Opin Ophthalmol 25: 177-185.

Shields CL, Shields JA, Milite J, De Potter P, Sabbagh R, Menduke H. 1991a. Uveal melanoma in teenagers and children. A report of 40 cases. Ophthalmology 98: 1662-1666.

Shields CL, Cater J, Shields JA, Singh AD, Santos MC, Carvalho C. 2000. Combination of clinical factors predictive of growth of small choroidal melanocytic tumors. Arch Ophthalmol 118: 360-364.

Shields CL, Honavar SG, Shields JA, Demirci H, Meadows AT, Naduvilath TJ. 2002b. Factors predictive of recurrence of retinal tumors, vitreous seeds, and subretinal seeds following chemoreduction for retinoblastoma. Arch Ophthalmol 120: 460-464.

Shields CL, Fulco EM, Arias JD, Alarcon C, Pellegrini M, Rishi P, Kaliki S, Bianciotto CG, Shields JA. 2013. Retinoblastoma frontiers with intravenous, intra-arterial, periocular, and intravitreal chemotherapy. Eye (Lond) 27: 253-264.

Shields JA, Shields CL, Donoso LA. 1991b. Management of posterior uveal melanoma. Surv Ophthalmol 36: 161-195.

Shields JA, Shields CL, De Potter P. 1994. Clinical management of retinoblastoma. Curr Opin Ophthalmol 5: 83-88.

Shields JA, Parsons HM, Shields CL, Shah P. 1991c. Lesions simulating retinoblastoma. J Pediatr Ophthalmol Strabismus 28: 338-340.

Shields JA SC, ed. 1992. Introduction to melanocytic tumors of the uvea Philadelphia, Pa: Saunders.

Singh AD, Topham A. 2003a. Survival rates with uveal melanoma in the United States: 1973-1997. Ophthalmology 110: 962-965.

Singh AD, Topham A. 2003b. Incidence of uveal melanoma in the United States: 1973-1997. Ophthalmology 110: 956-961.

Singh AD, Bergman L, Seregard S. 2005. Uveal melanoma: epidemiologic aspects. Ophthalmol Clin North Am 18: 75-84, viii.

Singh AD, Santos CM, Shields CL, Shields JA, Eagle RC, Jr. 2000. Observations on 17 patients with retinocytoma. Arch Ophthalmol 118: 199-205.

Singh AD, Rennie IG, Kivela T, Seregard S, Grossniklaus H. 2004. The Zimmerman-McLean-Foster hypothesis: 25 years later. Br J Ophthalmol 88: 962-967.

Singh AD, Aronow ME, Sun Y, Bebek G, Saunthararajah Y, Schoenfield LR, Biscotti CV, Tubbs RR, Triozzi PL, Eng C. 2012. Chromosome 3 status in uveal melanoma: a comparison of fluorescence in situ hybridization and single-nucleotide polymorphism array. Invest Ophthalmol Vis Sci 53: 3331-3339.

Sivakumaran TA, Ghose S, Kumar H, A S, Kucheria K. 2000. Parental age in Indian patients with sporadic hereditary retinoblastoma. Ophthalmic Epidemiol 7: 285-291.

Smith AL, Iwanaga R, Drasin DJ, Micalizzi DS, Vartuli RL, Tan AC, Ford HL. 2012. The miR-106b-25 cluster targets Smad7, activates TGF-beta signaling, and induces EMT and tumor initiating cell characteristics downstream of Six1 in human breast cancer. Oncogene 31: 5162-5171.

Soti C, Racz A, Csermely P. 2002. A Nucleotide-dependent molecular switch controls ATP binding at the C-terminal domain of Hsp90. N-terminal nucleotide binding unmasks a C-terminal binding pocket. J Biol Chem 277: 7066-7075.

Sotiropoulou G, Pampalakis G, Lianidou E, Mourelatos Z. 2009. Emerging roles of microRNAs as molecular switches in the integrated circuit of the cancer cell. RNA 15: 1443-1461.

Srougi MC, Burridge K. 2011. The nuclear guanine nucleotide exchange factors Ect2 and Net1 regulate RhoB-mediated cell death after DNA damage. PLoS One 6: e17108.

Stannard C, Lipper S, Sealy R, Sevel D. 1979. Retinoblastoma: correlation of invasion of the optic nerve and choroid with prognosis and metastases. Br J Ophthalmol 63: 560-570.

Stempor PA, Cauchi M, Wilson P. 2012. MMpred: functional miRNA--mRNA interaction analyses by miRNA expression prediction. BMC Genomics 13: 620.

Stiller CA, Parkin DM. 1996. Geographic and ethnic variations in the incidence of childhood cancer. Br Med Bull 52: 682-703.

Stravopodis DJ, Margaritis LH, Voutsinas GE. 2007. Drug-mediated targeted disruption of multiple protein activities through functional inhibition of the Hsp90 chaperone complex. Curr Med Chem 14: 3122-3138.

Su F, Overholtzer M, Besser D, Levine AJ. 2002. WISP-1 attenuates p53-mediated apoptosis in response to DNA damage through activation of the Akt kinase. Genes Dev 16: 46-57.

Subramanian N, Navaneethakrishnan S, Biswas J, Kanwar RK, Kanwar JR, Krishnakumar S. 2013. RNAi Mediated Tiam1 Gene Knockdown Inhibits Invasion of Retinoblastoma. PLoS One 8: e70422.

Subramanian N, Raghunathan V, Kanwar JR, Kanwar RK, Elchuri SV, Khetan V, Krishnakumar S. 2012. Target-specific delivery of doxorubicin to retinoblastoma using epithelial cell adhesion molecule aptamer. Mol Vis 18: 2783-2795.

Sudhakar J, Venkatesan N, Lakshmanan S, Khetan V, Krishnakumar S, Biswas J. 2013. Hypoxic tumor microenvironment in advanced retinoblastoma. Pediatr Blood Cancer 60: 1598-1601.

Szczepanski MJ, et al. 2013. PRAME expression in head and neck cancer correlates with markers of poor prognosis and might help in selecting candidates for retinoid chemoprevention in pre-malignant lesions. Oral Oncol 49: 144-151.

Tang D, Khaleque MA, Jones EL, Theriault JR, Li C, Wong WH, Stevenson MA, Calderwood SK. 2005. Expression of heat shock proteins and heat shock protein messenger ribonucleic acid in human prostate carcinoma in vitro and in tumors in vivo. Cell Stress Chaperones 10: 46-58.

Tang MJ, Tai IT. 2007. A novel interaction between procaspase 8 and SPARC enhances apoptosis and potentiates chemotherapy sensitivity in colorectal cancers. J Biol Chem 282: 34457-34467.

Taraboletti G, Morbidelli L, Donnini S, Parenti A, Granger HJ, Giavazzi R, Ziche M. 2000. The heparin binding 25 kDa fragment of thrombospondin-1 promotes angiogenesis and modulates gelatinase and TIMP-2 production in endothelial cells. FASEB J 14: 1674-1676.

Tatsumoto T, Xie X, Blumenthal R, Okamoto I, Miki T. 1999. Human ECT2 is an exchange factor for Rho GTPases, phosphorylated in G2/M phases, and involved in cytokinesis. J Cell Biol 147: 921-928.

Tchougounova E, Jiang Y, Brasater D, Lindberg N, Kastemar M, Asplund A, Westermark B, Uhrbom L. 2009. Sox5 can suppress platelet-derived growth factor B-induced glioma development in Ink4a-deficient mice through induction of acute cellular senescence. Oncogene 28: 1537-1548.

Thapa DR, Li X, Jamieson BD, Martinez-Maza O. 2011. Overexpression of microRNAs from the miR-17-92 paralog clusters in AIDS-related non-Hodgkin's lymphomas. PLoS One 6: e20781.

Theriault BL, Dimaras H, Gallie BL, Corson TW. 2014. The genomic landscape of retinoblastoma: a review. Clin Experiment Ophthalmol 42: 33-52.

Thomson DW, Bracken CP, Goodall GJ. 2011. Experimental strategies for microRNA target identification. Nucleic Acids Res 39: 6845-6853.

Trabulo S, Cardoso AM, Santos-Ferreira T, Cardoso AL, Simoes S, Pedroso de Lima MC. 2011. Survivin silencing as a promising strategy to enhance the sensitivity of cancer cells to chemotherapeutic agents. Mol Pharm 8: 1120-1131.

Trepel J, Mollapour M, Giaccone G, Neckers L. 2010. Targeting the dynamic HSP90 complex in cancer. Nat Rev Cancer 10: 537-549.

Trompeter HI, Abbad H, Iwaniuk KM, Hafner M, Renwick N, Tuschl T, Schira J, Muller HW, Wernet P. 2011. MicroRNAs MiR-17, MiR-20a, and MiR-106b act in concert to modulate E2F activity on cell cycle arrest during neuronal lineage differentiation of USSC. PLoS One 6: e16138.

Ts'o MO, Fine BS, Zimmerman LE. 1969. The Flexner-Wintersteiner rosettes in retinoblastoma. Arch Pathol 88: 664-671.

Tu SP, et al. 2003. Suppression of survivin expression inhibits in vivo tumorigenicity and angiogenesis in gastric cancer. Cancer Res 63: 7724-7732.

Tzatsos A, Bardeesy N. 2008. Ink4a/Arf regulation by let-7b and Hmga2: a genetic pathway governing stem cell aging. Cell Stem Cell 3: 469-470.

Uusitalo MS, Van Quill KR, Scott IU, Matthay KK, Murray TG, O'Brien JM. 2001. Evaluation of chemoprophylaxis in patients with unilateral retinoblastoma with high-risk features on histopathologic examination. Arch Ophthalmol 119: 41-48.

Vallone D, Battista S, Pierantoni GM, Fedele M, Casalino L, Santoro M, Viglietto G, Fusco A, Verde P. 1997. Neoplastic transformation of rat thyroid cells requires the junB and fra-1 gene induction which is dependent on the HMGI-C gene product. EMBO J 16: 5310-5321.

Van Raamsdonk CD, et al. 2010. Mutations in GNA11 in uveal melanoma. N Engl J Med 363: 2191-2199.

Vandhana S, Deepa PR, Jayanthi U, Biswas J, Krishnakumar S. 2011. Clinico-pathological correlations of fatty acid synthase expression in retinoblastoma: an Indian cohort study. Exp Mol Pathol 90: 29-37.

Vandhana S, Coral K, Jayanthi U, Deepa PR, Krishnakumar S. 2013. Biochemical changes accompanying apoptotic cell death in retinoblastoma cancer cells treated with lipogenic enzyme inhibitors. Biochim Biophys Acta 1831: 1458-1466.

Vemuganti, Jalali S, Honavar SG, Shekar GC. 2001. Enucleation in a tertiary eye care centre in India: prevalence, current indications and clinicopathological correlation. Eye (Lond) 15: 760-765.

Vemuganti G.K. HSG, John R. 2000. Clinicopathological profile of retinoblastoma in Asian Indians. Invest. Ophthalmol. Vis. Sci. 46: E-Abstract 3396. 41: 790. (S).

Venkatesan N, Krishnakumar S, Deepa PR, Deepa M, Khetan V, Reddy MA. 2012. Molecular deregulation induced by silencing of the high mobility group protein A2 gene in retinoblastoma cells. Mol Vis 18: 2420-2437.

Venkatesan N, Kandalam M, Pasricha G, Sumantran V, Manfioletti G, Ono SJ, Reddy MA, Krishnakumar S. 2009. Expression of high mobility group A2 protein in retinoblastoma and its association with clinicopathologic features. J Pediatr Hematol Oncol 31: 209-214.

Ventura BV, Quezada C, Maloney SC, Fernandes BF, Antecka E, Martins C, Bakalian S, di Cesare S, Burnier MN, Jr. 2014. Expression of the metastasis suppressor BRMS1 in uveal melanoma. Ecancermedicalscience 8: 410.

Voorhoeve PM, et al. 2006. A genetic screen implicates miRNA-372 and miRNA-373 as oncogenes in testicular germ cell tumors. Cell 124: 1169-1181.

Wang C, Liu X, Huang H, Ma H, Cai W, Hou J, Huang L, Dai Y, Yu T, Zhou X. 2012. Deregulation of Snai2 is associated with metastasis and poor prognosis in tongue squamous cell carcinoma. Int J Cancer 130: 2249-2258.

Wang CL, Wan YL, Liu YC, Huang ZQ. 2006. TGF-beta1/SMAD signaling pathway mediates p53-dependent apoptosis in hepatoma cell lines. Chin Med Sci J 21: 33-35.

Wang Z, Sampath J, Fukuda S, Pelus LM. 2005. Disruption of the inhibitor of apoptosis protein survivin sensitizes Bcr-abl-positive cells to STI571-induced apoptosis. Cancer Res 65: 8224-8232.

Watanabe A, et al. 2011. The role of microRNA-150 as a tumor suppressor in malignant lymphoma. Leukemia 25: 1324-1334.

Watanabe M, Sheriff S, Lewis KB, Tinch SL, Cho J, Balasubramaniam A, Kennedy MA. 2012. HMGA-targeted phosphorothioate DNA aptamers

increase sensitivity to gemcitabine chemotherapy in human pancreatic cancer cell lines. Cancer Lett 315: 18-27.

Watanabe S, Ueda Y, Akaboshi S, Hino Y, Sekita Y, Nakao M. 2009. HMGA2 maintains oncogenic RAS-induced epithelial-mesenchymal transition in human pancreatic cancer cells. Am J Pathol 174: 854-868.

Weis E, Shah CP, Lajous M, Shields JA, Shields CL. 2006. The association between host susceptibility factors and uveal melanoma: a meta-analysis. Arch Ophthalmol 124: 54-60.

Whitesell L, Lindquist SL. 2005. HSP90 and the chaperoning of cancer. Nat Rev Cancer 5: 761-772.

Wikman H, Kettunen E, Seppanen JK, Karjalainen A, Hollmen J, Anttila S, Knuutila S. 2002. Identification of differentially expressed genes in pulmonary adenocarcinoma by using cDNA array. Oncogene 21: 5804-5813.

Wilson MW, Fraga CH, Rodriguez-Galindo C, Hagedorn N, Leggas ML, Stewart C. 2009. Expression of the multi-drug resistance proteins and the pregnane X receptor in treated and untreated retinoblastoma. Curr Eye Res 34: 386-394.

Wilson MW, Fraga CH, Fuller CE, Rodriguez-Galindo C, Mancini J, Hagedorn N, Leggas ML, Stewart CF. 2006a. Immunohistochemical detection of multidrug-resistant protein expression in retinoblastoma treated by primary enucleation. Invest Ophthalmol Vis Sci 47: 1269-1273.

Wilson TR, Longley DB, Johnston PG. 2006b. Chemoresistance in solid tumours. Ann Oncol 17 Suppl 10: x315-324.

Witt O, Deubzer HE, Milde T, Oehme I. 2009. HDAC family: What are the cancer relevant targets? Cancer Lett 277: 8-21.

Wolffe AP. 1994. Architectural transcription factors. Science 264: 1100-1101.

Woll E, Bedikian A, Legha SS. 1999. Uveal melanoma: natural history and treatment options for metastatic disease. Melanoma Res 9: 575-581.

Wong TS, Liu XB, Wong BY, Ng RW, Yuen AP, Wei WI. 2008. Mature miR-184 as Potential Oncogenic microRNA of Squamous Cell Carcinoma of Tongue. Clin Cancer Res 14: 2588-2592.

Workman P, Burrows F, Neckers L, Rosen N. 2007. Drugging the cancer chaperone HSP90: combinatorial therapeutic exploitation of oncogene addiction and tumor stress. Ann N Y Acad Sci 1113: 202-216.

Worley LA, Long MD, Onken MD, Harbour JW. 2008. Micro-RNAs associated with metastasis in uveal melanoma identified by multiplexed microarray profiling. Melanoma Res 18: 184-190.

Worley LA, Onken MD, Person E, Robirds D, Branson J, Char DH, Perry A, Harbour JW. 2007. Transcriptomic versus chromosomal prognostic markers and clinical outcome in uveal melanoma. Clin Cancer Res 13: 1466-1471.

Wu J, Liu Z, Shao C, Gong Y, Hernando E, Lee P, Narita M, Muller W, Liu J, Wei JJ. 2011. HMGA2 overexpression-induced ovarian surface epithelial transformation is mediated through regulation of EMT genes. Cancer Res 71: 349-359.

Wunderlich V, Bottger M. 1997. High-mobility-group proteins and cancer--an emerging link. J Cancer Res Clin Oncol 123: 133-140.

Xi Y, Nakajima G, Gavin E, Morris CG, Kudo K, Hayashi K, Ju J. 2007. Systematic analysis of microRNA expression of RNA extracted from fresh frozen and formalin-fixed paraffin-embedded samples. RNA 13: 1668-1674.

Xu B, et al. 2011a. miR-143 decreases prostate cancer cells proliferation and migration and enhances their sensitivity to docetaxel through suppression of KRAS. Mol Cell Biochem 350: 207-213.

Xu CX, et al. 2012. MicroRNA miR-214 regulates ovarian cancer cell stemness by targeting p53/Nanog. J Biol Chem 287: 34970-34978.

Xu X, Jia R, Zhou Y, Song X, Wang J, Qian G, Ge S, Fan X. 2011b. Microarray-based analysis: identification of hypoxia-regulated microRNAs in retinoblastoma cells. Int J Oncol 38: 1385-1393.

Xu XL, Fang Y, Lee TC, Forrest D, Gregory-Evans C, Almeida D, Liu A, Jhanwar SC, Abramson DH, Cobrinik D. 2009. Retinoblastoma has properties of a cone precursor tumor and depends upon cone-specific MDM2 signaling. Cell 137: 1018-1031.

Yamashita S, Masuda Y, Kurizaki T, Haga Y, Murayama T, Ikei S, Kamei M, Takeno S, Kawahara K. 2007. Survivin expression predicts early recurrence in early-stage breast cancer. Anticancer Res 27: 2803-2808.

Yamazaki K, Masugi Y, Sakamoto M. 2011. Molecular pathogenesis of hepatocellular carcinoma: altering transforming growth factor-beta signaling in hepatocarcinogenesis. Dig Dis 29: 284-288.

Yan LX, Huang XF, Shao Q, Huang MY, Deng L, Wu QL, Zeng YX, Shao JY. 2008. MicroRNA miR-21 overexpression in human breast cancer is

associated with advanced clinical stage, lymph node metastasis and patient poor prognosis. RNA 14: 2348-2360.

Yang C, Wei W. 2011. The miRNA expression profile of the uveal melanoma. Sci China Life Sci 54: 351-358.

Yang H, Schilling H, Effert R, Wessing A. 1999. [Morphologic classification of choroidal invasion of retinoblastoma]. J Tongji Med Univ 19: 149-154.

Yang H, et al. 2008. MicroRNA expression profiling in human ovarian cancer: miR-214 induces cell survival and cisplatin resistance by targeting PTEN. Cancer Res 68: 425-433.

Yang Z, Strickland DK, Bornstein P. 2001. Extracellular matrix metalloproteinase 2 levels are regulated by the low density lipoprotein-related scavenger receptor and thrombospondin 2. J Biol Chem 276: 8403-8408.

Yap-Veloso MI, Simmons RB, Simmons RJ. 1997. Iris melanomas: diagnosis and management. Int Ophthalmol Clin 37: 87-100.

Yin G, Chen R, Alvero AB, Fu HH, Holmberg J, Glackin C, Rutherford T, Mor G. 2010. TWISTing stemness, inflammation and proliferation of epithelial ovarian cancer cells through MIR199A2/214. Oncogene 29: 3545-3553.

Yokoyama K, Kamata N, Hayashi E, Hoteiya T, Ueda N, Fujimoto R, Nagayama M. 2001. Reverse correlation of E-cadherin and snail expression in oral squamous cell carcinoma cells in vitro. Oral Oncol 37: 65-71.

Yoshida M, Kijima M, Akita M, Beppu T. 1990. Potent and specific inhibition of mammalian histone deacetylase both in vivo and in vitro by trichostatin A. J Biol Chem 265: 17174-17179.

Young JC, Moarefi I, Hartl FU. 2001. Hsp90: a specialized but essential protein-folding tool. J Cell Biol 154: 267-273.

Yu J, Zhang L, Hwang PM, Kinzler KW, Vogelstein B. 2001. PUMA induces the rapid apoptosis of colorectal cancer cells. Mol Cell 7: 673-682.

Zhang B, Chen X, Bae S, Singh K, Washington MK, Datta PK. 2014. Loss of Smad4 in colorectal cancer induces resistance to 5-fluorouracil through activating Akt pathway. Br J Cancer 110: 946-957.

Zhang J, Han L, Ge Y, Zhou X, Zhang A, Zhang C, Zhong Y, You Y, Pu P, Kang C. 2010. miR-221/222 promote malignant progression of glioma through activation of the Akt pathway. Int J Oncol 36: 913-920.

Zhang J, et al. 2012a. A novel retinoblastoma therapy from genomic and epigenetic analyses. Nature 481: 329-334.

Zhang JF, Zhang JG, Kuai XL, Zhang H, Jiang W, Ding WF, Li ZL, Zhu HJ, Mao ZB. 2013. Reactivation of the homeotic tumor suppressor gene CDX2 by 5-aza-2'-deoxycytidine-induced demethylation inhibits cell proliferation and induces caspase-independent apoptosis in gastric cancer cells. Exp Ther Med 5: 735-741.

Zhang X, Liu S, Hu T, He Y, Sun S. 2009. Up-regulated microRNA-143 transcribed by nuclear factor kappa B enhances hepatocarcinoma metastasis by repressing fibronectin expression. Hepatology 50: 490-499.

Zhang Y, Fan KJ, Sun Q, Chen AZ, Shen WL, Zhao ZH, Zheng XF, Yang X. 2012b. Functional screening for miRNAs targeting Smad4 identified miR-199a as a negative regulator of TGF-beta signalling pathway. Nucleic Acids Res 40: 9286-9297.

Zhao JJ, Yang J, Lin J, Yao N, Zhu Y, Zheng J, Xu J, Cheng JQ, Lin JY, Ma X. 2009. Identification of miRNAs associated with tumorigenesis of retinoblastoma by miRNA microarray analysis. Childs Nerv Syst 25: 13-20.

Zhao ZN, et al. 2012. TSA suppresses miR-106b-93-25 cluster expression through downregulation of MYC and inhibits proliferation and induces apoptosis in human EMC. PLoS One 7: e45133.

Zhou J, Rossi JJ. 2008. Bivalent aptamers deliver the punch. Chem Biol 15: 644-645.

Zhou J, Rossi JJ. 2009. The therapeutic potential of cell-internalizing aptamers. Curr Top Med Chem 9: 1144-1157.

Zhou J, Rossi JJ. 2010. Aptamer-targeted cell-specific RNA interference. Silence 1: 4.

Zhou X, Benson KF, Ashar HR, Chada K. 1995. Mutation responsible for the mouse pygmy phenotype in the developmentally regulated factor HMGI-C. Nature 376: 771-774.

Zhou X, Benson KF, Przybysz K, Liu J, Hou Y, Cherath L, Chada K. 1996. Genomic structure and expression of the murine Hmgi-c gene. Nucleic Acids Res 24: 4071-4077.

Zimmerman LE, McLean IW, Foster WD. 1980. Statistical analysis of follow-up data concerning uveal melanomas, and the influence of enucleation. Ophthalmology 87: 557-564.